Spring 5-1-2021

Modeling Hydrochemical and Vegetation Responses of High-elevation Forested Watersheds to Future Climate and Atmospheric Deposition Changes in the Southeastern U.S.

Hailong Huang

MODELING HYDROCHEMICAL AND VEGETATION RESPONSES OF HIGH-ELEVATION FORESTED WATERSHEDS TO FUTURE CLIMATE AND ATMOSPHERIC DEPOSITION CHANGES IN THE SOUTHEASTERN U.S.

by

Hailong Huang

A Dissertation
Submitted to the Graduate School,
the College of Arts and Sciences
and the School of Ocean Science and Engineering
at The University of Southern Mississippi
in Partial Fulfillment of the Requirements
for the Degree of Doctor of Philosophy

Approved by:

Dr. Wei Wu, Committee Chair
Dr. Patrick Biber
Dr. Kevin Dillon
Dr. Robert Leaf

May 2021

Published by the Graduate School

ABSTRACT

Changes in climate and atmospheric acidic deposition alter biogeochemical cycles in forested ecosystems. I investigated the responses of vegetation, soil, and hydro-related processes to changes in climate and acidic deposition at five high-elevation forests in the southeastern U.S. using a biogeochemical model - PnET-BGC model. I focused on change-points and thresholds concepts that were less studied in forest ecosystems as well as seasonal variability of responses and extreme events. I applied principal component analysis (PCA) to reduce the dimensionality of data. I developed a Bayesian multi-level model to derive key biogeochemical variables response to temperature and precipitation (local) and latitude and elevation (regional) with uncertainty accounted for. The first principal components (PC1s) explain 50-60% and 40-50% of the variance in the 17 main biogeochemical variables simulated from the model at the Coweeta Basin (CWT) and Shenandoah National Park (SNP) respectively. PC1s at CWT are highly correlated to transpiration, gross and net primary production (GPP and NPP), soil base saturation, soil Al:Ca ratio, and stream chemistry (Ca^{2+} and K^{+}), while PC1s at SNP are highly correlated to NPP, transpiration, and stream base cations. The key biogeochemical processes show strong seasonality in their response to future climate change. Higher latitudinal sites have earlier but fewer change-points than lower latitudes from 1931 to 2100. Vegetation at higher-elevation forests appears more sensitive to climate change, while soil and streams are more sensitive at the lower-elevation forests. Flooding and drought will become more frequent, and soil and stream will become more acidic under climate change. Regional analysis demonstrates that temperature tends to drive key biogeochemical variables more significantly than precipitation. Winter shows the least sensitivity to climate change in

NPP, transpiration, and acid neutralization capacity 3 (ANC) at all five sites. In addition, latitude and elevation influence the sensitivity of these biogeochemical variables to temperature and precipitation at some degree. Change in acidic deposition will likely shift the biogeochemical processes response to climate change differently, depending on biogeochemical processes, season, and the direction and magnitude of change in acidic deposition. The effect is minimal for NPP, and summer and winter will have the largest shifts.

ACKNOWLEDGMENTS

I would like to express my sincere gratitude to my advisor, Dr. Wei Wu, who has given me the opportunity to pursue my Ph.D. under her guidance. Without her great patience and encouragement, I am not sure I could finish my study here through these years. Her insightful questions, challenging comments, and feedback always pointed me to the right direction especially toward the end of my study here. With her diligence and professionalism, she is not only my advisor but also my role model both in life and work. I could never ask for a better advisor to pursue my Ph.D. and I will be indebted to her for the rest of my life. My profound gratitude also goes to my other committee members: Dr. Patrick Biber, Dr. Kevin Dillon, and Dr. Robert Leaf, as well as my previous committee member Dr. Katherine Elliott from the USDA Forest Service at the Southern Station at Coweeta, NC. With their extremely generous support, guidance, encouragement, and professionalism, I have eventually completed my dissertation project successfully. I would also like to thank the Environmental Protection Agency through the STAR program for providing the funding for this research. I want to say thanks to the following professors and their labs: Dr. Katherine Hayhoe and Anne Stoner, for providing the downscaled climate data; Dr. Charles Driscoll and Dr. Afshin Pourmokhtarian, for helping with the PnET-BGC model, data, and manuscripts; Dr. Chelcy Miniat and Dr. Jennifer Knoepp, for sharing data, papers, and insights on Coweeta Basin; Dr. Deepak Mishra, for financially supporting me for one year through one NASA proect; Dr. Tina Masterson and the Department of Chemistry of the University of Southern Mississippi, for supporting me through many years of studying here. 5 I would like to give thanks to my department and school, as well as my current and past lab members and friends who

have impacted my life deeply: Dr. Shuo Shen, Jason Tilley, Tyler Hardy, Yimu Yang, Evan Grimes, Devin Jen, Kodi Feldpausch, Dr. David Cotton, and many others. Finally, I would like to say thanks to my family and especially to my mom. I feel sorry for keeping her waiting for so long.

DEDICATION

To my beloved parents, for their endless love, support, and encouragement.

TABLE OF CONTENTS

LIST OF TABLES

LIST OF ILLUSTRATIONS

LIST OF ABBREVIATIONS

ANC	Acidic Neutralization Capability
AOGCMs	Atmosphere-Ocean General Circulation Models
BS	Soil Base Saturation
CASTNET	Clean Air Status and Trends Network
CCSM4	Community Climate System Model Version 4
CWT	Coweeta Basin
DayMET	Daily Surface Weather and Climatological Summaries
GPP	Gross Primary Production
GrossNImmob	Gross Nitrogen Immobilization
HadGEM2	Hadley Centre Global Environment Model version 2
IPCC	Intergovernmental Panel on Climate Change
LTER	The Long-Term Ecological Research Network
MIROC5	Model for Interdisciplinary Research on Climate version 5
MRI-CGCM3	Meteorological Research Institute Coupled Global Climate Model Version 3
NADP	National Atmospheric Deposition Program

NCDC	National Climatic Data Center
NetNMin	Net Nitrogen Mineralization
NMAE	Normalized Mean Absolute Error
NME	Normalized Mean Error
NPP	Net Primary Production
PAR	Photosynthetically Active Radiation
PCA	Principal Components Analysis
PnET-BGC	Photosynthesis Evapotranspiration Biogeochemical
PRCP	Precipitation
RCPs	Representative Concentration Pathways
SLRD	Solar Radiation
STASTGO	State Soil Geographic
TotLitt	Total Litter Mass

CHAPTER I – INTRODUCTION

Climate has considerably changed in recent decades due to human activities (IPCC, 2007) and global climate change is expected to accelerate through the end of this century (IPCC, 2014). The Coupled Model Intercomparison Project Phase 5 (CMIP5) based on four greenhouse gas emission scenarios, representative concentration pathways - RCPs: RCP2.6, 4.5, 6.0, and 8.5, has predicted that the global mean surface temperatures for years 2081-2100 will be 0.3 to 4.8 ^{o}C warmer than those observed in 1986-2005. Higher–latitude regions are projected to experience greater temperature increases than regions at the lower-latitude. Global precipitation is also predicted to increase, driven by mean surface temperature with a 1% to 4% increase per ^{o}C by 2100. However, predication in the expected precipitation show high spatial variability (IPCC, 2014) and is projected to increase in the southeastern U.S. but decrease in the western U.S where there has experienced severe droughts in the recent years. Temporally, global temperature increases will be accompanied with larger contrasts in precipitation between wet and dry regions and also between wet and dry seasons in individual regions (IPCC AR5, 2014). In the south and southeastern U.S., temperature is expected to increase from less than 1.7 ^{o}C on the Atlantic coast to above 2.8 ^{o}C in northwestern Texas using the Global General Circulation Model Hadley Centre Climate Model, version 3 (HadCM3), under the B2 emission scenario (IPCC 2000 standard emission scenario - mid-range emission; Mitchell et al. 2014). Precipitation is expected to increase over most regions of the southeastern U.S. for all seasons except summer. The average annual precipitation is predicted to decrease by 2% to 4% in Louisiana and Southern Florida respectively, but increase up to 6% across North Carolina and Virginia (Keim et al. 2011).

1.1 Climate impacts to forested watershed

1.1.1 Impacts to forest

Temperature and precipitation are two important factors of climate that alter forest distribution, composition, and productivity (Shugart et al. 2003). The interactions between temperature and precipitation can be complex by the biogeochemical conditions such as geology, physiography, and vegetation type (e.g., conifers, hardwoods, and species-specific composition). Higher air temperature will increase the length of the growing season, and therefore increase annual gross primary production and carbon sequestration if soil water content is not limited (Boisvenue and Running, 2006). Elevated temperatures in summer, however, may begin to exceed physiological optima, resulting in decreased productivity (Coder, 1999; Buermann et al. 2013; Hatfield and Prueger, 2015). At the same time, vegetation and soil respiration will increase with temperature and may offset the increased carbon storage driven by increased primary production (Turnbull et al. 2001). Changes in precipitation affects hydrological cycles and soil water content, which are directly related to vegetation growth and health. In the western regions of the U.S., the projected decreases in precipitation will likely negatively affect vegetation (Vose et al. 2016). For most regions in the southeastern U.S., the annual precipitation is predicted to increase; however, the seasonal variability is predicted to become larger, with more droughts in summer /fall and more frequent flooding events in spring /winter (Wu et al. 2012). Other changes in temperature and precipitation characteristics such as extreme values, duration, intensity, timing, and frequency also have critical effects on forest vegetation responses because they can impact vegetation dispersion and influence disturbances such as fire, drought, invasive species, insect, and

extreme weather conditions (Elliott et al. 1994; Dale et al. 2001; Elliott et al. 2002; Elliott and Vose, 2006; Elliott et al. 2009). Climate can also alter carbon allocation between different parts of tree tissues. As an example, Lapenis (2013) reported 17 increased carbon allocated to roots instead of stemwood due to soil acidification and an earlier growing season in a calcium-depleted spruce forest.

1.1.2 Impacts to hydrology

The most direct and prominent impacts of climate change on forest hydrology are snowpack and runoff patterns (Furniss et al. 2010). Over the last century, many mountains in the western region of North America have exhibited declines in spring snowpack even though winter precipitation increased in many places (Mote et al. 2005). For the southeastern U.S., the average annual snowfall has declined at a rate of approximately one percent per year since the late 1930s (Kunkel et al. 2009). In the northern parts of the Appalachians and at greater elevations, spring runoff occurred earlier in snow- and glacier-dominated watersheds (Stewart et al. 2005; Hodgkins & Dudley, 2006). A longer growing season and higher temperature increased evapotranspiration, leading to declines in spring and summer soil moisture (Meehl et al. 2007; Wu et al. 2012). In some cases, (Kaskawulsh Glacier, Canada, for instance), an extreme and sudden change of river flow path, “river piracy”, occurred when the precipitation patterns changed and could no longer sustain the previous river flow (Shugar et al. 2017). Precipitation distribution is likely to be more spatially and temporally unevenly distributed in the U.S. by the end of this century (AR5, IPCC, 2014). Frequency of droughts, flash floods, and extreme temperature days would also likely increase in many areas. The frequency of droughts is predicted to increase in the

northern Gulf of Mexico and the western U.S., however there will be fewer droughts in the rest of the southeastern U.S. (Strzepek et al. 2010).

1.1.3 Impacts to soil

Higher temperature can decrease soil moisture through increased evapotranspiration. More frequent extreme precipitation events could increase erosion, and prolonged droughts may increase wildfire events and induce degradation and loss of vegetation and soil (Klos et al. 2009). Additionally, climate change will indirectly affect soil properties through biotic and abiotic processes such as carbon fixation (Jobbagy and Jackson, 2000; Barger et al. 2011), acid neutralization capability, nitrification/denitrification rates, and mineralization of plant litters (Stark & Firestone, 1995; Knoepp & Vose, 2007; Duran et al. 2016). As nitrogen is a major element in the RuBisCO enzyme and the light harvesting complexes that modulate photosynthesis, terrestrial biosphere models generally relate photosynthetic capacity to leaf nitrogen (Evans 1989; Aber & Federer, 1992; Croft et al. 2017). Bioactive nitrogen is usually contained in vegetation and soil. Human activities have increased the availability of reactive nitrogen, exceeding the demands of vegetation and microbes, which leads to nitrogen saturation and nitrogen leaching from soil into water bodies in some regions such as northeastern U.S. (Aber et al. 1989; Aber, 1992; Aber et al. 1998; Huang et al. 2015; Chen et al. 2016). Saturated nitrogen leaching (from deposition or forest soils) is one of the main drivers of stream acidification, and it is dependent on precipitation, snowmelt, and water infiltration in the soil below the root zone (Mitchell, 1939; Rascher et al. 1987). Bernal et al. (2012) reported that the snowpack decline at the Hubbard Brook Experimental Forest in New Hampshire, U.S. has made the soil a massive nitrate sink

because of flow path change, past harvesting, and extreme weather events (i.e., hurricanes or ice storms). Temperature and precipitation changes can alter other nutrient cycles (Ca^{2+}, Mg^{2+}, and K^{+}) by increasing water and temperature stress and depressing soil microbial activity (Bassirirad, 2000; Weih et al. 2002; Rennenberg et al. 2006). Campbell et al. (2009) has predicted there will be an increase in net primary production due to longer growing seasons, an increase in nitrate leaching due to enhanced net mineralization and nitrification, as well as declines in mineral weathering due to reduced soil moisture under climate change in the northeastern U.S.

1.2 Atmospheric deposition impacts to forested watershed

Acidic deposition has caused a number of environmental issues since fossil fuel has been largely used in the last century (Driscoll et al. 2001). Atmospheric deposition has been monitored intensively across the U.S. by the National Atmospheric Deposition Program (NADP) since 1978 (currently with 250 sites), and the Clean Air Status and Trends Network (CASTNET) since 1991 (currently with 95 locations throughout the U.S. and Canada; USEPA, 2017a). Acidic atmospheric deposition, largely comprised of sulfuric acid and nitric acid from SO_2 and NOx fossil fuel emissions, is the major concern of the NADP and CASTNET programs. Ammonia, mainly from agricultural activities, plays an ever-increasing role in acid deposition (NH_4^+ and NO_3^- conversion by microbes through nitrification and NH_3 converts to NH_4^+ aerosols and NO_3^- leaching to underneath soils, Driscoll et al. 2001). Acid deposition adversely affects ecosystems, leading to base nutrient depletion, aluminum toxicity, nitrogen saturation, and eutrophication (Aber, 1989; Shortle & Bondietti, 1992; Driscoll et al. 2001; Driscoll et al. 2003).

Acidic deposition reduction and environment recovery may not happen concurrently and could be complicated and uncertain under future emission and human activity projections. Since the Clean Air Act and its amendments in the 1970s and 1990s, SO_2 and NO_x emission have dramatically decreased in the U.S. There has been an 84% decrease in the national average for SO_2 between 1980 and 2015 and a 59% decrease for NO_x over the same period (USEPA, 2017b). However, the recovery of ecosystems seems to lag behind the reduction of acidic deposition (Zhou et al. 2014, Wu and Driscoll 2010). In addition, it is widely accepted that ammonia deposition from increased agricultural activities has and will continue to increase if no reduction policy is implemented (Li et al. 2016). This makes recovery of ecosystems from reduced SO_2 and NO_x emissions more uncertain and acidic deposition an ongoing concern on forest ecosystems' structure and function.

1.3 PnET-BGC model and modeling approach

Modeling is a useful and efficient tool to address the questions arising in complex ecosystems such as how forest ecosystems respond to the changes in climate and acidic deposition. Observations and manipulated experiments, which are generally conducted in short-terms and narrow spatial scales, have provided some insights on above question, but the long-term effects of climate change on hydrological and biogeochemical processes in forested watersheds need to be better understood (Pourmokhtarian et al. 2012). Models can synthesize state-of-the art knowledge and make predictions under varied future or hypothetical scenarios (Medlyn et al. 2011). A number of models have been developed to study biogeochemical cycles in forests affected by atmospheric deposition and/or climate, such as the Very Simple Dynamic Model (Posch & Reinds,

2009), Simple Mass Balance Model (Prado et al. 2016), Model of Acidification of Groundwater in Catchment (MAGIC, Cosby et al. 1985), and PnET (photosynthesis and evapotranspiration) family models including PnET, PnET-II, PnET-CN and PnET-BGC (Aber et al. 1992; Aber et al. 1995; Aber et al. 1996; Gbondo-Tugbawa et al. 2001).

PnET-BGC (Fig. 1-1) is a lumped-parameter watershed model that can simulate the stocks and fluxes of the major elemental cycles including carbon, nitrogen, sulfur, and base cations (K^+, Na^+, Ca^{2+}, and Mg^{2+}) in vegetation, soil, and water. It includes processes of forest canopy exchange, primary productivity, litter decomposition, soil organic matter dynamics, weathering, and chemical equilibrium reactions between solid and solution phases in soil, hydrology cycle, and water chemistry at a monthly time step (Gbondo-Tugbawa & Driscoll, 2002; Chen et al. 2004a, b; Zhai et al. 2008; Wu & Driscoll, 2009; Zhou et al. 2015; Fakhraei et al. 2016). PnET-BGC integrates the PnET model (Aber & Federer, 1992) and a soil equilibrium model BGC model (Gbondo-Tugbawa et al. 2001). PnET, representing photosynthesis and evapotranspiration, was first developed in 1992 (Aber & Federer, 1992) to simulate water and carbon cycles in vegetation. It has gone through a few stages of improvement and refinement, including incorporation of nitrogen cycles in PnET-CN (Aber et al. 1997), and addition of the BGC (biogeochemical cycle) submodules which simulates biogeochemical cycles of other major elements (Ca^{2+}, Mg^{2+}, K^+, Na^+, Cl^-, Al^{3+}, and SO_4^{2-}) as well as chemical equilibrium reactions between solid and solution phases in the soil (Gbondo-Tugbawa et al. 2001). The outputs of the PnET-BGC model include estimates of streamflow, primary productivity, mineralization rates, immobilization rates, and concentrations of major

chemical elements in soil solution and streams. They also include base saturation of soil and acid neutralization capacity (ANC) of streams.

So far, PnET-BGC has been intensively applied in northeastern U.S. forests (Gbondo-Tugbawa et al. 2001; Chen et al. 2004a, b; Zhai et al. 2008; Wu & Driscoll, 2009; Zhou et al. 2015; Fakhraei et al. 2016). In this research, I will extend the application of the PnET-BGC model to the southeastern U.S. region (south and central Appalachians), where the climate, atmospheric acidic deposition, vegetation species, soil, and stream properties differ from the northeastern U.S. Additionally, I will use downscaled predictions of future climate including monthly air temperature, precipitation, and solar radiation, combined with a variety of atmospheric deposition scenarios, to drive the simulations of biogeochemical cycles in forests.

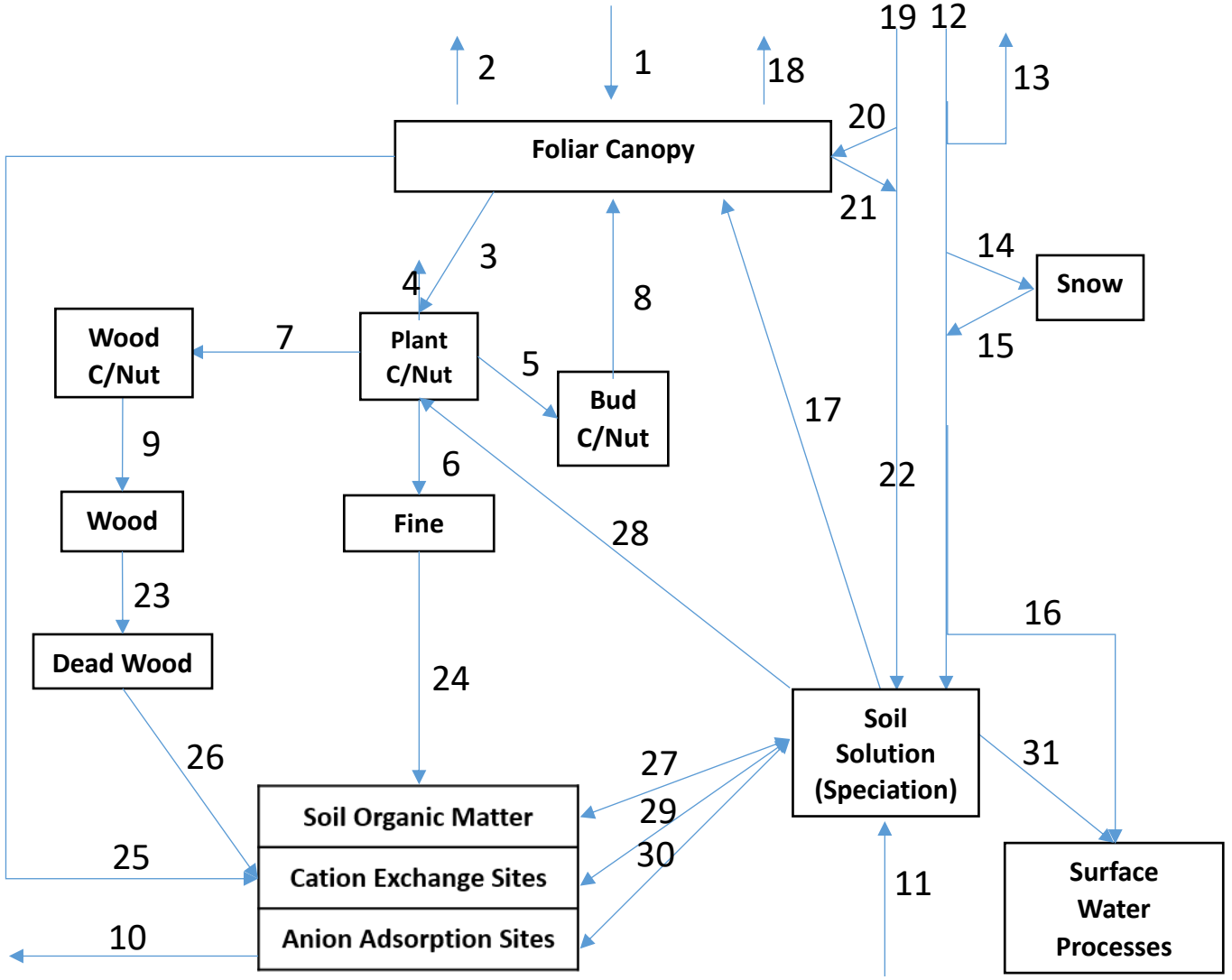

Fig. 1-1 Structure of PnET-BGC model (adapted from Gbondo-Tugbawa et al. 2001. Specific processes see next page)

1. Gross Photosynthesis
2. Foliar Respiration
3. Transfer to Mobil C
4. Growth and Maintenance Respiration
5. Allocation to Buds
6. Allocation to Fine Roots
7. Allocation to Wood
8. Foliar Production
9. Wood Production
0. Soil Respiration
1. Weathering Supply
12. Precipitation
13. Interception
14. Snow-Rain Partition
15. Snowmelt
16. Shallow Flow
17. Water Uptake
18. Transpiration
19. Deposition (Wet and Dry)
20. Foliar Nutrient Uptake
21. Foliar Exudation
22. Throughfall & Stemflow
23. Wood Litter
24. Root Litter
25. Foliar Litter
26. Wood Decay
27. Mineralization/Immobilization
28. Nutrient Uptake
29. Cation Exchange Reactions
30. Anion Adsorption Reactions
31. Drainage

1.4 Study sites

In this work, I selected five forested-watersheds which cover both the southern (the Coweeta Basin – CWT, NC) and central (the Shenandoah National Park – SNP, VA) Appalachians (Fig. 1-2 and Table 1-1). The watersheds' elevation ranges from 300 to over 1,500 meters and the latitude is between 38^{o}26'40.6"N and 35^{o}2'2.4"N. The smallest-sized watershed (watershed 18 – WS18) is located in CWT and the largest one (White Oak Run – WOR) is in SNP. Watershed 27 (CWT) has the highest elevation, the greatest precipitation, and the largest annual streamflow among these five sites (based on observation data between 1986 and 2015). Except WS18 (CWT), the remaining four watersheds show similar cooler temperatures during the same period (~ 10.0 ^{o}C). Within all watersheds, Chestnut Oak (*Quercus montana*), Northern Red Oak (*Quercus rubra*), and maples (*Acer spp.* such as red maple - *Acer rubrum*) are the dominant species and at colder and higher latitude or elevation sites. Birch (*Betula spp.*) are also common. Detailed descriptions of each study area and modeling data preparation are provided in

the following chapters (Chapter 2 – Coweeta Basin WS18 and WS27; Chapter 3 – Shenandoah National Park PR, WOR, and SR).

1.5 Overall objective and general hypotheses

I will predict how climate change, combined with changes in atmospheric deposition, affects 1.) hydrology (surface runoff), 2.) primary production, 3.) soil processes, and 4.) streamwater chemistry in forested watersheds in the southeastern U.S. using the PnET-BGC model and derive latitudinal and elevational dependences in key watershed processes with climate change and their seasonality changes using a Bayesian modeling approach. Even though there are large uncertainties in climate and atmospheric deposition predictions, the following patterns are likely to emerge:

1) climate seasonality will become stronger and spatial variability in climate will become more extreme, 2) extreme climate events such as drought, storms, and extreme temperature events will become more frequent and intense, 3) atmospheric deposition of sulfur will continue to decline, and 4) nitrogen deposition would be complex due to projected increases in NH_3 emissions, mainly from agricultural activities, and decreasing NO_x emission, mainly from fossil fuel combustion (van Vuuren et al. 2011).

I will explicitly test the following hypotheses:

Hypothesis 1: Climate change will affect the local hydrological cycle, primary productivity, soil and stream water chemistry, with the largest impact occurring in vegetation processes (ET, nutrient uptake, productivity).

Hypothesis 2: Climate change will affect vegetation, soil, and stream water processes in each season differently, with the most pronounced effect happening in summer and winter.

Hypothesis 3: The response of the hydrological and biogeochemical cycles to climate change in the five forested watersheds will vary, with the largest response occurring in higher elevation and higher latitude watersheds.

Hypothesis 4: Atmospheric deposition changes will likely synergistically intensify climate change impacts on key watershed processes such as vegetation, hydrology, and soil and stream chemistry, but this will also depend on the season.

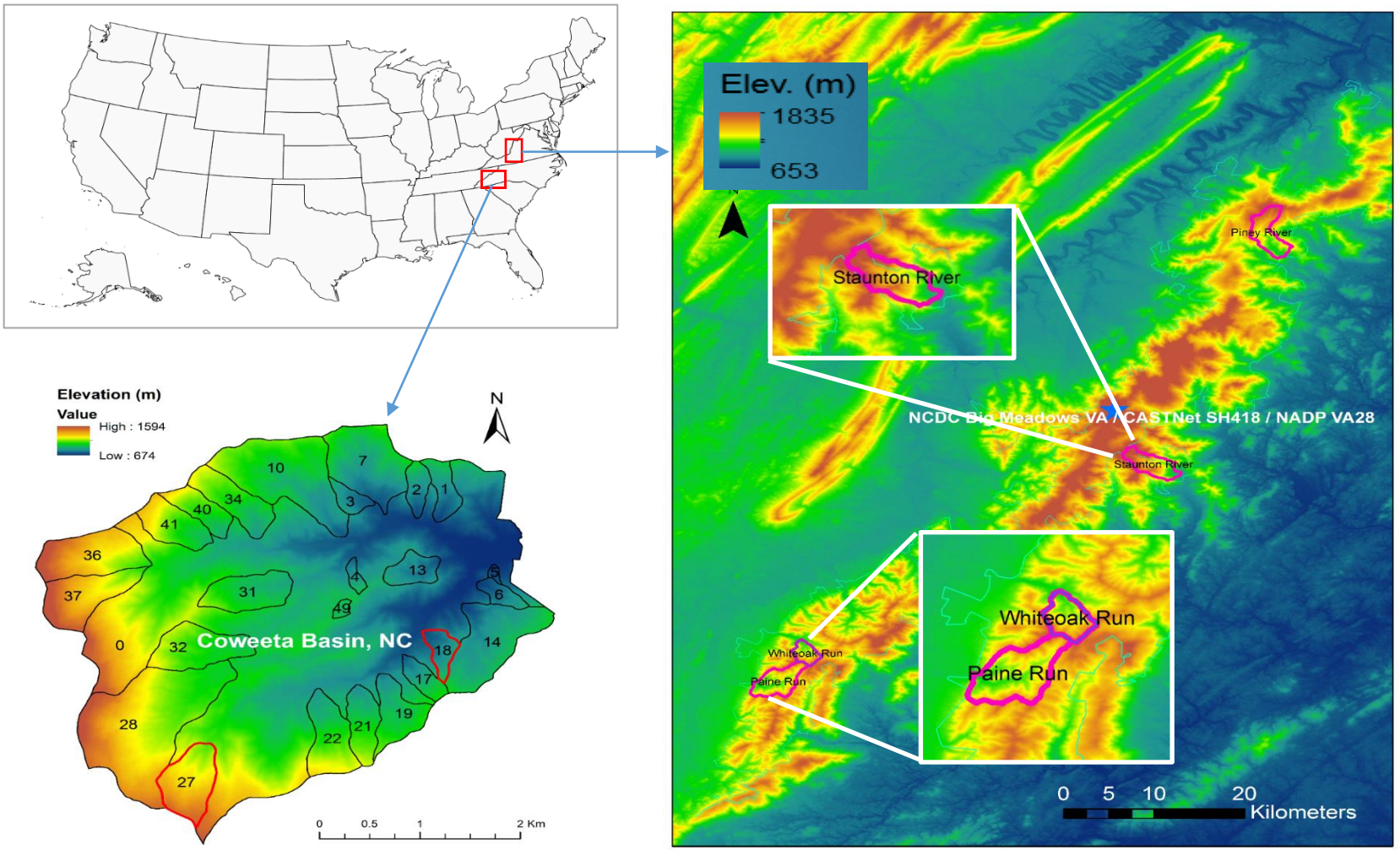

Fig. 1-2 Study watersheds: Coweeta Basin – CWT, NC (Watershed 18 and Watershed 27); Shenandoah National Park – SNP, VA (Paine Run, White Oak Run, and Staunton River).

Table 1-1. Summary of the five study watersheds' features
(Temperature and precipitation data based on observations collected between January 1986 and December 2015)

	Lat. (°)	Elev. (m)	Area (ha)	Prcp. (cm/yr)	Annual Temp. (°C)	Streamflow (cm/yr)	Dominant tree and shrub species*
Staunton River (SR)	38.4446	309-1,181 (768)	1,010	132	9.9 (4.7-15.2)	69	*Quercus montana, Quercus rubra, Acer, spp., Betula spp.*
White Oak Run (WOR)	38.2508	674-1,594 (685)	1,480	124	10.2 (4.7-15.6)	37	*Quercus montana, Quercus rubra, Acer spp., Betula spp., Fraxinus spp., Tilia americana*
Paine River (PR)	38.1986	434-1,040 (657)	1,390	128	10.4 (4.9-15.9)	40	*Quercus montana, Quercus rubra, Acer spp., Betula spp., Fraxinus spp., Tilia Americana, Liriodendron tulipifera*
WS27	35.0340	1,061-1,454 (1,398)	39	229	10.2 (5.9-14.5)	163	*Acer rubrum, Quercus montana (Q. prinus), Quercus rubra, Betula lenta, Betula alleghaniensis, Tsuga canadensis, Tilia americana, Liriodendron tulipifera, Rhododendron maximum, Nyssa sylvatica*
WS18	35.0495	726-993 (887)	13	192	14.0 (8.9-19.6)	96	*Liriodendron tulipifera, Quercus montana (Q. prinus), Carya spp., Acer rubrum, Quercus coccinea, Pinus rigida, Quercus rubra, Kalmia latifolia, Tsuga canadensis, Betula lenta*

Where * denotes the data, for SNP, is from the National Park Service NPSpecies database and can be accessed at https://irma.nps.gov/NPSpecies and accessed on 1/1/2021; for the CWT, tree species data is from the 2010 USDA Forest Services Southern Station Coweeta Hydrologic Laboratory field survey; the values in Elevation parentheses are whole watersheds' averaged elevations.

CHAPTER II IMPACT OF CLIMATE CHANGE ON HYDROCHEMICAL PROCESSES AT TWO HIGH-ELEVATION FORESTED WATERSHEDS IN THE SOUTHERN APPALACHIANS, U.S.

Abstract

Climate change alters primary productivity and biogeochemical cycles in forested ecosystems. In this work I studied the holistic response of vegetation, soil, and hydrologically related processes to climate change by applying the PnET-BGC model at two high-elevation forested watersheds (WS18 and WS27) in the basin of the Coweeta Hydrologic Laboratory, NC, US. I investigated change-points and threshold concepts that focus on nonlinear responses of forest ecosystems to climate change, as well as seasonal variability and extreme events.

Through the principal component analysis, I find the first three principal components (PC1s) that explain more than 80% of total variance in the 17 variables simulated in the model are highly correlated with transpiration, gross and net primary production (GPP and NPP), soil base saturation (BS), soil exchangeable Al:Ca ratio, stream Ca^{2+} and K^{+} concentrations, nitrogen mineralization, streamflow, and acid neutralization capacity (ANC). With climate change, GPP, NPP, transpiration, nitrogen mineralization, and streamflow are projected to increase, while soil base saturation, and base cation concentration, and ANC of streamwater are projected to decrease and show strong changes in seasonal variability. I detect five change-points of PC1 that occur between 1931 and 2100, with the last change-point projected to occur twenty years earlier under representative concentration pathway (RCP)8.5 than under RCP4.5 at both watersheds. The change-points are simulated to have occurred earlier at WS18 than at

WS27 in 1980s and 2010s but in the future are projected to occur earlier in WS 27 relative to WS18, implying that changes in biogeochemical cycles may be accelerated at higher-elevation WS27. I also find an increase of 3 ºC and decrease of precipitation by 40% will likely trigger a rapid change of key forest processes at the lower-elevation watershed but not at higher-elevation watershed with less water stress. While vegetation at higher-elevation forests appears more sensitive to climate change, soil and streams are more sensitive at the lower-elevation forests. Overall, the two forested watersheds will likely show substantial ecosystem alteration as they experience more frequent streamflow extremes, and an extended period when some indicators of acidification stress fall below critical values required for healthy soil and streams.

This findings from this study will contribute to more-informed policy making in mitigating the impact of climate change in forest resource management.

2.1 Introduction

Global climate has changed considerably over the past few decades and these changes will continue due to increases of greenhouse gas emissions, mainly through burning of fossil fuels and land disturbance (IPCC AR5, 2014; C2ES, 2019). In the IPCC AR5 report (2014), global air temperature between 2081 and 2100 is projected to be 0.3 to 4.8 ^{o}C higher than the average between 1986 and 2005 with high confidence. Precipitation will likely increase as well (1% to 4% more per ^{o}C increment) with high spatial variability.

Climate change has impacted and will impact forested ecosystems' distribution, composition, and productivity (McKenney-Easterling et al. 2000; Shugart et al. 2003; McKenney et al. 2007; Albrich et al. 2020) by altering biogeochemical cycles in vegetation, soil, and streams within forests that lead to changes in habitat suitability and species competition. Considering forests represent 30% of the world's land surface and provide a wide variety of ecosystem services, including carbon sequestration, water quality improvement, timber products, wildlife habitats and recreational opportunities etc. (Lindquist et al. 2012; Peters et al. 2013; United Nations, 2020, https://www.un.org/en/observances/forests-and-trees-day), alteration of biogeochemical cycles will likely degrade forests' ecosystem services and affect human's livelihood or quality of life. It is important to predict impact of climate change on forests in order to design effective mitigation measures to minimize potential adverse consequences to ecosystems and humans due to climate change. However, such predictions involve large uncertainties as the response of biogeochemical processes to climate change is complex due to different controlling factors that interact at different spatial and temporal scales

(Grimm et al. 2013). Increases in air temperature lead to longer growing seasons, and therefore increase annual primary productivity (Zohner et al. 2020). Meanwhile, plant respiration tends to increase with temperature (Turnbull et al. 2001), which results in uncertain changes in the direction and magnitude of the combined effect of these two processes, i.e., net primary productivity. Precipitation and available soil water are critical to forest growth. Climate change could reduce soil water content due to higher evapotranspiration associated with increase in temperature or changes in plant processes, or it could increase soil water content due to increased precipitation. The change of soil water content further alters soil properties through biotic and abiotic processes such as nitrification/denitrification and mineralization of plant nutrients (Stark & Firestone, 1995; Knoepp & Vose, 2007). For example, decomposition of plant litters is mediated by soil microbial activity, which is dependent on temperature and soil moisture (Krishna & Mahesh, 2017). As temperature increases and precipitation patterns change, decomposition rates will likely accelerate, therefore, carbon and nutrient (K, Ca, Mg, and P except N) release will become more rapid, especially in the fall and winter seasons (Chen et al. 2000; Davidson & Janssens, 2006). These biogeochemical changes will further impact water availability and quality (Delpla et al. 2009). Floods and droughts will likely become more frequent under climate change (e.g., Wu et al. 2014) and water quality can be degraded either because of drought-caused or flood-induced changes in temperature, pH, and concentrations of dissolved oxygen, nutrients, and dissolved organic matter (Stanke et al. 2013).

In addition to chronic changes in temperature and precipitation, the duration, intensity, and frequency of extreme events, such as drought and intense precipitation and

runoff events mentioned above as well as wildfire and heat waves, are projected to increase with climate change (IPPC, 2014; Rita et al. 2019, Vose & Swank, 1994; Kloeppel et al. 2003; Martin et al. 2017). Studies show the southeastern U.S. has already experienced increasing droughts and heavy storms in recent decades (Furniss et al. 2010; Diffenbaugh & Ashfaq, 2010) and this trend is projected to continue (McKenney-Easterling et al. 2000). Forests respond to these extreme events differently from to chronic change. More frequent and intensive extreme climate events may go beyond the ecological thresholds for forest stability, causing tree dieback, making trees vulnerable to insect/disease attacks (Kloeppel et al. 2003), or facilitating the expansion of invasive species to an irreversible extent (Hellmann et al. 2008; Pureswaran et al. 2018).

An ecological threshold is defined as a maximum or minimum value of an environmental driver (such as temperature, precipitation, disturbance frequency, and deposition loading etc.), that, if exceeded, will result in an abrupt change in ecosystem state and function, where small changes in the environmental driver(s) produce large changes in the ecosystem (Groffman et al. 2006). Exceeding an ecological threshold is anticipated to result in an alternate steady state for the ecosystem where recovery back to the previous state is constrained by hysteresis behavior (Andersen et al. 2009), also known as a regime shift. The identification of an ecological threshold and understanding when a state shift occurs could be facilitated by dynamic process models (Wu et al. 2017), in which environmental factors can be set to extreme conditions and then the resultant model outputs describing ecosystem status can be evaluated and compared. In the southern Appalachian forests, ecological thresholds may exist and could be exceeded due to climate induced warming and precipitation change (Albrich et al. 2020).

To improve the understanding of the nonlinear responses of forest processes to climate change, I aim to address the following questions: 1). What processes of forested ecosystems explain the largest component of variability in the impacts of climate change and does the impact of climate change on these processes' present seasonal variability? 2). Do change-points of these processes exist over time? Do they correspond to change-points of temperature and precipitation? 3). Do these processes show threshold behavior in response to temperature or precipitation change? 4). How do frequency and intensity of extreme hydrological events and acidification status of soil and streams change in response to climate change? 5). How do the impacts of climate change on forest ecosystem processes contrast between lower and higher elevation watersheds?

2.2 Methods

I applied the PnET-BGC (Photosynthesis-EvapoTranspration and BioGeoChemistry) model, an integrated and dynamic biogeochemical model (Gbondo-Tugbawa et al. 2001), to evaluate the impact of climate change on coupled vegetation-soil-stream processes at the two watersheds at the Coweeta Basin in the southern Appalachian Mountains of North Carolina. I focused on average and extreme conditions. I implemented principal component analysis to derive the main biogeochemical processes that explain the majority of variance of all the processes / states and evaluated their seasonal changes. I next derived the change-points of ecosystem processes over time. I also studied potential thresholds of temperature and precipitation for stability of main biogeochemical variables. I further investigated the hydrological extremes in streams and extreme acidic events in streams and soil. The multiple aspects I focused on provide a comprehensive understanding on how forests respond to climate change.

2.2.1 Study area

The Coweeta Experimental Forest at the Coweeta Basin was established in 1934 by USDA Forest Service near Otto, North Carolina and was then renamed as Coweeta Hydrologic Laboratory in 1948 (35º03' N, 83º25'W, Fig. 1-1). The climate in this region is classified as marine, humid temperate, and features cool summers and mild winters, with less than 5% of annual precipitation occurring as snow (Swift et al. 1988). Two reference watersheds with detailed meteorology, vegetation, soil, and stream chemistry data were selected for this study to calibrate the PnET-BGC model: lower-elevation watershed 18 (WS18) and higher-elevation watershed 27 (WS27) (Fig. 1-1). WS18 is a 12.5 ha watershed drained by Grady Branch, with an elevation range from 726 m to 993 m and a northwest facing slope of 52%. From 1986 and 2015, over half of the precipitation was returned in streamflow (average of 96 cm yr^{-1} streamflow vs. 182 cm yr^{-1} total precipitation). The average annual air temperature was 14.0 ºC with an average minimum of 8.9 ºC and an average maximum of 19.6 ºC. WS27 is a 39-ha watershed drained by Hard Luck Creek, and its elevation ranges from 1,061 m to 1,454 m with a northeast facing slope of 55%. From 1986 to 2015, over two third of precipitation was returned as streamflow (an average of 163 cm yr^{-1} streamflow vs. 229 cm yr^{-1} total precipitation). The average annual air temperature was 10.2 ºC with an average minimum of 5.9 ºC and an average maximum of 14.5 ºC (derived from USDA Forest Service Southern Research Station: https://www.srs.fs.usda.gov/coweeta/tools-and-data/ accessed 08/01/2020). Soils are deep sandy loams underlain by folded schist and gneiss. Under the uppermost true and biologically active soils consisting of Ultisols and Inceptisols, there is a porous, friable, and unconsolidated saprolite layer above bedrock, which is believed to

be a primary source of base flow, storm flow, and stream geochemistry (Velbel, 1988). Soil depth decreases with elevation with whole basin averaged soil depth around 3 meters (Swank & Crossley Jr., 1988). The dominant vegetation at both watersheds is southern mixed deciduous forests with overstory codominance by oaks (*Quercus*), maples (*Acer*), hickories (*Carya*) and tulip poplar (*Liriodendron tulipifera* L.) and an evergreen understory of rosebay rhododendron (*Rhododendron maximum* L.) and mountain laurel (*Kalmia latifolia* L.) (Day et al. 1988; Elliott & Swank, 2008).

These two watersheds have not been subject to human disturbances since the establishment of the experimental forest in 1934; however, they have experienced a variety of natural disturbances, including chestnut blight in the 1930s (Day & Monk, 1974; Elliott & Swank, 2008), fall cankerworm infestation in WS27 in the 1970s (Swank et al. 1981), extended drought in the 1980s (Elliott & Swank, 1994), and Hurricane Opal in 1995 (Elliott et al. 2002). In addition, the region has experienced increasing air temperature and extreme precipitation events over the years (Laseter et al. 2012).

2.2.2 Model description, inputs and calibration

PnET-BGC model has been applied, primarily in the northeastern region of the U.S., to study forest primary production, water and nitrogen cycling, hydrology, as well as soil and lake/stream acidification in response to acidic deposition, climate change, and disturbances (Gbondo-Tugbawa & Driscoll, 2002; Chen & Driscoll, 2004a; Chen & Driscoll, 2004b; Chen & Driscoll, 2005a; Chen & Driscoll, 2005b; Zhai et al. 2008; Wu & Driscoll, 2009, 2010; Zhou et al. 2015; Pourmokhtarian et al. 2016; Valipour et al. 2018; Robison & Scanlon, 2018). Recently the model has been applied to watershed in the mid and western U.S. (Niwot Ridge and Loch Vale Watershed, Colorado and The

H.J. Andrews Experimental Forest, Oregon, Dong et al. 2019). With the work presented herein, Coweeta Basin will be the southernmost U.S. region the PnET-BGC has been applied to. This model includes two major modules: 1) PnET, a module that simulates water, carbon, and nitrogen cycling, and 2) BGC, a module that includes vegetation and organic matter interactions of abiotic soil processes, solution speciation, and surface water process involving other major elements (Gbondo-Tugbawa et al. 2001). The main state variables simulated include primary productivity, transpiration, streamflow soil exchangeable cations, carbon and nitrogen mineralization, litter biomass, concentrations of sulfate, nitrate, potassium, calcium, magnesium, sodium and acid neutralization capacity (ANC) in stream at a monthly step. I applied variant of the model that accounts for the impact of CO_2 on primary productivity based on the results from the Duke University's Free-Air Carbon Dioxide Enrichment (FACE) project (Schlesinger et al. 2006) where gross primary productivity increases with atmospheric CO_2 concentration until 600 ppm. Increasing atmospheric CO_2 has two confounding effects that are depicted in this model: an increase in maximum photosynthetic rate (A_{max}) and a reduction in stomatal conductance (g_s). Stomatal conductance and photosynthesis are coupled (Jarvis & Davies, 1998; Ollinger et al. 2002; Ollinger et al. 2009). Stomatal conductance changes in proportion to difference between atmospheric CO_2 (C_a) and internal CO_2 (C_i) across the boundary of stomata. C_i is estimated from relatively constant C_i/C_a (Ollinger et al. 2009; $C_i/C_a \sim 0.7$ in Lavergne et al. 2019). The stomatal conductance and maximum photosynthetic rate are used to calculate CO_2 assimilation. Additionally, water use efficiency (WUE) is a function of CO_2 assimilation and vapor pressure (VPD), adjusted by C_i/C_a and increases in A_{max} (ΔA_{max}). When atmospheric CO_2 increases, A_{max} will

increase and g_s will decrease, which results in an increase of WUE. Plant transpiration is constrained by both ΔA_{max} and adjusted conductance (Delgs) when C_a is high and is calculated from gross primary productivity and WUE. I further modified the PnET-BGC model by adding a base flow component in order to obtain more accurate simulations of streamflow. The previous PnET-BGC model would return zero streamflow if there is no precipitation in that month, which is not consistent with the observed streamflow (such as December 2006 at WS18, and October 2000 at WS27). Based on observed non-zero streamflow when monthly precipitation was zero between 1936 and present, I added base flows of 0.6 cm/mo at WS18 and 0.9 cm/mo at WS27.

In order to run the PnET-BGC model, data of meteorology and atmospheric deposition of major elements are required as inputs (Table S2-1). Streamflow, vegetation productivity, soil and stream chemistry data are needed for model calibration. These data are described as follows.

Meteorological data: Meteorological inputs include monthly maximum and minimum air temperature (T_{max} and T_{min}, ^oC), photosynthetic active radiation (PAR) ($\mu mol \cdot m^{-2} \cdot s^{-1}$), and precipitation ($cm \cdot mo^{-1}$). The daily maximum and minimum temperature were available from 1985 (WS18) /1992 (WS27) to 2015 (https://www.srs.fs.usda.gov/coweeta/tools-and-data/, last accessed on 05/28/2020). The longer monthly time series of temperature was available at Climate Station 1 (CS01) in Coweeta (1935 – 2015). I derived a regression model based on monthly temperature measured at CS01 and at WS18/27 (WS18: 1985 to 2015, $R^2 = 0.90$ for maximum temperature: $T_{max\text{-}WS18} = 0.9968 \times T_{max\text{-}WS01} - 0.6957$ and $R^2 = 0.91$ for minimum temperature: $T_{min\text{-}WS18} = 1.0029 \times T_{min\text{-}WS01} + 1.8471$; WS27: 1992 to 2015, $R^2 = 0.96$ for

maximum temperature: $T_{max\text{-}WS27} = 1.0137 \times T_{max\text{-}WS01} - 6.1392$ and $R^2 = 0.96$ for minimum temperature: $T_{min\text{-}WS27} = 1.0091 \times T_{min\text{-}WS01} - 0.7467$). After deriving climate data from 1935 to 1985 or 1992 for WS18 and WS27 based on the regression models, the monthly means of maximum and minimum temperature from 1935 to 1985 or 1992 were used as the temperature inputs before 1935 at each watershed. The monthly averages from 2016 to 2100 in the base climate scenario were derived using monthly mean temperatures from 2006 to 2015 (Hansen et al. 2006).

Monthly precipitation was available from August 1936 to 2015 at WS18 and April 1958 to 2015 at WS27. I derived the average total precipitation values for each month and applied them before 1936 and to the base scenario in the future.

Measured PAR was available only for a limited period: May 2010 to December 2011 at WS18 and 27. In order to obtain a longer-term series of PAR, I applied the simulated solar radiation from 1980 to 2010 based on the Daily Surface Weather and Climatological Summaries (DayMET), I converted solar radiation to PAR using Eq. 1. (Both et al. 2002):

$$48.3 \text{ W m}^{-2} \text{ (solar radiation)} = 100 \text{ μmol m}^{-2} \text{ s}^{-1} \text{ (PAR)} \text{ - Eq. 1}$$

Then the monthly averages of PAR between 1980 and 2010 were used as inputs for the years before 1980 and after 2011 under the base climate scenario.

The climate change scenarios were statistically downscaled from four global atmosphere-ocean general circulation models (AOGCMs: CCSM4, HadGEM2, MIROC5, and MRI-CGCM3) with two representative concentration pathways (RCPs, RCP4.5 and RCP8.5). A Station-based Asynchronous Regional Regression Model was based on the long-term, and daily observed climate data collected from Coweeta WS18

(1982-2015) and WS27 (1992-2015) (Hayhoe et al. 2004; Hayhoe et al. 2007; Hayhoe et al. 2008; Pourmokhtarian et al. 2016). The spatial resolution of the AOGCMs (~100 km) is too coarse for WS18 or 27 because small watersheds in complex mountainous terrain are strongly affected by local weather patterns (Pourmokhtarian et al. 2012). The station-based technique generally returns higher precipitation projection than the Bias Correction-Spatial Disaggregation grid-based downscaling technique, another common downscaling approach (Pourmokhtarian, 2013). The RCP8.5 represents the most aggressive greenhouse gas (GHG) emission scenario. By 2100, the atmospheric CO_2 concentration is projected to be 1,370 ppm (Moss et al. 2010). RCP4.5 represents a scenario with some mitigation plans, and atmospheric CO_2 concentration is projected to reach 580 ppm in 2100. To simplify the study and follow atmospheric CO_2 trends between 1970 and 2020 (a linear increase from 330 to 403 ppm), I applied a linear extrapolation to derive annual predictions of atmospheric CO_2 concentrations from 2016 to 2100 as other studies have done (Kienast, 1991), based on the target CO_2 concentrations in 2100 in RCP4.5 and RCP8.5 and CO_2 concentration of 403 ppm in 2016. The predicted temperature and precipitation changes in all four seasons under climate change are similar between WS18 and 27 under each RCP scenario, except that the increase of precipitation under RCP8.5 at WS27 is predicted to be smaller than that at WS18, especially in spring and summer. RCP8.5 show higher temperature and precipitation increase than RCP4.5 and temperature kept increasing from past (1936-1965) to current (1986-2015) and then to future (2071-2100) while precipitation first decreased from past to current then increase in the future.

The wet and dry depositions of major elements (Na^+, Mg^{2+}, K^+, Ca^{2+}, NH_4^+, Cl^-, NO_3^-, and SO_4^{2-}) were obtained from National Atmospheric Deposition Program (NADP) (http://nadp.slh.wisc.edu/) and The Clear Air Status and Trend Network (CASTNET) (https://www.epa.gov/castnet) respectively. The closest NADP site to the Coweeta Basin is NC25 (35º03'36.1" N, 83º25'50.7"W, located within the Coweeta Basin, http://nadp.slh.wisc.edu/data/ntn/plots/ntntrends.html?siteID=NC25, accessed on 08/01/2020) and the wet deposition record is from July 1978 to 2015. For the dry deposition, the CASTNET COW137 station (35º03'36.1" N, 83º25'50.7"W), which is located at the same location as the NADP station, was used with the data available from November 1987 to 2015. Atmospheric deposition data before 1987 was reconstructed from national emission record from 1930 to 1978 and after 2015, and the relationship between emission and atmospheric deposition of SO_2 and NO_x between 1978 or 1987 and 2015 (USEPA, 2000; Driscoll et al. 2001; Chen et al. 2004b). From 1850 (pre-industrial) to 1930 when the emission data were not available, I assume a 50% increase of SO_2 and NO_x emission during this period and a linear increment was applied to reconstruct sulfur and nitrogen emissions and wet depositions from 1850 to 1930. After wet deposition data was fully constructed, the monthly average dry-to-wet-deposition-ratios derived from observed CASTNET and NADP data were used to reconstruct missing dry deposition data for the period outside the observations from the CASNET station. In addition to S and N (SO_4^{2-} and NO_3^-), other chemical constituents include NH_4^+, Ca^{2+}, Mg^{2+}, K^+, Na^+, and Cl^-. For these elements, re-construction of deposition data before and after the observed NADP record period, a 5-year averages of monthly values were applied (i.e., monthly deposition before 1978 and after 2015 was calculated using observation between

1979 and 1983). For those elements that are not measured through NADP (dissolved organic carbon - DOC, Al^{3+}, F^-, PO_4^{3-}, and Si), I used the input data in reference to previous work from the northeastern U.S (https://ctdrisco.expressions.syr.edu/pnet-bgc-model/ and accessed on 08/01/02020).

To calibrate the model, I applied data provided by the Coweeta Hydrologic Laboratory, including streamflow, steam concentrations of Na^+, Mg^{2+}, K^+, Ca^{2+}, Cl^-, NH_4^+, NO_3^-, and SO_4^{2-}. Other data used to calibrate different modules of the model included net primary productivity (NPP), net soil mineralization rates, and soil base saturation were available in the literature (Day & Monk, 1977; Knoepp & Swank, 1998; Knoepp et al. 2016) (Table S2-3).

To quantify how well model simulations matched the site observations, I applied normalized mean error (NME) and normalized mean absolute error (NMAE, Janssen & Heuberger, 1995). The NME (Eq. 2) provides the average prediction bias and NMAE (Eq. 3) indicates the absolute error between predicted and observed values. NME and NMAE closer to 0 indicates a better model fit.

$$NME = \frac{\bar{p} - \bar{o}}{\bar{o}} \quad \text{- Eq. 2}$$

$$NMAE = \frac{\sum_{t=1}^{n} (|p_t - o_t|)}{n\bar{o}} \quad \text{- Eq. 3}$$

Where p is model prediction and $\bar{p}$ is the mean of predictions; o is observation and $\bar{o}$ is the mean of observations, and n is the number of observations.

2.2.3 Principal component analysis (PCA)

To reduce the data dimensions of the many coupled vegetation-soil-stream processes analyzed, I applied principal component analyses based on 17 vegetation-hydrology-soil-stream variables simulated from 1931 to 2100 for each climate model under both RCP4.5 and 8.5 climate scenarios (i.e., totally 8 runs for each watershed) with the PCA analysis tool package 'FactoMineR' in R. The simulated variables are gross primary production (GPP), net primary production (NPP), total litter mass, streamflow, transpiration, soil base saturation, soil Al:Ca, net nitrogen mineralization, gross nitrogen mineralization, gross nitrogen immobilization, nitrogen uptake, concentrations of NO_3^-, SO_4^{2-}, Ca^{2+}, Mg^{2+}, and K^+, and the acid neutralizing capacity of streamwater (μeq/L). Note the application of PCA is for data dimension reduction and identification of important watershed process variables. Due to its exploratory nature, normality of the data is not a strict requirement (Vaughan & Ormerod, 2005; Jolliffe et al. 2016).

2.2.4 Seasonal analysis

I evaluated the changes of the ecological processes/states under changing climate for spring (March to May), summer (June to August), fall (September to November), and winter (December to February). I focused on the variables that had high correlations with Principal Component 1 and 2 and these include transpiration, GPP, NPP, soil base saturation, N mineralization, base cation (potassium and calcium) concentrations, ANC of stream. I subtracted the ecological conditions under current climate (1971-2000 or 1996-2015) from the predicted ecological conditions under different scenarios of climate change (2071-2100), and plotted probability density functions based on the differences. Based on these plots, I derived whether changes are mostly positive or negative by

determining the area under the curve to the right or left of zero (zero indicating no change).

2.2.5 Change-points detection and large climate variability

Identifying a change-point in the time series is the first step in identifying a potential driver of change, and, therefore a mechanism for a potential regime shift (Andersen et al. 2009), even though the existence of an abrupt change-point does not necessarily lead to instability and hysteresis or regime shift. To further investigate the impact pf climate change on watershed processes, I conducted change-point analyses in the time series (1931-2100) of PCA score means of the principal component 1 (PC1s) that explained the largest variance of the variables (Andersen et al. 2009), to identify the years when PC1s exhibited or will exhibit significant shifts, using the R-package of 'changepoint' (Killick & Eckley, 2014). I have selected the binary segmentation ('BinSeg' in R) method and checked for the normality between each change points (i.e., years) identified and they all met the normal distribution requirement (on annual basis). The same change point detection methods are used for the climate data between 1931 and 2100 with climate data after 2016 being the averaged output of four climate models for each RCP scenarios (RCP4.5 and 8.5). For both PC1s and climate data (1931 – 2100) change-points detection, I set up number of change-points from 3 to 10 in the program. However, the results did not change once the set-up reached 5.

At broad spatial scales, climate variability like *El Niño-Southern Oscillation* (*ENSO*) may enhance changes in temperature or precipitation (El Niño and La Niña Years and intensities at https://ggweather.com/enso/oni.htm and accessed on 08/01/2020). Accordingly, I expect to observe concurrence in change-points in both

climate and watersheds processes (represented by PC1s), and they may correspond to timing of strong ENSO events.

2.2.6 Threshold analysis

I ran the PnET-BGC model under different combinations (132 scenarios) in temperature increase from 0.5 to 6 ºC with a step increment of 0.5 ºC (12 scenarios), and in precipitation change from -50 to +50% of the current conditions with a step change of 10% (11 scenarios). I then evaluated the change in NPP (representing vegetation), transpiration (representing hydrology), and ANC (representing stream chemistry) to identify whether there existed threshold behaviors (abrupt change) of these three variables in response to changes in temperature and precipitation.

2.2.7 Hydrological extremes and acidification status

In addition to chronically changing average conditions, the extreme occurrence can impact the function of ecosystems. Extreme events are highly relevant to resource managers and the public as they incur greater societal consequences and costs (Grimm et al. 2013). As a result, increases in extreme events or shifts in seasonality have been considered in climate change mitigation plans and management strategies. In terms of extremes, I evaluated the streamflow extremes and the extreme acidic status in reference to critical chemical values in soil and streams.

Coweeta has experienced increasing droughts and heavy storms in the recent decades (Furniss et al., 2010), and the frequency of such extreme meteorological conditions is projected to increase further under changing climate. I conducted a flood and drought frequency analysis between 1931 and 2100. I fit a Generalized Pareto (GP) distribution to the observed streamflow above a set threshold (15 cm/mo for WS18 and

25 cm/mo for WS27) to analyze flood frequency using the extRemes package in R (Wu et al., 2012, Gilleland & Katz, 2016). To determine the flooding threshold, I used the 'mean residual life plot' that aims to find the lowest streamflow threshold that allows the thresholds vs. mean excess flow to be nearly linear and then I fit the GP distribution model over a range of thresholds (i.e., fit threshold ranges - GDP) to determine the final threshold (a graphical method to make selection of threshold above which the underlying GP shape parameter ξ to be approximately constant, Coles 2001). For drought frequency analysis, I used a truncation level (q_0, 30% quantile of observed streamflow, Engeland *et al*., 2004; Wu *et al*., 2012) which was determined to be 4.1 cm/mo for WS18 and 8.0 cm/mo for WS27.

To evaluate the acidification status of the Coweeta ecosystem, I compared the total months that soil base saturation (BS) and stream ANC are below the critical chemical values under changing climate compared to the current climate scenario. Soil BS and stream ANC values that are lower than critical values of acidification indicators suggest that soil or water body may be susceptible to detrimental effects from ongoing acidic deposition or legacy sulfur and nitrogen that has accumulated in soil from historical atmospheric deposition and may become mobilized following changes in soil conditions. These critical values that are used to calculate critical loads of sulfur and nitrogen inform air quality management goals. They include (1) the molar Al:Ca ratio of soil water of 1.0, or soil percent base saturation of 10% -20% to protect the acid-base status of soil and forest vegetation; and (2) pH of 6.0, ANC of 50/20/0 μeq/L, or Al of 2 μmol/L in stream to protect surface waters (Driscoll et al. 2001). Lower critical values of ANC (20/0 μeq/L) are used to protect against chronic acidification while higher critical

values are used to protect against episodic acidification (https://www.nrs.fs.fed.us/pubs/gtr/gtr_nrs71.pdf). I chose the critical limits of stream ANC and soil BS as 20 μeq/L and 10% to be protective of acidification stress. Values below these could result in detrimental effects.

2.3 Results

The key findings relevant to my research questions include: 1) The impacts of climate change on the forest ecosystem at Coweeta vary by season. There is not a particular season that will be impacted the most as this depends on the biogeochemical processes considered. 2) Five change-points have been found from 1930 to 2100 for PC1s, which explained 50-60% of the variance of the key biogeochemical processes/states, driven primarily by temperature or precipitation. 3) Net primary productivity, transpiration, and ANC show abrupt changes when precipitation decreases by 40% and temperature increases by 3 °C at the lower-elevation WS18, but the same threshold behavior does not show up at the higher-elevation WS27. 4) Drought and flooding will become more frequent under changing climate and the duration when soil and water chemistry (e.g., ANC and BS) are below the critical limits becomes longer with changing climate, indicating deterioration of ecosystem health with changing climate in terms of streamflow extremes and acidic status. 5) Vegetation seems to be impacted by climate change more at the higher-elevation WS27 than lower-elevation WS18, while soil and stream processes seem to be more impacted at WS18. Both WS27 and WS18 are sensitive to temperature increase, with greater sensitivity in WS27. WS18 is sensitive to precipitation when temperature increases by 3 °C and reduction of precipitation is larger than 40%, while WS27 is less sensitive to precipitation.

2.3.1 Climate change

For the two studied watersheds in the Coweeta Basin, observed air temperature increased from past (1936 – 1965) to current (1986 – 2015) and is projected to continue to increase between 2.5 and 4.8 ^{o}C from current to the future (2071 – 2100) on an annual basis (Fig. 2-1 and Table 2-1a). WS27 shows a slightly greater temperature increase than WS18 from current to the future, especially under RCP8.5 (+4.6 ^{o}C at WS18 vs. +4.8 ^{o}C at WS27). At WS18, spring and fall has larger temperature rise than summer and winter, while at WS27, summer is predicted to experience greater temperature increase in addition to spring and fall (Fig. 2-1a).

Observed precipitation showed a decrease in all the seasons with the exception of fall from past to current. However, precipitation is predicted to increase ranging from 2.2 to 4.0 cm/mo in all seasons in the future compared to current with the fall showing the smallest increment (Table 2-1). Both air temperature and precipitation in this basin follow the trend of regional climate projections for the southeast U.S. (IPCC, 2014). Noticeably, the temperature and precipitation in each season under changing climate scenario (2071-2100) is statistically significant different from those under current climate scenario (1986-2015) (Table 2-1b).

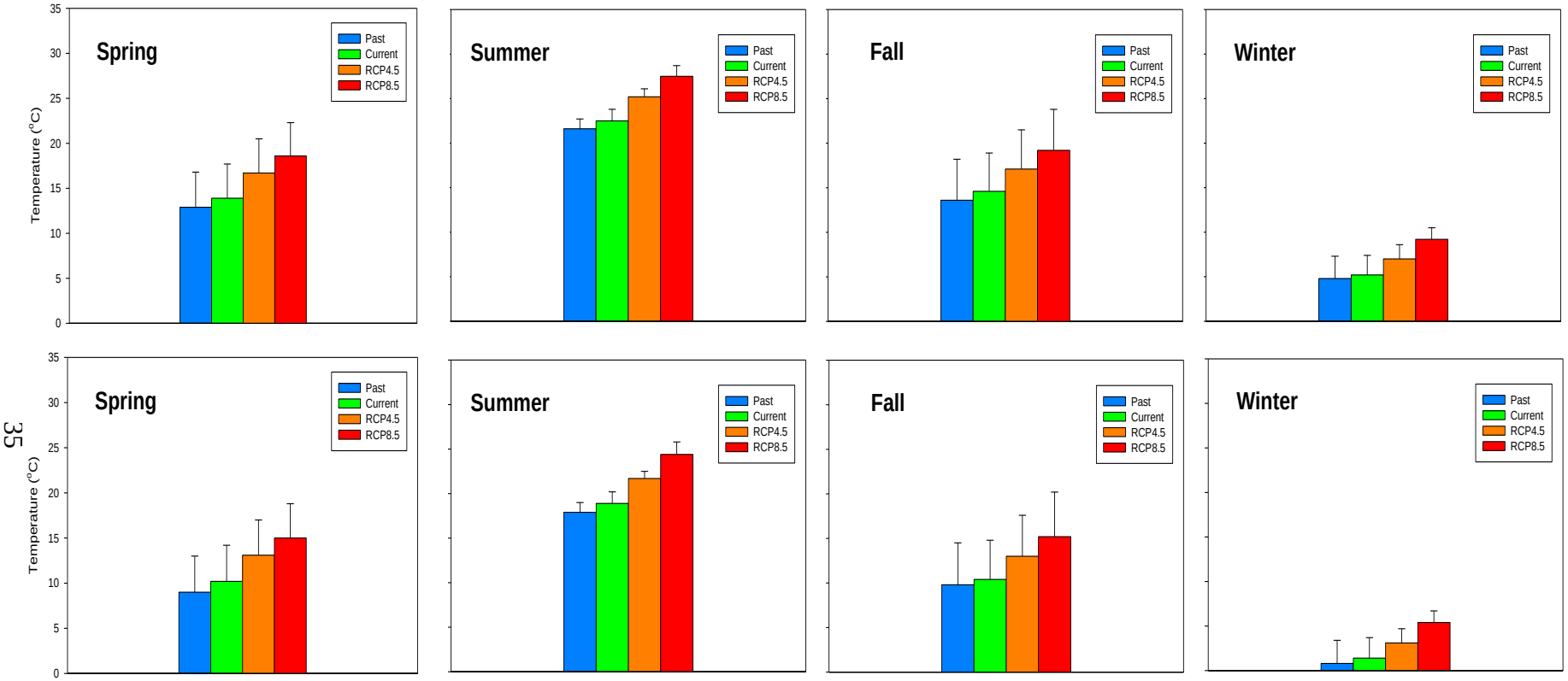

Fig. 2-1a Seasonal temperature comparison between past (1936–1965), current (1986–2015), and future (2071–2100) at Watershed 18 (top) and Watershed 27 (bottom); spring (Mar.–May), summer (Jun.–Aug.), fall (Sep.–Nov.), and winter (Dec.– Feb.).

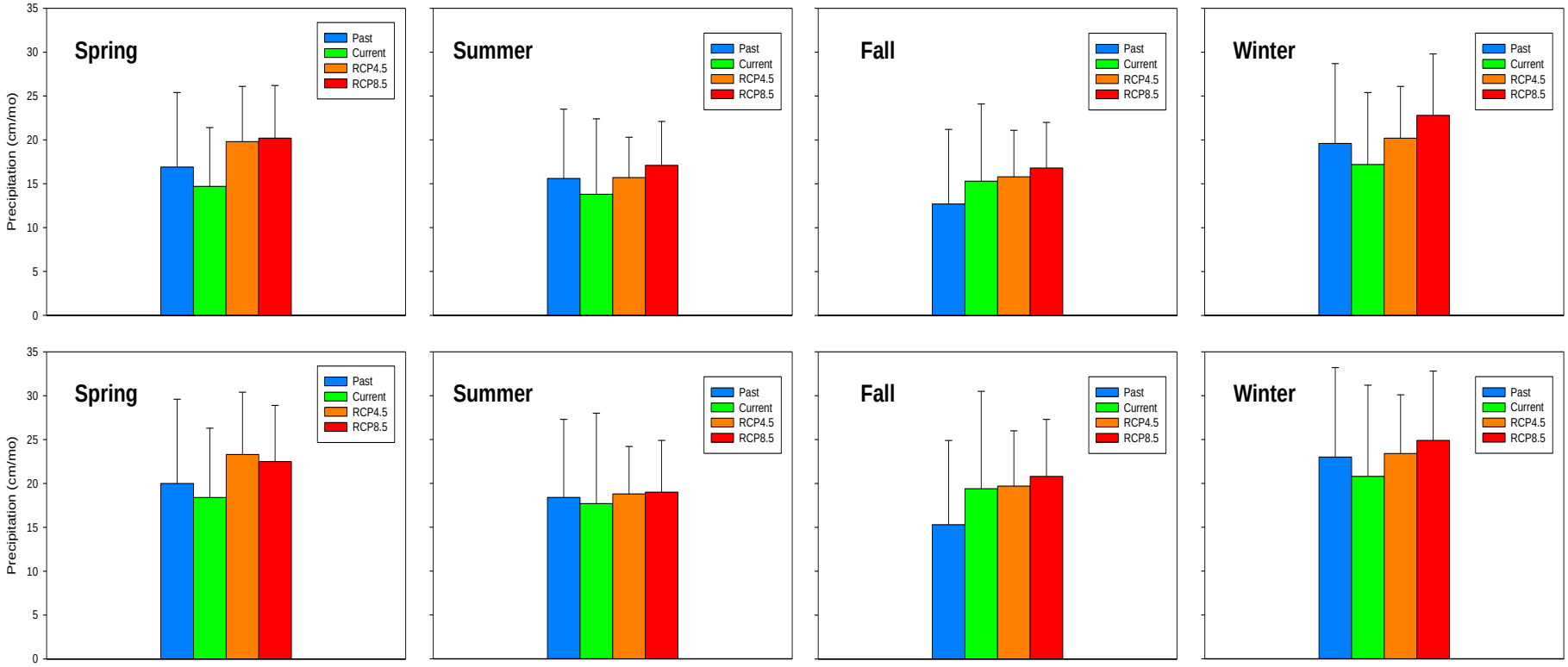

Fig. 2-1b Seasonal precipitation comparison between past (1936–1965), current (1986–2015), and future (2071–2100) at Watershed 18 (top) and Watershed 27 (bottom); spring (Mar.–May), summer (Jun.–Aug.), fall (Sep.–Nov.), and winter (Dec.–Feb.).

Table 2-1a. Seasonal temperature and precipitation in the past, current, and future (RCP4.5 and RCP8.5) at WS18 and WS27

		Spr	Sum	Fall	Win	Mean	Differ. [2]	Var.[3]
	Climate[1]				Temperature (°C)			
WS18	Past	12.9	21.6	13.6	4.8	13.2		
	Current	13.9	22.5	14.6	5.2	14.1	0.8*	
	RCP4.5	16.7	25.2	17.1	7.0	16.5	2.5^	0.5
	RCP8.5	18.6	27.5	19.2	9.2	18.6	4.6^	0.4
WS27	Past	9.0	17.9	9.8	0.8	9.4		
	Current	10.2	18.9	10.4	1.4	10.2	0.9*	
	RCP4.5	13.1	21.7	13.0	3.1	12.7	2.5^	0.5
	RCP8.5	15.0	24.4	15.2	5.4	15.0	4.8^	0.6
					Precipitation (cm/mo)			
WS18	Past	16.9	15.6	12.7	19.6	16.2		
	Current	14.7	13.8	15.3	17.2	15.3	-1.0*	
	RCP4.5	19.8	15.7	15.8	20.2	17.9	2.6^	1.9
	RCP8.5	20.2	17.1	16.8	22.8	19.2	4.0^	2.0
WS27	Past	20.0	18.4	15.3	23.0	19.2		
	Current	18.4	17.7	19.4	20.8	19.1	-0.1*	
	RCP4.5	23.3	18.8	19.7	23.4	21.3	2.2^	2.0
	RCP8.5	22.5	19.0	20.8	24.9	21.8	2.7^	1.6

Note: 1. Past climate refers to between 1936 and 1965, current climate between 1986 and 2015, and future climate between 2071 and 2100 from four GCMs under either RCP4.5 or RCP8.5 scenario; 2. "Differ" refers to mean of difference of climate between scenarios, either current climate minus past climate (*) or future climate minus current climate (^); 3. seasonal variability – variance of future climate minus current climate. Seasons: Spr – March to May, Sum – June to August, Fall – September to November, and Win – December to February.

Table 2-1b. Statistical test result of temperature and precipitation between current and changing climate scenarios

	TEMPERATURE							
	RCP4.5-Current				RCP8.5_Current			
	Spr	Sum	Fall	Win	Spr	Sum	Fall	Win
WS18	***	***	***	***	***	***	***	***
WS27	***	***	***	***	***	***	***	***
	PRECIPITATION							
WS18	***	**	-	-	***	***	*	-
WS27	***	**	-	-	***	***	-	-

Note: * indicates 0.01<p <0.05; ** indicates 0.001 < p <0.01; *** indicates p <0.001; and – indicates no significant difference has been detected. Color green means increasing from current to the future. In each season from 1986 to 2000 and from 2071 to 2100, monthly climate data were averaged first, then the 30 data points in each of the current and changing climate scenarios were checked for temporal autocorrelation ("acf" function in R) and normality (Shapiro test). As the checks show lack of temporal autocorrelation and met normality requirement, t-test was implemented to test whether the seasonal climate variables under current and changing climate scenarios were statistically significant different or not.

2.3.2 Model performance

The PnET-BGC model simulated well most of monthly and annual vegetation-soil-stream processes at both WS18 and WS27 from 1970s to 2014 (stream chemistry) or from 1930s/1940 to 2014 (streamflow), with NME ranging from -0.06 to 0.09 (Table 2-2). However, NO_3^- was underestimated at both WS18 and WS27 and SO_4^{2-} was overestimated at WS18. The model also underestimated the variance of NO_3^- and SO_4^{2-}. There was an unexplainable increasing concentration of SO_4^{2-} at WS18 between 1980s and 1990s, even though the atmospheric deposition of S continuously decreased during the same period after implementation of the Clean Air Act (1970) and Clean Air Act Amendments (1990) (US EPA: https://www.epa.gov/clean-air-act-overview/evolution-clean-air-act). The nitrogen cycle is more complex than other element cycles, and therefore, PnET-BGC simulation of stream NO_3^- involves larger uncertainties than other solutes (Fakhraei et al. 2017; Shao et al. 2020). In addition, contrary to a decrease in both observed nitrogen deposition and simulated nitrate leaching since the 1970s, both watersheds show an unexplainable increasing trend of observed nitrate concentration in streams, which helped to explain why the nitrate model simulation performance is poor.

In addition to the long-term observed streamflow and stream chemistry concentrations, our model simulations were consistent with other published data (Table S2-3), including net primary productivity (NPP), soil base saturation, and net nitrogen mineralization rate. Model simulated aboveground NPPs at WS18 and WS27 using the averages between 1971 and 1980 are close to published data from Day and Monk (1977) (8,056 vs. 7,965 kg/ha/yr). For net nitrogen mineralization, the ten-year averages (1971-1980) are 2.5 and 3.1 mg N/kg soil/mo at WS18 and WS27, which are within the range

reported by Knoepp and Swank (1998) based on the samples from an elevation gradient. The elevation over 1,000 m showed highest values. WS18 at the lower elevation has higher base saturation (BS) of 24.9% while the higher elevation WS27 has lower BS of 4.0% with simulated data from 2001 to 2010, Table S2-3, and this simulated range covers data obtained from USDA Forest Services in 2008 soil survey from 9.2 to 19.7%.

Table 2-2. Observed and simulated streamflow (unit: cm/month) and stream chemistry variables (unit: µmol/L) at WS18 and WS27

WS18	Observed		Simulated		Model Performance	
	mean	S.D.*	mean	S.D.	NME	NMAE
Na^+	40.4	2.0	41.6	2.2	-0.02	0.08
Mg^{2+}	12.4	0.6	11.5	0.7	0.01	0.09
K^+	11.3	0.9	10.7	0.4	0.01	0.08
Ca^{2+}	15.7	1.0	16.4	0.8	0.002	0.08
Cl^-	14.6	0.6	16.0	2.2	0.000	0.12
NO_3^-_N	0.8	0.5	0.3	0.2	-0.65	0.74
SO_4^{2-}_S	4.7	1.2	6.0	0.5	0.30	0.38
ANC	83.7	5.7	80.6	5.2	-0.04	0.08
Streamflow	8.2	2.5	9.0	2.3	0.09	0.15

WS27	Observed		Simulated		Model Performance	
	mean	S.D.	mean	S.D.	NME	NMAE
Na^+	22.1	1.6	22.3	2.0	-0.02	0.09
Mg^{2+}	8.4	0.6	8.7	0.7	-0.03	0.08
K^+	5.8	0.7	5.6	0.1	-0.04	0.09
Ca^{2+}	8.9	0.9	8.4	0.5	-0.06	0.08
Cl^-	13.2	1.4	13.5	1.8	-0.02	0.08
NO_3^-_N	2.3	1.1	1.1	0.9	-0.50	0.69
SO_4^{2-}_S	11.8	1.6	11.3	1.1	-0.05	0.13
ANC**	23.6	2.5	25.3	4.0	0.07	0.13
Streamflow	14.1	3.3	14.0	3.0	-0.003	0.06

* S.D. denotes standard deviation.
** ANC denotes acidic neutralization capacity (Driscoll et al., 1994)
Note: The water chemistry data ranged from 1972 to 2014 (ANC from 1973 to 2014), streamflow ranged from 1936 to 2015 at WS18, and from 1947 to 2015 at WS27.

2.3.3 PCA analysis

The PCA analysis indicated that the first three principal components explained ~ 85% of variance of the 17 variables analyzed (Table 2-3 and Table 2-4). Particularly, PC1 explained 63.2% and 68.8% of total variances under RCP4.5 and RCP8.5 respectively at WS 18. PC1s explained 50.6% and 57.1% of variances under RCP4.5 and RCP8.5 respectively at WS 27. Based on the loadings of the principal components, PC1s represent the contrast between primary production and transpiration vs. soil and stream alkalinity, and the second principal components (PC2s) depict nitrogen mineralization rate. The third principal components (PC3s) represent the concentrations of sulfate in stream at WS18 under RCP4.5 and at WS27 under both RCP4.5 and RCP8.5, while the PC3 at WS18 under RCP8.5 represents streamflow.

Table 2-3. Results of PCA analysis - loadings of the first three principal components at WS18 and WS27 under different climate change scenarios. (The high loading values are highlighted).

	WS18			WS27		
RCP4.5	Comp 1	Comp 2	Comp 3	Comp 1	Comp 2	Comp 3
GPP	0.98	-0.07	0.02	0.94	-0.18	0.15
NPP	0.96	-0.10	0.04	0.93	-0.18	0.13
TotLitterMass	-0.49	0.26	-0.26	0.48	0.04	0.18
Streamflow	-0.21	-0.29	0.67	-0.02	-0.36	0.01
Transpiration	0.93	0.10	-0.06	0.87	-0.14	0.25
Base Saturation	-0.97	0.05	0.06	-0.93	0.03	0.35
Al/Ca	0.97	-0.02	0.04	0.93	0.01	-0.34
NetNMin	0.75	-0.62	0.03	0.27	0.80	0.48
GrossNMin	-0.01	-0.97	-0.02	0.56	0.74	0.34
GrossNImmob	-0.83	-0.46	-0.06	0.76	0.57	0.14
N_uptake	0.79	-0.57	0.05	0.68	0.60	0.36
ANC	-0.92	-0.21	0.28	-0.74	-0.16	0.60
NO_3^-	-0.75	0.07	-0.16	-0.80	-0.04	0.43
SO_4^{2-}	-0.07	-0.44	-0.75	0.11	0.55	-0.81
Ca^{2+}	-0.96	-0.19	-0.13	-0.88	0.45	0.01
Mg^{2+}	-0.89	-0.10	0.11	-0.63	0.68	-0.10
K^+	-0.94	-0.30	0.02	-0.60	0.66	-0.38
Cumulative Variance (%)	63.2	77.4	84.6	50.6	71.3	84.3

	WS18			WS27		
RCP8.5	Comp 1	Comp 2	Comp 3	Comp 1	Comp 2	Comp 3
GPP	0.96	-0.15	0.02	0.97	-0.15	0.03
NPP	0.91	-0.22	0.02	0.94	-0.10	0.00
TotLitterMass	-0.74	-0.00	0.21	-0.05	0.45	0.21
Streamflow	-0.02	-0.02	-0.91	0.19	-0.42	-0.14
Transpiration	0.95	0.07	0.14	0.91	-0.15	0.17
Base Saturation	-0.97	0.10	-0.04	-0.93	-0.12	0.33
Al/Ca	0.98	0.01	-0.00	0.94	0.07	-0.27
NetNMin	0.82	-0.50	-0.12	0.71	0.28	0.57
GrossNMin	-0.28	-0.92	-0.09	0.68	0.53	0.46
GrossNImmob	-0.88	-0.40	0.02	0.51	0.72	0.25
N_uptake	0.86	-0.44	-0.13	0.89	0.17	0.36
ANC	-0.94	-0.06	-0.27	-0.78	-0.32	0.49
NO_3^-	-0.78	0.13	0.07	-0.77	-0.26	0.43
SO_4^{2-}	-0.35	-0.58	0.43	-0.10	0.75	-0.61
Ca^{2+}	-0.98	-0.18	0.02	-0.93	0.33	0.12
Mg^{2+}	-0.92	0.02	-0.01	-0.77	0.51	0.11
K^+	-0.96	-0.23	-0.09	-0.77	0.58	-0.14
Cumulative Variance (%)	68.8	80.4	87.5	57.1	73.7	84.5

Table 2-4. Results of PCA analysis – eigenvalues (EV) of 17 watershed processes variables (data from 1931 to 2100) at WS18 and WS27 under different climate change scenarios

WS18	RCP4.5 EV	% of Variance	Cumulative % of variance	RCP8.5 EV	% of Variance	Cumulative % of variance
comp 1	10.7	63.2	63.2	11.7	68.8	68.8
comp 2	2.4	14.3	77.4	2.0	11.6	80.4
comp 3	1.2	7.2	84.6	1.2	7.1	87.5
comp 4	0.9	5.3	89.9	0.7	4.3	91.8
comp 5	0.7	4.3	94.2	0.5	2.9	94.7
comp 6	0.5	2.7	96.9	0.3	2.0	96.8
comp 7	0.2	1.2	98.1	0.3	1.7	98.5
comp 8	0.1	0.8	98.9	0.1	0.7	99.1
comp 9	0.1	0.5	99.4	0.1	0.5	99.6
comp 10	0.1	0.4	99.8	0.0	0.2	99.8
comp 11	0.03	0.17	99.9	0.0	0.1	99.9
comp 12	0.01	0.03	100	0.00	0.02	100
comp 13	0.00	0.02	100	0.00	0.01	100
comp 14	0.00	0.02	100	0.00	0.01	100
comp 15	0.00	0.01	100	0.00	0.01	100
comp 16	0.00	0.00	100	0.00	0.00	100
comp 17	0.00	0.00	100	0.00	0.00	100

WS27	RCP4.5 EV	% of Variance	Cumulative % of variance	RCP8.5 EV	% of Variance	Cumulative % of variance
comp 1	8.6	50.6	50.6	9.7	57.1	57.1
comp 2	3.5	20.6	71.3	2.8	16.6	73.7
comp 3	2.2	13.1	84.3	1.8	10.9	84.5
comp 4	1.2	7.2	91.5	1.0	5.8	90.3
comp 5	0.7	4.2	95.7	0.9	5.0	95.4
comp 6	0.3	1.5	97.2	0.3	1.8	97.2
comp 7	0.2	0.9	98.1	0.2	1.3	98.4
comp 8	0.1	0.7	98.8	0.1	0.7	99.1
comp 9	0.1	0.5	99.3	0.1	0.4	99.5
comp 10	0.0	0.2	99.6	0.0	0.2	99.7
comp 11	0.0	0.2	99.8	0.0	0.2	99.9
comp 12	0.02	0.14	99.9	0.01	0.08	99.9
comp 13	0.01	0.05	100	0.00	0.03	100
comp 14	0.01	0.03	100	0.00	0.02	100
comp 15	0.00	0.01	100	0.00	0.01	100
comp 16	0.00	0.00	100	0.00	0.01	100
comp 17	0.00	0.00	100	0.00	0.00	100

2.3.4 Seasonal variability

Based on the PCA analysis, my evaluation of the impacts of climate change on watersheds of Coweeta focused on the processes with high correlations with PC1s and PC2s in different seasons. Particularly I only included the figures of seasonal changes of transpiration, NPP, and stream ANC in the main text. The figures for other processes variables are described in Appendix Figure (Fig. S2-1 to Fig. S2-7).

For both watersheds, transpiration (Fig. 2-2) is projected to increase under changing climate. However, the increase in transpiration at WS18 is smaller than WS27, probably due to higher water stress. Even though transpiration increases, annual streamflow (Fig. S2-1) under future climate is projected to increase with increasing precipitation (26.8% and 32.7% at WS18 under RCP4.5 and 8.5; 11.9% and 14.7% for WS27 under RCP4.5 and 8.5, respectively). Seasonally, streamflow tends to decrease in fall and winter at WS18. While at WS27, streamflow tends to decrease in summer and fall.

The simulated impact of climate change on GPP is not as dramatic as for the water cycle (Fig. S2-2). However, it shows increases in summer under RCP4.5, but the direction of the change (i.e., decrease or increase) in summer with RCP8.5 depends on the climate model considered. The increase of GPP at WS27 is more dramatic, especially in summer and winter. Overall, annual GPP is projected to increase due to the extended growing season (2071-2100 compared to 1986-2015: increase by 13.8% and 17.9% for WS18, and 26.9% and 43.0% for WS27 under RCP4.5 and 8.5 scenarios, respectively). The simulated impact of climate change on NPP is moderate (Fig. 2-3). On an annual basis, NPP is projected to increase although summer shows strong decreases due to

increases in respiration. Under RCP8.5, NPP shows some decrease in summer and larger variance in winter, with some high values. During summer, NPP is lowered in WS18 as much as 43.2 g biomass/m^2/mo or 23.1% under RCP8.5. For WS27, NPP increases somewhat during all seasons under RCP4.5. With RCP8.5, NPP shows decrease during summer. NPP is projected to increase to a greater degree in WS27 than WS18 due to less water stress associated with temperature increase.

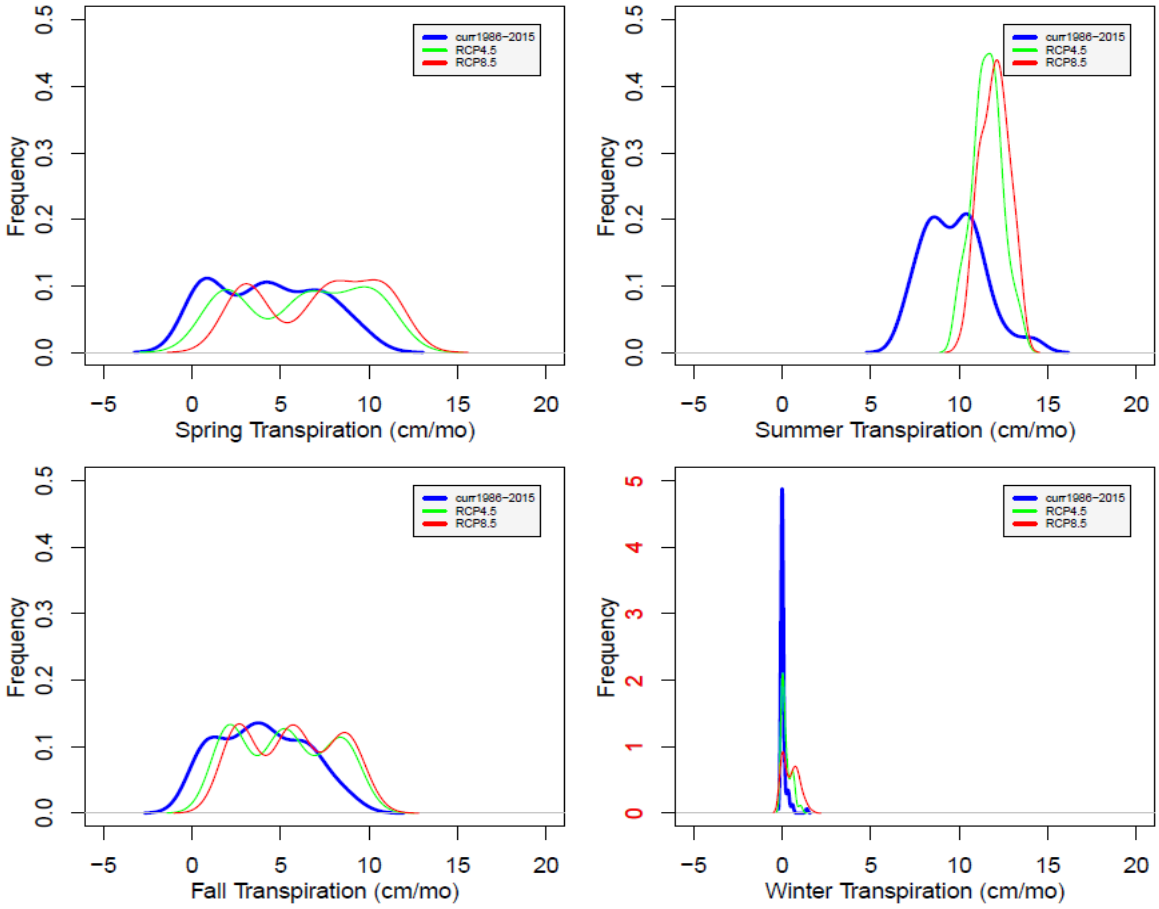

Fig. 2-2a Transpiration at WS18 under future climate compared to current by seasons. Current (blue), RCP4.5 (green), and RCP8.5 (red), and hereafter the same.

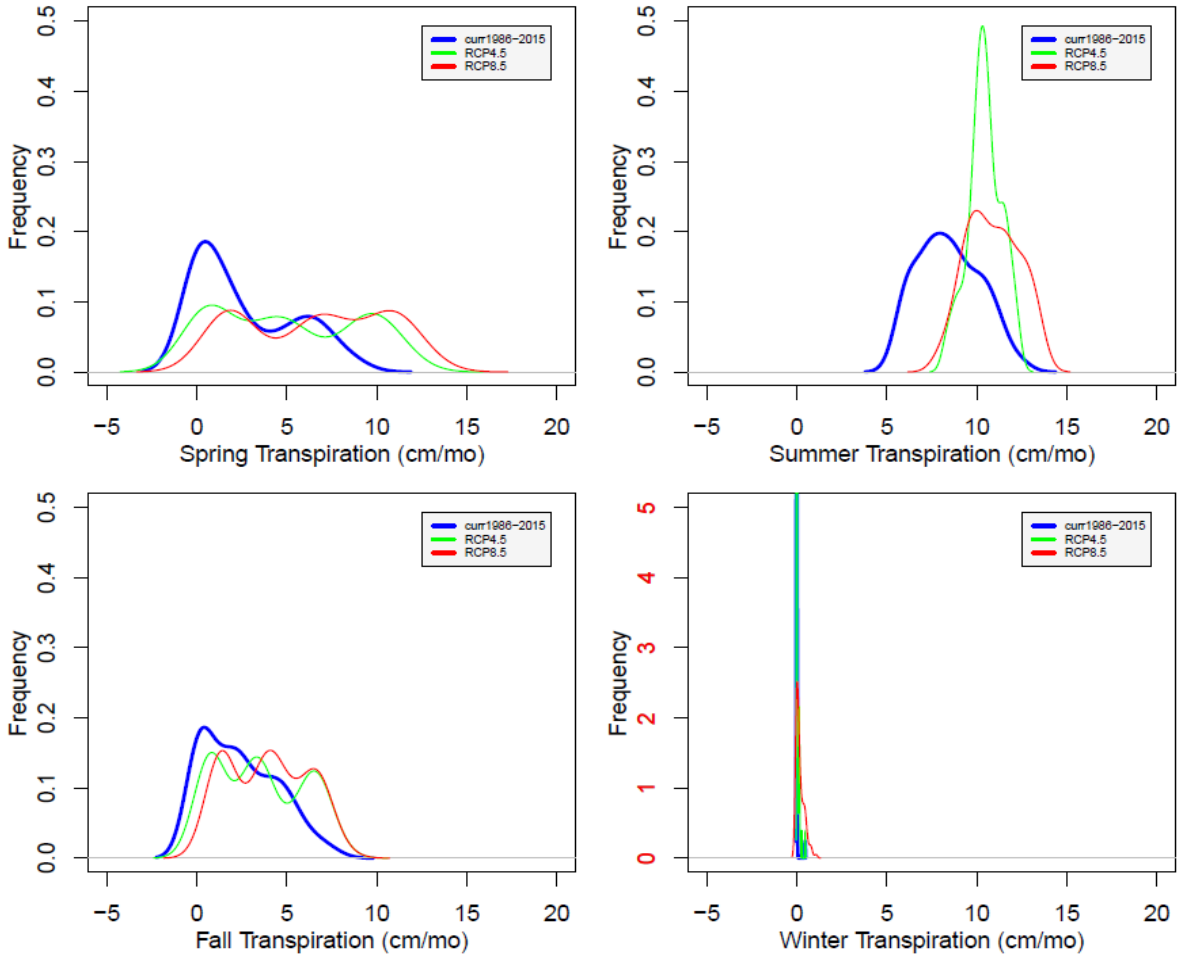

Fig. 2-2b Transpiration at WS27 under future climate compared to current by seasons.

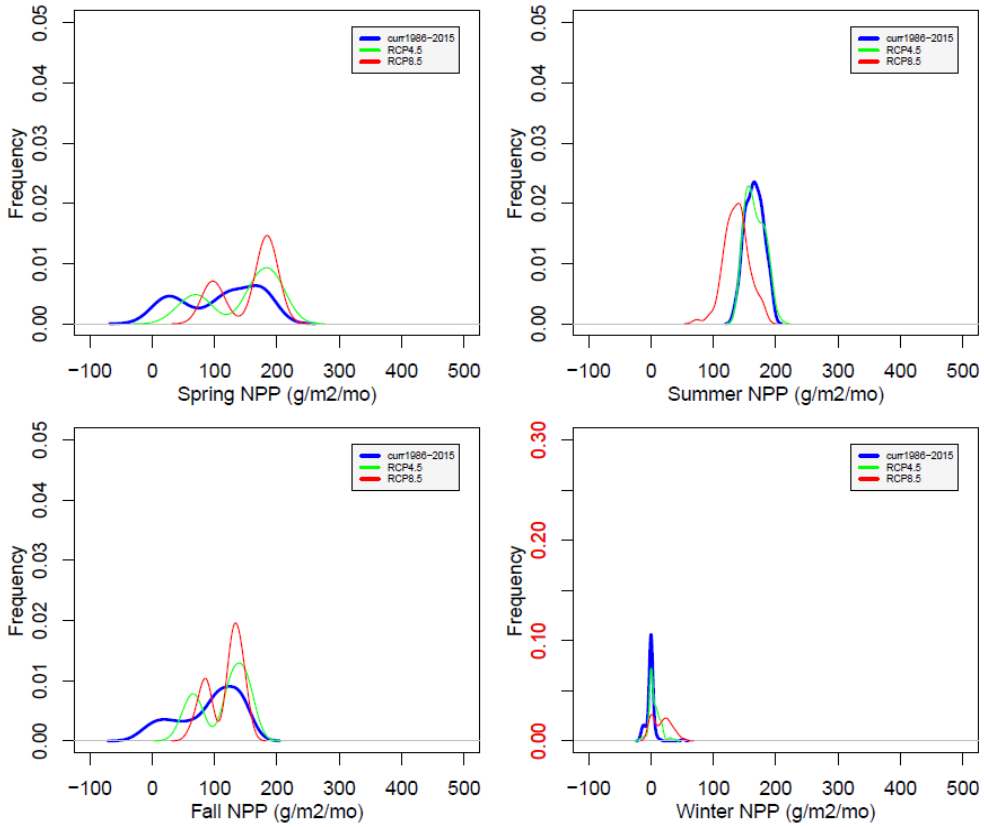

Fig. 2-3a NPP at WS18 under future climate compared to current by seasons.

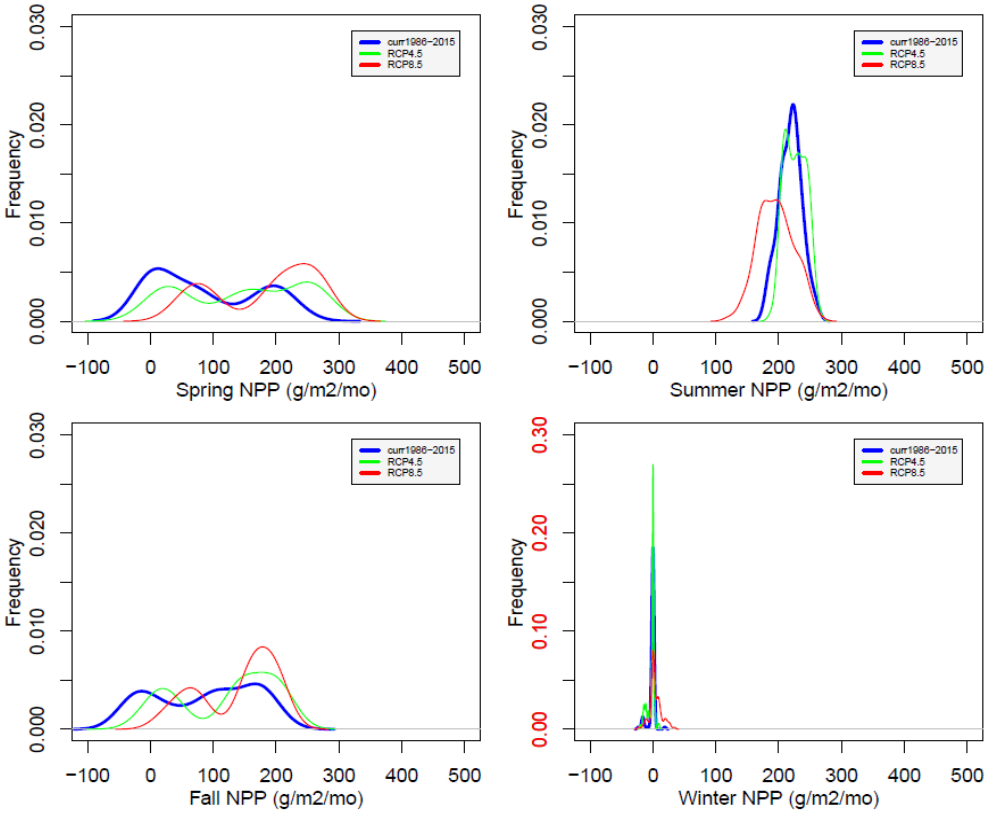

Fig. 2-3b NPP at WS27 under future climate compared to current by seasons.

Stream ANC is projected to decrease during all seasons under future climate with the largest decrease in summer and the smallest during winter at WS18 (Fig. 2-4). The variance in ANC largely increases during summer and fall at WS18, demonstrating that extremely low ANC values will become more frequent. The impact of climate change on stream ANC is minimal at WS27, with small decreases under RCP8.5.

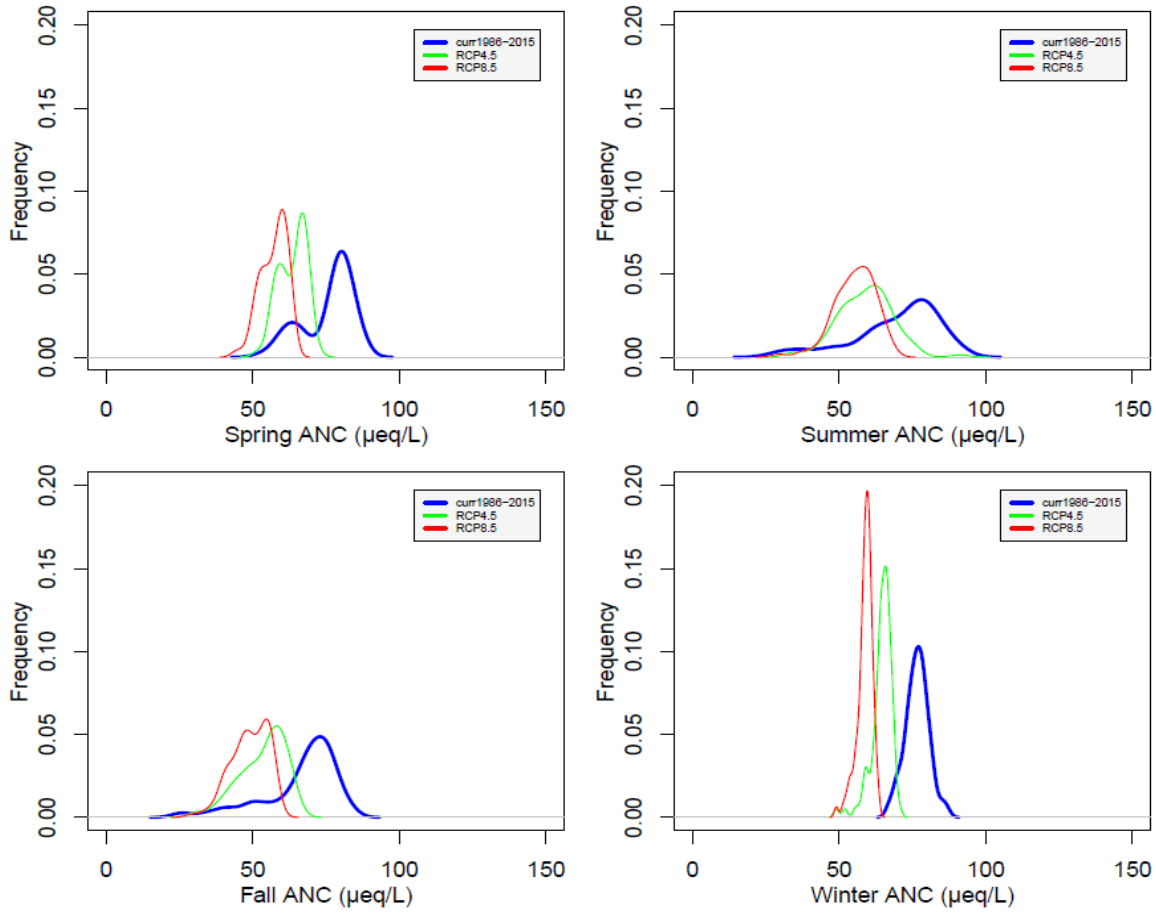

Fig. 2-4a ANC at WS18 under future climate compared to current by seasons.

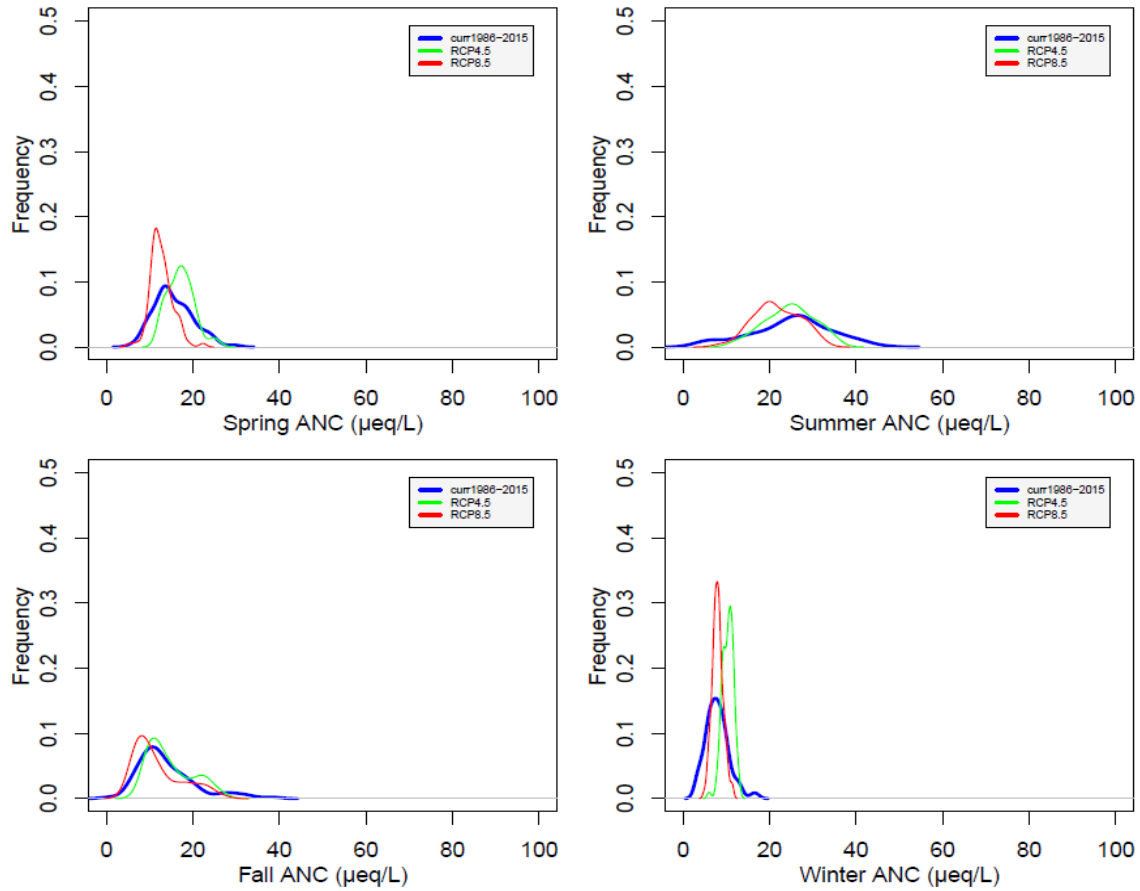

Fig. 2-4b ANC at WS27 under future climate compared to current by seasons.

Under climate change, the most conservative element, Cl^-, as well as basic cations (Na^+, K^+, Ca^{2+}, and Mg^{2+}) and SO_4^{2-} exhibited decreases in concentration but increases in total flux as streamflow increases. The increased flux of the base cations in soil is mainly due to release from wood litter. Calcium concentration (Fig. S2-3) in stream decreases dramatically in all seasons at WS18. A similar decrease is also evident in WS27, but not as marked. Potassium concentrations decrease (Fig. S2-4) in stream water during all seasons at WS18 with the most distinct change occurring in winter and spring. Decreases in potassium are also evident at WS27 with all seasons showing similar trends. Potassium and calcium showed clear seasonal changes with streamflow variations (higher

concentration in late spring through early autumn and lower concentration during winter). Sulfate concentration (Fig. S2-5) in stream water decreases in both watersheds, especially in winter under RCP8.5 and with lower values than projected under RCP4.5. Compared to conditions under current climate, future sulfate concentration will be less varied in WS27 but showing greater decrease than WS18. WS18 has the highest (median) sulfate concentration in summer while in WS27, the highest concentrations occur in fall and winter.

Soil base saturation (Fig. S2-6) shows decreases during all the seasons at both watersheds under RCP4.5 and 8.5. Decreases are significant under both climate scenarios in WS18, but only marginal under RCP8.5 in WS27. Al:Ca in soil shows a significant increase in all the seasons, but increases are most pronounced during summer, at WS18 under RCP4.5 and 8.5. Al:Ca in soil increases particularly during summer in WS27 as well, but significant increases are only for some climate models (CCSM4 and HadGEM2) under RCP8.5.

The simulated impact of climate change on N mineralization is small (Fig. S2-7). In WS18 under RCP8.5, the N mineralization rate shows some decrease. At WS27, the mineralization shows some decrease in winter with RCP4.5 and during summer and winter under RCP8.5

Overall, the response of individual forest processes to climate change varies by season. Furthermore, vegetation seems to be more sensitive to climate change at WS27 than WS18, while soil processes and stream chemistry seem to be more impacted by climate change at WS18 than WS27.

2.3.5 Temporal trend of biogeochemical processes and change-points

From the time series of the scores of the PC1s that explained more than 50% of the total variances, I derived five similar decadal change-points for WS 18 and 27 (Table 2-5, Fig. 2-5). The change-points were earlier at WS18 than at WS27 during 1980s and 2010s but are projected to occur at similar time points or even earlier at WS 27 relative to WS18 under future changing climate, implying accelerated changes of biogeochemical processes at the higher-elevation WS27 site. The last change-points are predicted to occur 20 years earlier and showing a more marked response under RCP8.5 compared to those under RCP4.5 at the lower- and higher-elevation forests.

When I compared the change-points of temperature and precipitation to those of PC1, I found the first few change-points of PC1 matched those of temperature at WS18, showing temperature is the main driver of watershed response (Table 2-5, Fig. S2-8). However, precipitation is the main driver for the change-point of PC1 in 2079 at WS18. Precipitation is likely to be the main driver for the change-points in 2010s and the 2070s, while temperature is the main driver for the change-point in 2030s and around 2060. Both precipitation and temperature are important for the change-point in 1989, and the driver is not clear for the change-point in 2069.

Table 2-5. Change-points of the scores of the first principal components (PC1s) s and climate (temperature and precipitation)

			CP1*	**CP2**		**CP3**	**CP4**	**CP5**
WS18	PC1-RCP4.5	—	1981	2010	—	2039	—	2079
	PC1-RCP8.5	—	1985	2010	2023	2039	2059	—
	Temperature-RCP4.5	—	1984	—	2023	—	—	—
	Temperature-RCP8.5	—	—	2010	—	2038	2067	—
	Precipitation-RCP4.5	—	—	—	—	—	—	2076
	Precipitation-RCP8.5	—	—	—	—	2043	—	2081
WS27	PC1-RCP4.5	1969	1989	2015	—	2038	—	2074
	PC1-RCP8.5	1969	1989	2017	—	—	2059	—
	Temperature-RCP4.5	—	1989	—	—	2038	—	—
	Temperature-RCP8.5	—	1997	—	—	2038	2067	—
	Precipitation-RCP4.5	—	1998	2012	—	—	—	2076
	Precipitation-RCP8.5	—	1998	2012	—	—	—	2081

Note: where the results are average of four climate models for two future climate scenarios; and (*) indicates that only those years that were within the same decade and at both watersheds were identified as the changing point in PC1

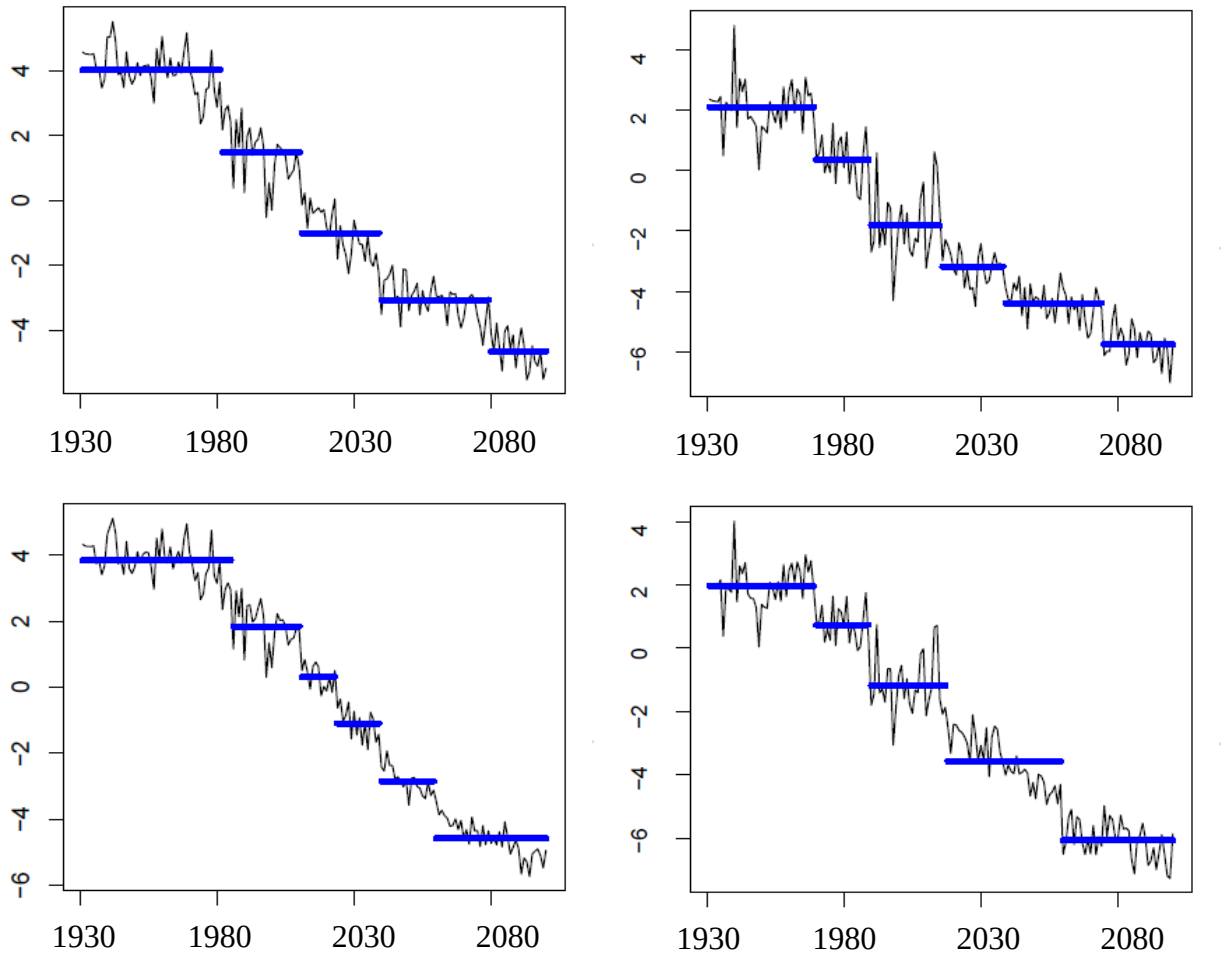

Fig. 2-5 PC1 change-points at WS18 and WS27 (top left – WS18 RCP4.5, bottom left – WS18 RCP8.5, top right – WS27 RCP4.5, and bottom right – WS27 RCP8.5)

2.3.6 Thresholds of temperature and precipitation driving ecosystem change

I further studied the potential thresholds of temperature or precipitation that could drive the shift of three processes with large loadings in PC1 representing vegetation – net primary productivity (NPP), hydrology – transpiration, and stream chemistry – stream acid neutralizing capacity (ANC) respectively.

At WS18, NPP increases with temperature initially and then decreases following temperature increases of more than 1 ºC (Fig. 2-6). The decrease is especially dramatic under a 40% decrease in precipitation and temperature increases larger than 3 ºC. Decreases in precipitation do not have as large an impact on NPP at WS27 as WS18. NPP increases with temperature until temperature increase reaches 5 ºC at WS27.

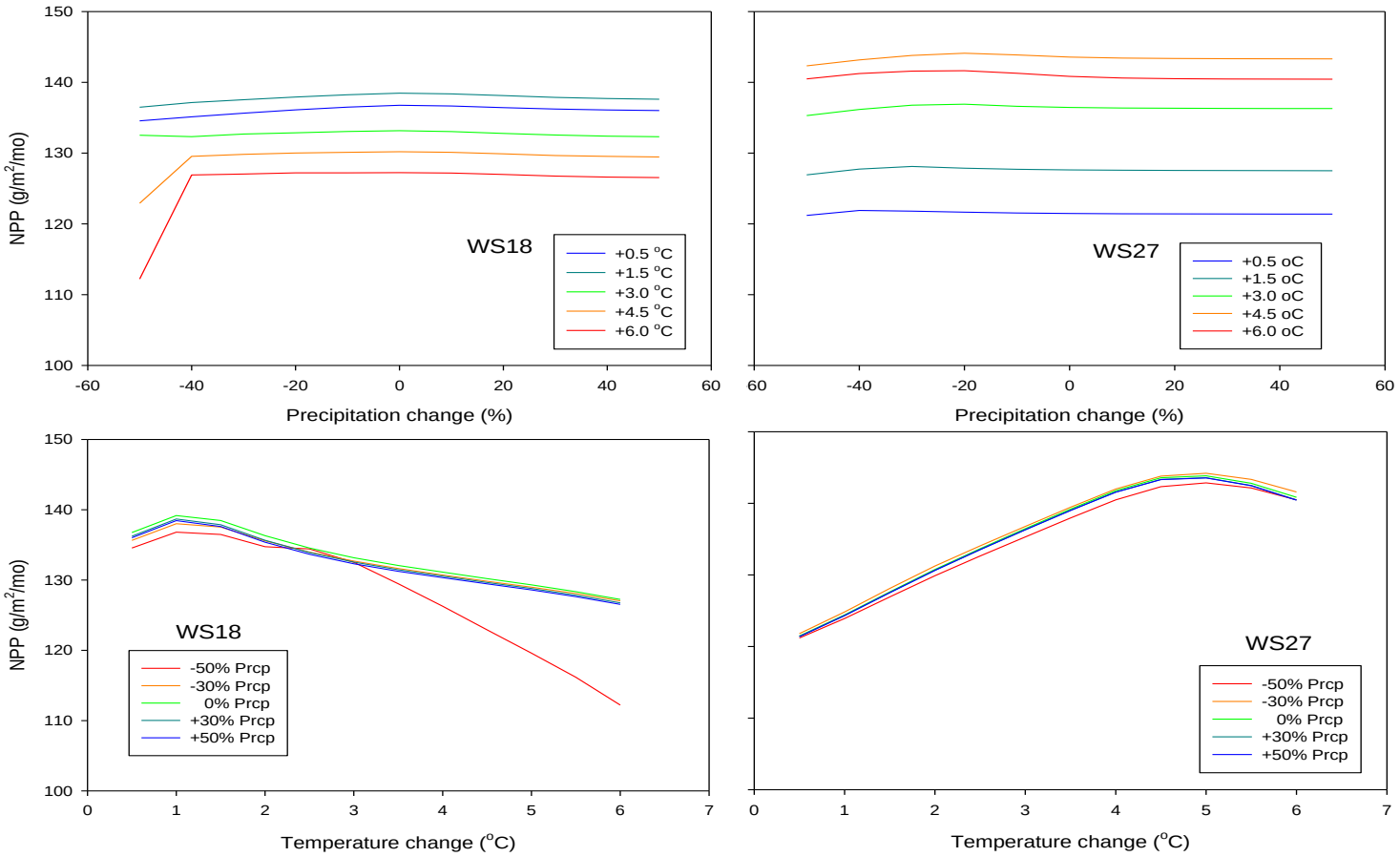

Fig. 2-6 Threshold of temperature (top) and precipitation (bottom) change impact to NPP (2016-2100) at WS18 (left) and WS27 (right)

At WS18, transpiration increases with temperature except when precipitation is reduced by 40% or more (Fig. 2-7). When the temperature increase is greater than 3 ºC, decreases in precipitation of 40% or more will reduce transpiration. At WS27, transpiration increases with temperature and unlike WS18 water is not limited.

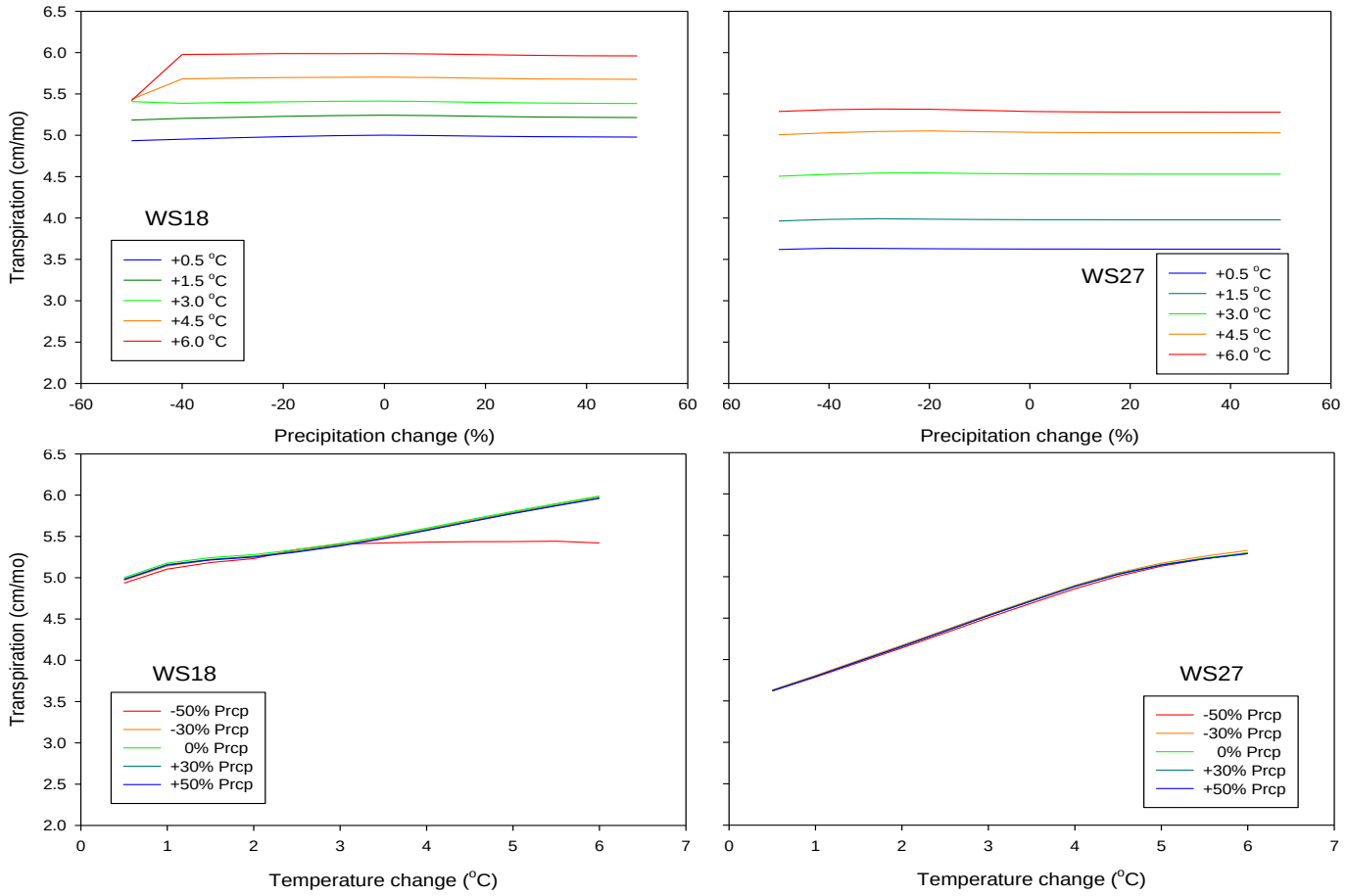

Fig. 2-7 Threshold of temperature (top) and precipitation (bottom) change impact to Transpiration (2016-2100)

The response of stream ANC to changes temperature and precipitation associated with changing climate is more complex (Fig. 2-8). At WS18, ANC decreases with increases in temperature and the decrease is particularly pronounced when precipitation experiences a 40% reduction. Similarly, at WS27, ANC slowly decreases with increases in temperature when precipitation experiences a 40% reduction or more.

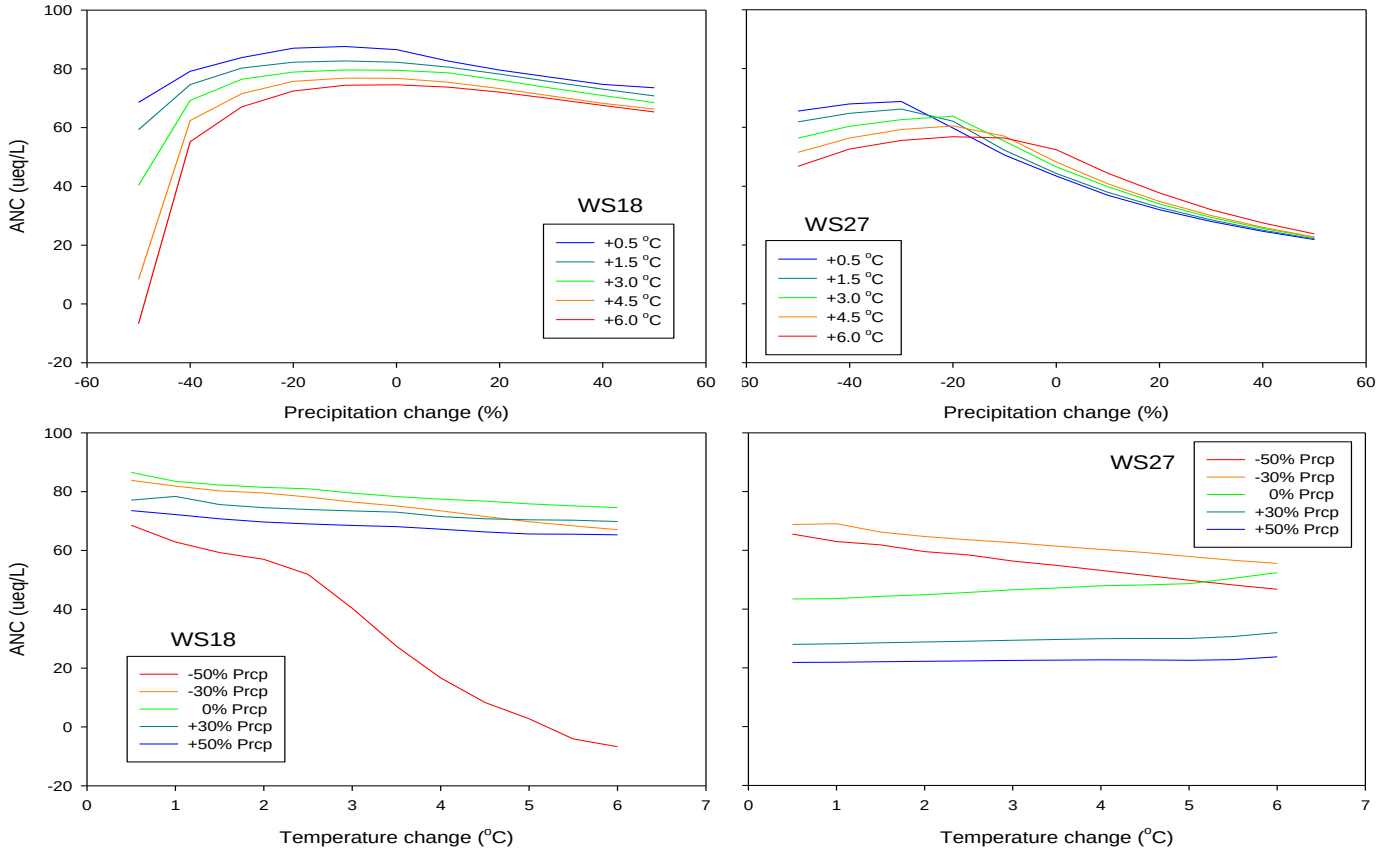

Fig. 2-8 Threshold of temperature (top) and precipitation (bottom) change impact to ANC (2016-2100) at WS18 (left) and WS27 (right)

Overall, WS18 is affected by both precipitation and temperature while WS27 is more impacted by temperature due to its relatively abundant precipitation supply. At WS27, NPP and transpiration are impacted by temperature, with response greater than simulated for WS18. Stream ANC responds to both changes in temperature and precipitation. In addition, simulations suggest smooth changes in NPP, transpiration and ANC at WS27, while threshold behavior occurs in WS18 when temperature increases above 3 °C and precipitation is reduced by 40%.

2.3.7 Extremes in streamflow and acidic conditions

Compared to current climate (1986-2015), the total number of months that ANC is above the critical limit of 20 μeq/L are projected to decrease under future changing climate scenario (Table 2-6). In addition, it is found that the duration is even shorter with RCP8.5 than with RCP4.5. The exception is RCP4.5 at WS27. For the base saturation (BS), the WS27 has lower BS than WS18 as the pH in soil solution is lower at the higher elevation (Table 2-6). BS at WS27 never exceeds 10% under both current and changing climate scenarios. At WS18, the number of months when BS exceeds 10% becomes less under changing climate scenarios than the current climate condition. The analysis of stream ANC and soil BS indicate soil and water will become more acidic, which will affect biota in the ecosystems further (Maaroufi & De Long 2020).

By comparing the current (1986 to 2015) to future (2071 to 2100) scenarios, I found that both the duration and frequency of flooding and drought are predicted to increase (Table 2-7 & 2-8). The return levels (defined as 'the m-year *return level* as the *streamflow* for which the expected number of events in an m year period is one' Cooley, 2013) at the same return periods under future climate conditions are much

greater than under the current climate scenario. For instance, for current climate, the 50-year streamflow return levels are 34.6 and 54.8 cm/mo for WS18 and WS27 (Table 2-8). However, the same streamflow will become as frequent as 5-year event or 10-year event for WS18 and WS27, respectively under changing climate (RCP4.5). Meanwhile, RCP8.5 shows more frequent flooding than RCP4.5 even though the difference is relatively small. Under both climate scenarios, WS18 and WS27 are predicted to have substantial increase in frequency of droughts (in months). WS18 and WS27 have over 50% and near 90% increase respectively in drought events compared to current (2071 to 2100 vs. 1986 to 2015).

Table 2-6. Total number of months in 30 years (1986-2015 or 2071-2100) of ANC and BS that are above the critical values under current and changing climate scenarios

	WS18		WS27	
	ANC	BS	ANC	BS
CM1_4.5	344	348	118	0
CM1_8.5	343	348	71	0
CM2_4.5	329	348	122	0
CM2_8.5	339	348	80	0
CM3_4.5	346	348	75	0
CM3_8.5	346	348	55	0
CM4_4.5	348	348	110	0
CM4_8.5	348	348	90	0
CURRENT	360	360	91	0
RCP4.5	342	348	106	0
RCP8.5	344	348	74	0

Table 2-7. Duration of flooding and drought (unit: months) at two watersheds, based on flooding threshold

	WS18		*WS27*	
	drought (<4.1 cm/mo)	flooding (>15 cm/mo)	drought (<8.0 cm/mo)	flooding (>25 cm/mo)
Current	107	46	66	17
CM1_rcp4.5	172	71	135	58
CM1_rcp8.5	171	86	141	63
CM2_rcp4.5	176	68	141	60
CM2_rcp8.5	182	76	147	76
CM3_rcp4.5	153	73	114	62
CM3_rcp8.5	172	77	129	74
CM4_rcp4.5	143	83	108	61
CM4_rcp8.5	130	82	95	63
current	107	46	66	17
*RCP4.5_avg**	161 (+50.5%)	74 (+60.9%)	125 (+89.4%)	60 (+253%)
*RCP8.5_avg**	164 (+53.3%)	80 (+73.9%)	128 (+93.9%)	69 (+306%)

Note: The numbers in brackets indicate =percentage increase compared to current results

Table 2-8. Flooding frequency analysis under both current and future climate at WS18 and WS27

WS18 Return Period (Years)	**Return level (cm/mo)**										
	Current	S1*	S2	S3	S4	S5	S6	S7	S8	**RCP4.5**	**RCP8.5**
2	21.1	28.9	29.8	28.7	34.9	26.1	28.7	28.2	28.9	28.0	30.6
5	25.3	35.8	38.8	36.5	45.4	30.7	34.9	36.4	35.1	34.9	38.5
10	28.1	40.6	46.3	42.2	53.1	33.6	39.0	43.2	39.3	39.9	44.4
20	30.6	44.9	54.5	47.8	60.6	36.0	42.7	50.7	43.2	44.9	50.3
50	33.6	50.1	66.4	55.0	70.2	38.6	47.1	61.5	47.9	51.3	57.9
100	35.6	53.7	76.3	60.3	77.3	40.3	49.9	70.6	51.1	56.2	63.7

WS27 Return Period (Years)	**Return level (cm/mo)**										
	Current	S1*	S2	S3	S4	S5	S6	S7	S8	**RCP4.5**	**RCP8.5**
2	30.1	40.3	42.7	40.1	49.0	36.0	40.3	38.2	38.7	38.7	42.7
5	36.1	48.0	53.3	50.4	61.1	43.9	48.3	47.1	46.8	47.3	52.4
10	41.2	52.9	61.1	58.4	69.6	50.2	54.0	54.1	52.6	53.9	59.3
20	46.7	56.9	68.7	66.6	77.7	57.1	59.5	61.3	58.1	60.5	66.0
50	54.8	61.4	78.4	77.7	87.6	66.8	66.5	71.1	65.1	69.3	74.4
100	61.6	64.2	85.5	86.4	94.7	74.8	71.5	78.7	70.2	76.0	80.5

Note: S1 through S8 represents climate model 1 to 4 under RCP4.5 and 8.5 scenarios (*: S1, S3, S5, and S7 are climate model 1 to 4 under RCP4.5 scenario and S2, S4, S6, and S8 are climate model 1 to 4 under RCP8.5 scenario). Above is the return level estimate of current climate streamflow flooding (data used are 1936-2015 at WS18 and 1946-2015 at WS27) using L-moments method (vs. MLE, GMLE, Bayesian as L-moments method gave better fitting between simulated and observed streamflow).

2.4 Discussion

2.4.1 Spatial and seasonal variability

The specific impacts of climate change on the hydrochemical processes have shown large spatial variability. Evapotranspiration and streamflow are predicted to increase under both moderate (RCP4.5) and high-end (RCP8.5) climate change scenarios at both WS18 and WS27. The predicted increase of evapotranspiration with climate change is consistent with patterns found in seven forest watersheds across four northeastern states in the U.S. (Pourmokhtarian et al. 2016). Annual streamflow, however, is highly variable among these watersheds, with some watersheds predicted to increase while others predicted to decrease, depending on whether the increase of evapotranspiration is offset by the increase of precipitation or not (Campbell et al. 2011). The hydrological predictions are different at the Andrews Experimental Forest in the northwestern U.S., where it is predicted that there will be a 20% to 71% decreases in annual transpiration under future climate change corresponding to 49% to 86% decreases in foliar biomass due to drought stress and 56% to 77% increases in stomatal conductance (Dong et al. 2019). The decrease in evapotranspiration will contribute to higher streamflow at this forest. In the western U.S. where future climate is projected to become warmer and dryer, gross and net nitrogen mineralization are predicted to increase, and net primary productivity is predicted to increase by 32%, due to feedbacks between warmer temperatures and enhanced nitrogen mineralization in forests. In Coweeta Basin, Knoepp and Swank (1998 and 2002) found that temperature and temperature-moisture interactions significantly affected net soil nitrogen mineralization based on a series of long-term studied plots at different elevations. When temperature was warmer and soil

moisture content was higher, nitrogen mineralization was reported to be greater. From the relatively low elevation oak-pine dominated watershed to the higher elevation watershed dominated by northern hardwoods, net nitrogen mineralization (NetNMin) rate showed a strong spatial pattern with the highest NetNMin observed at the highest site, even though there were other factors besides temperature and soil moisture that also influenced nitrogen cycle both in the laboratory and *in situ*.

Climate change is projected to have variable effects on ecosystem responses across the seasons. Even though annual streamflow is projected to increase, these increases are less pronounced in fall and winter at WS18, and in summer and fall at WS27. Spring is important because of loss of snowpack and leaf-out timing that can extend the growing season and exacerbate drought stress. A hotter summer together with a warmer spring, coupled with temporally unevenly distributed precipitation, could increase drought stress and risks of wildfire. The drought stress could extend to other seasons. The fall season presents the lowest percent increase of precipitation among all the seasons. With higher evapotranspiration driven by higher temperature, streamflow is projected to decrease thereby causing more droughts. During winter, relative temperature increases are particularly pronounced, which decreases precipitation inputs as snow and the degree and duration of snow coverage (Campbell et al. 2011; Pourmokhtarian et al. 2016). Here I found that the responses of individual biogeochemical processes varied across seasons.

Effects of climate change are difficult to evaluate during the “shoulder seasons” due to the large year to year variability. As a result, impacts during these periods are generally ignored, however more and more research shows transitional seasons are

affected by climate change to a greater degree than previously thought (Xie et al. 2015; Goss et al. 2020). Traditional definition and transition between seasons are predicted to become less clear as we may see shorter spring and fall, while winter and summer will become longer, and most of the year will fall into more extreme hot and cold temperatures (Thomson 2009).

2.4.2 The impact of CO_2 on ecosystems

Elevated CO_2 associated with climate change tends to increase plant water use efficiency, i.e., increases primary productivity and reduces evapotranspiration (Reyer et al. 2015), which benefits forests by increasing their drought tolerance although there are counteracting effects to consider. Elevated CO_2 could also increase plant leaf area, therefore, making trees less drought tolerant (Ghannoum & Way, 2011). Reduced evapotranspiration could lead to increases in leaf temperature, thereby increasing temperature stress. Increased productivity under elevated CO_2 may increase litter (Hyvonen et al. 2007), leading to increased litter accumulation and higher vulnerability to fire.

Many studies on the response of forest habitats to increased CO_2 are at the small scale of individual trees or small plots. Scaling up the effect to the ecosystem scales involves large uncertainties. Furthermore, the fertilizing effect of CO_2 is commonly found only in young trees (Korner et al. 2007). When I assume elevated CO_2 increases primary productivity at the entire watershed, as I have done in this study, it is likely an optimistic estimate on primary productivity.

2.4.3 The impact of large-scale climate variability and extremes

Generally, during El Niño years, the southeastern U.S. would experience cooler temperatures and wetter winters (https://www.weather.gov/tae/enso). Together with the North Atlantic Oscillation (NAO), it was found that the southern Appalachians had higher snowfall and cooler temperature in winter during El Niño and negative NAO phases (Eck et al. 2019). In contrast, La Niña and positive NAO years had warmer and drier winter weather. I evaluated how ENSO could affect biogeochemical processes. The analysis shows that Oceanic Ni*ño* Index (ONI which indicates ENSO) had a negative relation with the integrated biogeochemical processes (PC1) in the winter and early spring (January to April) at WS18 and WS27 (Fig. S2-9). Strong El Ni*ño* years generally had lower PC1 (Fig. S2-9 and S2-10), indicating lower productivity and higher alkalinity in soil and streams. In addition, the larger precipitation more likely leads to flooding. Therefore, El Ni*ño* years can enhance extremes in streamflow and acidic conditions (flushing high amount of decomposed organic matter downstream to ponds or lakes), a major concern to society. On the other hand, the prediction of El Ni*ño's intensity* using current climate models involves large uncertainty (Wang et al. 2019), which makes predictions of extreme events more challenging under climate change.

2.4.4 Ecological thresholds

The changing-points in history are mostly driven by temperature, however the main driver shifts to precipitation in the different scenarios of future climate change, consistent with predictions from other studies in temperate forest (Peters et al. 2013; Charney et al. 2016; Novick et al. 2016). The change-points may represent critical transitions between states and align with the concept of ecological thresholds.

Although simulation of individual ecosystem processes changes in different directions and show strong seasonality at the two study sites, overall ecosystem functions will likely degrade as the frequency of extreme streamflow and duration of extreme acidic conditions increase with climate change. The negative impact will likely compromise forest resilience (such as droughts and flash-flooding impacts to soil and surface water). It is increasingly important to understand whether and how climate change leads to reduced resilience and potential thresholds (Reyer et al. 2015). Threshold-based concepts emphasize abrupt change and nonlinear (or rarely linear) responses of ecosystems to abiotic and biotic drivers. It can guide natural resource management with proper use, for example, providing early warning signs of ecosystem transitions (Munson et al. 2018). However, these concepts have rarely been tested in forests, probably due to the difficulty of predicting forests' responses to climate change arising from large heterogeneity across spatial and temporal scales. Predicting the thresholds based on empirical data remains challenging (Moore, 2018) due to multiple interactions, different scales, and stochasticity. A more effective approach is using a combination of models and long-term observations or short-term experiments. As such, time-series data that exist in long-term ecological research sites are very valuable. Furthermore, process models that account for important underlying mechanisms, such as the PnET-BGC model I applied in this study, can facilitate threshold analysis.

However, one needs to take extra caution to interpret the change-points or potential thresholds based on simulations of the ecosystem models. Most models (including PnET-BGC) are not designed to simulate thresholds due to the inclusion of equilibrium pools, which represent average steady state responses and/or lack of

feedbacks between vegetation and climate (Reyer et al. 2015). Nevertheless, these models can provide a diagnostic tool for ecosystem's resilience to environmental driver changes.

The abrupt changes of NPP, transpiration, and stream ANC at and above 3 ℃ coupled with 40% decreases in precipitation at WS18 is consistent with a previous study that showed considerable ecosystem change is expected under local temperature change of 4 ℃ in the temperate zone (Heyder, 2011). Sensitivity to temperature change increases with decreasing precipitation in WS18. Though a reduction in precipitation of 40% or more is not likely at WS18, drought is projected to become more frequent and this condition will likely push ecosystems closer to abrupt changes in function.

I applied the threshold concepts to a variety of key ecosystem processes. Ecosystem performance was commonly measured by changes in plant growth, with metrics of foliar cover to the tree ring growth, as primary production is the basis of ecosystem functions. However, different structures of vegetation can have different responses to disturbance, creating unique thresholds/tipping points that need to be identified (Munson et al. 2018). Furthermore, biogeochemical processes interact with plant growth and likely lead to different threshold responses. For example, simulations for WS18 suggest that NPP increases with increases in temperature initially but will decrease when temperature rises more than 1 ℃ at WS18, transpiration will increase with temperature until the temperature increase reaches 3 ℃.

2.4.5 Caveats of PnET-BGC

PnET-BGC is a watershed-scale model that was operated on a monthly time step, so it is not well suited to address finer spatial and temporal resolutions (Merganicova et al. 2019). This model treats the vegetation in the watershed as a big leaf, therefore, it does

not consider the difference among tree types and fine structure (Elliott et al. 2015), adaption (Jandi et al. 2019), or shift of vegetation types. Recent studies show that the critical transitions of vegetation type in mountain forests (Albrich et al. 2020) may change the fundamental relationships between foliar N concentration and maximum photosynthesis rate, which is one of the two fundamental relations that PnET-BGC is built on. Reich et al. (1995) has studied the photosynthesis-foliage nitrogen relation, for deciduous hardwood and evergreen coniferous tree species. Broadleaf deciduous forest species have the highest correlation with leaf nitrogen content (r^2 = 0.75, P<0.001) while evergreen conifers show a weaker yet significant correlation (r^2 = 0.59, P<0.001), whereas the slope of the regression is higher than for broadleaf trees, which means broadleaf has higher photosynthesis rate under same foliage nitrogen content. Furthermore, the function of understory shrub vegetation in cycling nutrients, carbon, and water is another component this model lacks. Different stages of vegetation not only have different capabilities of nutrient uptake, photosynthesis, cycling of carbon and water, but larger and older trees may be also more susceptible to stress such as drought and storms (Clinton et al. 1993; Clinton & Baker, 2000; Clinton et al. 2003), which is not depicted in the model.

This model requires a number of empirical data to calibrate, some of which are not available for the study watersheds (such as Al and DOC concentrations), making calibration for these parameters less robust. In addition, the model under-predicts nitrate concentrations in streamwater, suggesting the need to critically review this submodule for applications at Coweeta watersheds. Other simulations using PnET-BGC have been challenged to accurately simulate nitrogen dynamics (e.g., Shao et al. 2020). This model

is designed to predict long-term hydrologic and biogeochemical changes at the watershed scale (Aber & Federer, 1992; Gbondo-Tugbawa et al. 2001), combined with the lack of feedback between vegetation and climate, it is not an ideal tool to derive regime shifts. However, the change-point and threshold analysis show the potential of regime shifts under higher temperature and drought conditions at the lower-elevation watershed.

Despite these caveats, the PnET-BGC model provides a useful tool to evaluate the impact of climate change on forested ecosystems over long time scales (multiple decades to centuries). When depicting complex ecosystems, as many other ecological models have done, it is necessary to make assumptions and inherent uncertainties exist (Aber et al. 1992; Aber & Federer, 2001). In order to capture the uncertainty, I have applied multiple climate change scenarios. The consistent response of biogeochemical cycles provides projections with higher confidence, while inconsistent predictions indicate larger uncertainties involved and can generate important hypotheses in future studies.

2.5 Conclusion

I studied the impact of climate change on the function of two high-elevation forested watersheds in the southern Appalachians, focusing on the nonlinear responses by studying change-points of biogeochemical processes and identifying the potential thresholds of some climatic drivers. Even with the general positive response of vegetation to warming and overall increased precipitation, simulations show signs of potential degradation in future ecosystem health, driven by more frequent hydrological extreme events and longer extreme acidic conditions in soil and streams. I detected earlier change-points of PC1 occurring under RCP8.5 compared to RCP4.5, and at the higher elevation WS27 than at WS18, indicating potential accelerating change of key biogeochemical

processes under more extreme warming and at higher-elevations. The potential thresholds at the lower elevation watershed (WS18) shows the forest is less resilient to climate changes under warming conditions. This analysis may provide useful information for resource managers to anticipate the potential risks that the forests will likely face under climate change. Therefore, forest managers can consider possible measures such as tree planting and forest restoration, wildfire control, establishment of mixed stands, planting better adapted species or varieties, and vegetation insects and diseases control (etc.) to mitigate future adverse impacts.

CHAPTER III THE IMPACT OF CHANGE IN ACIDIC DEPOSITION AND CLIMATE ON FIVE FORESTED WATERSHEDS IN THE SOUTHEASTERN U.S.

Abstract

Climate change disproportionally affects forest ecosystems at different latitudes and elevations. This pattern will be further complicated due to interactions with change in acidic depositions. There have been limited studies on the combined effect of change in climate and acid deposition on forested ecosystems. In addition, the regional analysis on climate change impact involves large uncertainties. In this study, I predict the impact of climate change on hydrology, vegetation dynamics, soil processes, and stream chemistry in five forested watersheds that cover both southern and central Appalachians with a variety of latitudes and elevations. I also examine if predicted changes in acidic atmospheric deposition exacerbate climate change impacts. Furthermore, I synthesize the response of key biogeochemical variables to climate change regionally.

I applied an integrated biogeochemical model PnET-BGC at three forested watersheds in the Shenandoah National Park (SNP) in Virginia and two forested watersheds in the Coweeta Basin in North Carolina, U.S. under different climate change scenarios (RCP4.5 and RCP8.5) that were downscaled to watershed scales and included interactions with a variety of scenarios of sulfate, nitrate, and ammonia depositions. I applied multi-level Bayesian models to synthesize the response of biogeochemical processes to climate change.

The results show transpiration and stream base cations are closely related to the first principal components (PC1) of seventeen main biogeochemical variables simulated by the PnET-BGC at SNP. They show seasonal variability in response to climate change.

There are more change points detected for the PC1s at the SNP than at the Coweeta Basin, and the first change point occurred in the 1940s at the SNP, 40 years earlier than estimated for the Coweeta Basin. In general, the watersheds at higher latitude or elevation showed fewer but earlier changing points than their lower latitude, lower elevation counterparts. The change of acidic deposition affects the response of some key biogeochemical variables to climate change. The effects depend on the biogeochemical processes, seasons and the direction and magnitude of the change in acidic deposition. The effect is minimum for net primary productivity. Seasonally, summer and winter are the two seasons that will be most impacted by acidic deposition based on the percent changes between current (1986 to 2015) and future (2071 to 2100) over the selected watershed process variables (NPP, ANC, BS, and transpiration, and discharge). Across all five sites from southern to central Appalachians, the response of the key biogeochemical variables to precipitation is less significant than to temperature. Winter shows the least sensitivity to climate change among the four seasons in NPP, transpiration, and ANC except the NPP's response to precipitation under RCP8.5 and ANC's response to temperature under RCP8.5. In addition, latitude and elevation affects the sensitivity of these biogeochemical variables to temperature and precipitation, but with large uncertainties. Therefore, the latitudinal and elevation pattern of climate change impact is not conclusive based on the five sites I studied.

I evaluated the climate change impacts at the season, site and regional scales. I quantified the uncertainties of the responses of different biogeochemical processes to temperature and precipitation and the role of latitude and elevation in affecting the responses. The consideration of multi-scale drivers and uncertainties is important for

local and regional policy to improve forest conservation and mitigation plans under climate change.

3.1 Introduction

Accumulating evidence has shown the change of global climate in recent decades has affected forest ecosystems (IPCC, 2007; Campbell et al. 2011; Pourmokhtarian et al. 2012; Caldwell et al. 2016). Some climate change impacts are sudden and dramatic while others can be gradual and subtle. In arid and semi-arid regions, drought and wildfire are becoming more frequent as temperature increases and precipitation decreases or becomes more unevenly distributed, negatively affecting primary productivity and altering biogeochemical cycles in forests (Westerling et al. 2014). In the areas where precipitation is not limiting or where it is cold, such as at higher latitudes or elevations, increased temperature can increase primary productivity (Ruiz-Perez & Vico, 2020).

Climate change is projected to continue to accelerate through the end of this century. The global mean surface temperature in years 2081-2100 is predicted to be 0.3 to 4.8 ^{o}C higher than in 1986-2005 (Intergovernmental Panel on Climate Change, IPCC, 2014). Precipitation is also predicted to increase with mean surface temperatures with a 1% to 4% increase per 1^{o}C by 2100 with high spatial variability. The climate in southeastern U.S. is expected to follow this trend and its temperature is projected to increase even more (up to 6 ^{o}C by end of this century) as land heats faster than oceans (Mitchell et al. 2014; Anandhi & Bentley; 2018).

In addition to general projections of future climate, local climate can have substantial variation over short distance in both altitude and latitude (Lee, 2014; Pepin et al. 2015; Wang et al. 2016; Serreze et al. 2000). Higher latitudes may experience larger impact due to climate change as they warm faster than the lower latitude regions (Roots, 1989). Additionally, higher elevation normally shows greater changes in temperature than

nearby areas at lower elevations (Wang et al. 2014; Pepin et al. 2015; Wang et al. 2016). Wang et al. (2014) found that high-elevation regions are warming 26% faster than the nearby low-elevation regions on average using a paired comparison method. Higher elevation mountainous watersheds typically receive more precipitation than lower watersheds. Meanwhile temperature has seasonal differences in relation to latitude and altitude (Lu et al. 2009). In summer, temperature is more strongly related to elevation than to latitude, while in winter it is more closely related to latitude. As air temperature is predicted to increase the most in winter, the correlation between latitude and temperature will be weakened in winter because of uneven warming/cooling at different latitudes. In summer, however, when temperature increases, the correlation between temperature and altitude is expected to become even stronger due to both altitude and topographical effects (Lu et al. 2009). Therefore, climate change had disproportional impact on forested ecosystems in different seasons and at different elevations and latitudes.

Temperature and precipitation, as mentioned previously, are the two most important factors in climate, and can affect forest in many processes, such as primary productivity, carbon sequestration (Turnbull et al. 2001; Boisvenue & Running, 2006; Buermann et al. 2013; Hatfield & Prueger, 2015), and hydrology (such as snowpack, droughts, and flooding: Kunkel et al. 2009; Furniss et al. 2010; Giang et al. 2014; Wu et al. 2014) as well as soil properties such as soil moisture and loss of organic carbon storage from drought, flooding, and wildfire (Stark & Firestone, 1995; Jobbagy & Jackson, 2000; Knoepp & Vose, 2007; Duran et al. 2016).

Human activities have increased the availability of reactive nitrogen, exceeding the demands of vegetation and microbes, leading to nitrogen saturation and nitrogen

leaching from soil into water bodies (Aber et al. 1989; Aber, 1992; Aber et al. 1998; Huang et al. 2015; Chen et al. 2016). Nitrogen leaching is dependent on precipitation, snowmelt, and water infiltration in the soil below the root zone and causes stream acidification (Mitchell, 1939; Rascher et al. 1987). While reactive nitrogenous atmospheric deposition is expected to increase, sulfate deposition is expected to continue to decrease since passage of the Clean Air Act. The impact of changes in acidic deposition rates on ecosystem processes is relatively well understood (Chen et al. 2004; Zhai et al. 2008; Wu & Driscoll, 2009), however the research on how changes in acidic deposition interacting with climate change affect ecosystems is limited (Wu & Driscoll, 2010).

In this work, I aim to address the following questions: 1) What biogeochemical processes/variables explain the largest variability in the impact of climate change in the Shenandoah National Park (SNP) and how do these compare to the Coweeta Basin? What is the seasonal variability of these processes? 2) How do the change points of PC1s at the SNP compare to those at the Coweeta Basin? 3) How do changes in acidic deposition rates interact with climate change to affect key biogeochemical processes? 4) What is the spatial pattern of sensitivity of the key biogeochemical processes to temperature and precipitation?

3.2 Methods

I first investigated the impact of climate change on three watersheds within the Shenandoah National Park (SNP). I applied PnET-BGC model to simulate biogeochemical processes under current climate and changing climate scenarios. The climate change scenarios were downscaled from the general circulation models (GCMs)

at the watershed scales (Hayhoe et al. 2004; Hayhoe et al. 2007; Hayhoe et al. 2008). I then applied principal component analysis based on a variety of biogeochemical processes to simplify the high-dimensional problem. Next, I studied the seasonality of these processes that are closely related to the first principal components (PC1s), including gross primary productivity, transpiration, and Ca^{2+} and ANC in stream. I also detected the change points of the PC1s over time and the potential drivers from past (1931) to the future (2100).

I further combined the three sites at SNP with the two sites at the Coweeta Basin (CWT, Chapter 2), and evaluated how change of acidic deposits affect climate change impact by implementing the PnET-BGC model in scenarios with different climate and acidic depositions. To synthesize the regional pattern of the impact of changes of climate and acidic depositions, I applied multi-level Bayesian models to analyze how these key processes respond to precipitation and temperature across five watersheds in different seasons under different scenarios of acidic depositions.

3.2.1 Study sites

The five forested watersheds cover both south and central Appalachians with two at the Coweeta Basin in North Carolina, and three at the Shenandoah National Park in Virginia. I described the two watersheds at the Coweeta Basin in Chapter 2. So, in this chapter, I will only focus on the three watersheds in the SNP.

The three watersheds in Shenandoah National Park are located in a temperate climate zone with cool summers and short, mild winters. They are Staunton River (SR, 38°02’40”N, 78°22’15”W), White Oak Run (WOR, 38°15’03”N, 78°44’53”W), and Paine Run (PR, 38°11’55”N, 78°47’36”W), from north to south (Fig. 1-1). Annual total

precipitation at these three watersheds is 128 cm which is ~40 percent lower than the two watersheds at the Coweeta Basin (Table S3-1). Snow occupies a relative larger proportion of precipitation in these watersheds compared to the Coweeta Basin. For instance, snow was up to 14% of annual precipitation at the Big Meadows National Climate Data Center-NCDC weather station between 1935 and 2012 (station ID: USC00440720, elevation: 1,079 m at 38º31'18"N, 78º26'08W, https://www.ncdc.noaa.gov/cdo-web/datasets/GSOM/stations/GHCND:USC00440720/detail and accessed on 08/01/2020) compared to 5% at the Coweeta Basin. The three watersheds have lower precipitation and streamflow compared to the Coweeta Basin (Table S3-1). In addition, the watersheds have lower ratio of streamflow to precipitation (1/3 to 1/2 in SNP vs. 1/2 to 2/3 in Coweeta). During the same time, the watersheds in the SNP showed lower annual temperature than that at the Watershed 18 but similar to that at the Watershed 27 at the Coweeta Basin (Table S3-1).

The SR is closest to the wet deposition (NADP VA28), dry deposition (CASTNET SH418), and climate (NCDC station: Big Meadows) stations among the three watersheds (Fig. 1-1). This watershed covers about 1,050 ha and ranges from 335 to 1,056 m in elevation. In 1941, the dominant tree species were chestnut oak (*Quercus prinus*) (33% of area) and red oak (*Quercus rubra*) (23% of area) (Fievet et al. 2003). In 1985, the chestnut oak became even more prevalent, covering 48% of the watershed. There have been no significant fires since the formation of the park (1935). WOR watershed has an area less than 1,000 ha and ranges from 480 to 968 m in elevation and chestnut oak dominates in this watershed as well with 47% of area in 1941 and 82% of

area in 1985. There were no significant fires in WOR. Like SR, anthropogenic activities and constructions (such as road and buildings) in the WOR are very limited. PR has the largest area among the three watersheds (1,240 ha). Its elevation ranges from 434 to 1,040 m and chestnut oak is also the dominant species in this watershed. In 1998, a large fire affected about half of the area of PR. The sizes of the Shenandoah watersheds are much larger than the two watersheds at the Coweeta Basin (~1,000 ha or more in the Shenandoah National Park vs. 13 to 30 ha at the Coweeta Basin).

3.2.2 Input data and data for model calibration

The required input data for the PnET-BGC model include climatic conditions, atmospheric depositions, vegetation properties, and soil characteristics (Table S3-2).

3.2.2.1 Climate data

The climate data was obtained from the Big Meadows station (Network ID: GHCND: USC00440720) at the National Climatic Data Center (NCDC), which includes monthly precipitation, maximum and minimum temperature (Tmax and Tmin), and solar radiation (http://www.ncdc.noaa.gov/cdo-web/datasets/GHCND/stations/GHCND:USC00440720/detail, accessed on 08/01/2020). The weather station is the only one close to these three watersheds in the SNP and it is near the Stanton River watershed (approximately 8.0 km from the weather station to the center of the watershed while approximately 45 km to the center of the other two watersheds, Fig.1-1) at an elevation of 1,079 m. The Tmax, Tmin, and precipitation measured from this weather station were not directly used due to the difference of elevations between the weather station and the three watersheds. I first derived regression models between temperature/precipitation and elevation in each month between 1935 and

2015 based on the weather stations at the Big Meadows and other fifteen weathers stations nearby (Table S3-3 and S3-4, R^2 ranges between 0.067 and 0.801 and with 12-month averaged R^2 0.45 for Prcp, 0.60 for Tmax, and 0.30 for Tmin). Then I calculated the ratios of temperature/precipitation at the SR, WOR, or PR to at the Big Meadows in each month based on the regression models and average elevation for each watershed. These ratios, combined with monthly climate data at the Big Meadows, I derived the temperature and precipitation at the SR, WOR, and PR watersheds from 1935 to 2015. I replaced negative precipitation derived with an arbitrarily small value of 0.1 cm mo^{-1}. During the years when there was no observed climate data (i.e., before 1935 and after 2015), I used the monthly averages of Tmax, Tmin, and precipitation from 1935 to 1985 as the climate inputs for the years between 1000 (the year the model runs start) and 1934 and the monthly averages between 2006 and 2015 as the climate inputs from 2016 to 2100 under the base climate scenario. I applied solar radiation derived from the Daily Surface Weather and Climatological Summaries (DayMET data, https://daymet.ornl.gov/, spatial resolution: 1 km) between 1980 and 2015. Meanwhile, I derived a regression model for the DayMET-modeled solar radiation as a function of observed solar radiation at the Big Meadows station between 1988 and 2015 (R^2 of 0.28). Based on the regression model, I derived solar radiation at the three watersheds from 1935 to 2015. I then used the monthly averages between 1935 and 2015 as the solar radiation before 1935 and after 2015.

In the future climate change scenarios, I used downscaled climate predictions of air temperature, solar radiation, and precipitation at the watershed scale from four global atmosphere-ocean general circulation models (Atmosphere-Ocean General Circulation

Models - AOGCMs: CCSM4, HadGEM2, MIROC5, and MRI-CGCM3) coupled with two Representative Concentration Pathways (RCP4.5 and RCP8.5). The downscaling is based on the long-term daily observations at the Big Meadows weather station (Hayhoe, et al. 2004; Hayhoe et al. 2007; Hayhoe et al. 2008; Pourmokhtarian et al. 2016). AOGCMs has a coarse spatial resolution of ~100 km, which has limitations when applied to small, high-elevation watersheds in complex mountainous which are strongly affected by local weather patterns (Pourmokhtarian et al. 2012). I then applied the same temperature and precipitation ratios between the three watersheds and the Big Meadows in Table S3-4 to derive future climate at each watershed.

3.2.2.2 Atmospheric depositions

I obtained wet and dry depositions of major elements (NO_3^--N, SO_4^{2-}-S, Cl^-, Na^+, Mg^{2+}, K^+, Ca^{2+}, NH_4^+) from the National Atmospheric Deposition Program (NADP) and The Clear Air Status and Trend Network (CASTNET) respectively. The closest NADP station for the SNP is VA28 that is close to the SR and the wet deposition data ranges from 1981 to 2015. The closest CASTNET station is SH418 and the dry deposition data ranges from 1988 to current. I constructed the data before the measurements based on the national sulfur dioxide (SO_2) emission records from 1931 to 1987 and the relation between the emission and atmospheric deposition of SO_4^{2-}-S and NO_x-N between 1988 and 2015 (EPA, 2000; Driscoll et al. 2001; Chen et al. 2004). From 1850 (pre-industrial) to 1930, I assumed a 50% increase of SO_2 and NO_x emissions and applied a linear increment to construct the emissions and wet deposition of SO_4^{2-}-S and NO_x-N. Between 1000 and 1850, I kept the sulfur and nitrogen wet deposition the same as in 1850. I applied a monthly-average dry to wet deposition ratios of sulfate, nitrate, ammonia,

chloride, and base cations of sodium, magnesium, potassium, and calcium derived from observed wet and dry depositions to construct the unobserved dry depositions.

3.2.2.3 Disturbance history

For the PR, there was a fire event that destroyed about half of the area and in order to incorporate it into model simulation, the parameters have been set are: fire intensity as 0.5 (from 0 to 1.0 and 1.0 indicates total destroyed), remain fraction as 0.5 (from 0 to 1.0 and 0.5 indicates that half of total vegetation remained after disturbance), and soil loss as 0. And the foliage regeneration time used is the model default value as 100 years (return to pre-disturbance status).

3.2.2.4 Soil and stream chemistry data

In order to calibrate the model, I applied measured data in the soil and streams provided by the Stream and Water Analysis System – Virginia Social Services System (SWAS-VSSS) program, including streamflow, concentrations of Na^+, Mg^{2+}, K^+, Ca^{2+}, Cl^-, NH_4^+, NO_3^- and SO_4^{2-} in streams from 1992 to 2012 (Table S3-2). Other data used to further calibrate different modules of the model included gross primary productivity (GPP, http://www.edc.uri.edu/ATMT-DSS/report_forecast/subsection_summaries/M221.html and accessed on 08/01/2020), net primary productivity (NPP, http://www.edc.uri.edu/atmt-dss/report_forecast/forest_health/M221_NPP.html and accessed on 08/01/2020), and nitrogen mineralization and immobilization rates (Lovett & Ruesink, 1995; Lovett & Tobiessen, 1993).

3.2.2.5 Model calibration and other methods

To quantify the model fit, I used normalized mean error and normalized mean absolute error to evaluate how close the model simulations are to the observed data in stream, soil, and vegetation, as described in Chapter 1. I also applied the PCA and detected change points of PC1, as in Chapter 1.

3.2.3 Bayesian analysis

I applied multi-level Bayesian models to examine the climate change's impact on NPP, transpiration, calcium concentration in stream, and ANC, the key biogeochemical variables that relate closely to PC1, from 2016 to 2100 under RCP4.5 and RCP8.5 across the five sites that vary in latitude and elevation (Fig. 3-1). Synthesis of the climate change impacts at the regional scale is challenging due to the large variances involved. Hierarchical models have the advantage of decomposing a complex question into manageable components and can account for uncertainties from data, models, and parameters (Clark, 2005). The posteriors of the coefficients for precipitation and temperature at the site scale and for latitude and elevation at the regional scale facilitate inference on the latitude and elevation's impact and difference in sensitivity of the biogeochemical variables to precipitation and temperature at different watersheds. More importantly, the variances are readily summarized in the credible intervals based on the posterior distributions.

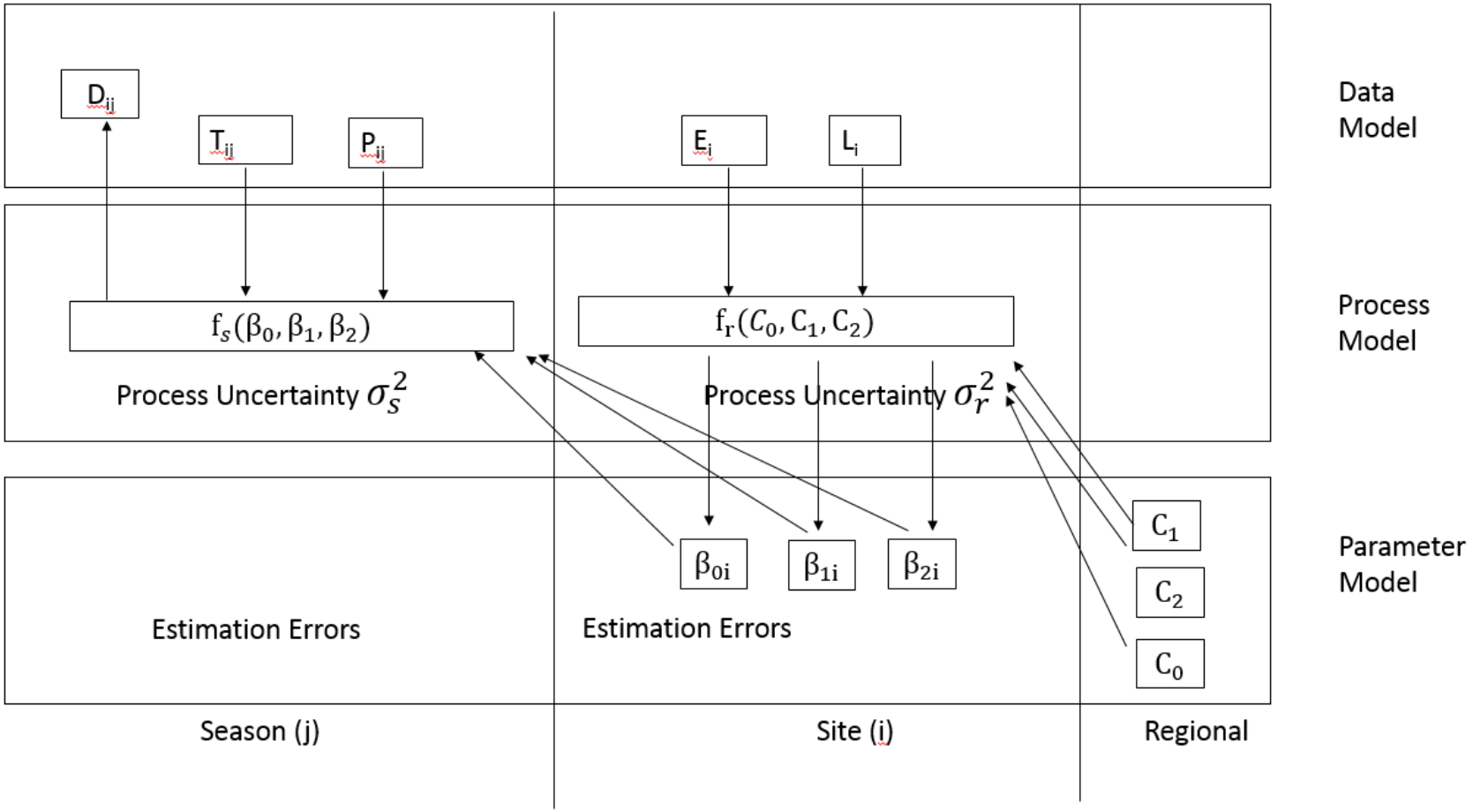

Fig. 3-1. Bayesian Model.

The model to illustrate the hierarchical structure with complexity decomposed into stages of data, processes, and parameters (vertical direction), and the association of different spatial scales (horizontal direction). Biogeochemical process (ANC, NPP, transpiration) (Dij) was a function of variables at the season scale (j) and site scale (i). j represents each season, while i represents the site j belongs to. The season-scale process was modeled using the temperature (Tij), precipitation (Pij) as the covariates. The site-scale process was modeled using elevation (Ei) and latitude (Li) as the covariates.

To represent the biogeochemical process D in season j at site i, let $D_{ij}.\mu$ represent the mean of D_{ij}, and σ_s^2 represent the variance of D at the site scale. D_{ij} was modeled by assuming it was distributed as (~) a normal distribution (Eq. 1):

$$D_{ij} \sim N(D_{ij.}\mu, \sigma_s^2) \quad (1)$$

Mean of the $D_{ij.}\mu$ was a linear function of the covariates at the season level: temperature (T_{ij}) and precipitation (P_{ij}) (Eq.2)

$$D_{ij}.\mu = f_s(\beta_{0i}, \beta_{1i}, \beta_{2i}) = \beta_{0i} + \beta_{1i} \times T_{ij} + \beta_{2i} \times P_{ij} \quad (2)$$

Where βs were the parameters dependent on regional covariates including latitude and elevation.

Therefore, the D at five sites in four seasons was modeled as in Equation 3:

$$p(D|\beta_0, \beta_1, \beta_2, \sigma_s^2) \propto \prod_{i=1}^{5} \prod_{j=1}^{4} N(D_{ij}| f_s(\beta_{0i}, \beta_{1i}, \beta_{2i}), \sigma_s^2) \quad (3)$$

At the site scale, the intercept βs were all modeled by assuming they were distributed as (~) normal distributions:

$$\beta_{0i} \sim N(\beta_{0i}.\mu, \sigma_{r0}^2) \quad (4)$$

$$\beta_{1i} \sim N(\beta_{1i}.\mu, \sigma_{r1}^2)$$

$$\beta_{2i} \sim N(\beta_{2i}.\mu, \sigma_{r2}^2)$$

Means of the intercept and slopes for temperature and precipitation were modeled as linear functions of elevation (E_i) and latitude (L_i) (Eq. 5)

$$\beta_{0i}.\mu = f_r(C_{00}, C_{01}, C_{02}) = C_{00} + C_{01} \times E_i + C_{02} \times L_i \quad (5)$$

$$\beta_{1i}.\mu = f_r(C_{10}, C_{11}, C_{12}) = C_{10} + C_{11} \times E_i + C_{12} \times L_i$$

$$\beta_{2i}.\mu = f_r(C_{20}, C_{21}, C_{22}) = C_{20} + C_{21} \times E_i + C_{22} \times L_i$$

To complete the Bayesian model, I defined prior distribution for unknown parameters ($C_{00}, \ldots C_{22}, \sigma_s^2, \sigma_{r0}^2 \ldots \sigma_{r2}^2$). I used conjugated priors for computation efficiency (Calder et al. 2003) therefore the priors and posteriors have the same probability distribution forms. The priors for $C_{00} \ldots C_{22}$ were normally distributed and the priors for $\sigma_s^2, \sigma_{r0}^2 \ldots \sigma_{r2}^2$ followed the inverse gamma distribution. The priors' distributions were flat and only weakly influenced the posteriors, which reflected the lack of knowledge on the parameters (Lambert, 2005).

By combining the parameter (priors), process, and data models, I derived the joint distribution of unknowns in Eq. 6:

$$
\begin{aligned}
& p(\beta_0, \beta_1, \beta_2, C_{00}, C_{01}, C_{02}, C_{10}, C_{11}, C_{12}, C_{20}, C_{21}, C_{22}, \sigma_s^2, \sigma_{r0}^2, \sigma_{r1}^2, \sigma_{r2}^2 | D, T, P, E, L) \quad (6) \\
& \propto p(D|\beta_0, \beta_1, \beta_2, \sigma_s^2) \times p(\beta_0|C_{00}, C_{01}, C_{02}, \sigma_{r0}^2) \\
& \times p(\beta_1|C_{10}, C_{11}, C_{12}, \sigma_{r1}^2) \times p(\beta_2|C_{20}, C_{21}, C_{22}, \sigma_{r2}^2) \\
& \times p(C_{00}) \times p(C_{01}) \times p(C_{02}) \\
& \times p(C_{10}) \times p(C_{11}) \times p(C_{12}) \times p(C_{20}) \times p(C_{21}) \times p(C_{22}) \\
& \times p(\sigma_s^2) \times p(\sigma_{r0}^2) \times p(\sigma_{r1}^2) \times p(\sigma_{r2}^2)
\end{aligned}
$$

The posterior distributions were computed using Markov Chain Monte Carlo Simulation (MCMC) (Robert, 2004) using the software JAGS 4.3.0 (Plummer, 2017). I summarized 95% and 50% credible intervals based on the posteriors. If the 95% credible interval of a parameter for a particular covariate does not contain 0, then I say the covariate's impact on D is significant.

3.3 Results

3.3.1 Climate change

Similar to the two Coweeta Basin (CWT) watersheds, the three Shenandoah National Park (SNP) watersheds are predicted to have higher air temperature and precipitation compared to current and past climate (3-14 ENSO Oceanic Niño Index vs. PC1 scores in PR (top), SR (middle), and WOR).

On an annual basis, the SNP watersheds are predicted to have even larger temperature increases (+4.1 to 6.5 ^{o}C vs. 2.5 to 4.8 ^{o}C at the Coweeta) from current (1986 – 2015) to the future (2071 – 2100), and air temperature contradiction between summer and winter in the SNP is greater than the Coweeta watersheds. RCP8.5 has higher temperature change than RCP4.5 for all seasons.

Annual precipitation on an annual basis is predicted to increase from 5.0 to 6.4 cm/mo in future (2071 – 2100) compared to current (1986 – 2015), which is also a greater change than the two CWT watersheds (2.2 – 4.0 cm/mo). By seasons, from past to current, the summer precipitation has barely changed whereas all the rest of the seasons have had considerable increases in precipitation, which is different from CWT in both spring and winter. Summer and fall are predicted to have greater precipitation under moderate climate scenario (i.e., RCP4.5) than under RCP8.5, largely attributed to higher predictions of precipitation for these two seasons under RCP 4.5 by one of the four climate models (HadGEM2).

In summary, both air temperature and precipitation are projected to significantly increase from now to the future across all three studied SNP watersheds (Table 3-1).

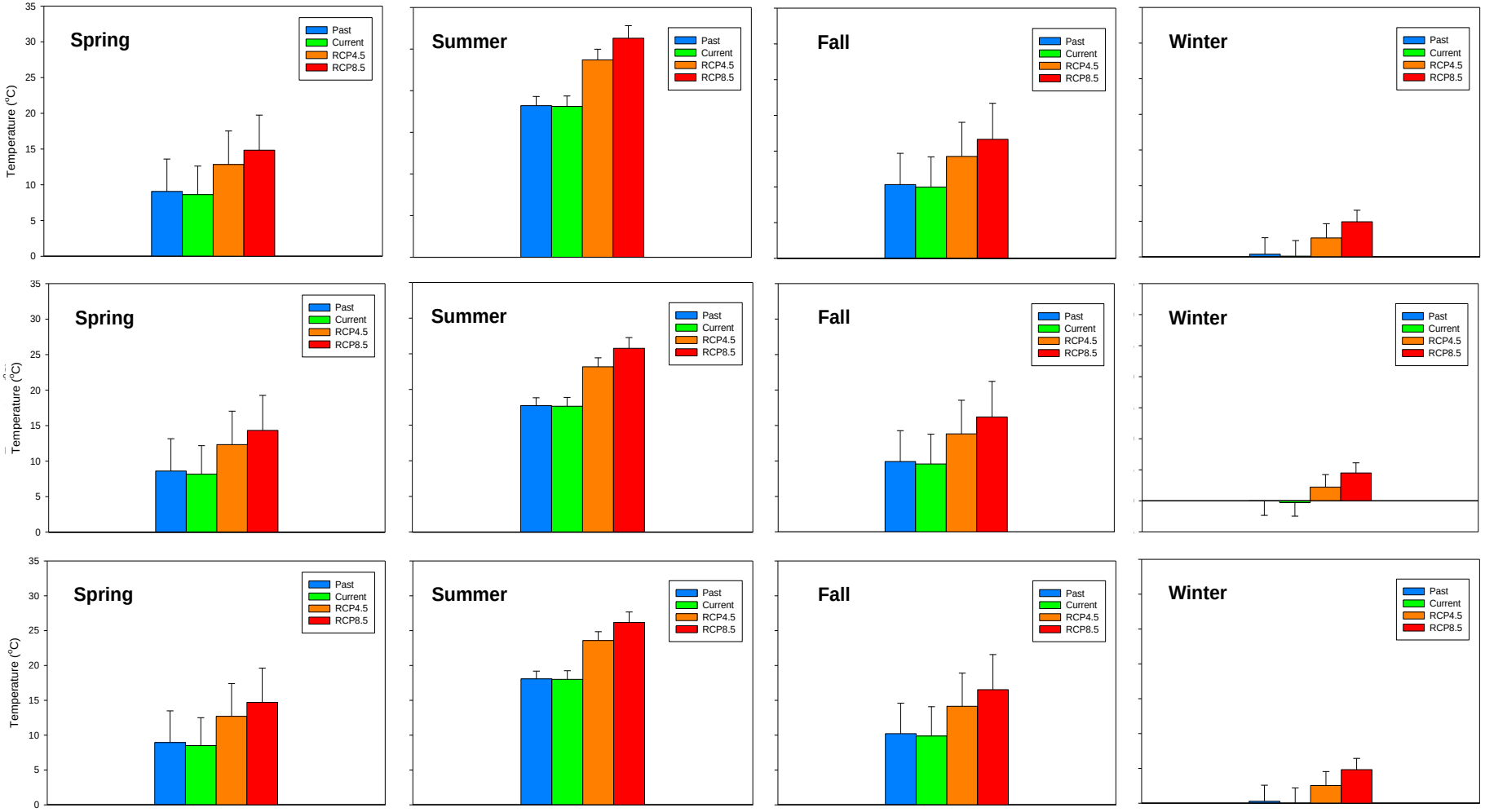

Fig. 3-2a Air temperature by seasons at the Shenandoah National Park (SNP): Paine Run (PR, top), Staunton River (SR, middle), and White Oak Run (WOR, bottom); past (1936-2015, blue), current (1986–2015, green), and future (2071-2100, orange–RCP4.5 and red–RCP8.5), hereafter the same.

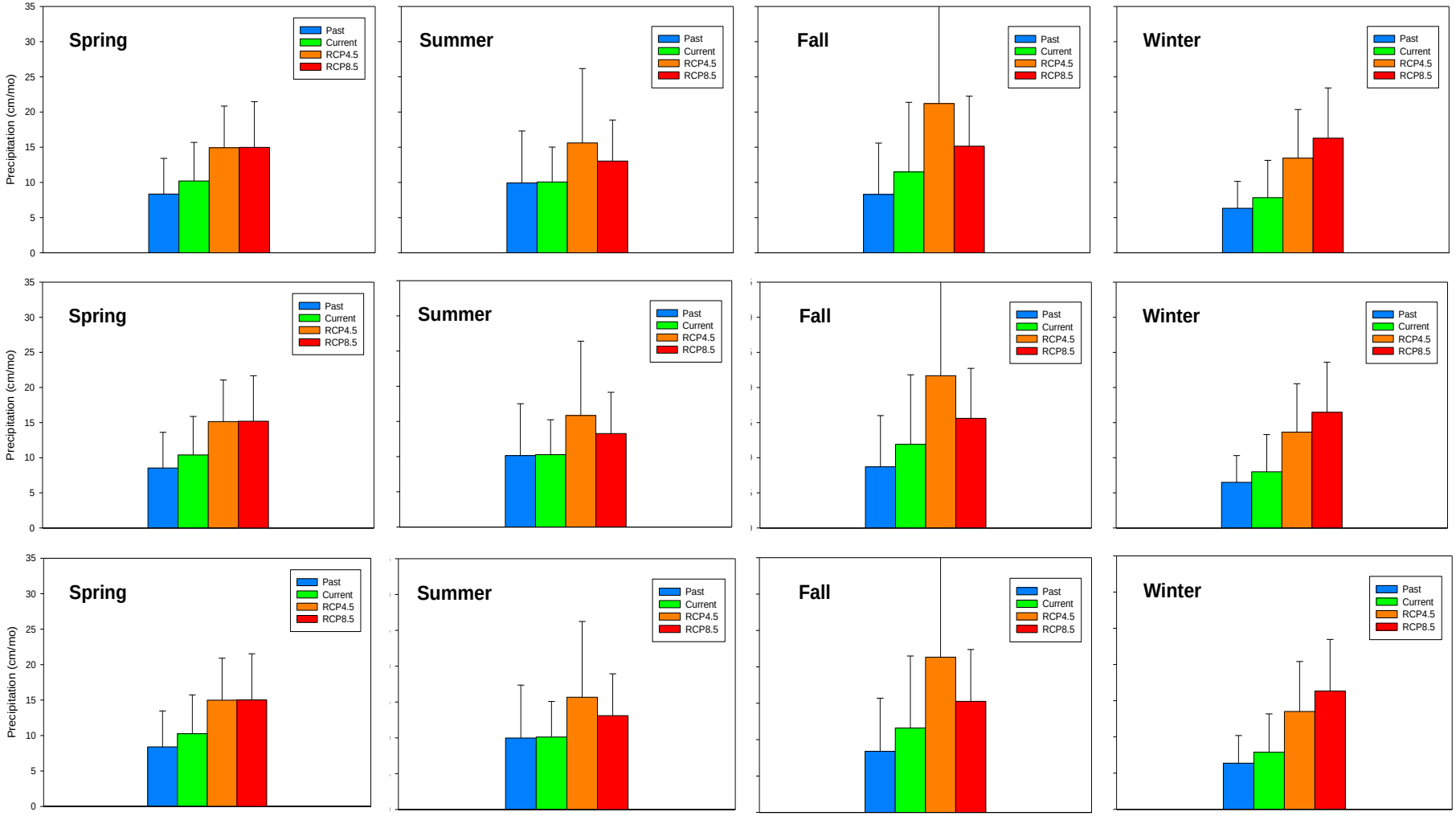

Fig. 3-2b Precipitation by seasons at the Shenandoah National Park (SNP): Paine Run (PR, top), Staunton River (SR, middle), and White Oak Run (WOR, bottom); past (1936-2015, blue), current (1986-2015, green), and future (2071–2100, orange–RCP4.5 and red–RCP8.5).

Table 3-1 Statistical test result of temperature and precipitation between current and changing climate scenarios

	TEMPERATURE							
	RCP4.5-Current				RCP8.5_Current			
	Spr	Sum	Fal	Win	Spr	Sum	Fal	Win
PR	***	***	***	***	***	***	***	***
SR	***	***	***	***	***	***	***	***
WOR	***	***	***	***	***	***	***	***
	PRECIPITATION							
PR	***	***	***	***	***	***	*	***
SR	***	***	***	***	***	***	*	***
WOR	***	***	***	***	***	***	*	***

Note: * indicates 0.01<p <0.05; ** indicates 0.001 < p <0.01; *** indicates p <0.001; and – indicates no significant difference has been detected. Color green means increasing from current to the future. In each season from 1986 to 2000 and from 2071 to 2100, monthly climate data were averaged first, then the 30 data points in each of the current and changing climate scenarios were checked for temporal autocorrelation ("acf" function in R) and normality (Shapiro test). As the checks show lack of temporal autocorrelation and met normality requirement, t-test was implemented to test whether the seasonal climate variables under current and changing climate scenarios were statistically significant different or not.

3.3.2 Model performance

The PnET-BGC model simulated the observed long-term streamflow and stream chemistry generally well at the three watersheds in the SNP (PR, SR, and WOR) except for nitrate concentrations. NME ranges from -0.07 to 0.09 for stream chemistry. ANC and the streamflow are mostly accurately simulated in the SR among the three watersheds (Table 3-2). The model had difficulty capturing the streamflow peaks and it overestimated the streamflow at PR and WOR, which caused the ANC simulations at PR or WOR not as good as at the SR or at the Coweeta Basin.

Table 3-2. Observed and simulated streamflow (unit: cm/month) and water chemistry variables (unit: µmol/L) at PR, SR, and WOR

PR	Observed		Simulated		Model Performance	
	mean	S.D.*	mean	S.D.	NME	NMAE
Na^+	23.6	1.0	25.6	2.7	0.09	0.12
Mg^{2+}	25.4	1.2	25.6	2.1	0.01	0.06
K^+	47.1	1.4	50.9	4.1	0.08	0.09
Ca^{2+}	14.7	0.5	15.0	1.2	0.02	0.06
Cl^-	23.0	1.2	22.4	1.4	-0.03	0.04
NO_3^-_N	4.2	6.0	0.9	0.7	-0.80	0.84
SO_4^{2-}_S	55.1	1.5	58.7	5.0	0.06	0.08
ANC	13.3	3.1	17.1	1.2	0.28	0.33
Streamflow	3.2	1.5	4.8	1.9	0.48	0.45

SR	Observed		Simulated		Model Performance	
	mean	S.D.	mean	S.D.	NME	NMAE
Na^+	62.4	1.9	59.9	2.8	-0.04	0.06
Mg^{2+}	14.2	1.1	14.8	0.7	0.04	0.07
K^+	10.9	0.5	11.2	0.6	0.03	0.05
Ca^{2+}	33.2	1.7	30.8	1.6	-0.07	0.08
Cl^-	22.8	1.0	22.2	1.3	-0.02	0.07
NO_3^-_N	0.8	1.2	0.8	0.5	-0.07	0.76
SO_4^{2-}_S	22.4	1.2	23.0	1.5	0.03	0.08
ANC**	99.6	7.0	93.3	4.5	-0.06	0.07
Streamflow	5.8	1.9	5.4	1.9	-0.06	0.18

WOR	Observed		Simulated		Model Performance	
	mean	S.D.	mean	S.D.	NME	NMAE
Na^+	22.1	1.0	24.3	2.4	0.10	0.10
Mg^{2+}	27.5	2.3	24.3	1.8	-0.12	0.12
K^+	43.7	5.2	43.7	3.4	0.00	0.10
Ca^{2+}	17.4	1.3	15.5	0.8	-0.11	0.12
Cl^-	21.2	1.9	21.8	1.5	0.03	0.07
NO_3^-_N	11.4	13.7	0.6	0.2	-0.95	0.94
SO_4^{2-}_S	39.7	2.3	51.9	3.5	0.31	0.29
ANC**	43.7	10.3	21.5	1.2	-0.51	0.52
Streamflow	3.9	2.0	6.2	1.9	0.58	0.37

* S.D. denotes standard deviation.

** ANC denotes acidic neutralization capacity (Driscoll et al., 1994)

Note: The water chemistry data ranged from 1992 to 2012.

3.3.3 PCA analysis and change-points detection

By conducting PCA analysis of 17 simulated hydrological and biogeochemical variables/processes in vegetation, soil, and streams, I have found the first three principal components explained around 70% of total variance (Table 3-3), compared to 85% of variance explained at the Coweeta Basin. In addition, I detected change-points of PC1 scores and climate data from 1931 to 2100 and identified any concurrence between them.

At the SNP watersheds, transpiration and stream chemistry (base cations) are closely related to PC1s, compared to Coweeta Basin where transpiration, primary production, and soil and stream chemistry are closely related to PC1s. Additionally, the variance explained by PC1s in the SNP is lower than at the Coweeta Basin (40-50% at SNP vs. 50-70% at Coweeta). Based on the loadings of the principal components, PC1s represent the contrast between hydrology and alkalinity in both soil and stream. The time series of the PC1 scores are similar between PR and WOR, while different from SR, which could be attributed to PR and WOR being geographically closer and having more similar climatic and biogeochemical conditions. PC2 explained an additional 10 to 20 % of variance and was closely related to nitrogen uptake and net mineralization. NPP, SO_4^{2-}, and/or gross nitrogen immobilization are closely related to PC3, depending on the watershed studied. At the Coweeta Basin, soil nitrogen cycling (e.g., GrossNMin) is also closely related to PC2 but the variable is gross net mineralization. Still at the Coweeta Basin, stream SO_4^{2-} is closely related to PC3.

Table 3-3. Results of PCA analysis - loadings of the first three principal components at PR, SR, and WOR under different climate change scenarios. (The high values of loadings are highlighted).

	PR			SR			WOR		
RCP4.5	Comp 1	Comp 2	Comp 3	Comp 1	Comp 2	Comp 3	Comp 1	Comp 2	Comp 3
GPP	0.65	-0.10	-0.70	0.65	-0.31	-0.37	0.81	-0.25	0.18
NPP	0.07	-0.10	-0.88	0.29	-0.27	-0.46	0.55	-0.20	0.08
TotLitterMass	-0.79	0.14	-0.25	-0.66	0.35	-0.50	-0.46	0.34	-0.66
Streamflow	0.82	-0.04	-0.00	0.81	-0.08	-0.12	0.84	0.08	-0.00
Transpiration	0.80	-0.24	-0.20	0.70	-0.49	0.12	0.66	-0.48	0.38
Base Saturation	-0.72	-0.02	0.04	-0.94	-0.02	0.21	-0.78	-0.21	0.29
Al/Ca	0.53	-0.40	0.28	0.92	0.05	0.11	0.89	0.21	-0.19
NetNMin	0.15	-0.92	-0.05	0.14	-0.88	-0.21	0.56	-0.71	-0.23
GrossNMin	-0.42	-0.77	-0.21	-0.33	-0.73	-0.48	0.19	-0.68	-0.65
GrossNImmob	-0.79	-0.19	-0.26	-0.69	-0.18	-0.54	-0.33	-0.27	-0.80
N_uptake	0.04	-0.89	0.06	0.02	-0.92	0.05	0.34	-0.86	-0.07
ANC	0.11	-0.06	-0.02	-0.95	-0.05	-0.11	-0.73	-0.15	0.31
NO_3^-	0.39	-0.62	0.38	-0.19	-0.66	0.53	-0.38	-0.63	0.41
SO_4^{2-}	-0.50	-0.04	-0.08	-0.24	0.29	-0.56	-0.49	-0.08	-0.34
Ca^{2+}	-0.90	-0.26	0.06	-0.94	-0.21	0.18	-0.94	-0.28	0.03
Mg^{2+}	-0.89	-0.15	0.06	-0.94	-0.14	0.16	-0.92	-0.25	0.13
K^+	-0.93	-0.19	0.01	-0.93	-0.22	0.18	-0.95	-0.22	-0.05
Cumulative Variance (%)	40.5	58.3	68.5	47.5	67.3	78.8	46.2	63.5	76.8

Table 3-2 continued (RCP8.5).

	PR			SR			WOR		
RCP8.5	Comp 1	Comp 2	Comp 3	Comp 1	Comp 2	Comp 3	Comp 1	Comp 2	Comp 3
GPP	0.72	-0.20	-0.28	0.75	-0.37	0.02	0.89	-0.08	-0.21
NPP	0.10	-0.21	-0.26	0.26	-0.47	0.12	0.54	-0.28	-0.14
TotLitterMass	-0.81	-0.07	0.26	-0.81	-0.05	0.39	-0.74	-0.46	0.22
Streamflow	0.71	-0.12	0.02	0.70	-0.10	0.14	0.71	-0.02	0.14
Transpiration	0.83	-0.09	-0.37	0.84	-0.17	-0.32	0.83	0.19	-0.39
Base Saturation	-0.75	0.26	-0.59	-0.91	0.08	-0.30	-0.71	0.39	-0.53
Al/Ca	0.36	-0.39	0.02	0.43	0.27	-0.40	0.44	0.28	0.22
NetNMin	-0.00	-0.94	-0.13	0.38	-0.85	-0.12	0.70	-0.43	-0.49
GrossNMin	-0.51	-0.80	0.01	-0.35	-0.88	0.07	0.02	-0.83	-0.45
GrossNImmob	-0.81	-0.31	0.14	-0.80	-0.40	0.20	-0.64	-0.65	-0.11
N_uptake	-0.08	-0.83	-0.14	0.33	-0.78	-0.29	0.64	-0.33	-0.54
ANC	-0.75	0.20	-0.55	-0.94	-0.20	-0.00	-0.68	0.40	-0.52
NO_3^-	0.36	-0.42	-0.19	0.38	0.09	-0.75	0.50	0.51	-0.20
SO_4^{2-}	-0.31	-0.17	0.84	-0.14	-0.09	0.77	-0.44	-0.50	0.39
Ca^{2+}	-0.90	-0.04	-0.18	-0.87	-0.11	-0.44	-0.90	0.09	-0.29
Mg^{2+}	-0.87	0.01	0.06	-0.88	-0.01	-0.32	-0.84	0.15	-0.23
K^+	-0.92	-0.11	-0.22	-0.84	-0.14	-0.48	-0.90	-0.01	-0.31
Cumulative Variance (%)	42.2	59.2	70.3	45.9	62.5	76.4	47.5	63.3	75.3

I have identified fewer and earlier change-points in the PC1 scores at the SNP between 1931 and 2100 compared to the same temporal span at the Coweeta Basin. They occurred in the 1940s, 2010s, and 2060s (Table 3-4 and Fig. 3-3). The first two change-points were most likely driven by temperature change (Figure S3-1), while the third change-points are likely driven by both precipitation and temperature (Table 3-4). The change-points in the 2010s were also detected at the Coweeta Basin (Table 2-5). The

change-points of PC1 in 2040s and 2070s, driven by temperature or precipitation, at the Coweeta Basin are not detected in the SNP though there seems a shift in climate at the SNP during this time. At the Coweeta Basin, the change points of PC1 in the future were driven by precipitation at the lower-elevation watershed while the likely driver shifts to temperature at the higher-elevation watershed.

*Table 3-4. Change points of the scores of the first principal components (PC1s) in contrast to change points of climate (temperature and precipitation, * indicates change points of PC1s fall into the same decades in all three watersheds)*

		CP1*				CP2*			CP3*	
PR	PC1-RCP4.5	—	—	—	1988	2019	2024	—	—	—
	PC1-RCP8.5	1948	—	—	1989	—	2022	—	2063	—
	Temperature-RCP4.5	—	—	—	—	—	2024	—	—	—
	Temperature-RCP8.5	—	—	—	—	2011	—	2038	2067	—
	Precipitation-RCP4.5	—	1959	1970	—	2012	—	—	—	2092
	Precipitation-RCP8.5	—	1959	1970	—	2009	—	—	2058	—
SR	PC1-RCP4.5	1944	—	—	—	2018	—	2038	—	—
	PC1-RCP8.5	1944	—	—	—	2018	—	—	2063	2097
	Temperature-RCP4.5	—	—	—	—	—	2023	—	—	—
	Temperature-RCP8.5	—	—	—	—	2011	—	2038	2067	—
	Precipitation-RCP4.5	—	1959	1970	—	2012	—	—	—	2092
	Precipitation-RCP8.5	—	1959	1970	—	2009	—	—	2058	—
WOR	PC1-RCP4.5	1944	1959	1971	—	2011	—	—	—	—
	PC1-RCP8.5	1944	—	—	1994	2017	—	—	2058	—
	Temperature-RCP4.5	—	—	—	—	—	2023	—	—	—
	Temperature-RCP8.5	—	—	—	—	2011	—	2038	2067	—
	Precipitation-RCP4.5	—	1959	1970	—	2012	—	—	—	2092
	Precipitation-RCP8.5	—	1959	1970	—	2009	—	—	2058	—

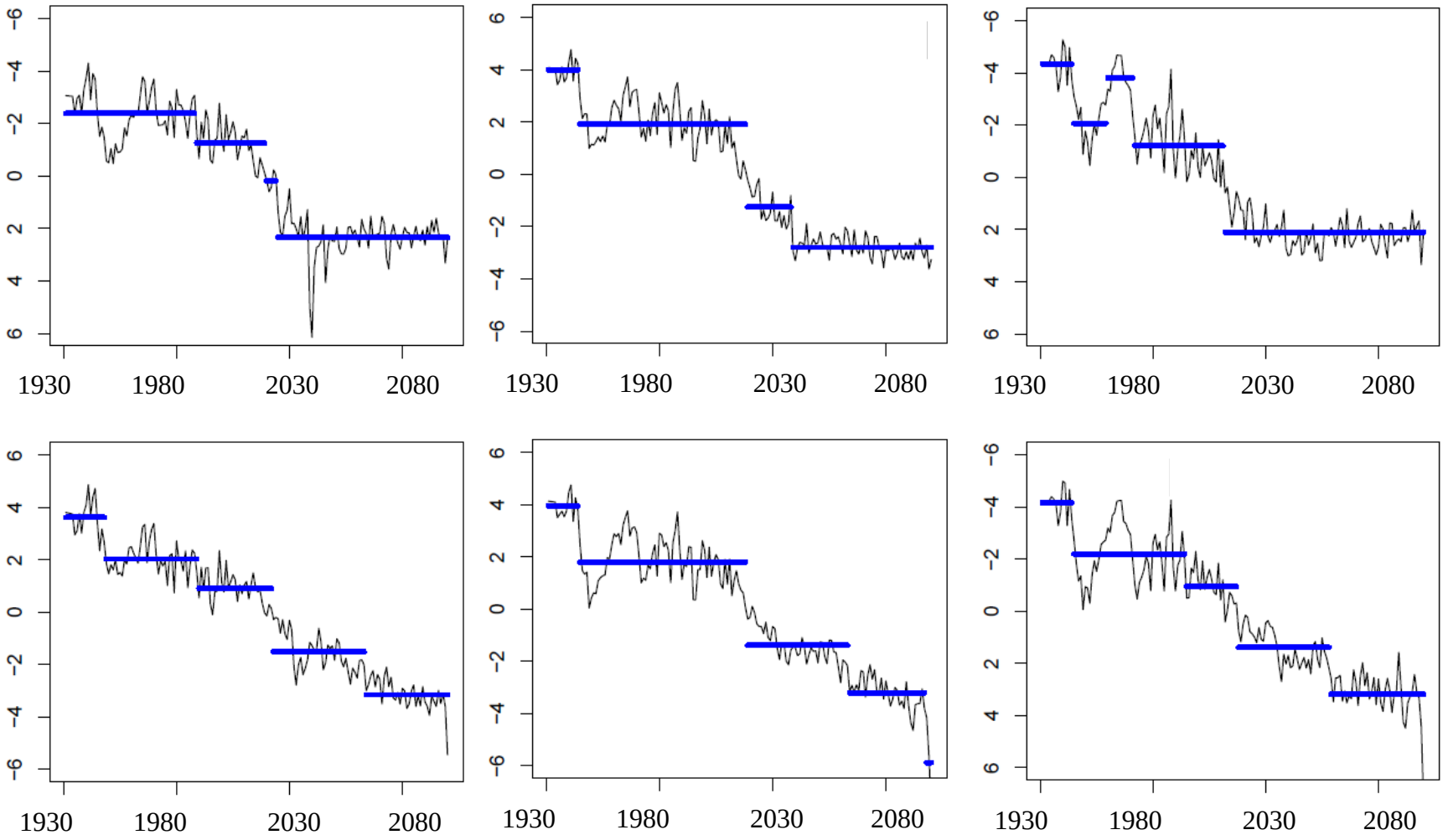

Fig. 3-3 Change points of the PC1 scores between 1931 and 2100 based on means at PR (left), SR (middle), and WOR (right); and RCP4.5 (Top) and RCP8.5 (Bottom).

3.3.4 Seasonality of climate change impacts

I focused on the biological and chemical variables that are closely related to the first three principal components. In general, all three watersheds in the SNP show similarly seasonal pattern for these key processes / variables (transpiration, NPP, and ANC).

Transpiration (Fig.3-4) increases in all four seasons across all the three watersheds under climate change. However, the increase is relatively small in summer and winter compared to spring and fall. In addition, the change under RCP8.5 is larger than RCP4.5. While streamflow is predicted to increase under changing climate and more so under RCP8.5, summer generally shows the lowest increase in streamflow at three watersheds among the four seasons (Fig. S3-2).

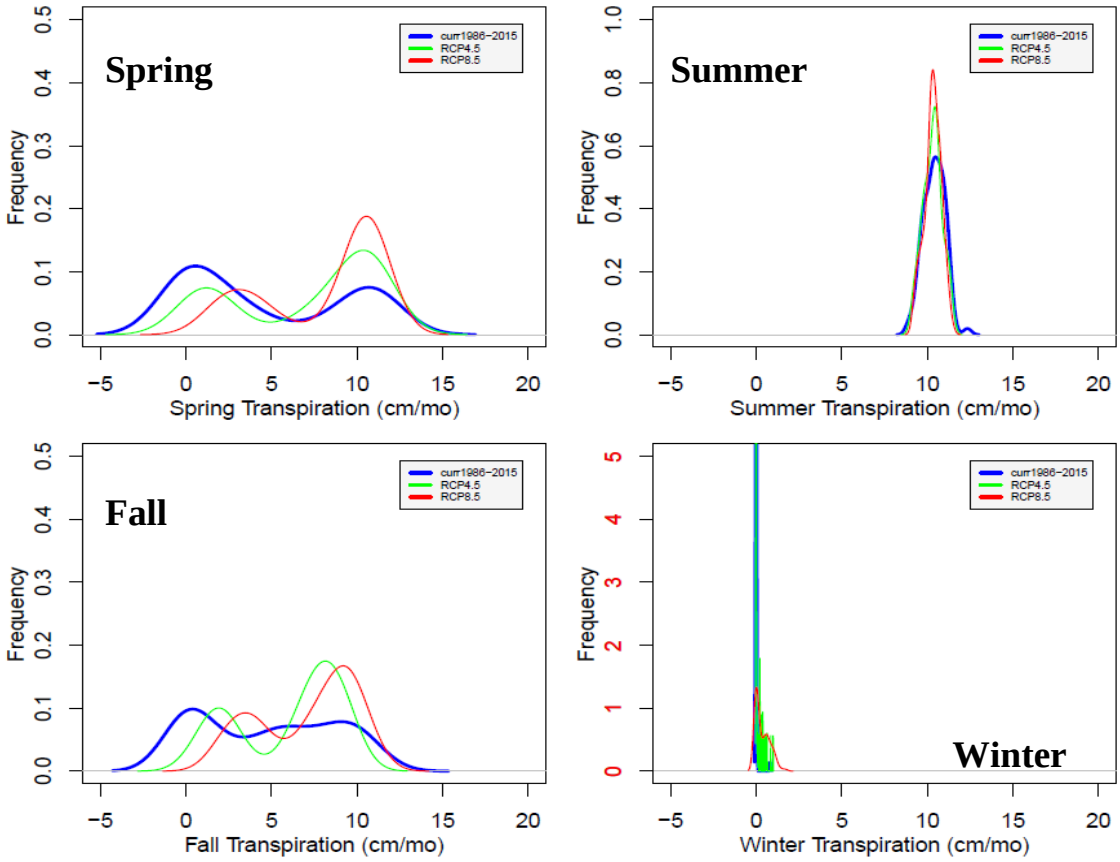

Fig. 3-4a PR comparison of transpiration by seasons between current (1986-2015) and future climate scenarios (2071-2100, RCP4.5 and 8.5 – average of four climate models)

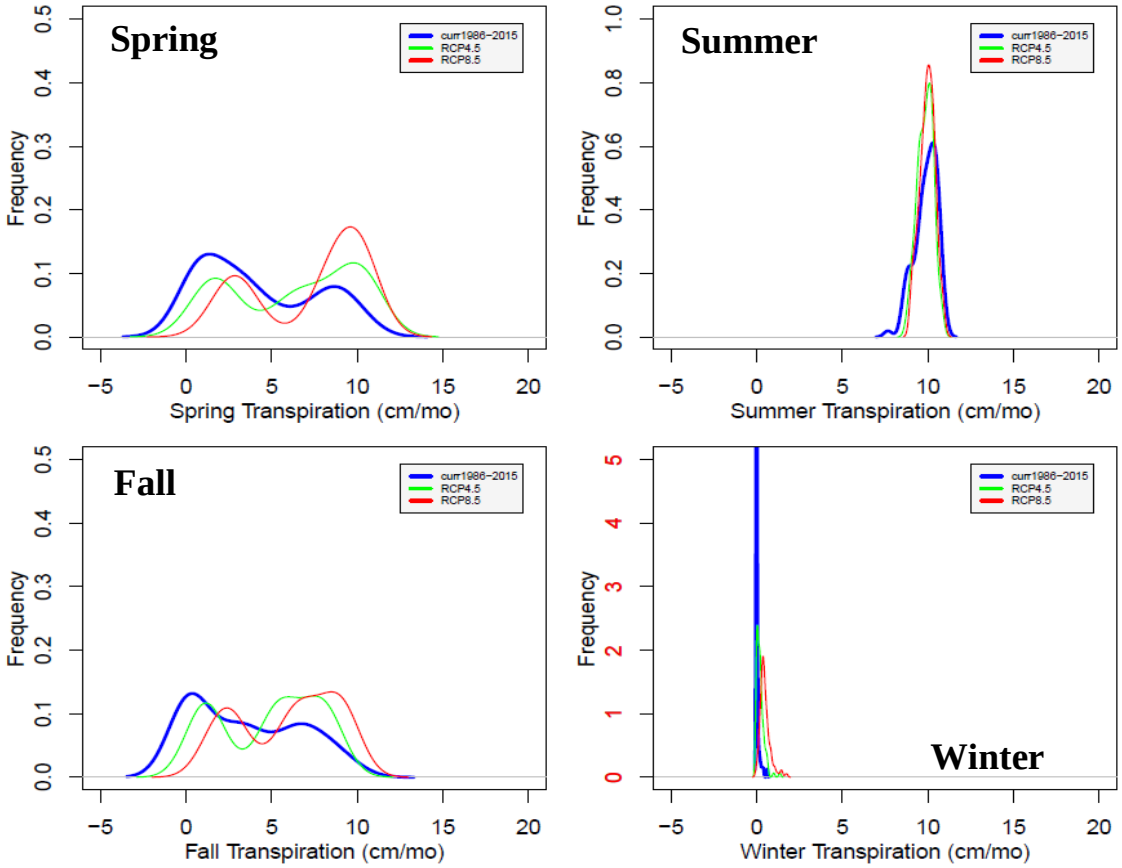

Fig. 3-4b WOR comparison of transpiration by seasons between current (1986-2015) and future climate scenarios (2071-2100, RCP4.5 and 8.5 – average of four climate models)

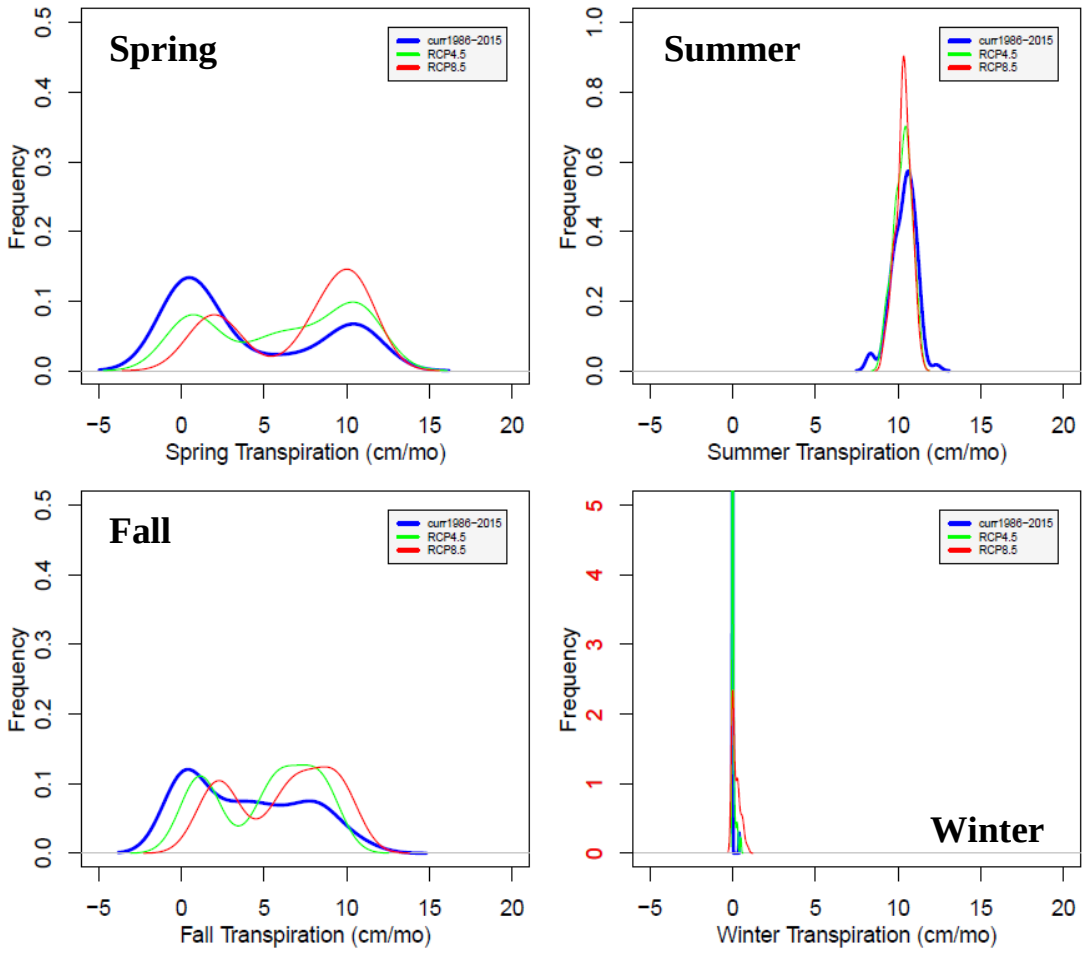

Fig. 3-4c SR comparison of transpiration by seasons between current (1986-2015) and future climate scenarios (2071-2100, RCP4.5 and 8.5 – average of four climate models)

The largest change of both NPP and GPP (Fig. 3-5, Fig. S3-3) is predicted to occur in summer, and they will decrease under both climate scenarios with more decrease under RCP8.5. GPP and NPP will increase slightly in spring and fall and the variance becomes smaller. In winter, SR and PR show minimal changes in NPP while WOR shows a slight increase in NPP. At the Coweeta Basin, both watersheds show clear increasing trends in spring and fall. In summer, there is minimum change of NPP under RCP4.5 and it decreases under RCP8.5. The change of NPP and GPP is also very small in

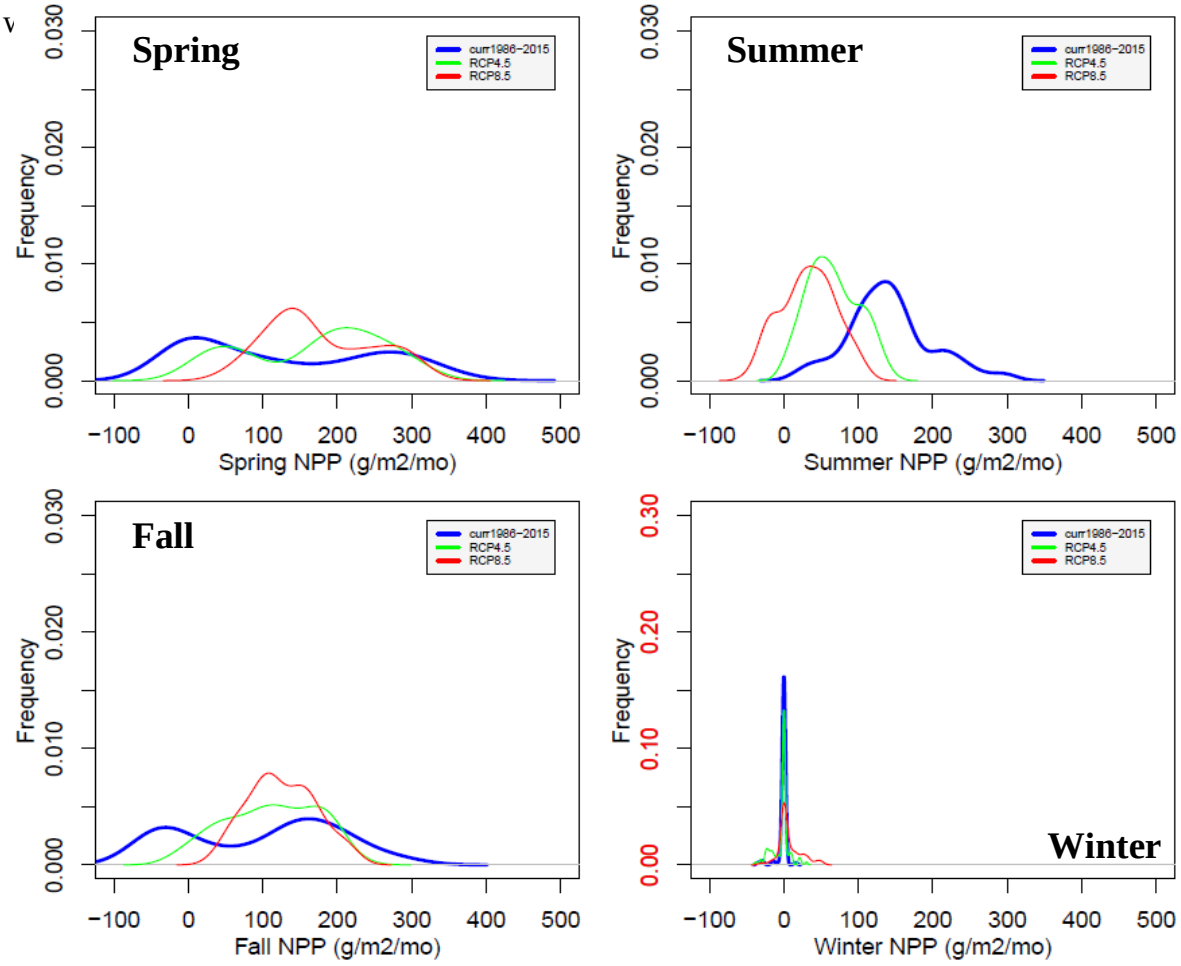

Fig. 3-5a PR comparison of NPP by seasons between current (1986-2015) and future climate scenarios (2071-2100, RCP4.5 and 8.5 – average of four climate models)

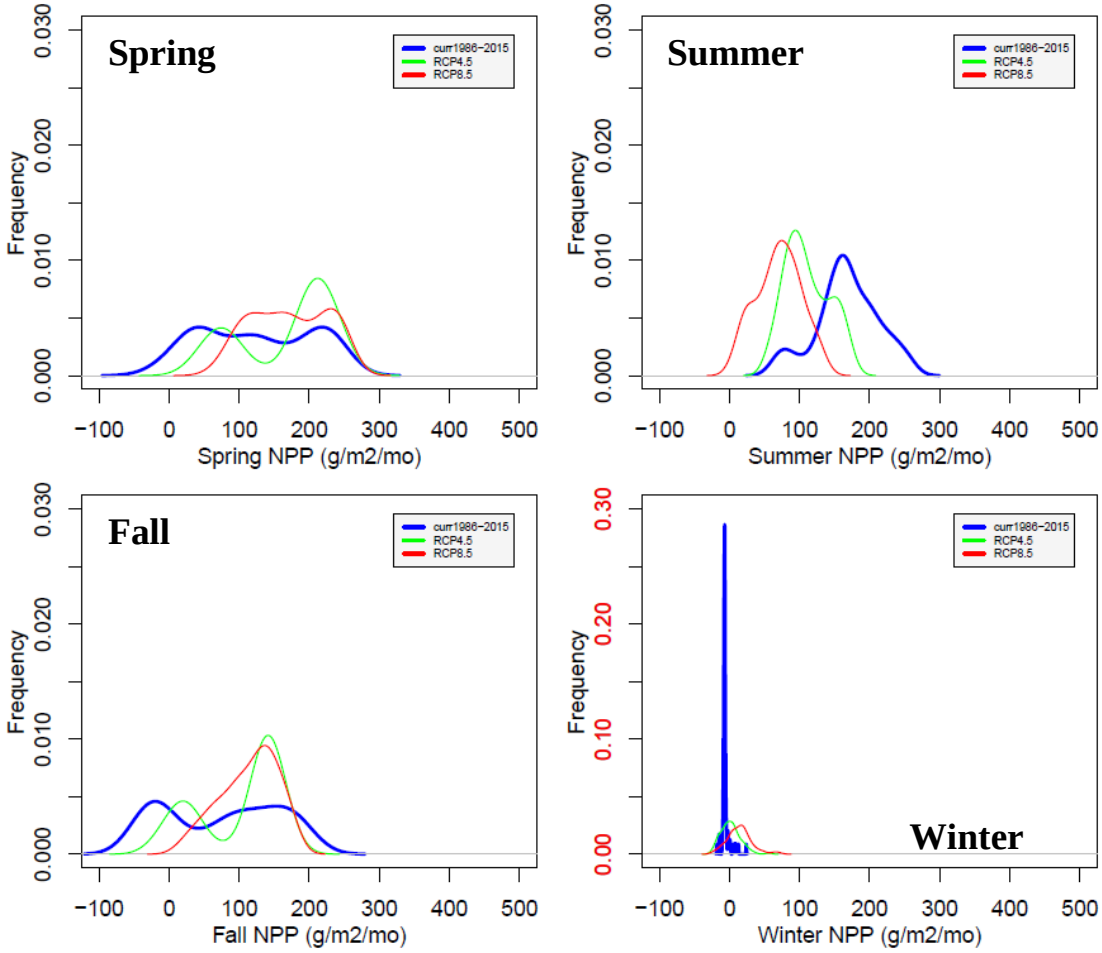

Fig. 3-5b WOR comparison of NPP by seasons between current (1986-2015) and future climate scenarios (2071-2100, RCP4.5 and 8.5 – average of four climate models)

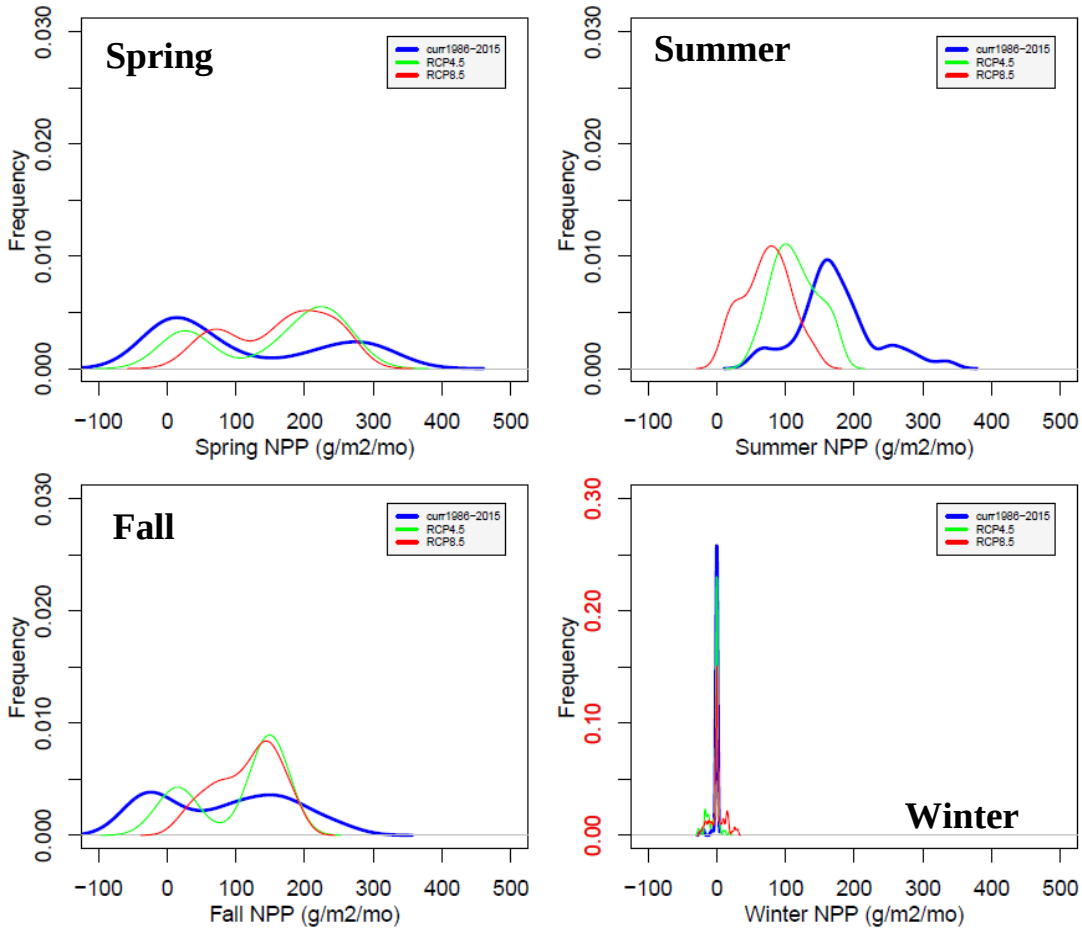

Fig. 3-5c SR comparison of NPP by seasons between current (1986-2015) and future climate scenarios (2071-2100, RCP4.5 and 8.5 – average of four climate models)

ANC (Fig. 3-6) and concentrations of Ca^{2+}, K^{+}, and SO_4^{2-} in streams (Fig. S3-4 to S3-6) are predicted to decrease under changing climate for all seasons compared to current climate at all three watersheds, except a slight increase of ANC at the WOR. The decrease of ANC is very similar or even slightly larger in RCP4.5 compared to RCP8.5, probably driven by larger precipitation predictions in one of the climate models (HadGEM2) under RCP4.5 than under RCP8.5. Generally, winter and fall have the greatest decrease in ANC at PR and SR (>40%). At SR, the reduction of ANC is more pronounced under RCP8.5 than under RCP4.5. Similar decreasing trend in ANC is also

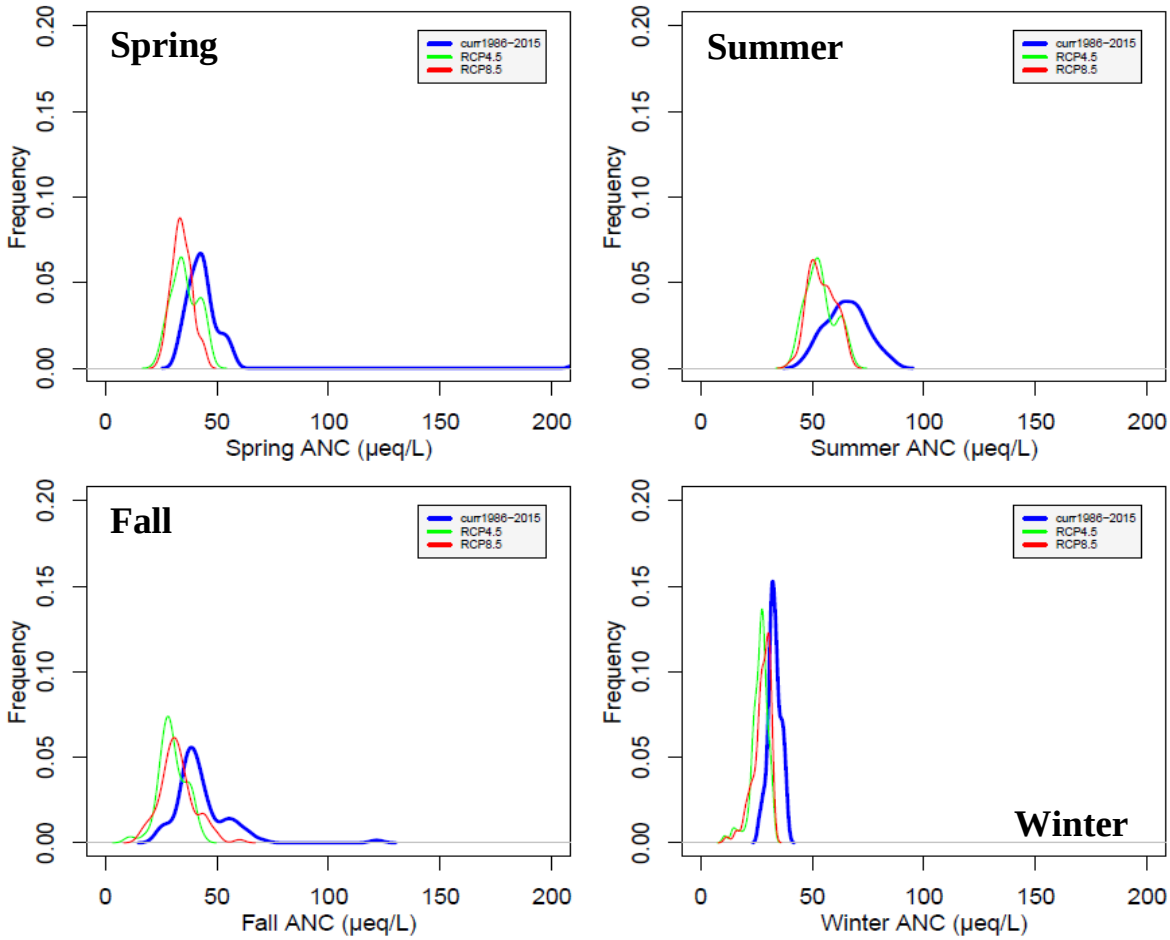

Fig. 3-6a PR comparison of ANC by seasons between current (1986-2015) and future climate scenarios (2071-2100, RCP4.5 and 8.5 – average of four climate models)

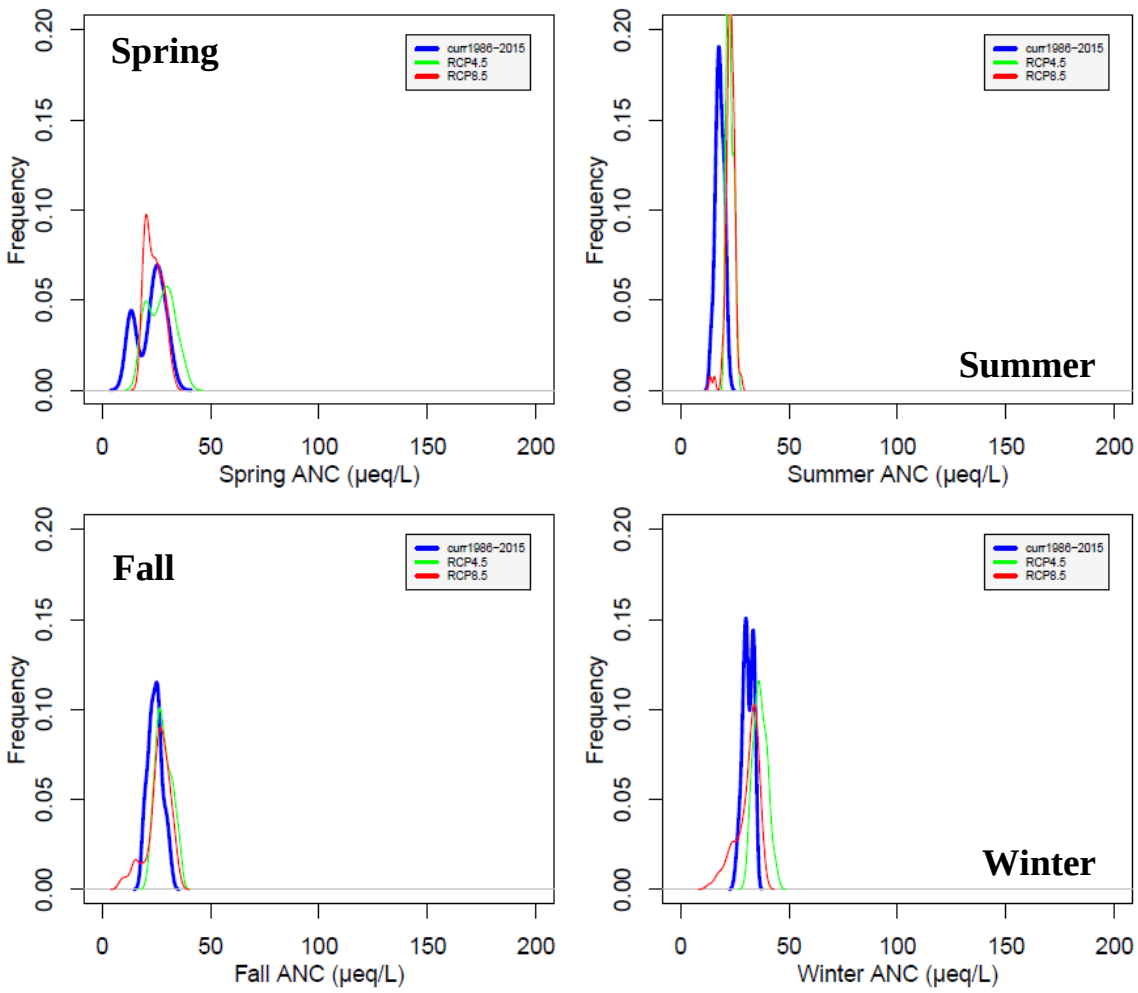

Fig. 3-6b WOR comparison of ANC by seasons between current (1986-2015) and future climate scenarios (2071-2100, RCP4.5 and 8.5 – average of four climate models)

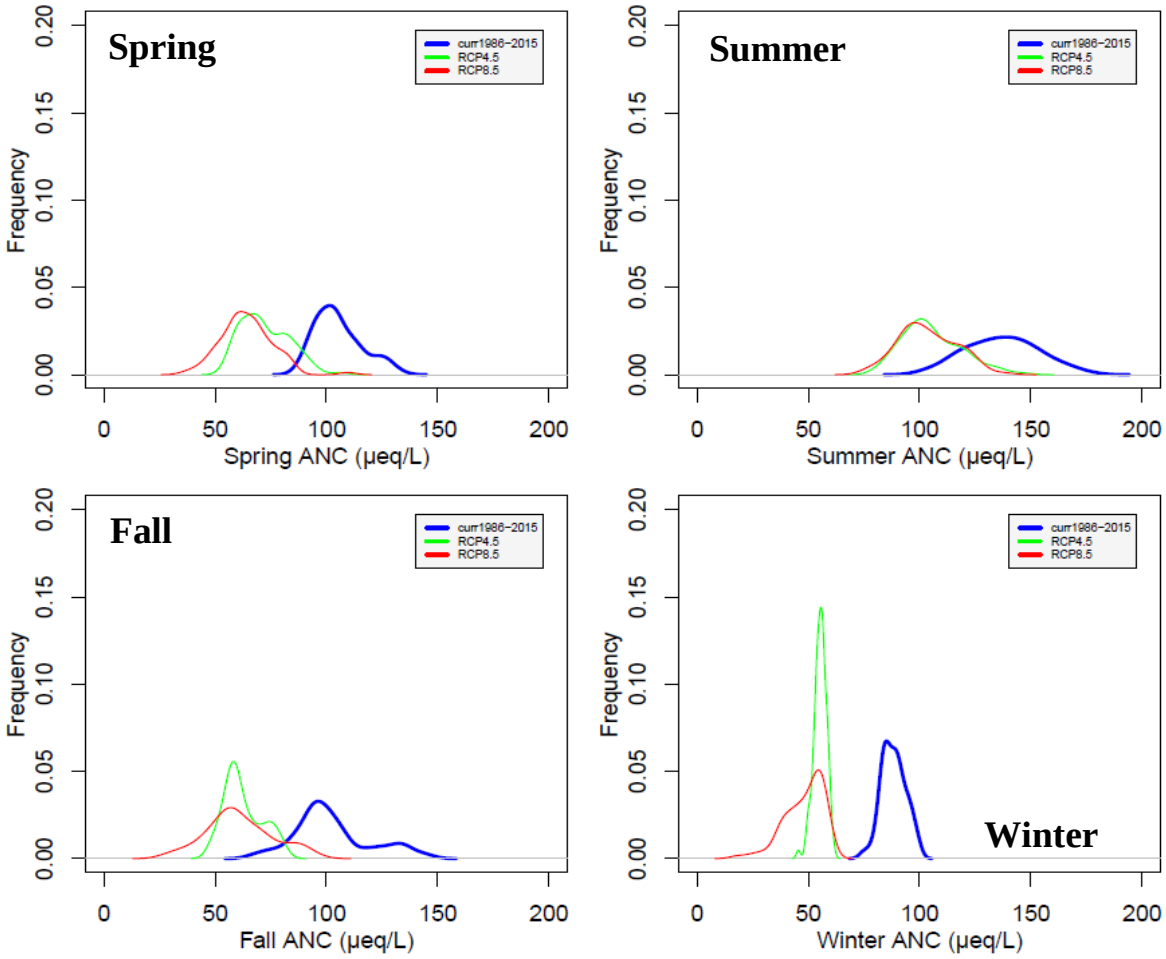

Fig. 3-6c SR comparison of ANC by seasons between current (1986-2015) and future climate scenarios (2071-2100, RCP4.5 and 8.5 – average of four climate models)

3.3.5 Combined impacts of change in climate and acidic deposition

The change in deposition of NO_3^-, SO_4^{2-}, and NH_4^+ follows a linear increase/decrease from current (i.e., 2016) to 2036 and deposition is maintained constant after 2036 (Fig. 3-7) (Fakhraei et al. 2016). Each level differs from next by ±10% of current level with the change ranging from –100% to +100% of current level.

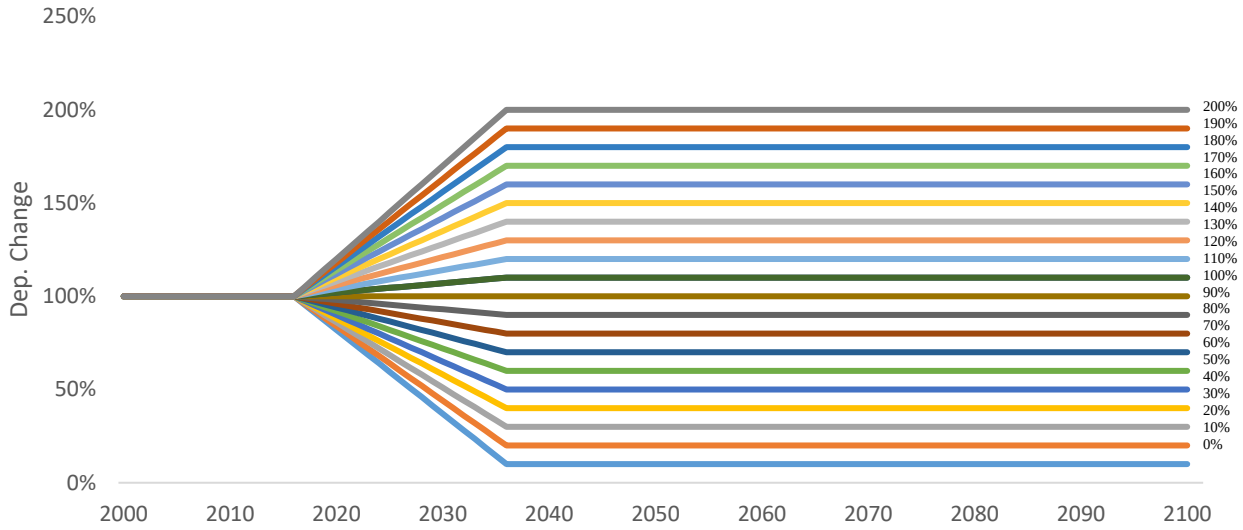

Fig. 3-7 Deposition change regime from 2016 to 2036 and to 2100 (2015 as current level). Each line represents a percentage of current deposition level indicated on the figure, with a total of 21 scenarios.

The change of acidic deposition is likely to shift the response of the key biogeochemical variables to climate change, especially in ANC in streams. In general, the shift is more pronounced with RCP8.5 than with RCP4.5. ANC decreases when sulfate, nitrate and ammonia deposition increases under climate change across the five sites (Fig. 3-7). The watersheds with lower ANC under the current climate scenario (i.e., WS27 and PR) are predicted to show greater sensitivity in response to deposition change than the other watersheds. Under the current climate, PR has the lowest ANC among the five watersheds (13.3 μeq/L, based on observation data from 1992 to 2012, Table 3-2). When depositions of sulfate, nitrate and ammonia double the current level under RCP4.5, ANC

is predicted to drop to the level the same as that under RCP 8.5 but without changes of the acidic depositions. At the Coweeta Basin WS27, it takes only 50% of increase in acidic depositions for the ANC under RCP4.5 to decrease to the same ANC level that is under RCP8.5 without change of the depositions. Meanwhile, same percentage change of deposition leads to larger change of ANC under RCP8.5 than the RCP4.5, and this pattern is more distinct at the watersheds in the SNP.

When I applied reduction of acidic deposition, the ANC is predicted to increase, however, the increase at WS18 is less than the decrease of ANC with the same percentage of increase in the acidic deposition for both RCP4.5 and 8.5 (Fig. 3-8). This shows recovery of ANC will be delayed even with a reduction of acidic deposition under climate change.

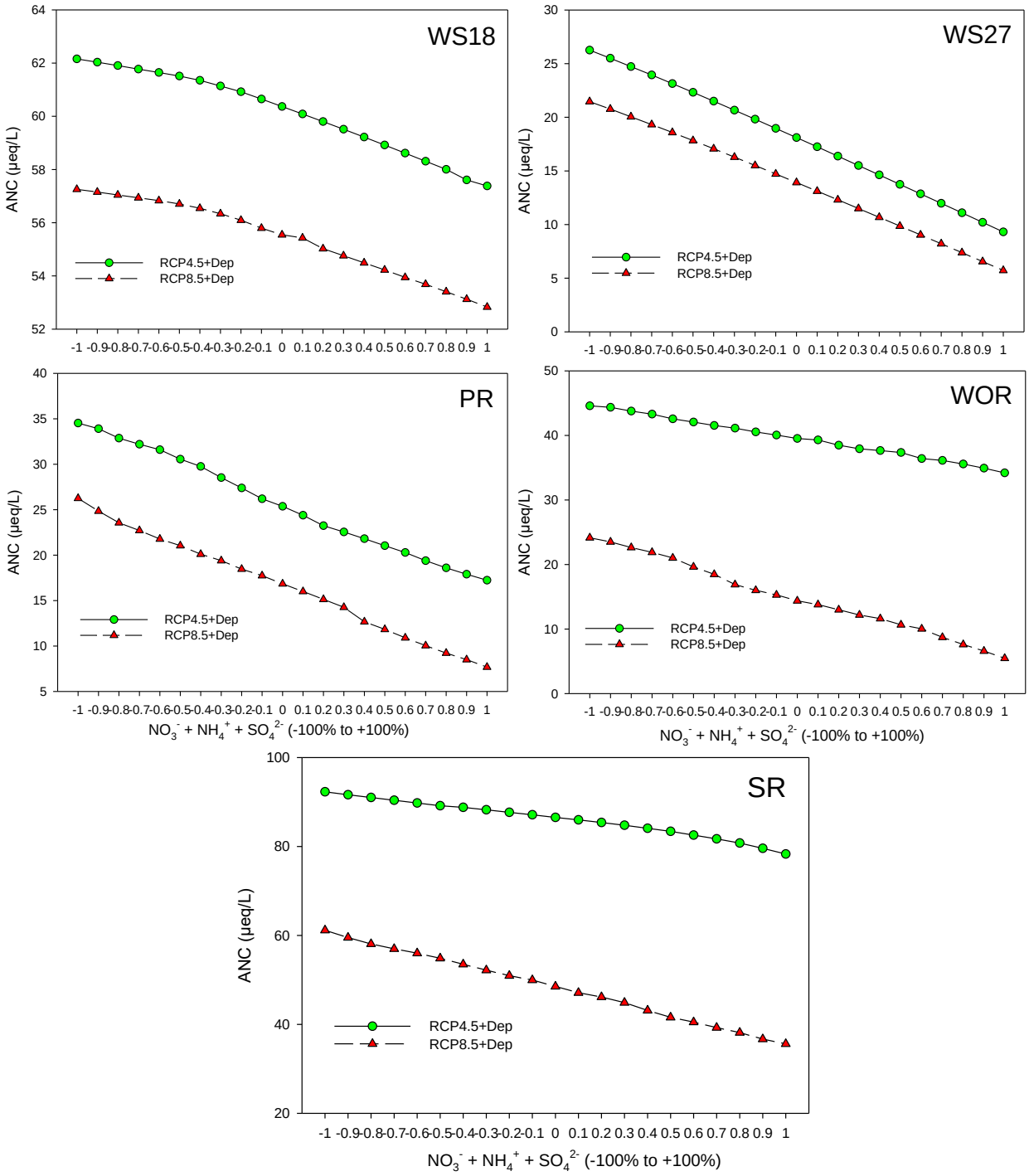

Fig. 3-8 ANC vs. Deposition changes in NO_3^-, NH_4^+, and SO_4^{2-} (ANC data between 2071 and 2100)

NPP's response to change of acidic deposition varies by watershed studied (Fig. 3-9). At WS18 in Coweeta Basin, NPP is similar under both climate scenarios. At the Coweeta Basin watersheds, NPP will increase as deposition rises for both climate change scenarios although NPP is higher under RCP8.5 than RCP4.5. At the three watersheds in the SNP, NPP is higher under RCP4.5 than RCP8.5. The increase of acidic deposition has little impact on NPP under RC8.5 while it leads to decrease of NPP in the SNP under RCP4.5.

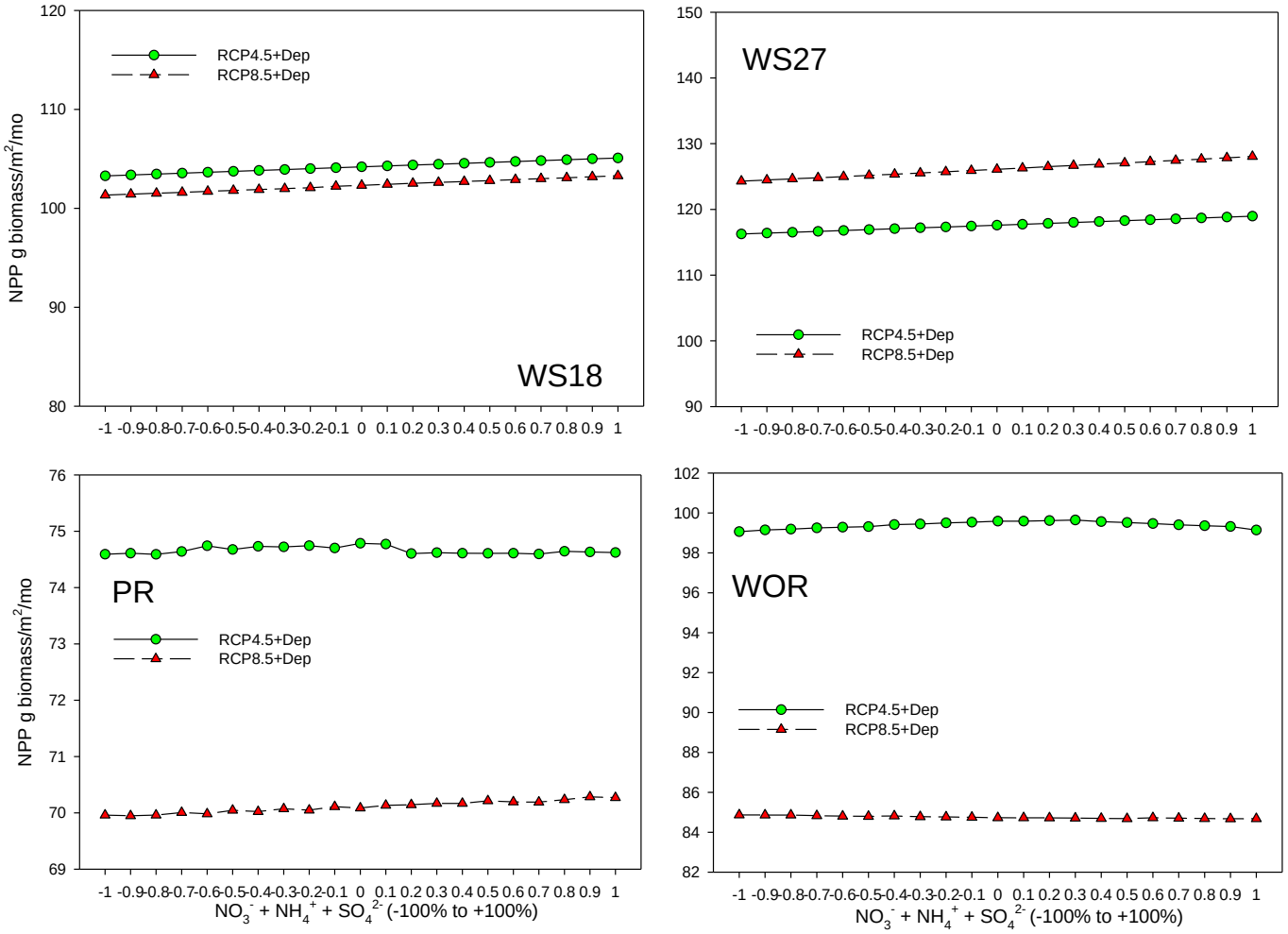

Fig. 3-9 NPP vs. Deposition changes in NO_3^-, NH_4^+, and SO_4^{2-} (NPP data between 2071 and 2100) for all 21 scenarios.

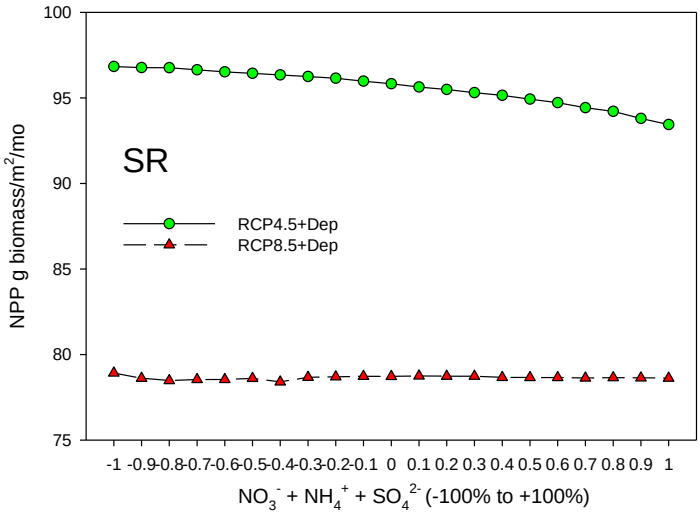

Fig. 3-9 Continued.

Transpiration (Fig. 3-10) is predicted to increase when depositions increase at the majority of the watersheds under both climate change scenarios. I detected the increase at the Coweeta Basin for both scenarios, while the increase is only clear at the SR and WOR in the SNP under RCP4.5. The change of transpiration with change of depositions is small at the PR for both RCP4.5 and 8.5. Meanwhile, transpiration under RCP8.5 is higher than RCP4.5 at all five watersheds.

Streamflow (Fig. S3-7), on the other hand, shows decreases with increase of acidic depositions at all five watersheds under RCP4.5 and Coweeta Basin under RCP8.5.

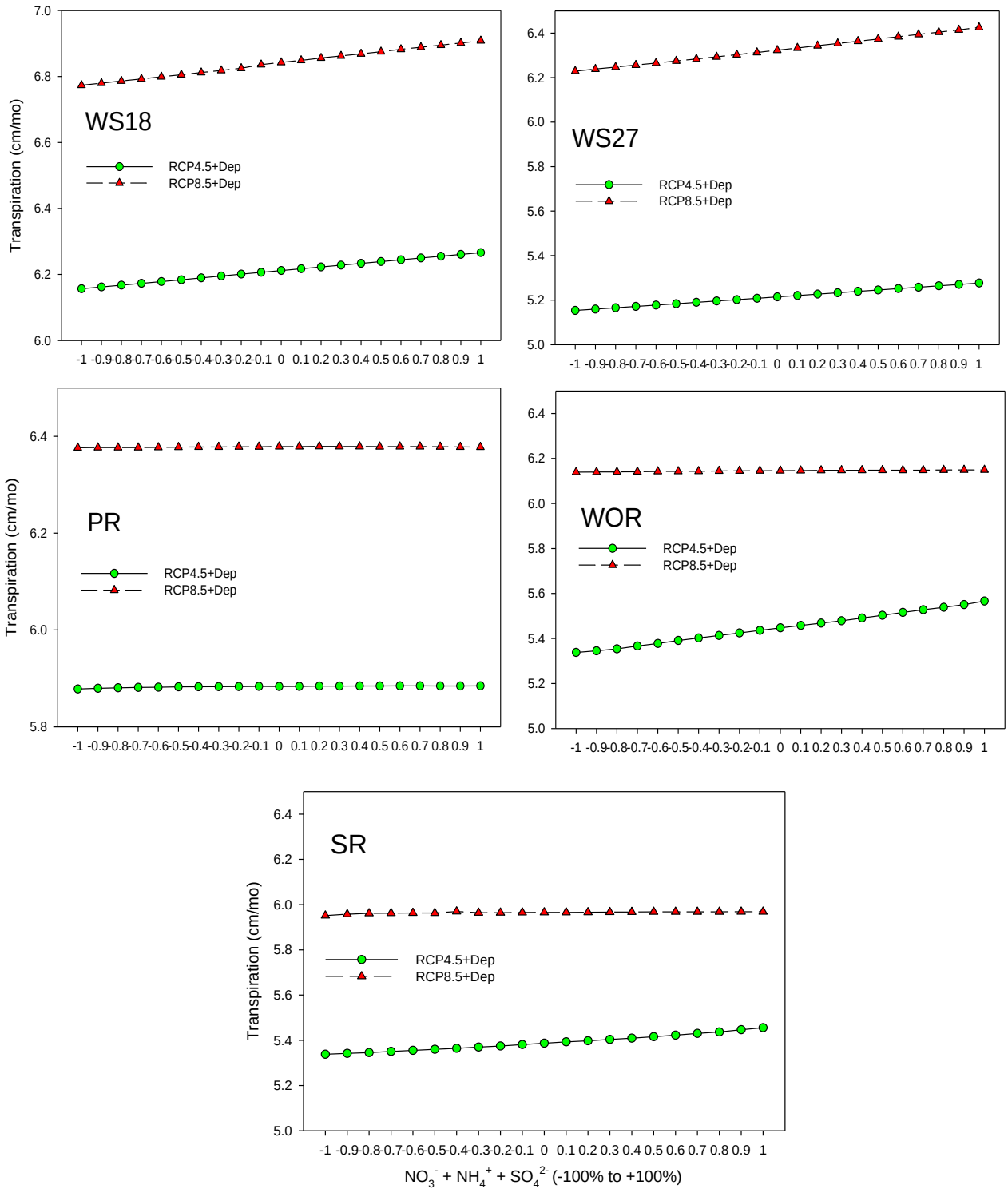

Fig. 3-10 Transpiration vs. Deposition changes in NO_3^-, NH_4^+, and SO_4^{2-} (NPP data between 2071 and 2100) for all 21 scenarios.

3.3.6 Synthesis of five watersheds with and without deposition change

The spatial pattern of the impact of climate change is complicated by the climate change scenarios, biogeochemical processes, and seasons. The 95% credible intervals of the coefficients for elevation and latitudes all contain 0, which shows a lack of significantly latitudinal or elevational patterns based on the five sites. However, some 50% credible intervals contain 0, especially in elevation or latitude's impact on the response of biogeochemical cycles to temperature, indicating some weak latitudinal or elevational pattern.

NPP is more sensitive to temperature in spring, summer, and fall than in winter (Fig. 3-11) with positive temperature impacts on NPP in spring and fall, and a negative impact on NPP in summer. Temperature's impact on NPP in winter is mixed but is mostly positive based on 50% and 95% of credible intervals (CIs) of the coefficient for temperature under RCP8.5 when modeling NPP. However, the impact is either positive at WS18 and WOR (95% CIs) or negative at PR and SR (50% CI) or negligible at WS27 under RCP4.5. NPP at the WS27 in the Coweeta shows the largest increase per unit increase of temperature in spring and fall. NPP responds positively to increase of precipitation in summer under RCP4.5 and 8.5 at the high-latitude sites in the SNP while the increase is negligible at the low-latitude sites at the Coweeta Basin. There are fewer significant effects of precipitation compared to temperature on NPP across the five sites. Elevation enhances response of NPP to temperature under RCP8.5. Latitude mitigates its response to temperature under RCP4.5 but enhances its response to temperature under RCP8.5.

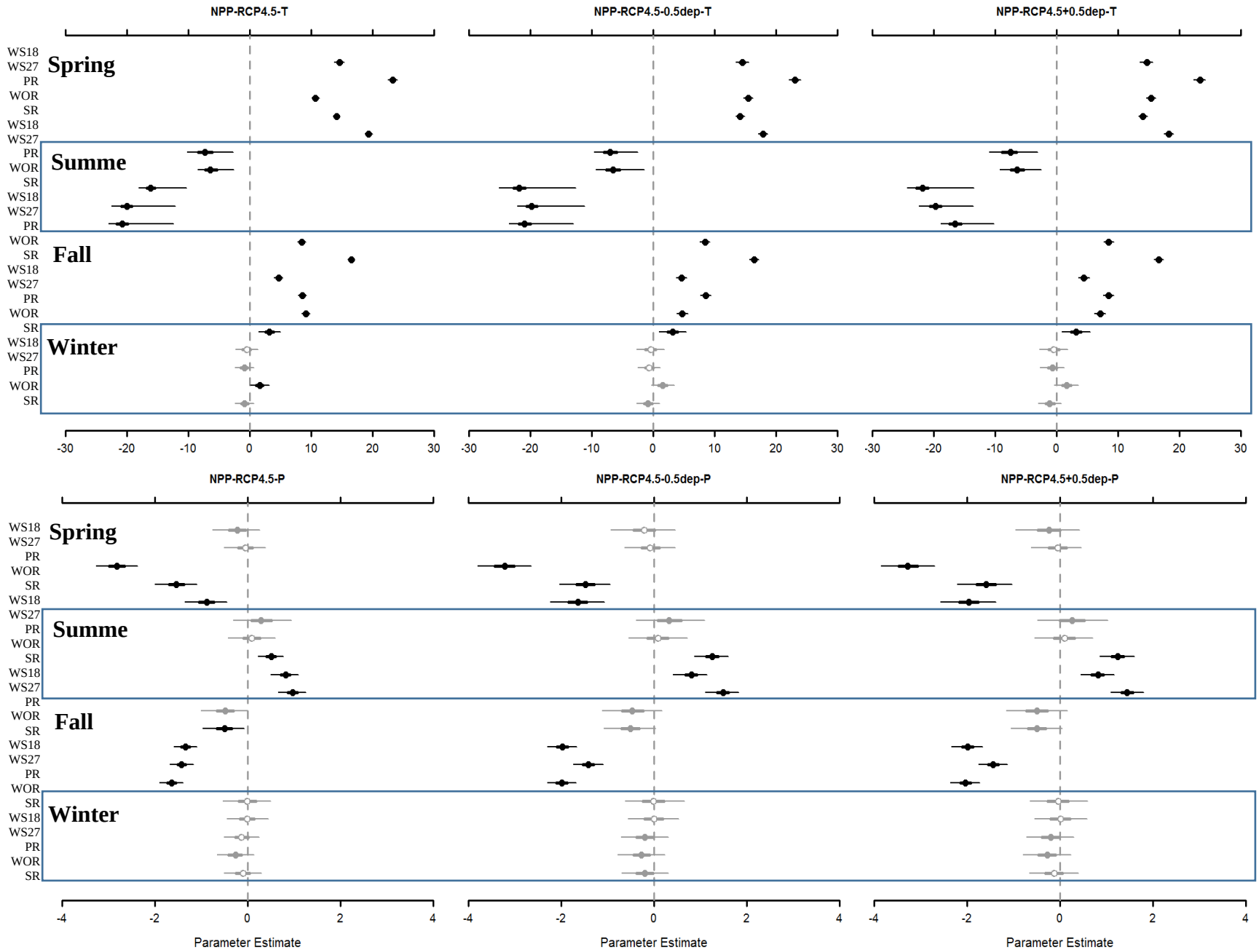

Fig. 3-11a NPP's sensitivity to Temperature (top) and Precipitation (bottom) without (left) and with deposition change (-50%: middle and +50%: right) by seasons (y-axis from top to bottom each season grouped by sites are spring, summer, fall, and winter) under RCP4.5.

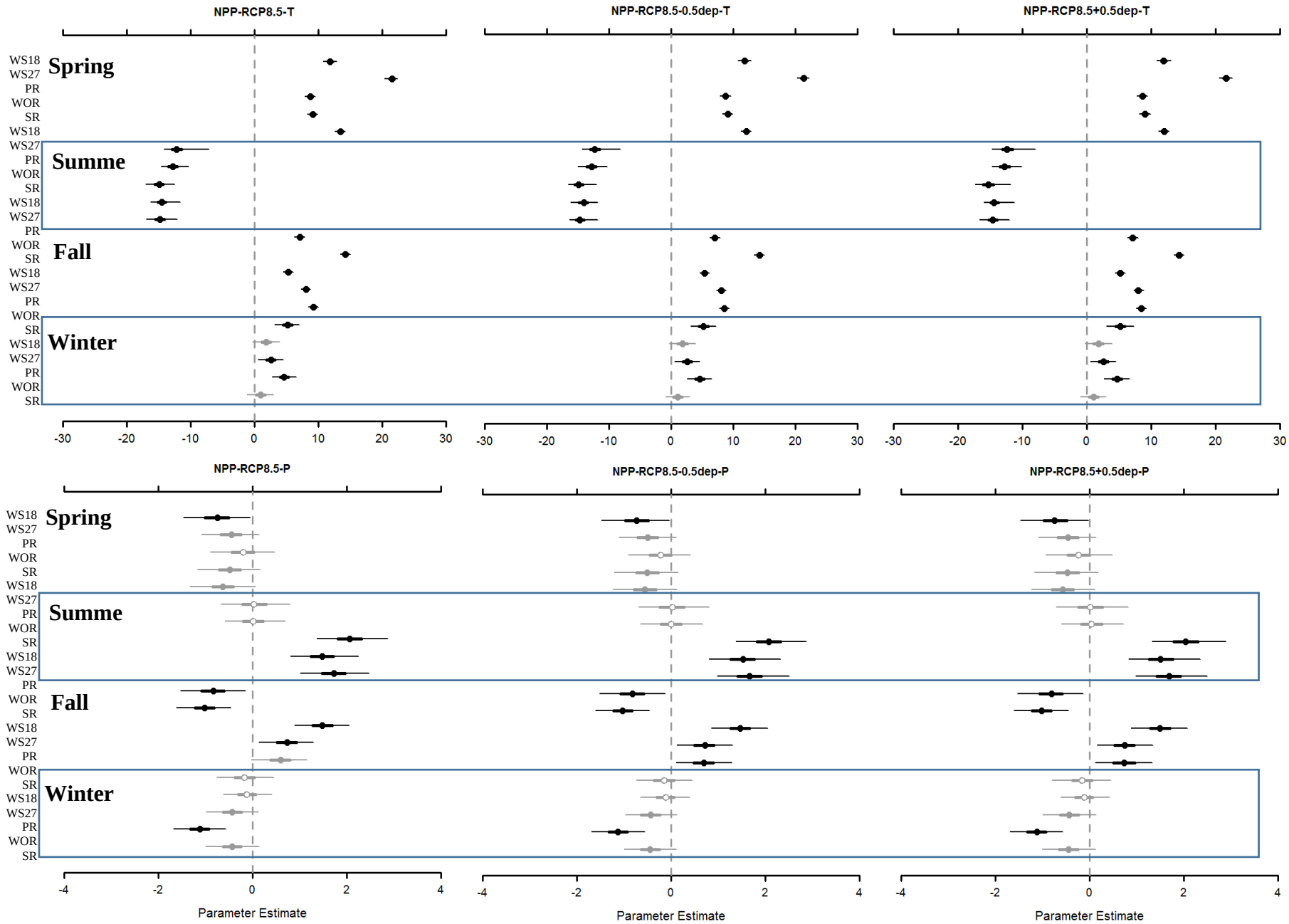

Fig. 3-11b NPP's sensitivity to Temperature (top) and Precipitation (bottom) change without (left) and with deposition change (-50%: middle and +50%: right) by seasons (y-axis from top to bottom each season grouped by sites are spring, summer, fall, and winter) under RCP8.5.

Transpiration positively responds to temperature except at the Paine Run under RCP4.5 and three high-latitude sites under RCP8.5 (Fig. 3-12). The response of transpiration to precipitation is negligible at most of the sites and seasons except at Paine Run in spring (negative), summer (positive) and fall (negative) under RCP4.5. Under RCP8.5, precipitation has a negative impact on transpiration at most of the sites in most seasons except the three high-latitude sites in summer. Latitude increases the response of transpiration to precipitation under RCP8.5. Other impacts of latitude or elevation on the responses of transpiration to temperature or precipitation are negligible.

The more integrated in-stream variables including calcium concentrations and ANC have more mixed responses to temperature and precipitation than NPP or transpiration depending on season, site, and climate change scenarios. ANC's response to climate change is enhanced by elevation under both scenarios (Fig. 3-13), while latitude enhances the response under RCP4.5, and to temperature under RCP8.5, but mitigates the response to precipitation under RCP8.5. Latitude and elevation play negligible roles in affecting calcium's response to climate change (Fig. 3-14).

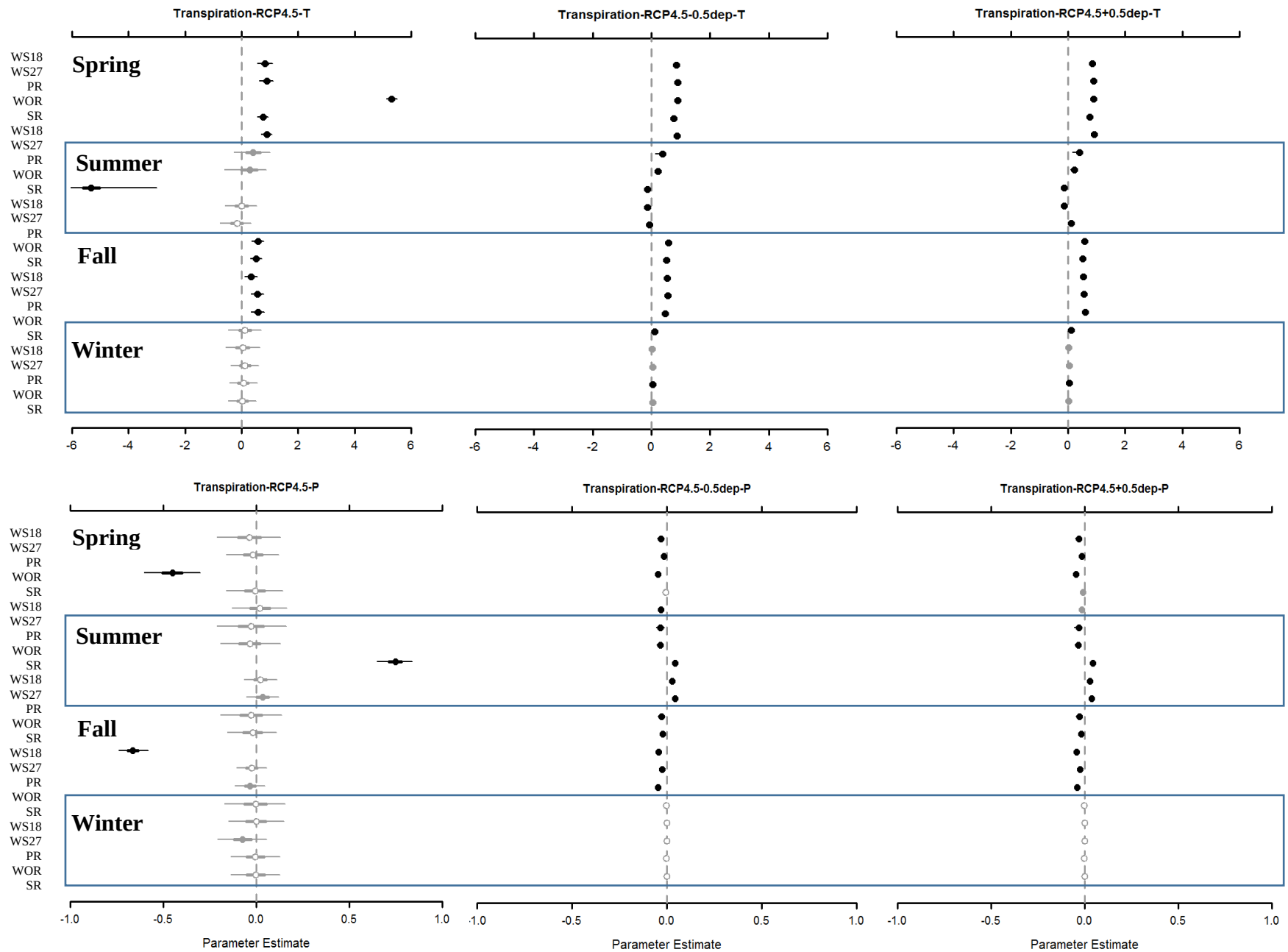

Fig. 3-12a Transpiration's sensitivity to Temperature (top) and Precipitation (bottom) change without (left) and with deposition change (-50%: middle and +50%: right) by seasons (y-axis from top to bottom each season grouped by sites are spring, summer, fall, and winter) under RCP4.5.

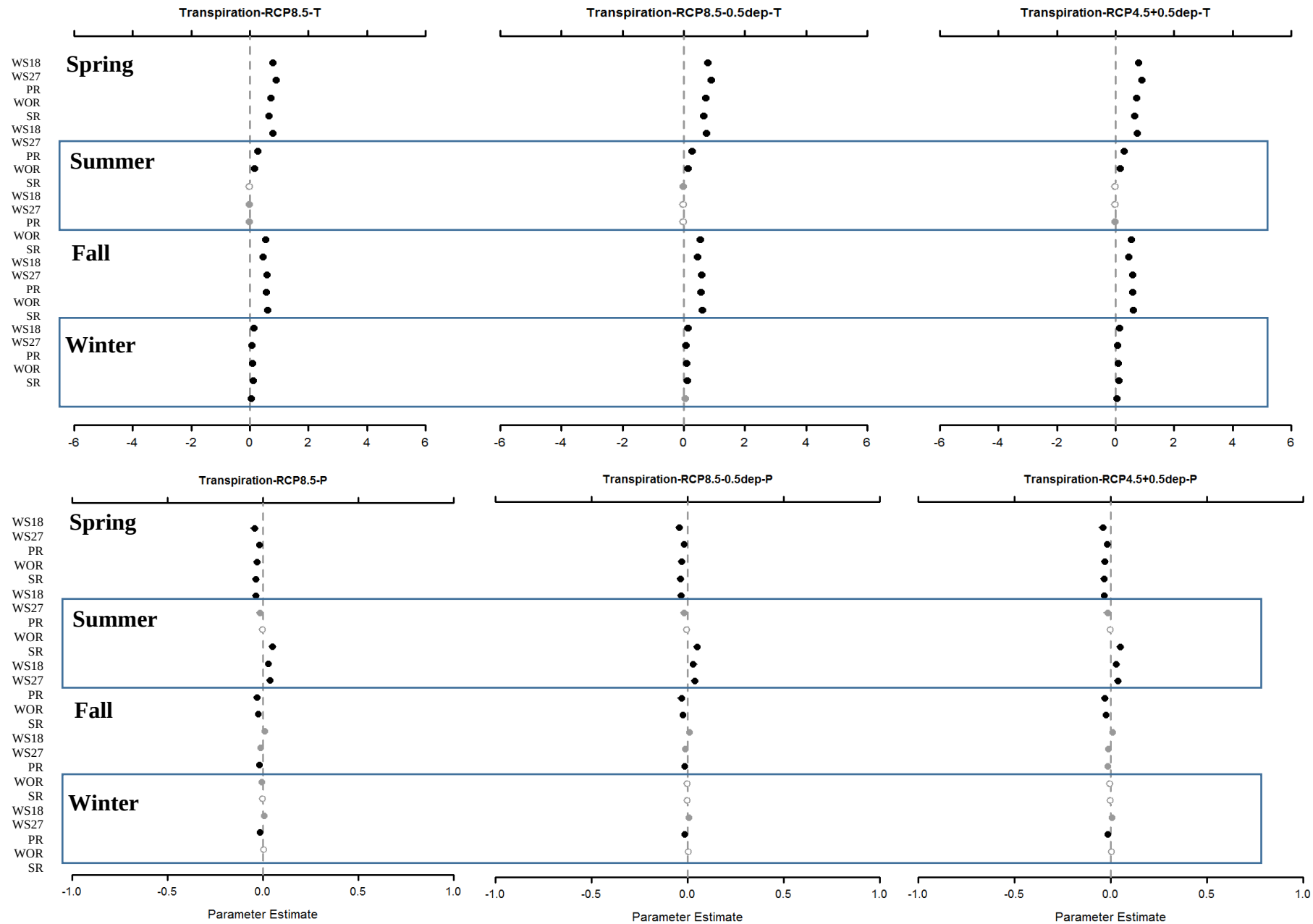

Fig. 3-12b Transpiration's sensitivity to Temperature (top) and Precipitation (bottom) change without (left) and with deposition change (-50%: middle and +50%: right) by seasons (y-axis from top to bottom each season grouped by sites are spring, summer, fall, and winter) under RCP8.5.

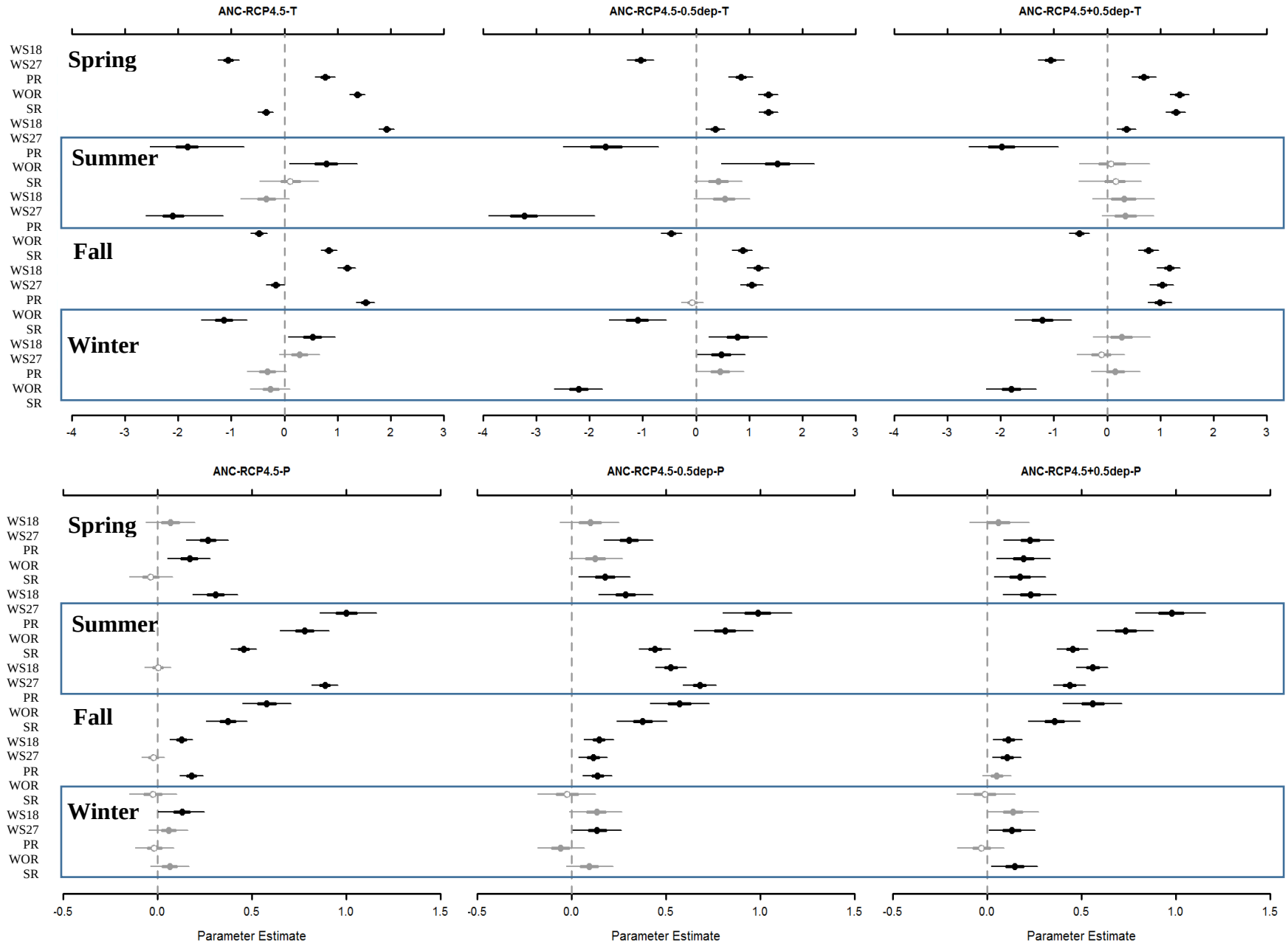

Fig. 3-13a ANC's sensitivity to Temperature (top) and Precipitation (bottom) change without (left) and with deposition change (-50%: middle and +50%: right) by seasons (y-axis from top to bottom each season grouped by sites are spring, summer, fall, and winter) under RCP4.5.

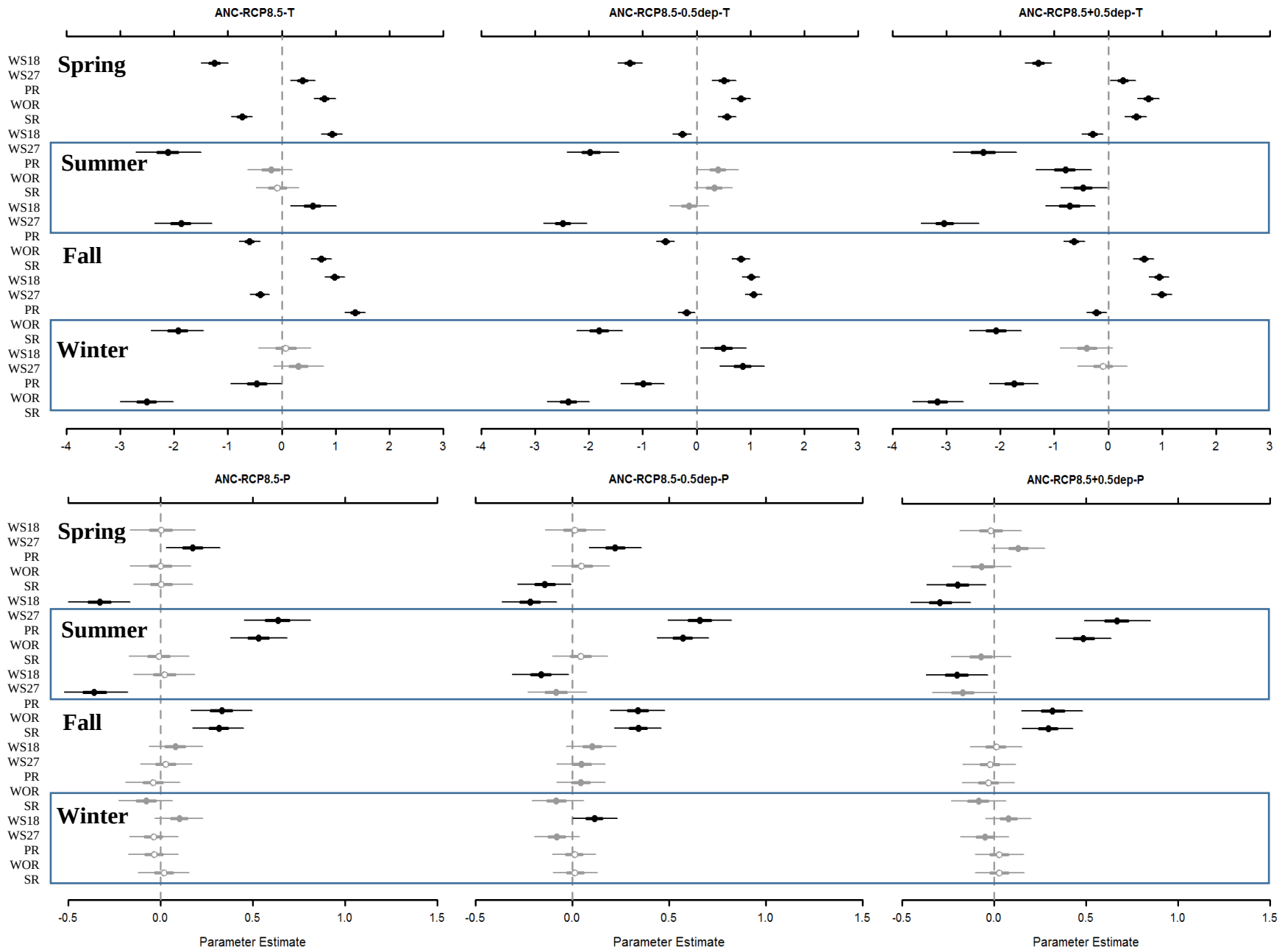

Fig. 3-13b ANC's sensitivity to Temperature (top) and Precipitation (bottom) change without (left) and with deposition change (-50%: middle and +50%: right) by seasons (y-axis from top to bottom each season grouped by sites are spring, summer, fall, and winter) under RCP8.5.

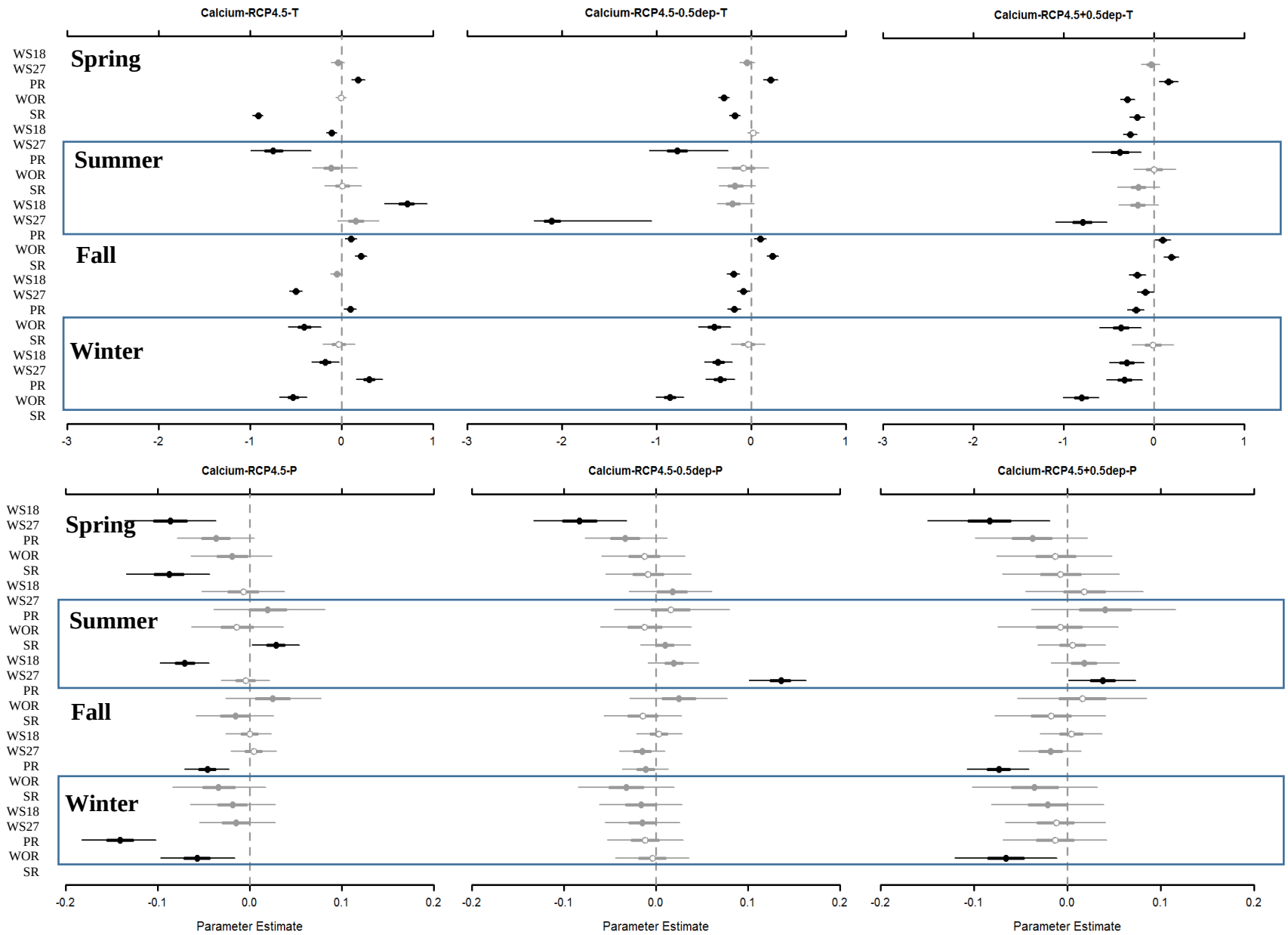

Fig. 3-14a Stream calcium's sensitivity to Temperature (top) and Precipitation (bottom) change without (left) and with deposition change (-50%: middle and +50%: right) by seasons (y-axis from top to bottom each season grouped by sites are spring, summer, fall, and winter) under RCP4.5.

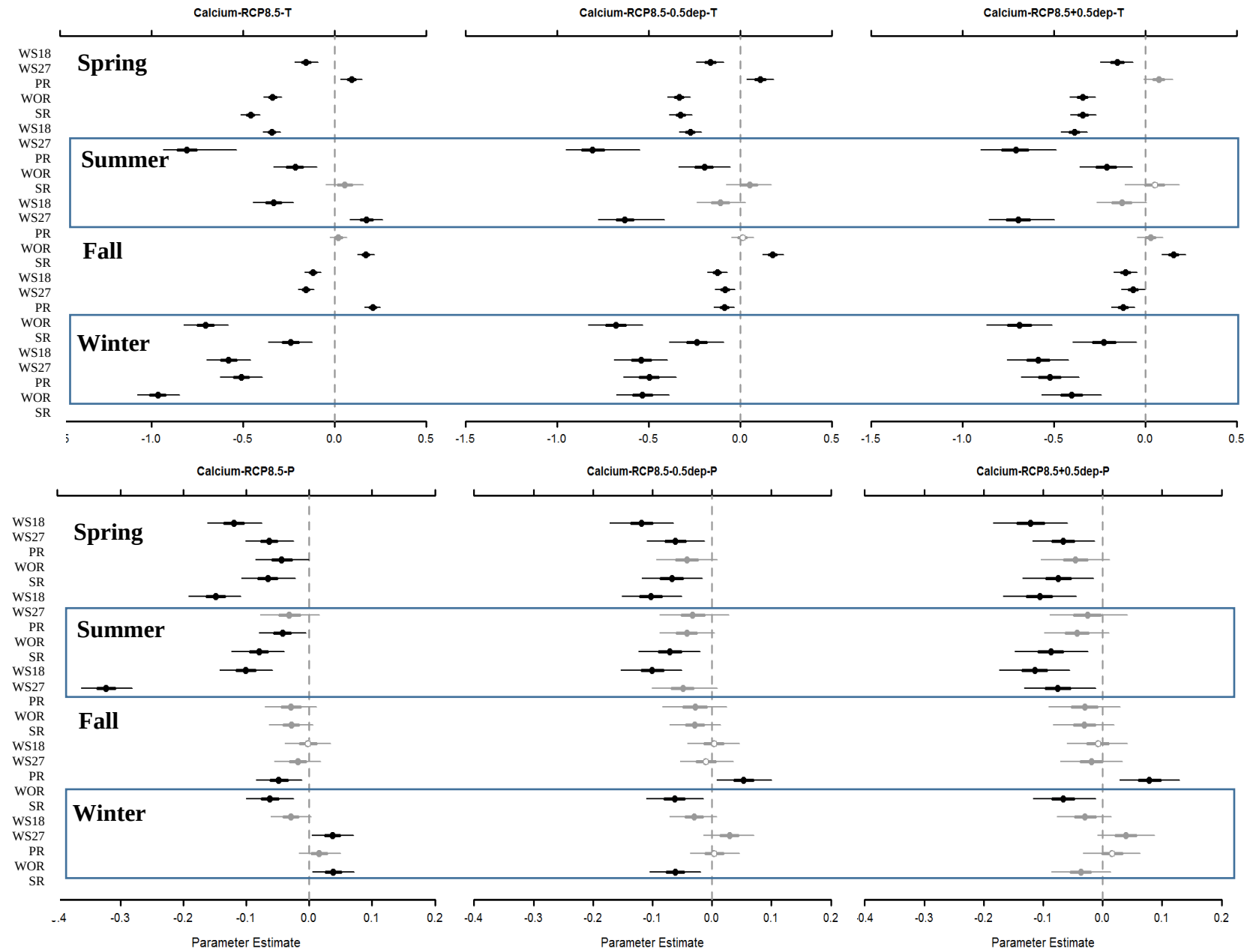

Fig. 3-14b Stream calcium's sensitivity to Temperature (top) and Precipitation (bottom) change without (left) and with deposition change (-50%: middle and +50%: right) by seasons (y-axis from top to bottom each season grouped by sites are spring, summer, fall, and winter) under RCP8.5.

3.4 Discussion

3.4.1 Uncertainty in regional pattern of climate change impact

Climate models show that warming is faster at higher latitudes and elevations (Lee, 2014; Pepin et al. 2015; Wang et al. 2014; Wang et al. 2016; Serreze et al. 2000, Rangwala et al. 2013). In addition, seasonal change of climate shows strong variability among temperate forest regions due to differences in latitude, topographic features (e.g., mountains) and proximity to the ocean (Gilliam, 2016). However, research on latitudinal and elevational responses of forested ecosystems to climate change is limited.

As biogeochemical processes, climate change scenarios, seasons, vegetation types, and soil types etc. act at multiple spatial scales, prediction of complicated latitudinal and elevational patterns of climate change impacts and synthesis of regional impacts involve large uncertainties. Quantifying these uncertainties is essential for more efficient forest management, but uncertainty estimates are not often provided in previous evaluations. A modeling technique that can assimilate errors from different sources at multi-scales to quantify uncertainties in model predictions is needed. Bayesian multi-level models provide such a tool which I applied in my study to synthesizing the response of the key biogeochemical variables to temperature and precipitation across different latitudes and elevations.

Bayesian frameworks are capable of exploiting diverse sources of information at multiple scales to account for uncertainties and prior information and have the ability to draw inferences on large numbers of inferred variables and parameters that describe complex relationships (Clark, 2005; Clark & Gelfand, 2006, Wu et al. 2018). The simulation results are informative and uncertainties can be quantified using credible

intervals from resulting model posteriors (Wu et al. 2012a; Wu et al. 2012b). Bayesian–based models have previously been applied to forest ecosystem models at the site scale/watershed scale (Augustynczik et al. 2017, Clark et al. 2013, Keenan 2015).

The Bayesian multi-level (regional, site and season-scale) models developed herein show potential seasonal effects of temperature and precipitation (seasonal scale), combined with latitude and elevation (site scale) on NPP, transpiration, calcium concentration in streams, and ANC in streams. The resultant posterior probabilities demonstrate the complexity of spatial and seasonal patterns of the responses of forested ecosystems to climate change. Even though the medians of the posteriors of the coefficients for season-specific temperature and precipitation, and site-scaled latitude and elevation may not be close to 0 (average response), some posteriors include 0, showing a lack of significant effects of these variables on the key biogeochemical variables at some sites and in some seasons. In general, how latitude or elevation affects the temperature's impact are more defined as positive or negative with more of the 95% or 50% credible intervals being positive or negative compared to the impact of precipitation. Larger uncertainty involved in the forest's response to precipitation has also been investigated in other areas (Nielsen & Ball, 2014; Campo, 2016; Duveneck & Thompson, 2017; Jeong et al. 2018).

The sensitivity of NPP to climatic changes in temperature and precipitation has implications on forest carbon sequestration. Warming is predicted to increase NPP in all seasons except summer, with the largest NPP increases per unit of temperature in the spring followed by fall and winter. However, the magnitude of positive effects in spring and negative effects in summer are similar. These findings are consistent with the

previous work that suggests higher primary production in spring may by followed by greater respiration, resulting in decreased NPP, particularly in summer when precipitation is low and evapotranspiration is high (Oishi et al. 2018; Liu & Wu, 2020, Duveneck & Thompason 2017). On the other hand, increased precipitation tends to decrease NPP at all sites in summer under both RCP4.5 and 8.5 and at the three sites in SNP in fall under RCP8.5. Even under this more aggressive warming scenario, increases in NPP with higher precipitation is not predicted among the sites and seasons. Note the five sites I studied generally have abundant precipitation under the current and changing climate scenarios, so my findings cannot be extrapolated to regions where water availability is limited. Furthermore, increased NPP due to warming does not necessarily increase either soil organic carbon or carbon sequestration over long periods if the increased NPP is mainly stored in aboveground biomass (Suddick et al. 2013; Oishi et al. 2018).

All 95% credible intervals of the effect of latitude and elevation contain 0 while some 50% credible intervals do not, showing the general lack of significant spatial patterns along latitude or elevation, though they impact the sensitivity of the key biogeochemical variables to temperature or precipitation to some degree. In addition, the effect of latitude or elevation on precipitation's impact is even less significant. Note I only applied five sites in my study. Latitudinal and elevational patterns of the impact of climate change on forested ecosystems has been studied yet no consistent conclusion has been drawn (Serreze et al. 2000; Hwang et al. 2014; Pepin et al. 2015). The complexity is enhanced by different dominant vegetation species, which is only coarsely represented by hardwoods in my model simulations. The dominant species in the SNP is chestnut oak

(aka dry oaks), while the dominant species in the Coweeta Basin include dry mixed oaks at low elevation and mesic mixed oaks at high elevation (Knoepp et al. 2008).

The PnET-BGC model is a deterministic model which cannot account for all uncertainties of climate projections which likely influence biogeochemical simulations, though I considered different climate models (four climate models) and RCPs (RCP4.5 and 8.5). Furthermore, climate is determined by the local environment as well as by global-scale climatic variability such as *El Niño-Southern Oscillation* (ENSO). In my study, I find that the values of PC1, which represent transpiration, ANC, and stream base cations, were lower during the strong El Niño years when the Oceanic Nino Index (ONI) is large from 1950 to 2015 (Fig. 3-15) in the SNP. This is consistent with the finding at the Coweeta Basin (Chapter 2), although the relation at SNP is weaker. Current climate models can only coarsely predict ENSO which could introduce more uncertainty on the response of forested ecosystems to climate change (Smith et al. 2015; Wang et al. 2019). In face of these large uncertainties, policy making, and conservation management call for flexible climate adaption and mitigation strategies (Drechsler 2020; Martens et al. 2020). For instance, Keenan (2015) has reviewed a number of measures used on adaptive forest management that aims to reduce the vulnerability of forest to increasing threats (such as drought, flooding, insects, and disease, etc.) and 'shocks from natural disasters or extreme events' (such as hurricanes and wildfires, etc.), or to enhance forest's resilience to climate progressive or extreme changes (such as CO_2, high heat or freezing, spatial and temporal unevenly precipitation distribution etc.). Since changing climate impacts to a forest will vary locally, management needs to be flexible in ways that meet the specific

needs of the local conditions (Innes et al. 2009), which often requires ‘multiple forms of knowledge and new approaches to forest management decisions (Keenan 2015).

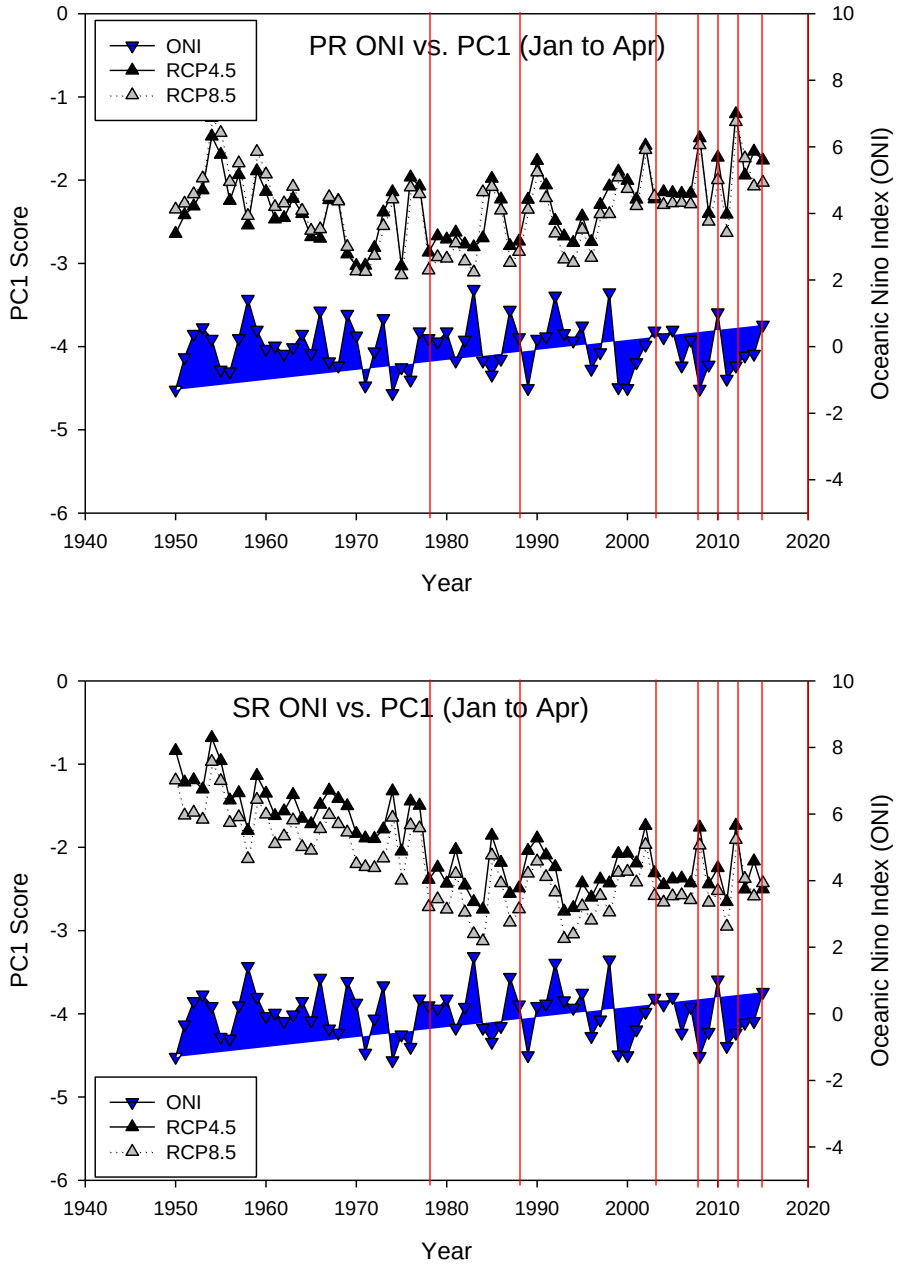

Fig. 3-15 ENSO Oceanic Niño Index vs. PC1 scores in PR (top), SR (middle), and WOR (bottom) (strong El Niño years are highlighted with red vertical lines).

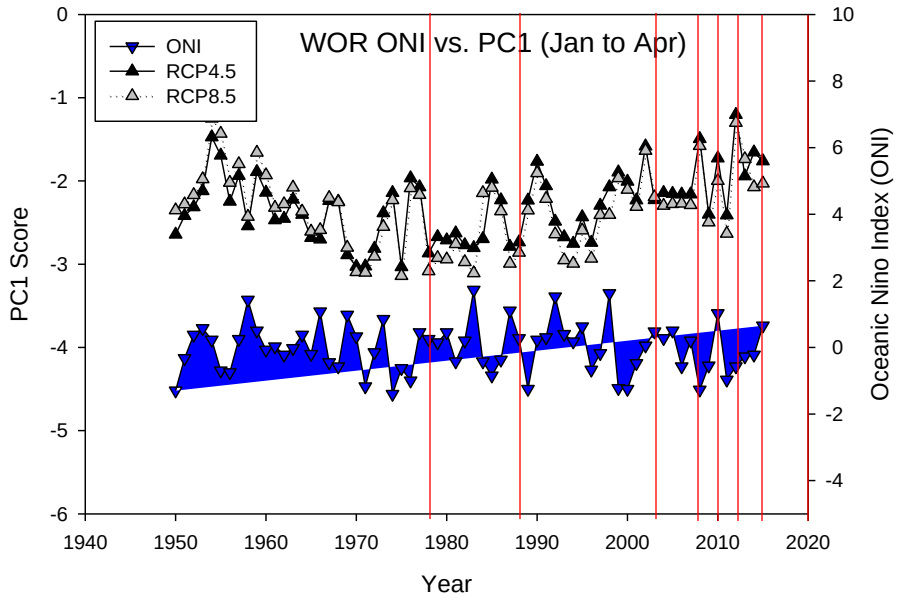

Fig. 3-15 Continued.

3.4.2 Combined effect of acidic deposition and climate change

There is very limited research on the impact of combined changes in acidic atmospheric deposition and climate on biogeochemical cycles (Wu & Driscoll, 2010; Greaver, et al. 2016; Lu et al. 2018; Robison & Scanlon, 2018; Wason et al. 2019). Wu and Driscoll (2010) show that critical load of sulfate and nitrogen based on the critical values of ANC will be smaller under climate change scenarios, indicating that water quality improvements require more substantial reductions in acidic deposition under changing climate compared to the current climate.

My study shows atmospheric acidic deposition changes are predicted to shift the response of key biogeochemical variables to temperature and precipitation depending on the variables studied, seasons focused, and climate change scenarios considered (Fig. 3-11 to 3-14). Among the four variables studied, NPP shows minimal response to acidic deposition, which may indicate that nitrogen is not limiting, especially for mature forests

where NPP is not projected to increase with increased nitrogen availability (Swank & Vose, 1997).

The lack of response of NPP to nitrogen additions indicates these ecosystems are nitrogen saturated (Aber et al. 1989, Aber et al. 2002). The different temporal trends of nitrate concentration between Coweeta Basin and SNP, i.e., increasing from 1970 to present at the Coweeta Basin, and decreasing from 1980 to present at the SNP, suggests Coweeta Basin has experienced nitrogen saturation while SNP has not. It helps explain why increasing nitrogen deposition at the Coweeta Basin leads to loss of base and nutrient cations, lower ANC, more acidified soil, and possibly lower primary productivity (Bowman et al. 2008; Horswill et al. 2008). Based on the increasing nitrate concentration in streams and increasing NPP (Swank & Vose 1997), the watersheds at the Coweeta Basin are in transition from stage 1 (nitrogen unsaturated condition) to stage 2 (impact of increased nitrate in streamflow still subtle) (Aber et al. 1989). In contrast, the SNP watersheds are not experiencing nitrogen saturation (stage 0) based on decreasing stream nitrate concentrations and decreasing NPP following the decreasing nitrogen until recently when NPP started to increase without increases in nitrate concentrations.

My study shows that changes in acidic deposition do not influence latitudinal or elevational effects on biogeochemical responses to temperature and precipitation. I applied the same magnitude of acidic deposition changes across all five sites. In reality, the change in acidic deposition may show spatial variability, which adds complexity to the evaluation of the combined effects of shifts in climate and acidic atmospheric deposition.

Atmospheric deposition of both nitrate and ammonium, especially dry deposition, has been decreasing since 1970s after passage of the Clean Air Act, however, emissions of ammonia (NH_3) are likely to increase as agriculture activity increases (Rice, et al. 2014; Ellis et al. 2013; Kanakidou et al. 2016; Li et al. 2016). It is probably worth investigating the impact of change of nitrogen deposition alone, then combined with change of climate, on forest ecosystems in a future study.

The majority of the biogeochemical variables show nonlinear responses to acidic deposition change. This indicates the unequal response of these processes to increases and decreases of acidic deposition. For example, the increase of ANC with the decrease of acidic deposition at WS18 and SR will be smaller than the decrease of ANC with the same magnitude of increase of acidic deposition. This shows slower recovery of the systems even though acidic deposition decreases. Recovery rate of ANC under decreased acidic deposition and its positive relation to elevation has been studied in Wu and Driscoll (2012), which is consistent with my study that lower elevations like WS18 and SR show a slower recovery rate of ANC (Fig. 3-8).

3.4.3 Disturbance

The impact of natural wildfire on watershed hydrology largely depends on fire intensity, frequency, and duration (Yao, 2003). Generally, watershed streamflow will increase in the early years of forest fire recovery due to lower evapotranspiration rates and reduced water holding capacity through loss of soil organic matter and increased soil bulk density (Verma et al. 2019). Meanwhile, peak flows and low flows are more frequent due to lack of vegetation buffering (Niemeyer et al. 2020). In my work, I did not detect increasing annual streamflow after fire at PR, however, the ratio of peak to low

flows increased after fire, compared to either pre-fire at the same watershed, or to WOR and SR, which indicates that fire disturbance made PR more vulnerable to flash flooding and drought.

I also compared the stream chemistry before and after the large fire event since soil and vegetation nutrients can be released and leached into streams (McColl & Grigal, 1977). In my results, I detected increases in Ca^{2+} and K^{+} fluxes. Other more conservative elements such as Na^{+} and Cl^{-} increased at a much smaller magnitude compared, probably attributed to precipitation increases. Flux of NO_3^{-} quickly dropped to near zero suggesting its quick uptake due to vegetation recovery. In addition, increased SO_4^{2-} indicates that forest floor burning released sulfate from the soil (Lydersen et al. 2014). Soil in the southern and central Appalachians generally has high SO_4^{2-} due to its large adsorption capacity of atmospheric SO_4^{2-} from coal combustion (Cosby et al. 2006).

Other disturbances such as hurricanes need to be further investigated as the frequency and intensity of hurricanes are projected to increase under climate change. Hurricane's impact on forest has been studied previously and the most direct impacts of hurricanes are blowdown of trees and large inputs of precipitation, which could cause short- or long-term release of nutrients, soil loss, and change in streamflow (Webster et al. 1992; Elliott et al. 2002). For watersheds controlled by marine climate, hurricanes can also pour large amounts of seawater-rich elements such as SO_4^{2-}, Cl^{-}, Ca^{2+}, Mg^{2+}, and Na^{+} on them (Heartsill-Scalley et al. 2007).

3.4.4 Implications for water quantity and water quality

Transpiration is important to vegetation function, hydrological cycle, and energy balance of the earth and it is predicted to increase with rising temperature. It could lead to

negative feedbacks that could reduce surface temperature. However, the increase of transpiration may be offset by a negative response to increased precipitation in the region.

Though streamflow is predicted to increase in the five watersheds, it does not directly lead to less concerns on water supply downstream, as the extreme hydrological events play an important role in actual water supply. Similar to Chapter 2, the flooding and drought under future climate (2081 to 2100) compared to current climate (1992 to 2011) at the SNP (Table 3-5) are predicted to become more frequent than in the current climate, except PR under RCP8.5. Furthermore, flooding is more frequent under RCP4.5 than RCP8.5 at PR and WOR, probably due to the higher precipitation projections in the HadGEM2 climate model under RCP4.5 than under RCP8.5. Furthermore, the streamflow becomes larger at the same return period in the changing climate scenario than in the current climate scenario for both RCP4.5 and 8.5 (Table 3-6).

ANC is an important indicator for water quality (Stumm & Morgan, 1981). ANC decreases in general, responding to climate change (Robison & Scanlon, 2018), more so under RCP8.5 than RCP4.5. The reduction will have important implications on acid-sensitive biota such as Brook Trout population (Bulger et al. 1995), especially in SNP where ANC tends to be smaller than at Coweeta Basin. The response of biota to ANC shows threshold behavior, meaning a sudden shift occurs once ANC drops below a threshold value, like 0, 25, or 50 μeq/L. I find the ANC are below thresholds for longer time periods under future climate change scenarios compared to the current climate scenario, indicating potential impairment to the biota.

Table 3-5. Duration of flooding and drought (unit: months) at two watersheds, based on flooding thresholds) (unit: cm/mo)

	PR		*SR*		*WOR*	
	drought (<0.66)	flooding (>6.0)	drought (<2.5)	flooding (>8.0)	drought (<0.69)	flooding (>6.0)
Current	66	36	66	54	77	66
CM1_rcp4.5	59	76	121	63	106	94
CM1_rcp8.5	70	60	131	58	112	76
CM2_rcp4.5	58	134	80	124	69	147
CM2_rcp8.5	46	91	111	92	96	108
CM3_rcp4.5	103	62	153	55	146	72
CM3_rcp8.5	69	91	117	88	105	105
CM4_rcp4.5	66	92	111	81	100	106
CM4_rcp8.5	52	97	107	89	92	119
current	66	36	66	54	77	66
*RCP4.5_avg**	72 (8.3%)	91 (153%)	116 (76.1%)	81 (49.5%)	105 (36.7%)	105 (58.7%)
*RCP8.5_avg**	59 (-10.2%)	85 (135%)	117 (76.5%)	82 (51.4%)	101 (31.5%)	102 (54.5%)

Note: The numbers in brackets indicate increasing percentage compared to current results. The thresholds for flooding were determined based on current streamflow data (1992 to 2011) and using mean residual life plot to depicts the thresholds vs. mean excess flow and fitting the Generalized Pareto distribution (GPD) model over a range of thresholds in determination of the final thresholds, and the drought level is based on the 30% quantile of observed streamflow, the same to Coweeta Basin study.

Table 3-6. Flooding frequency analysis under both current and future climate at PR, SR, and WOR

	Return Period (Years)	**Return level (cm/mo)**											
		Current	S1*	S2	S3	S4	S5	S6	S7	S8	**RCP4.5**	**RCP4.5***	**RCP8.5**
PR	2	12.8	18.3	19.9	70.7	32.6	37.0	45.5	28.7	25.1	38.7	28.0	30.8
	5	16.8	24.5	27.4	93.2	44.6	57.2	63.8	41.5	32.2	54.1	41.1	42.0
	10	19.6	29.2	33.2	110.3	54.1	75.4	78.5	53.0	37.4	67.0	52.5	50.8
	20	22.1	34.1	39.2	127.4	63.9	96.4	94.1	66.3	42.4	81.1	65.6	59.9
	50	25.2	40.7	47.5	150.1	77.5	129.3	116.2	87.1	48.6	101.8	85.7	72.5
	100	27.3	45.8	53.9	167.3	88.3	158.7	134.0	105.7	53.2	119.4	103.4	82.4
SR	2	17.5	20.3	20.7	72.4	33.4	39.8	47.5	29.9	26.3	40.6	30.0	32.0
	5	22.1	26.0	28.6	92.6	46.7	59.5	66.9	44.2	33.9	55.6	43.2	44.0
	10	25.5	30.1	35.1	107.0	58.0	76.0	82.9	57.6	39.7	67.7	54.6	53.9
	20	28.7	33.9	42.3	120.8	70.5	94.2	100.2	73.8	45.4	80.7	67.3	64.6
	50	32.8	38.6	52.6	137.9	89.2	120.8	125.3	100.6	53.0	99.5	86.7	80.0
	100	35.8	41.9	61.2	150.2	105.0	143.2	146.0	125.8	58.7	115.3	103.6	92.7
WOR	2	13.2	20.6	21.0	73.5	34.4	39.9	48.9	31.4	26.6	41.4	30.6	32.7
	5	17.8	25.9	28.4	99.2	45.8	60.0	66.7	45.5	33.4	57.7	43.8	43.6
	10	21.5	29.5	34.1	119.6	54.6	77.4	80.5	58.0	38.1	71.1	55.0	51.8
	20	25.5	32.8	39.9	140.9	63.4	96.9	94.7	72.5	42.5	85.8	67.4	60.1
	50	31.0	36.7	47.8	170.5	75.2	126.5	113.9	95.1	48.0	107.2	86.1	71.2
	100	35.4	39.3	53.9	194.1	84.2	152.1	128.7	115.3	51.8	125.2	102.2	79.7

Note: S1 through S8 represents climate model 1 to 4 RCP4.5 and 8.5 scenarios (*: S1, S3, S5, and S7 are climate model 1 to 4 under RCP4.5 scenario and S2, S4, S6, and S8 are climate model 1 to 4 under RCP8.5 scenario). In table above is the return level estimate of current climate streamflow flooding (data used are 1992-2011 at PR and SR, and 1988-2010 at WOR) using L-moments method. * is calculated without S3 (i.e., Climate model 2 RCP4.5).

3.5 Conclusion

Climate change alters forest ecosystem processes in a way that increases potential risks to forest sustainability. How to take advantage of potential benefits (such as increased NPP) and mitigate the negative consequences (such as droughts, floods and subsequent soil nutrient losses) in forest management with large uncertainties is challenging. My study presents some important findings that are under-studied at the regional scale with uncertainties accounted for.

The impacts of climate change on forest processes showed strong seasonality. Changes in acidic atmospheric deposition rates will likely further shift the seasonal impacts, and the magnitude will depend on local conditions such as deposition history, soil properties, vegetation composition, precipitation and temperature, as well as latitude and elevation. The large uncertainties involved in the responses of forest processes to climate change and depositional change call for more flexible adaption plans to mitigate the adverse impact of climate change on forest management.

CHAPTER IV CONCLUSION

The rapid increase in the global human population and activities has driven accelerated changes in global climate and atmospheric deposition especially in the last several decades and these changes are projected to continue into the future. Forest ecosystems, one of the main natural resources that can mitigate the impact of climate change through sequestering carbon dioxide, lowering air and surface temperatures, buffering storms and drought, and absorbing acidic deposition, are under great stress. As climate models predict greater warming tendency at higher elevations (Lee, 2014; Pepin et al. 2015; Wang et al. 2014; Wang et al. 2016; Serreze et al. 2000, Rangwala et al. 2013), high-elevation forests will likely experience higher risks under climate change than low-elevation forests. Furthermore, the negative effects of acid deposition on forests are magnified at higher elevations (over 4,000 feet) due to a much greater volume of precipitation there (Lewis, 2011). The research on the combined impacts of change in climate and acidic deposition is limited and requires more research attention. How to better manage, conserve, and restore high-elevation forest ecosystems is important, but challenging, due to the complexity involved in the responses of vegetation, soil, and streamflow to the combined changes in climate and atmospheric deposition in these ecosystems.

My research findings will facilitate more-informed policy making in forest ecosystems and natural resource management through an improved understanding of key hydrological and biogeochemical cycles. These findings apply to forests in the central and southern Appalachians of the U.S. in response to medium to aggressive climate change scenarios and low to high atmospheric depositions of nitrogen and sulfur. In

addition to the average response of forested ecosystems to a changing environment, I consider the effects in extreme hydrological and acidic deposition events, change-points over time, and potential thresholds of temperature and precipitation. The threshold-based concepts have rarely been tested in forests, probably due to the difficulty of predicting the range of forests' responses to climate change arising from the large heterogeneity across spatial and temporal scales. However, the thresholds emphasize abrupt change points and nonlinear (or rarely linear) responses of forest ecosystems to abiotic and biotic drivers, and can guide natural resource management with proper use, for example, by providing early warning signs of ecosystem transitions (Munson et al. 2018).

To better present the impact of climate change at the five studied watersheds in this work, I summarized the changes of the 17 model-derived key watershed process variables in each season between current (1986-2015) and future (2071-2100 for both RCP4.5 and 8.5) scenarios, particularly, the directions of the changes and the significance levels of the statistical tests (Table 4-1). The following can be concluded:

In vegetation: most GPP and NPP are predicted to increase significantly. However, during summer and at higher latitude sites, GPP and NPP will be significantly negatively impacted. This can be explained by higher water stress during this season coupled with less precipitation input at the SNP locations (compared to CWT sites). Additionally, RCP8.5 generally shows more significant reduction than RCP4.5 in both GPP and NPP, especially during summer and at the higher latitude sites.

In hydrology: transpiration will significantly increase during almost all seasons and across all sites as both precipitation and temperature are projected to increase from present day to the end of this century. However, all three SNP watersheds, having

relatively less precipitation input compared to the two CWT watersheds, show a non-significant decline in transpiration. Streamflow at CWT is trending to increase in winter and spring seasons and decrease in summer and fall seasons, but the predicted future changes are not significantly different from current conditions. For SNP watersheds, all seasons under RCP4.5 and summer and winter under RCP8.5 are predicted to have higher streamflow, which is most likely caused by less vegetation production and reduced transpiration.

In soil: base saturation across all sites and seasons is predicted to significantly decrease, which indicates a greater loss of base cations from the soil under changing climate. Along with the reduction of base saturation, the Al:Ca ratio is predicted to increase significantly at all seasons under both RCP4.5 and 8.5 at CWT and all seasons under RCP4.5 at SNP. Additionally, most nitrogen processes are negatively impacted, such as gross nitrogen mineralization and immobilization. For the net nitrogen mineralization, results are complicated due to counteracting processes being involved at the same time.

In streamwater chemistry: The concentration of major cations and sulfate are predicted to significantly decrease, even though soil loss of cations to nearby water flows (streams) are predicted to increase, probably due to the higher streamflow (not necessarily statistically significant though). ANC also shows similar results across most of the five sites (except WOR and WS27 during certain seasons). The change of nitrate concentration can increase or decrease depending on the site, season, and climate change scenario.

From the discussion of the above four processes, I conclude that under future climate change scenarios, most watersheds' processes will be significantly negatively impacted, and RCP8.5 will generally have greater negative impacts than RCP4.5. Particular sites in higher latitude and lower elevation are more sensitive and vulnerable to future climate change.

Table 4-1. Significance test of 17 watershed state variables between current (1986-2015) and future (2071-2100) for five studied watersheds

	WS18								*WS27*							
	RCP4.5				RCP8.5				RCP4.5				RCP8.5			
	Spr	Sum	Fall	Win	Spr	Sum	Fall	Win	Spr	Sum	Fall	Win	Spr	Sum	Fall	Win
GPP	***	***	***	***	***	-	***	***	***	***	***	**	***	***	***	***
NPP	***	-	***	***	***	***	***	***	***	***	***	-	***	***	***	***
Totlitter	***	***	***	-	***	***	***	***	***	***	***	***	***	***	***	***
Mg^{2+}	***	***	***	***	***	***	***	***	***	***	***	***	***	***	***	***
K^{+}	***	***	***	***	***	***	***	***	***	***	***	***	***	***	***	***
Ca^{2+}	***	***	***	***	***	***	***	***	***	***	***	***	***	***	***	***
NO_3^{-}	***	***	***	***	***	***	***	***	***	***	***	***	***	**	***	***
SO_4^{2-}	***	***	***	***	***	***	***	***	***	***	***	***	***	***	***	***
ANC	***	***	***	***	***	***	***	***	**	-	-	***	***	*	*	-
Streamflow	-	-	-	-	-	-	-	*	-	-	-	-	-	-	-	**
Trans	***	***	***	***	***	***	***	***	***	***	***	***	***	***	***	***
Al/Ca	***	***	***	***	***	***	***	***	***	***	***	***	***	***	***	***
BS	***	***	***	***	***	***	***	***	***	***	***	***	***	***	***	***
GrossNMin	-	-	-	**	***	***	***	***	-	-	-	**	-	**	-	**
GrossNImmob	***	***	***	***	***	***	***	***	*	-	-	*	*	-	**	***
NetNMin	***	***	-	-	***	***	*	-	-	-	-	***	-	***	*	-
Nuptake	***	***	*	**	***	***	**	***	*	-	-	-	***	***	***	***

Note: * indicates 0.01<p <0.05; ** indicates 0.001 < p <0.01; *** indicates p <0.001; and – indicates no significant difference has been detected. Color green means increasing from current to the future (red means decreasing). In each season from 1986 to 2000 and from 2071 to 2100, monthly climate data were averaged first, then the 30 data points in each of the current and changing climate scenarios were checked for temporal autocorrelation ("acf" function in R) and normality (Shapiro test). As the checks show lack of temporal autocorrelation and met normality requirement, t-test was implemented to test whether the seasonal climate variables under current and changing climate scenarios were statistically significant different or not.

Table 4-1. (Continued.)

	PR								*SR*							
	RCP4.5				RCP8.5				RCP4.5				RCP8.5			
	Spr	Sum	Fall	Win	Spr	Sum	Fall	Win	Spr	Sum	Fall	Win	Spr	Sum	Fall	Win
GPP	***	***	***	**	***	***	***	***	***	***	***	**	***	***	***	***
NPP	***	***	-	-	***	***	***	***	***	***	**	**	***	***	***	*
Totlitter	-	***	***	***	-	***	***	**	**	***	***	***	**	***	***	***
Mg^{2+}	***	***	***	***	***	***	***	***	***	***	***	***	***	***	***	***
K^{+}	***	***	***	***	***	***	***	***	***	***	***	***	***	***	**	***
Ca^{2+}	***	***	***	***	***	***	***	***	***	***	***	***	***	***	***	***
NO_3^{-}	***	**	**	***	***	*	***	***	**	-	*	*	***	*	***	***
SO_4^{2-}	***	***	***	***	***	***	***	***	***	***	***	***	***	***	***	***
ANC	***	***	***	***	***	***	***	***	***	***	***	***	***	***	***	***
Streamflow	*	***	***	***	-	***	-	***	*	***	***	***	-	***	-	***
Trans	***	-	***	**	***	-	***	***	***	-	***	**	***	-	***	***
Al/Ca	***	***	**	***	-	-	-	*	***	***	***	***	*	*	*	**
BS	***	***	***	***	***	***	***	***	***	***	***	***	***	***	***	***
GrossNMin	**	***	***	***	***	***	***	***	-	***	***	**	***	***	***	***
GrossNImmob	***	***	***	***	***	***	***	***	***	***	***	***	***	***	***	***
NetNMin	-	**	***	**	**	**	***	***	-	-	***	-	-	**	-	-
Nuptake	***	**	***	***	*	***	**	***	*	-	-	***	***	-	-	***

Table 4-1. (Continued.)

	WOR							
	RCP4.5				RCP8.5			
	Spr	Sum	Fall	Win	Spr	Sum	Fall	Win
GPP	***	***	***	***	***	***	***	***
NPP	***	***	***	***	***	***	***	***
Totlitter	***	-	***	***	***	**	***	***
Mg^{2+}	***	***	***	***	***	***	***	***
K^{+}	***	***	***	***	***	***	***	***
Ca^{2+}	***	***	***	***	***	***	***	***
NO_3^{-}	***	*	***	**	***	*	***	***
SO_4^{2-}	***	***	***	***	***	***	***	***
ANC	***	***	***	***	*	***	-	-
Streamflow	**	***	***	***	-	***	-	***
Trans	***	-	***	***	***	-	***	***
Al/Ca	***	***	*	***	-	-	-	-
BS	*	*	-	*	**	-	-	**
GrossNMin	-	*	***	-	**	***	***	***
GrossNImmob	*	***	***	**	***	***	***	***
NetNMin	*	*	**	-	*	***	*	-
Nuptake	**	-	-	***	***	***	-	***

My research is a comprehensive study both temporally and spatially. I emphasize seasonal variability and account for multiple spatial scales, including season, watershed, and regional scales. More importantly, I quantify the uncertainties in the sensitivity of key biogeochemical processes to changes in temperature and precipitation, and how latitude and elevation as well as changes in acidic depositions impact this sensitivity. This uncertainty information was largely lacking in previous studies but is important for resource managers to understand in the context of decision making.

The main findings from Chapter 2 and 3 include:

1) Strong seasonal variability exists in the response of biogeochemical cycles to climate change, and winter seems to be the season that will be impacted the least. (Chapters 2 & 3)

2) The change-points at the lower elevation and latitude watershed (WS18) were mainly driven by temperature, while they were mainly driven by temperature and precipitation at the other higher-elevation and/or higher latitude watersheds (WS27, PR, WOR, and SR). The main driver of the change points, however, is predicted to be precipitation across all five watersheds approaching the end of the 21st century. (Chapters 2 & 3)

3) The thresholds of temperature or precipitation depend on the biogeochemical processes studied. In general, a small reduction (20%) in precipitation at the higher latitudes (with already lower precipitation) can trigger large changes in biogeochemical processes compared to the lower latitudes that already have higher precipitation (40% of reduction). For instance, there are no identified thresholds of precipitation at WS27 on biogeochemical processes except for ANC. On the other hand, a smaller increase in temperature at the lower elevation (WS18) can trigger greater changes in biogeochemical processes compared to temperature increase at the other four higher-elevation sites. For instance, as low as a 1°C increase in temperature can reduce NPP rapidly at WS18. (Chapters 2 & 3)

4) The five forested ecosystems from the southern to central Appalachians will potentially experience more frequent streamflow extremes, and longer durations when soil and streams are in extreme acidic conditions (below critical chemical limits) under future climate change. (Chapters 2 & 3)

5) The regional analysis shows that the response of the key biogeochemical variables to precipitation is less significant than to temperature across all five sites. Winter shows the least sensitivity to potential changes in temperature and precipitation among the four seasons, corresponding to the least impact of climate change in winter (see Finding 1). (Chapter 3)

6) Latitude and elevation affect the sensitivity of biogeochemical processes to temperature and precipitation, but the effect is marginal. Therefore, the latitudinal and elevation patterns of climate change impact are not conclusive based on the five sites I studied. (Chapter 3)

7) Change of atmospheric deposition is predicted to shift the sensitivity of biogeochemical processes to temperature and precipitation to different extents based on season, biogeochemical processes, scenarios of climate change and atmospheric deposition. The shift is distinct in ANC's sensitivity to temperature and precipitation at higher latitudes under both RCP4.5 and 8.5, NPP's sensitivity to precipitation under RCP4.5, and transpiration's sensitivity to temperature and precipitation under RCP4.5. (Chapter 3)

To summarize and answer the general hypotheses listed in Chapter 1, based on my work here, I have concluded:

1. Future climate will affect the forested watersheds in all four major studied processes with the largest impacts focused not only on vegetation (GPP/NPP), but also extending to impacts to hydrology (transpiration and discharge), soil (base saturation), and stream chemistry (base cations).

2. The climate impacts show strong seasonality. Summer generally is impacted the most while winter is the least affected season, with spring and fall intermediate, even though the exact magnitude will also depend on the processes and variables studied.

3. Across all five studied Appalachian watersheds, higher elevations and/or latitudes will likely experience more impact of climate change.

4. Atmospheric deposition changes shift watersheds' response to climate change, and the magnitude are varied with different processes, variables, and seasons focused. Generally, ANC will be lowered and NPP and transpiration at most watersheds and under moderate climate change condition (i.e., RCP4.5) is predicted to increase as deposition simultaneously increased (SO_4^{2-}, NO_3^-, and NH_4^+).

There are a few areas where I envision that improvements in future studies relevant to my dissertation research can be made. First, the PnET-BGC model could be improved by including a submodule of vegetation community change. Recent studies show the critical transitions of vegetation community in mountain forests can change the fundamental relationships between foliar N concentration and maximum photosynthesis rate that the PnET-BGC is built on (Albrich et al. 2020). This will require close analysis of longer-term vegetation community structure where data is available. The modeling also needs improved accounting of uncertainties from different sources. Large uncertainties exist in predicting forest response to changes in climate and atmospheric deposition. I applied Bayesian analysis on the simulation results from the PnET-BGC model in the current study. The next step is to run the PnET-BGC model in the Bayesian framework so that uncertainties from data, model, parameters, scenarios of climate and

atmospheric depositions can be assimilated coherently. This could require higher computational power. In addition, soil processes need to be analyzed in more detail, such as the decomposition rate of buried organic carbon. Carbon sequestered in the soil can be stored for a longer term than in the woody vegetation, therefore, is important to mitigate future climate change impacts (Ontl and Schulte 2012). Furthermore, the impact of changes in ammonia deposition and climate on forested ecosystems needs further study. Ammonia deposition has increased due to agricultural activities (Butler et al. 2016) and is predicted to increase further in response to rising food demand. In the current study, I changed the deposition of ammonia, nitrate, and sulfate simultaneously, whereas the change of ammonia deposition itself is worth investigating in more detail.

The modeling approach used herein has advantages and disadvantages. To better use the model to solve ecological problems, it largely depends on the questions asked. PnET-BGC is a monthly lumped dynamic model that lowers the frequency requirement of observation data as input which inevitably sacrifices predictability for specific processes. Even though I successfully calibrated this model and applied it to predict the forest ecosystems' response to changes in climate and atmospheric deposition, uncertainties in the results could be substantial. A number of ecosystem processes are not included and accounted for, such as, change of forest composition over time, adaption of vegetation community structure to ambient environmental conditions, reproduction of vegetation (i.e., seeding and saplings), and soil microbial activities, etc. Therefore, precautions need to be taken to interpret the model simulations, and a balance needs to be considered between current knowledge, data available, the question to be investigated, and complexity of models applied.

In summary, interactions of atmospheric deposition and climate changes will impact high-elevation forests with primarily negative impacts, but with some positive effects. Though the impacts depend on watershed, season, different scenarios of climate and atmospheric deposition, and biogeochemical processes, some modeled predictions do have higher confidence than others. Streamflow will likely become more acidic, affecting the biota living in it. Transpiration will likely increase, potentially decreasing local air and surface temperature and, therefore, mitigating local temperature increase. NPP likely increases mostly in the spring, followed by fall and winter, but this increase could be offset by a decrease in NPP during the summer. Flooding and drought events will likely become more frequent and longer. As low as 1 ℃ of increase in temperature can lead to a rapid reduction of NPP in some watersheds. More importantly, we are facing an even more uncertain future than previously thought, based on 1) the prediction for precipitation is more uncertain than for temperature (IPCC, 2014), 2) precipitation is going to be the main driver for future change-points (my finding), and 3) the sensitivity of key biogeochemical processes to precipitation involves larger uncertainties than to temperature (my finding). Considering the change that may occur in high-elevation forests directly influences ecosystems downslope and downstream and the very uncertain future projections, immediate measures should be taken to protect, conserve and restore these high-elevation forests. The improved understanding of forests' nonlinear responses to a changing environment gained from my research can potentially enhance policy making in forest management even with large uncertainties. For example, detection of early warning signs of regime shift, detection of hotspots for conservation, and selection of species planted in restoration, etc.

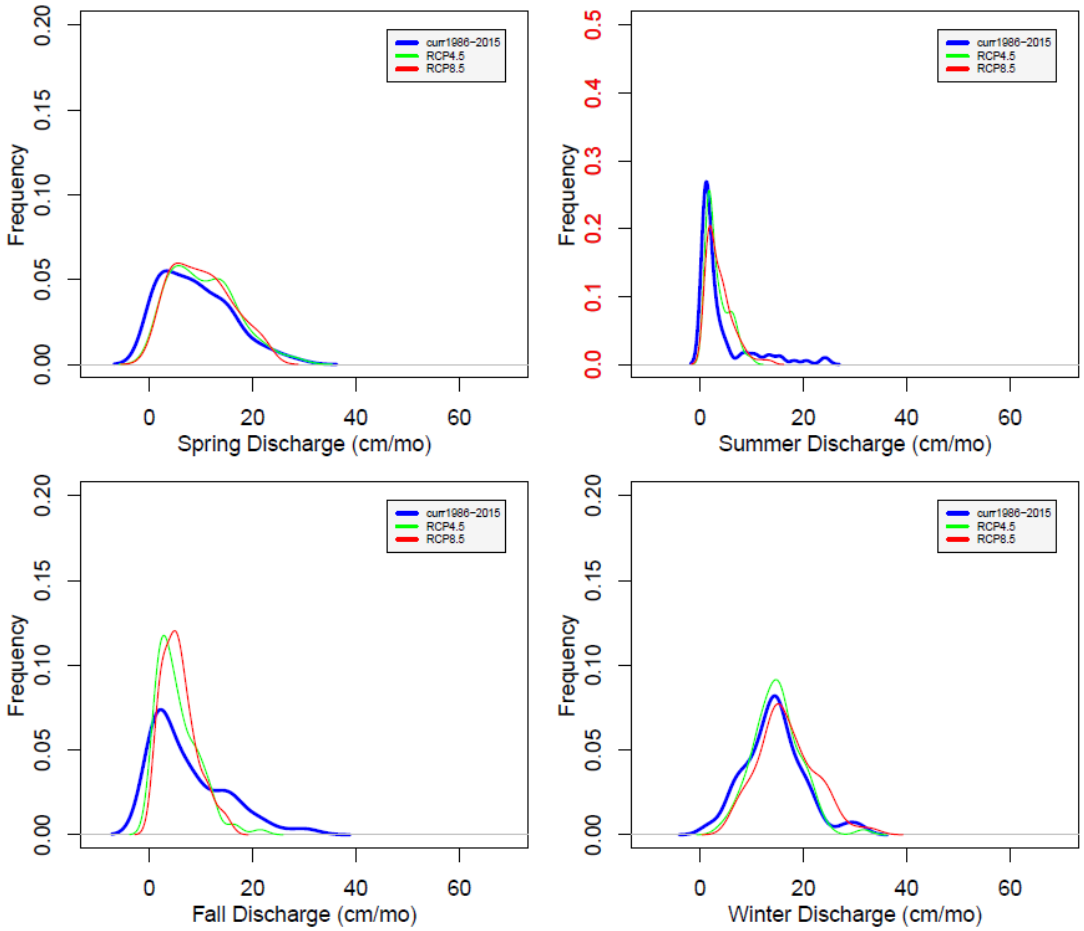

Fig. S2-1a WS18 comparison of Discharge between current (1986-2015) and future climate scenarios (2071-2100, RCP4.5 and 8.5 – average of four climate models)

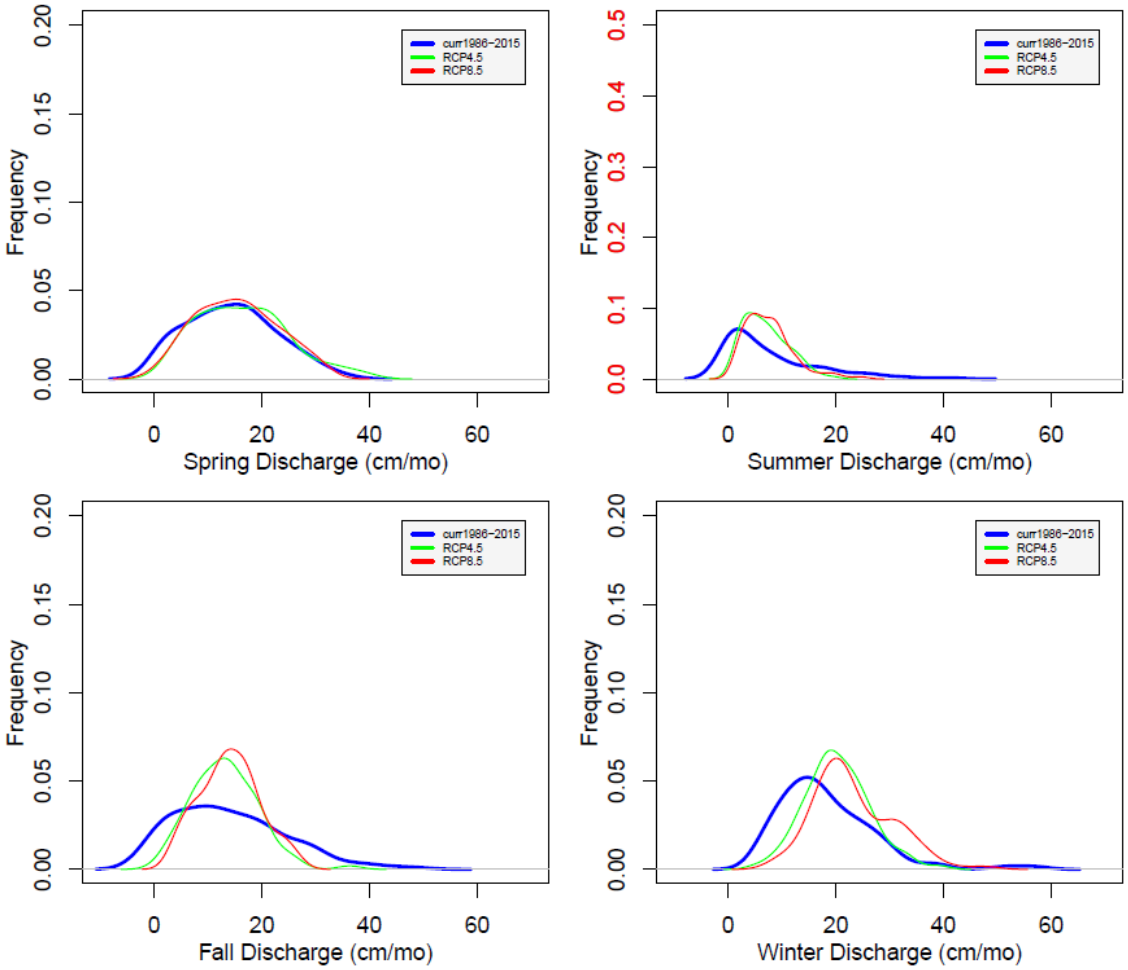

Fig. S2-1b WS27 comparison of Discharge between current (1986-2015) and future climate scenarios (2071-2100, RCP4.5 and 8.5 – average of four climate models)

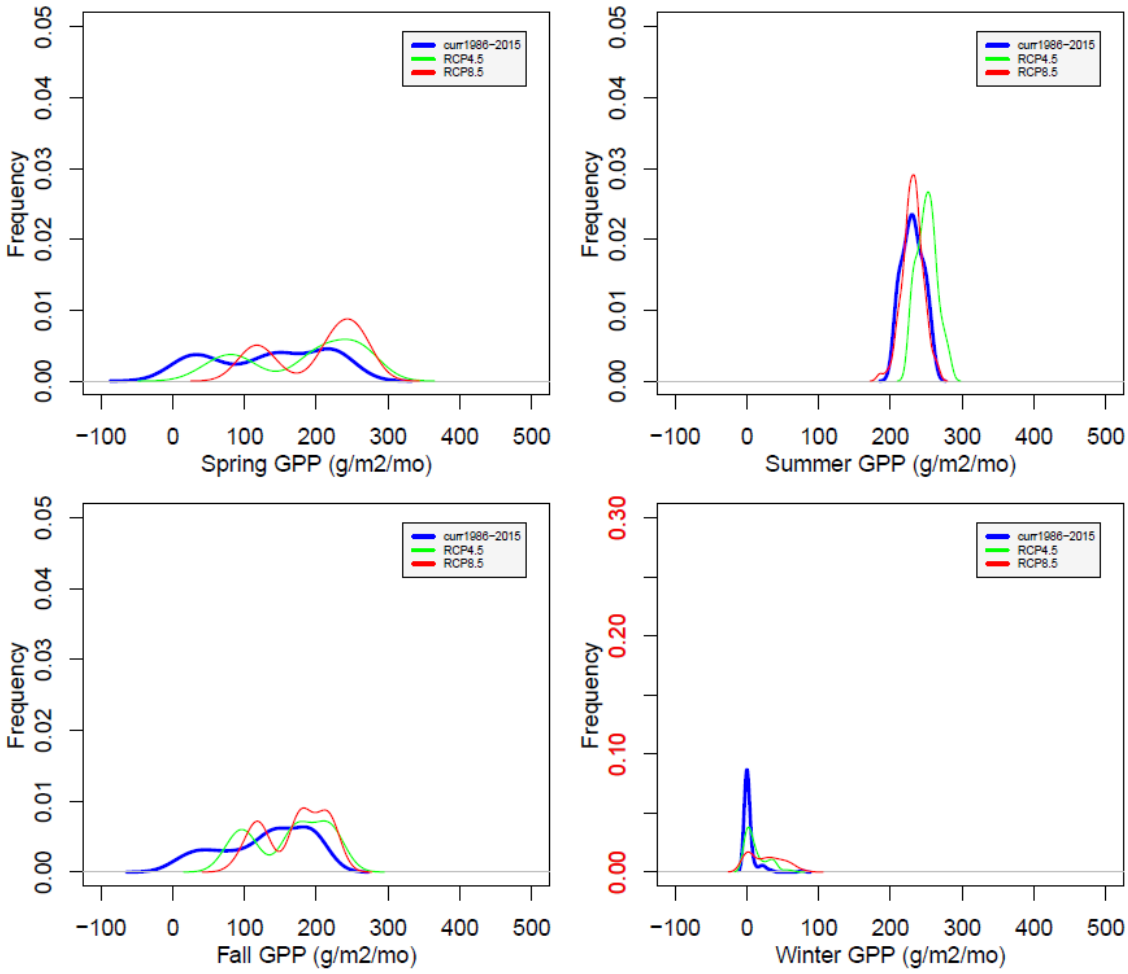

Fig. S2-2a WS18 comparison of GPP between current (1986-2015) and future climate scenarios (2071-2100, RCP4.5 and 8.5 – average of four climate models)

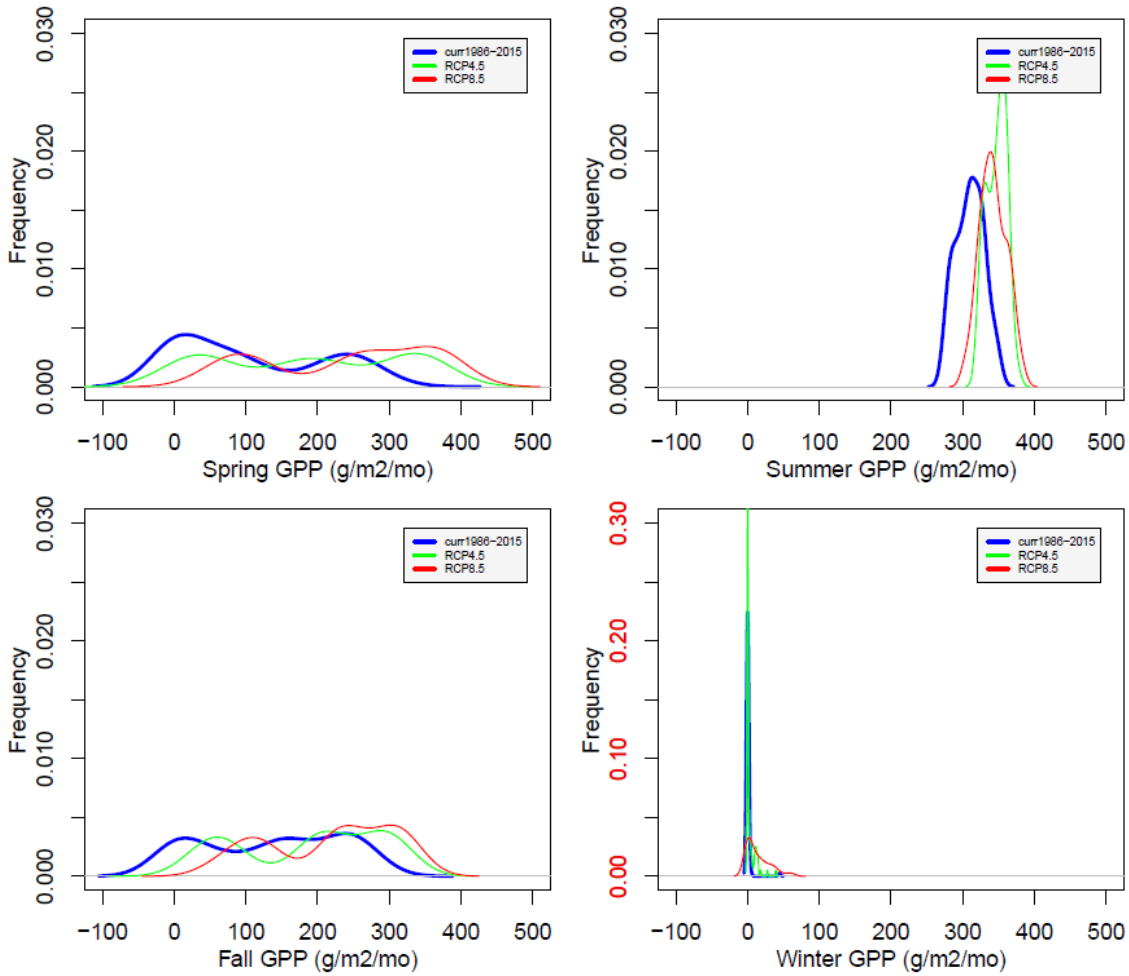

Fig. S2-2b WS27 comparison of GPP between current (1986-2015) and future climate scenarios (2071-2100, RCP4.5 and 8.5 – average of four climate models)

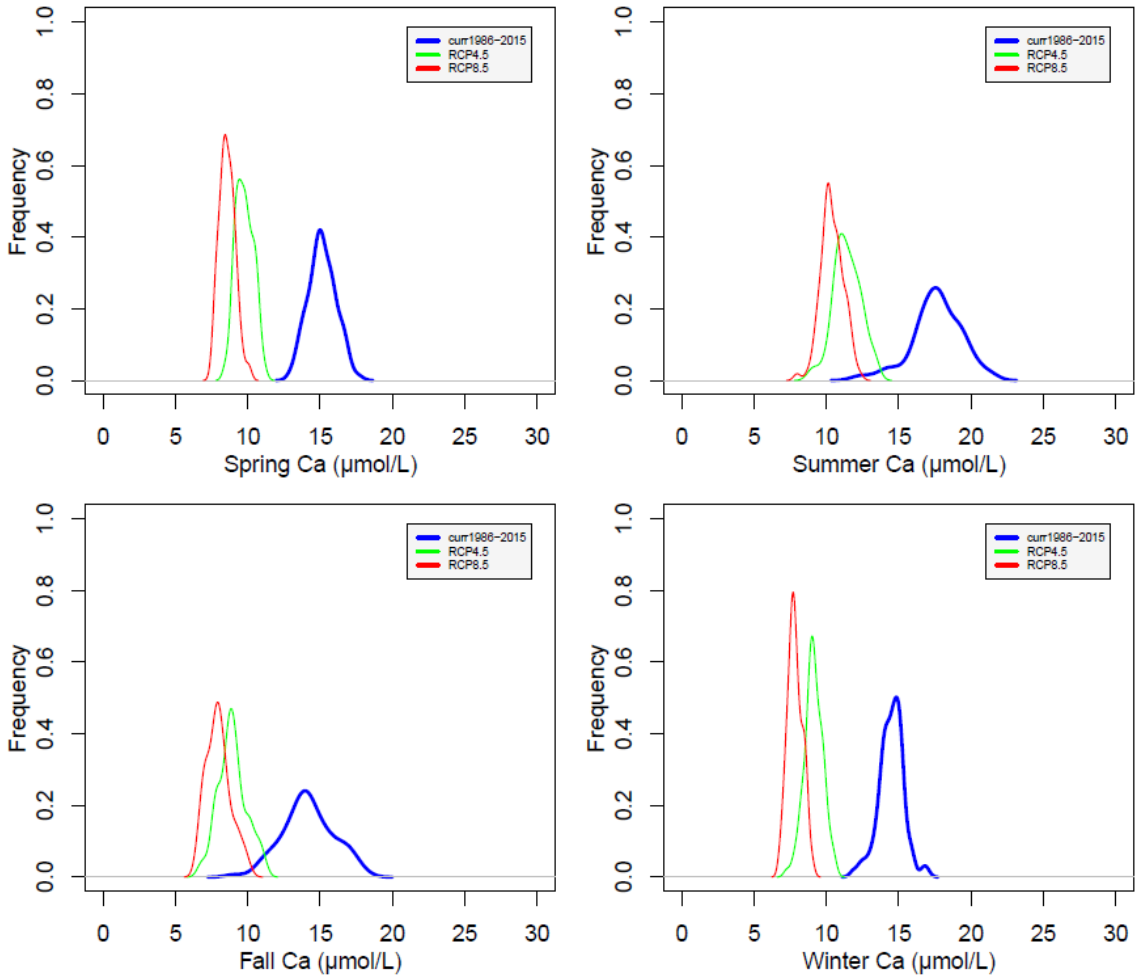

Fig. S2-3a WS18 comparison of stream Ca^{2+} between current (1986-2015) and future climate scenarios (2071-2100, RCP4.5 and 8.5 – average of four climate models)

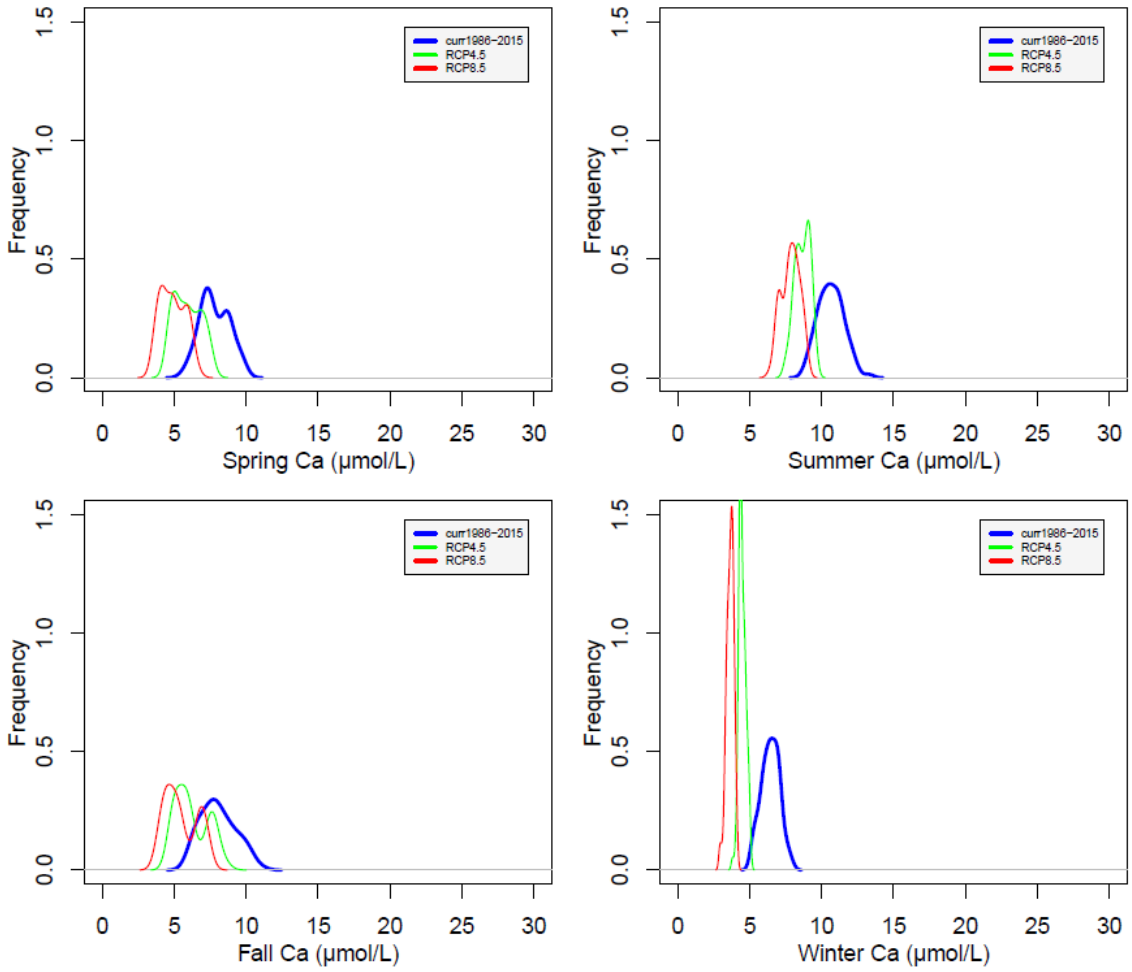

Fig. S2-3b WS27 comparison of stream Ca^{2+} between current (1986-2015) and future climate scenarios (2071-2100, RCP4.5 and 8.5 – average of four climate models)

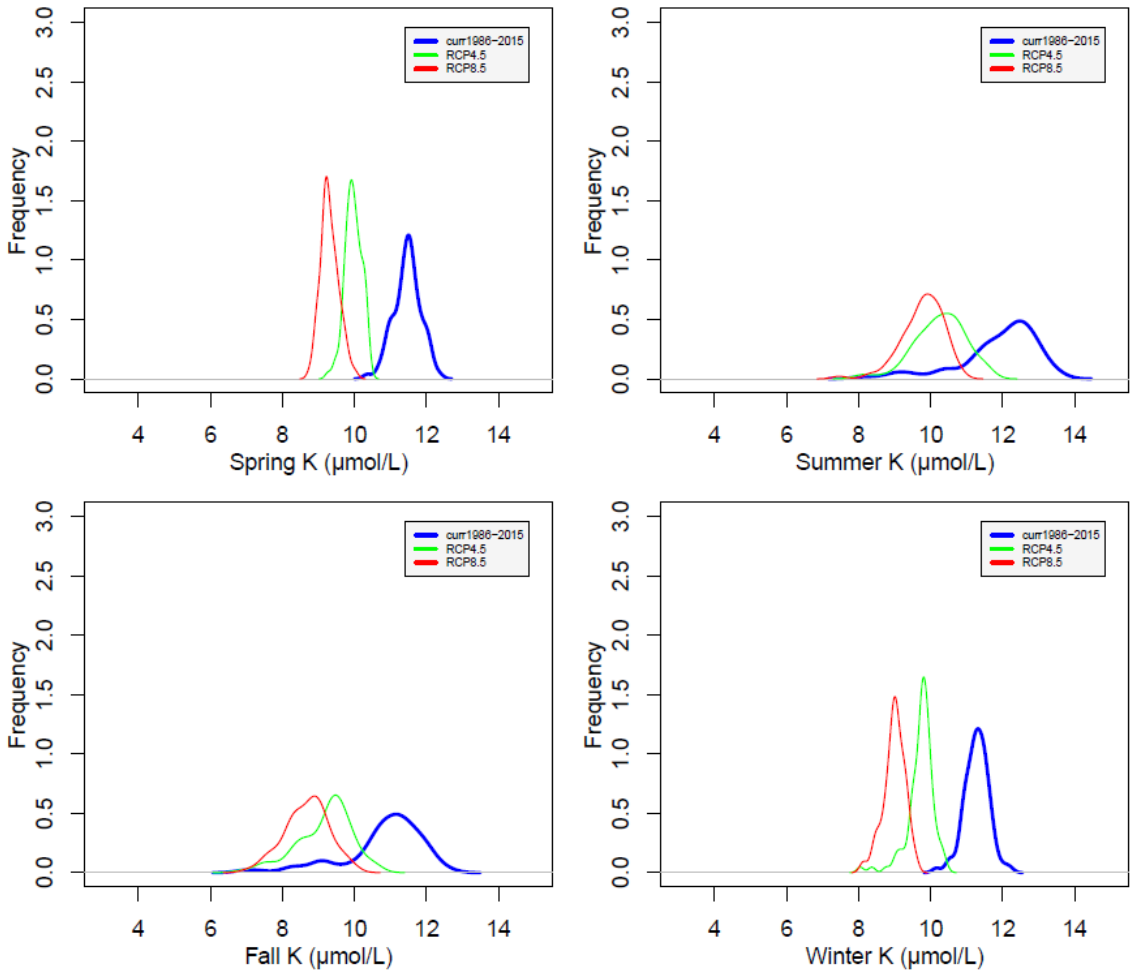

Fig. S2-4a WS18 comparison of stream K^+ between current (1986-2015) and future climate scenarios (2071-2100, RCP4.5 and 8.5 – average of four climate models)

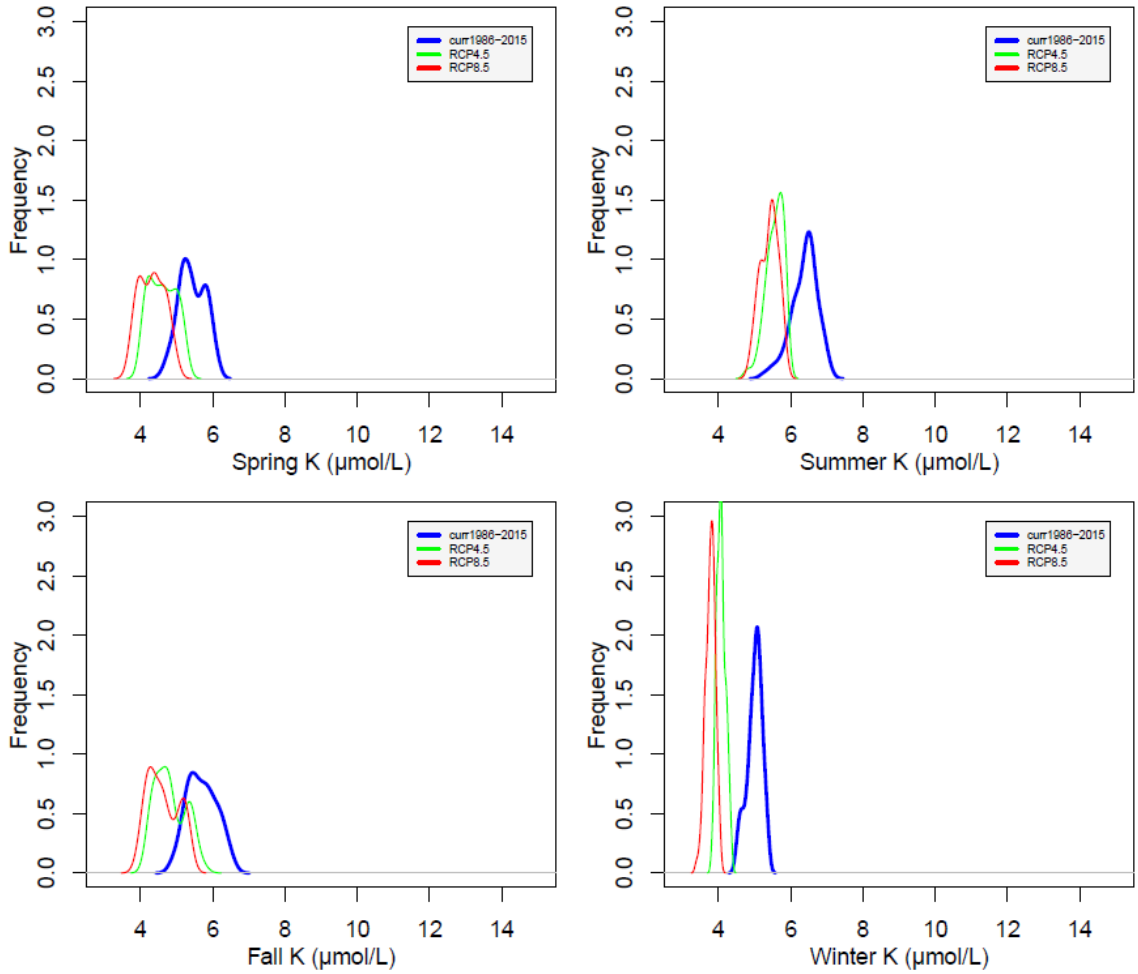

Fig. S2-4b WS27 comparison of stream K^+ between current (1986-2015) and future climate scenarios (2071-2100, RCP4.5 and 8.5 – average of four climate models)

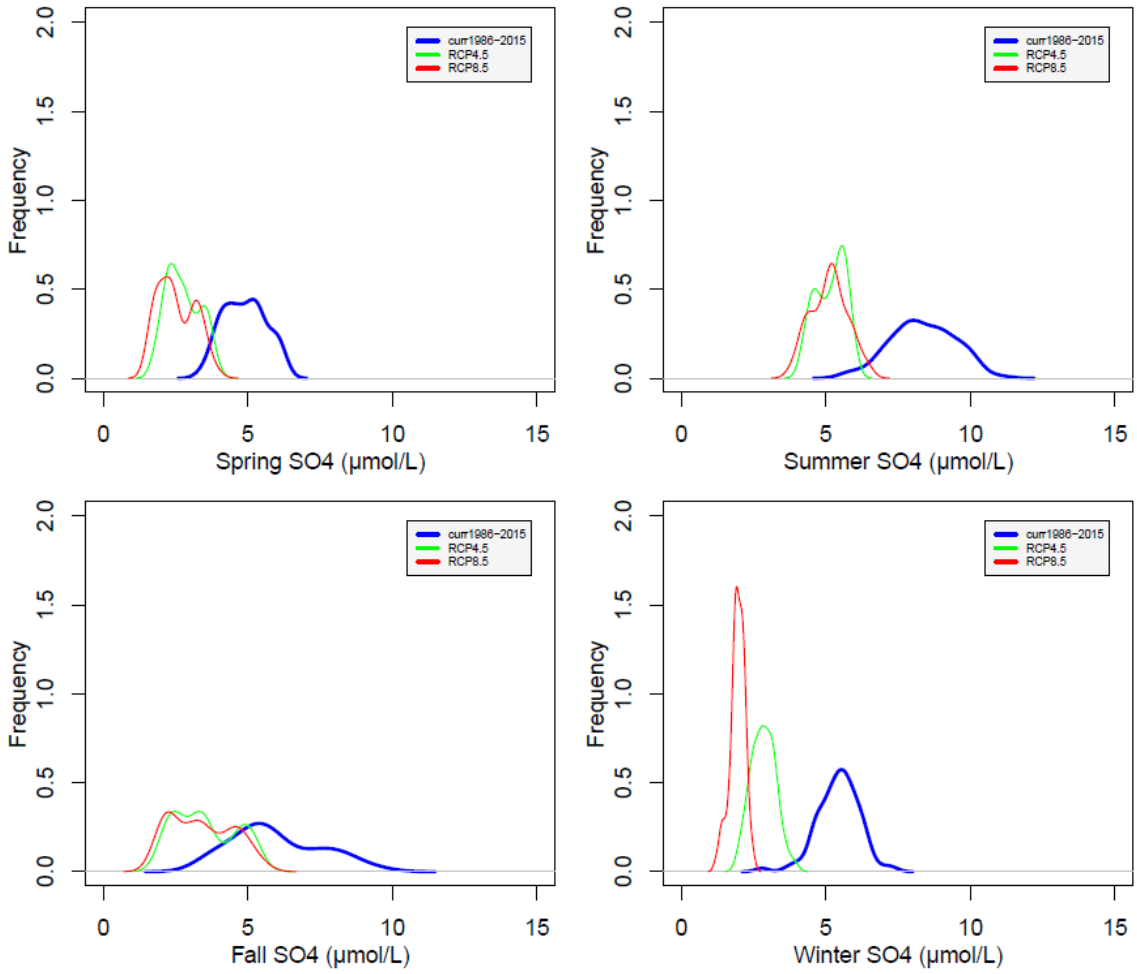

Fig. S2-5a WS18 comparison of stream SO_4^{2-} between current (1986-2015) and future climate scenarios (2071-2100, RCP4.5 and 8.5 – average of four climate models

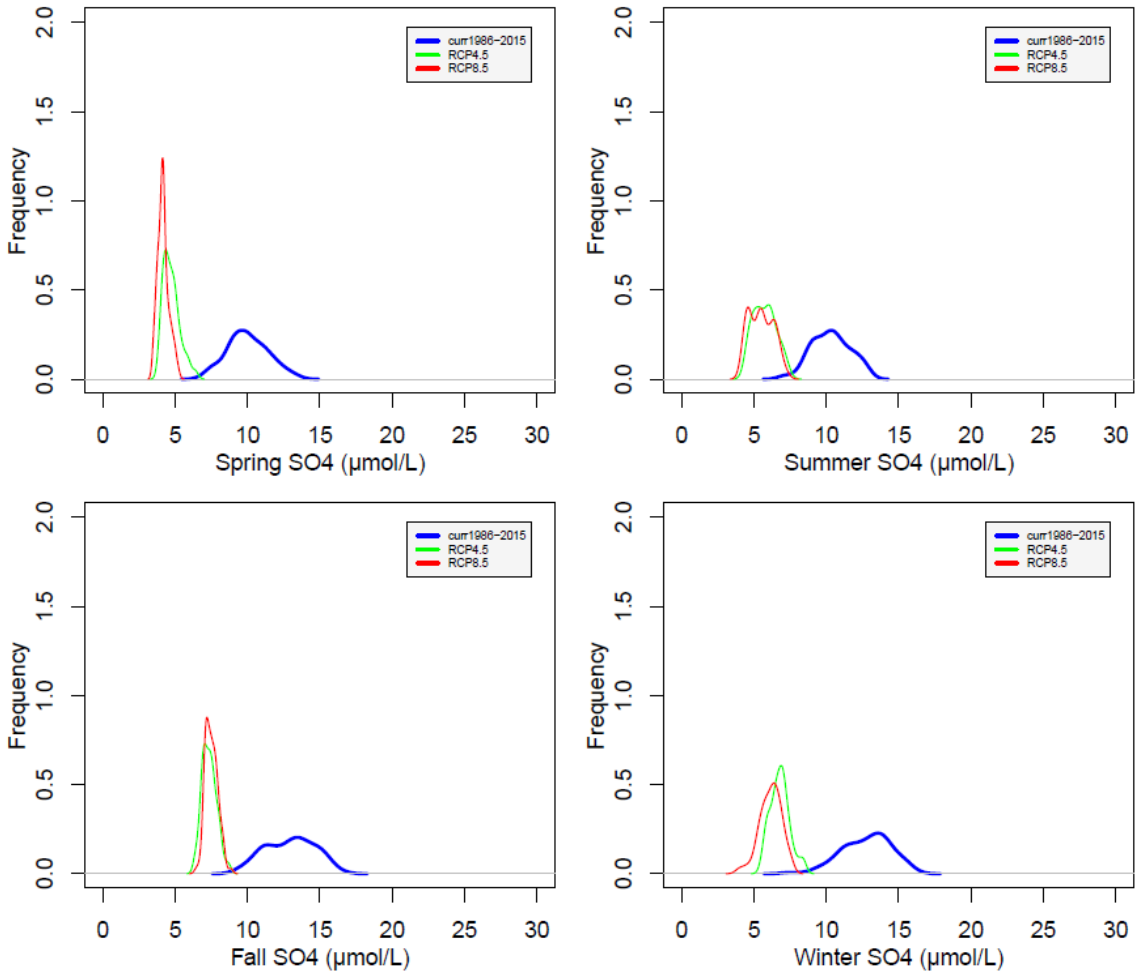

Fig. S2-5b WS27 comparison of stream SO_4^{2-} between current (1986-2015) and future climate scenarios (2071-2100, RCP4.5 and 8.5 – average of four climate models

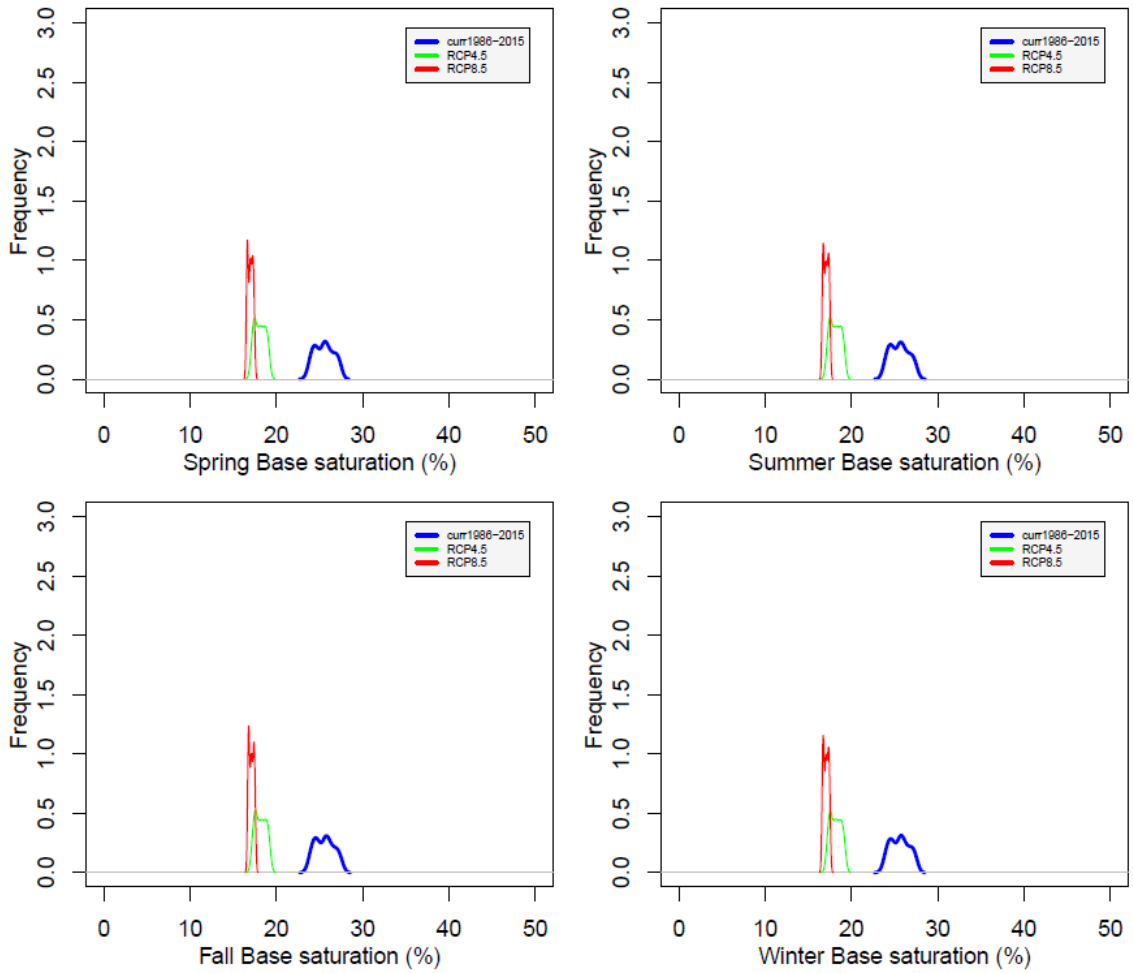

Fig. S2-6a WS18 comparison of base saturation between current (1986-2015) and future climate scenarios (2071-2100, RCP4.5 and 8.5 – average of four climate models

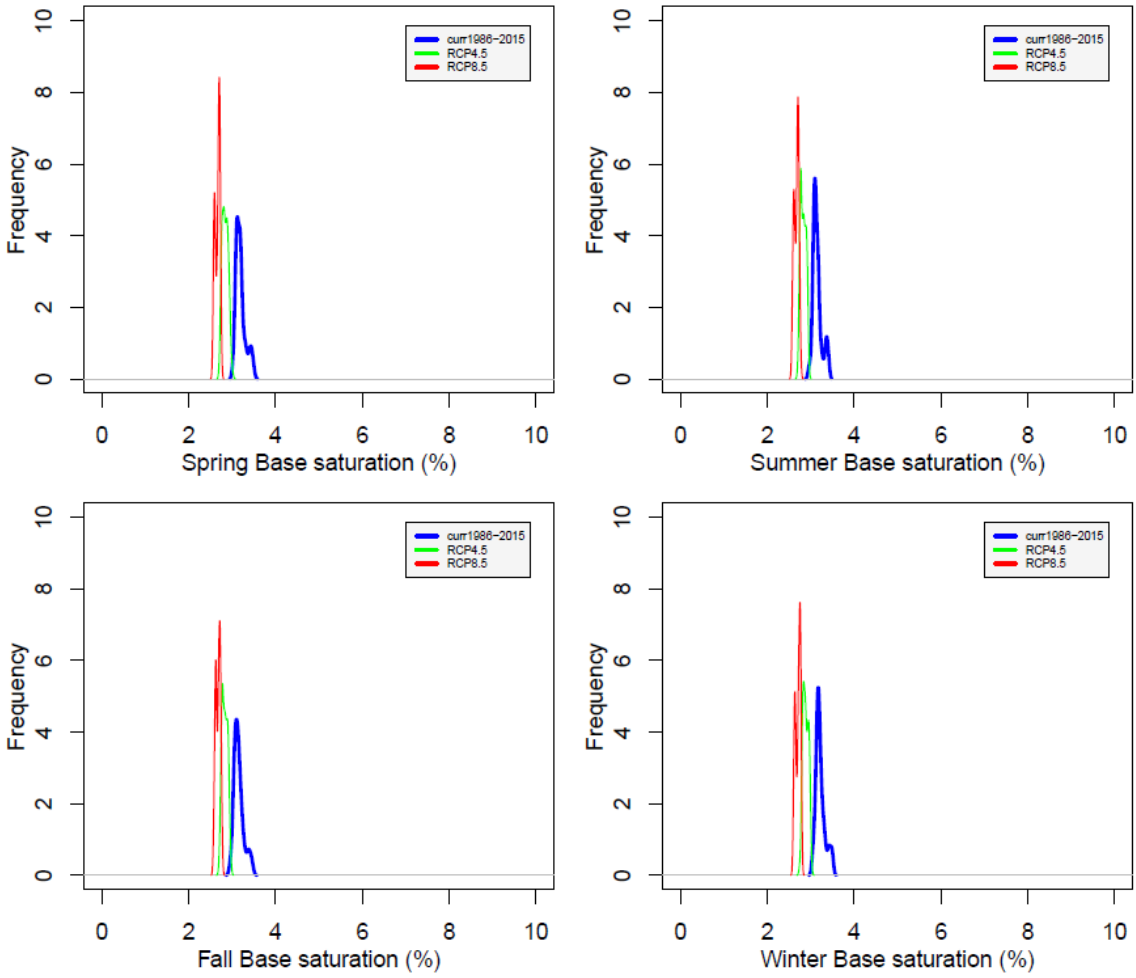

Fig. S2-6b WS27 comparison of base saturation between current (1986-2015) and future climate scenarios (2071-2100, RCP4.5 and 8.5 – average of four climate models

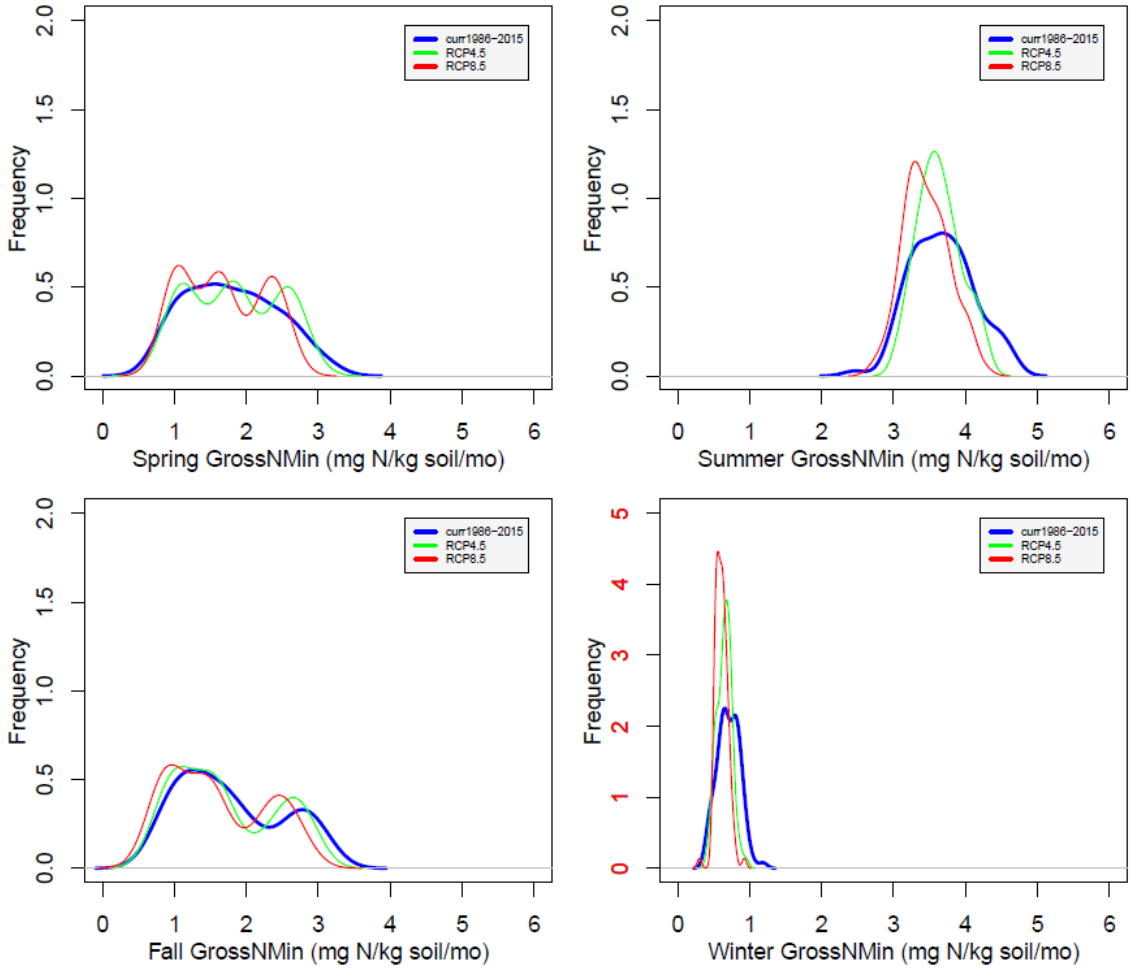

Fig. S2-7a WS18 comparison of gross nitrogen mineralization between current (1986-2015) and future climate scenarios (2071-2100, RCP4.5 and 8.5 – average of four climate models

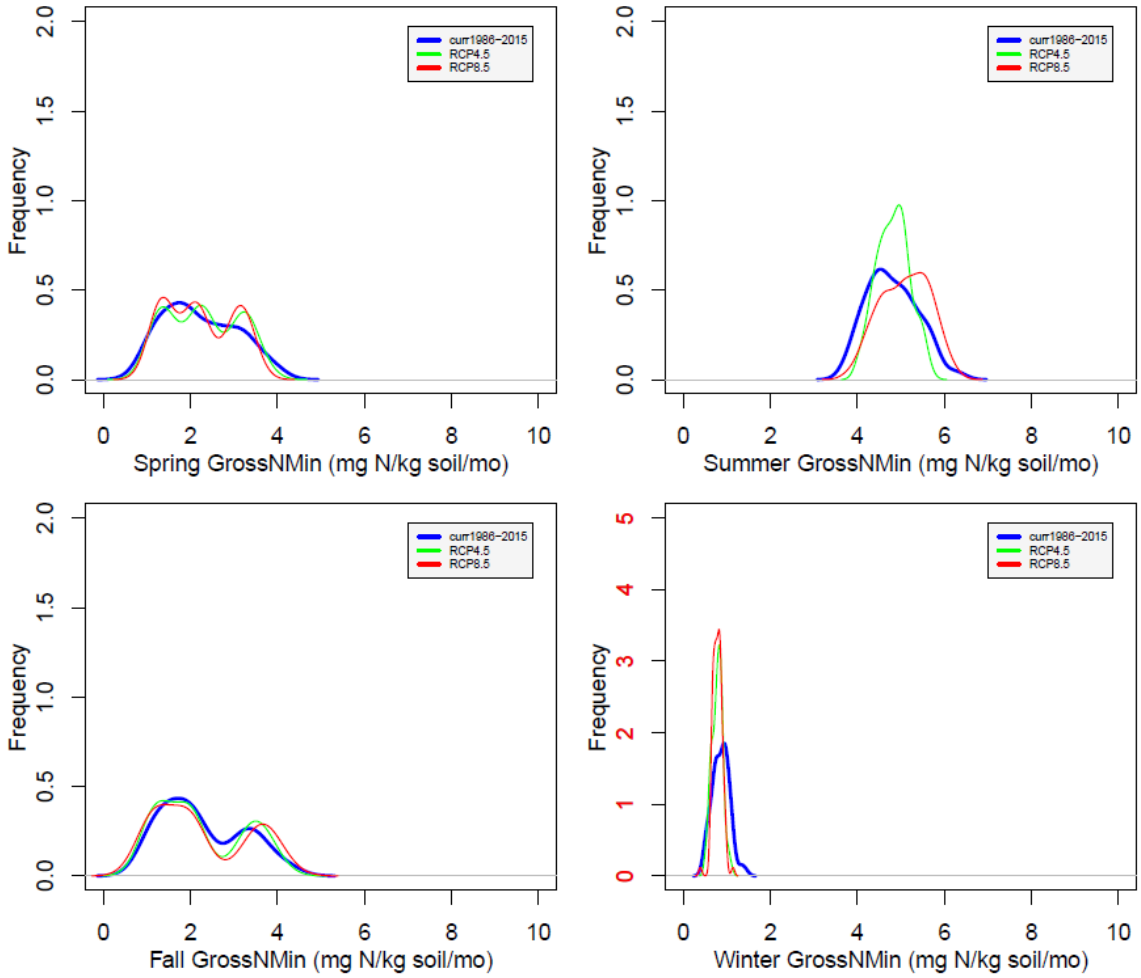

Fig. S2-7b WS27 comparison of gross nitrogen mineralization between current (1986-2015) and future climate scenarios (2071-2100, RCP4.5 and 8.5 – average of four climate models

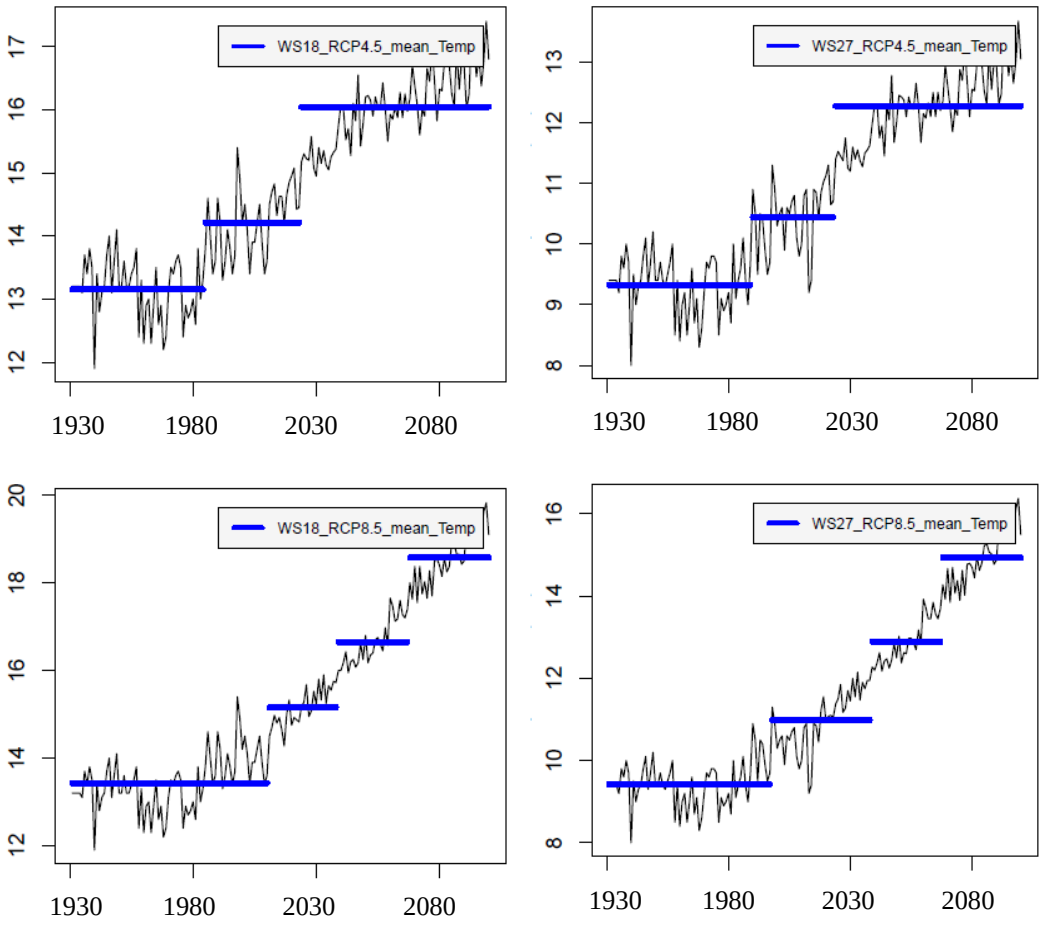

Fig. S2-8a WS18 and WS27 climate (Temperature) changing points (top right – WS18 RCP4.5, bottom right – WS18 RCP8.5, top left – WS27 RCP4.5, and bottom left – WS27 RCP8.5)

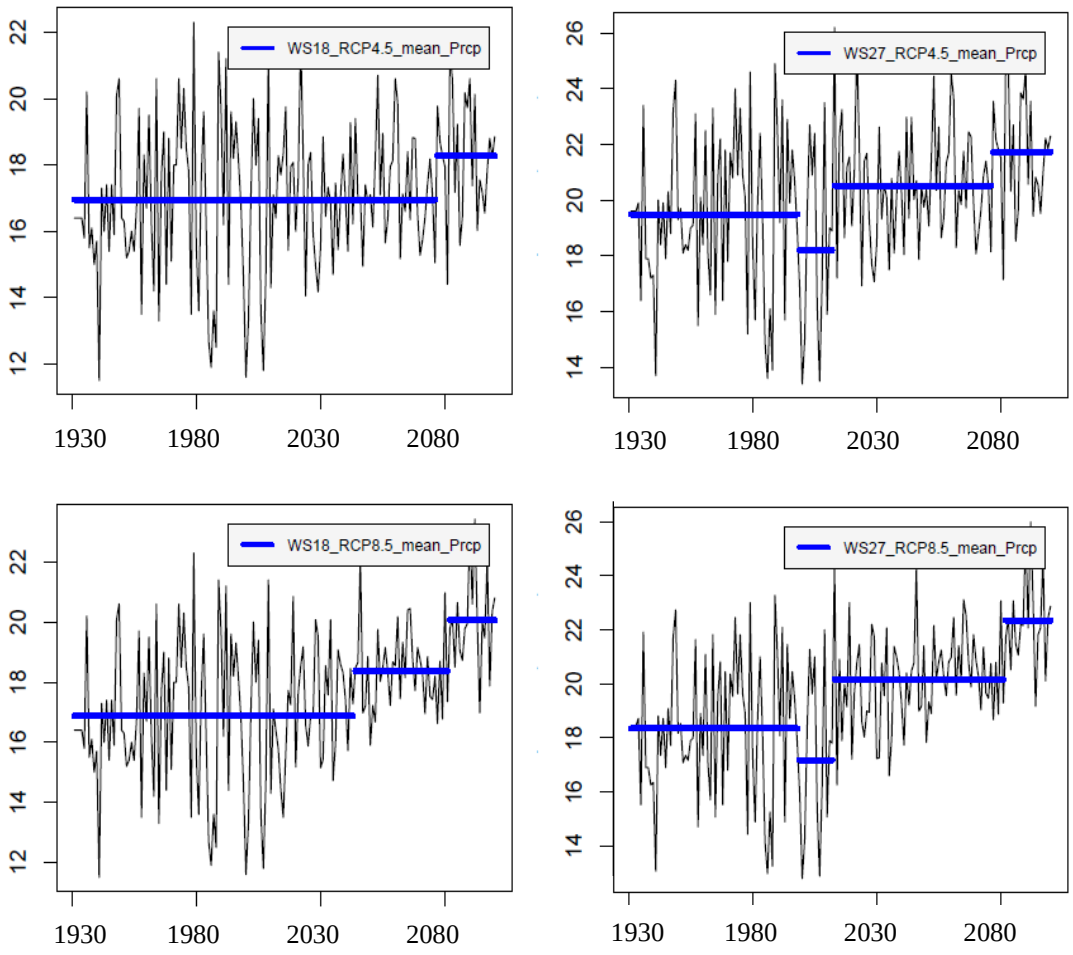

Fig. S2-8b WS18 and WS27 climate (Precipitation) changing points (top right – WS18 RCP4.5, bottom right – WS18 RCP8.5, top left – WS27 RCP4.5, and bottom left – WS27 RCP8.5)

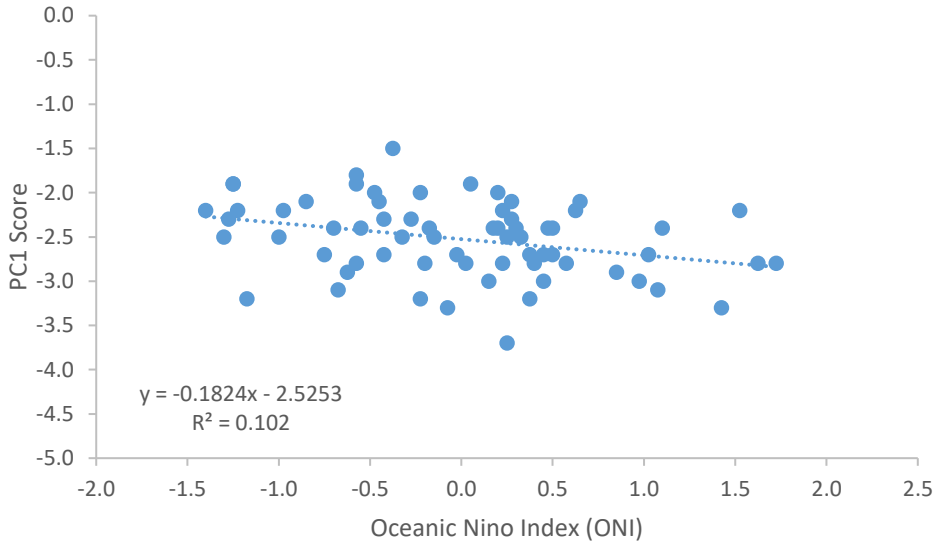

(A)

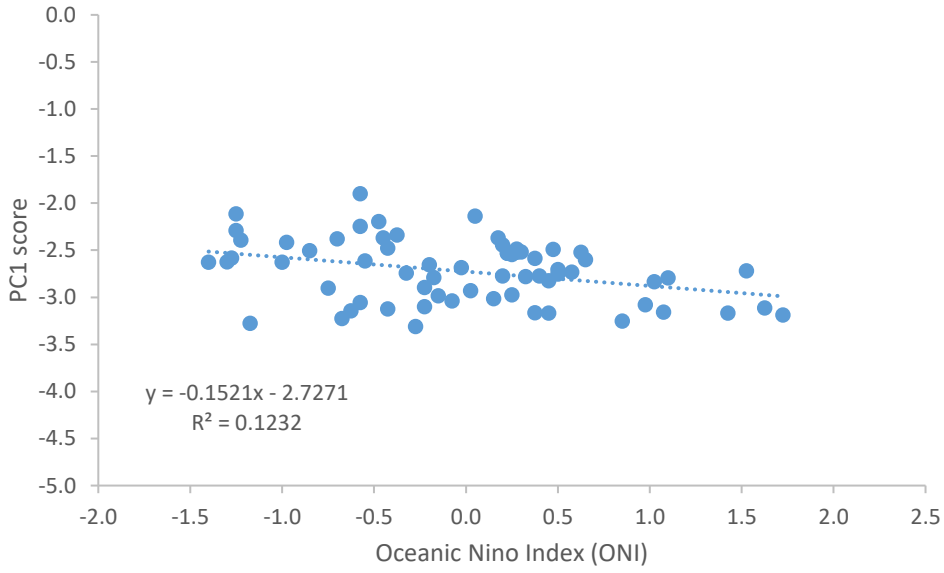

(B)

Fig. S2-9 PC1 scores in January to April from 1950 to 2015 vs. Oceanic Niño Index (ONI) at (A) WS18 and (B) WS27

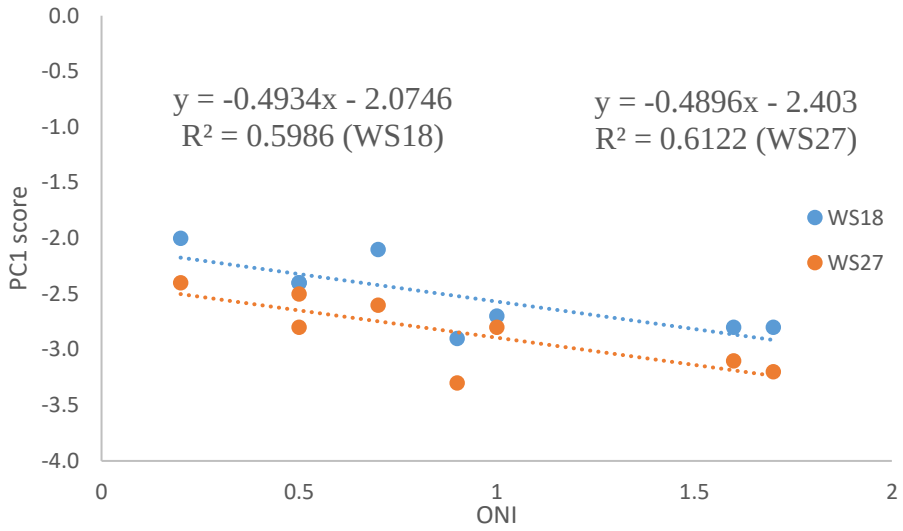

Fig. S2-10 PC1 score vs. ONI at El Niño years at both WS18 and WS27

Table S2-1. CWT WS18 and WS27 Climate and calibration data (monthly)

			Observation data	Source
WS18	Climate	Tmax	1985.01 - 2015.12 (1935.04 - 1984.12 using WS01 and WS18 regression between 1985.01 and 2015.12)	USDA FS
		Tmin	1985.01 - 2015.12 (1935.04 - 1984.12 using WS01 and WS18 regression between 1985.01 and 2015.12)	USDA FS
		Rain	1936.08 - 2015.12 (1934.08 - 1936.07 using WS01 and WS18 regression between 1936.08 and 2015.12)	USDA FS
		Solar	2010.05 - 2011.12 (1980.01 - 2010.04 using DayMET)	USDA FS
	Deposition	wet	1978.01 - 2015.12 (1930.01 - 1977.12 using SO_2 emission for SO_4^{2-})	NADP
		dry	1987.11 - 2015.12 (1978.01-1987.10 using monthly dry/wet deposition ratio derived with 1987.11-2015.12 data)	CASTNET
WS27	Climate	Tmax	1992.05 - 2015.12 (1935.04 - 1992.04using WS01 regression)	USDA FS
		Tmin	1992.05 - 2015.12 (1935.04 - 1992.04 using WS01 regression)	USDA FS
		Rain	1958.04 - 2011.12 (1934.08 - 1958.03 and 2012.01-2015.12 using WS01 regression)	USDA FS
		Solar	2010.05 - 2011.12 (1980 - 2010 using DayMET)	USDA FS
	Deposition	wet	1978.01 - 2015.12 (1930.01 - 1977.12 using SO_2 emission for SO_4^{2-})	NADP
		dry	1987.11 – 2015.12 (1978.01-1987.10 using monthly dry/wet deposition ratio derived with 1987.11-2015.12 data)	CASTNET
Vegetation			SHWDS - southern hardwoods	
Soil chemistry			varied soil chemistry from publications	
Soil properties			STATSGO	
Discharge			1936.07 - 2015.12 for WS18 and 1946.11 - 2015.12 for WS27	USDA FS
Water chemistry			1971.09-2014.12 for WS18 and 1971.09-2014.12 for WS27	USDA FS

Table S2-2. WS18 and WS27 past, current, and future (RCP4.5 and RCP8.5) seasonal climate

	*Climate*①	Spr	Sum	Aut	Win	Mean	Differ.②	Var.③
					Temperature (ºC)			
WS18	Past	12.9	21.6	13.6	4.8	13.2		
	Current	13.9	22.5	14.6	5.2	14.1	0.8*	
	RCP4.5	16.7	25.2	17.1	7.0	16.5	2.45^	0.5
	RCP8.5	18.6	27.5	19.2	9.2	18.6	4.58^	0.4
WS27	Past	9.0	17.9	9.8	0.8	9.4		
	Current	10.2	18.9	10.4	1.4	10.2	0.9	
	RCP4.5	13.1	21.7	13.0	3.1	12.7	2.50	0.5
	RCP8.5	15.0	24.4	15.2	5.4	15.0	4.78	0.6
					Precipitation (cm/mo)			
WS18	Past	16.9	15.6	12.7	19.6	16.2		
	Current	14.7	13.8	15.3	17.2	15.3	-1.0	
	RCP4.5	19.8	15.7	15.8	20.2	17.9	2.63	1.9
	RCP8.5	20.2	17.1	16.8	22.8	19.2	3.98	2.0
WS27	Past	20.0	18.4	15.3	23.0	19.2		
	Current	18.4	17.7	19.4	20.8	19.1	-0.1	
	RCP4.5	23.3	18.8	19.7	23.4	21.3	2.23	2.0
	RCP8.5	22.5	19.0	20.8	24.9	21.8	2.73	1.6

In this table, seasonal average climate in: ① – past climate between 1936 and 1965, – current climate between 1986 and 2015, and – future climate between 2071 and 2100 from four GCMs under either RCP4.5 or RCP8.5 scenario; ②– current climate minus past climate (*) or future climate minus current climate (^); ③: seasonal variability – future climate minus current climate. For seasons: Spr – March to May, Sum – June to August, Aut – September to November, and Win – December to February.

Table S2-3. Other variables PnET-BGC simulation vs published data

	Simulations-WS18	Simulations-WS27	Measured	Sources
NPP (kg/ha/yr) Aboveground (wood and foliage)	8,882 (1971-1980 average)	7,230 (1971-1980 average)	7,965	Day and Monk, 1977 at WS18
Base saturation (BS, %)	24.9 (2001- 2010 average)	4.0 (2001- 2010 average)	9.2 – 19.7 (top soil: <10 cm, soil: 10-30 cm, and bottom soil: 30-90 cm)	USDA FS 2008 soil survey provided by USDA FS Southern Research Station at Coweeta, NC
Net nitrogen mineralization (mg N/kg soil/mo)	2.5	3.1	<1.2 mg N /kg soil/ 28 days at lower elevation oak-pine; 3.8 mg N/kg soil/28 days @ cove hardwood; 13 mg N/kg soil/28 days @ higher elevation northern hardwoods	Knoepp and Swank, 1998 at WS18 and WS27

In above table, all the simulations results listed were ten years range covering the published work date, such as NPP (Day and Monk's work published in 1977 and then the NPP simulation results used was from 1971 to 1980).

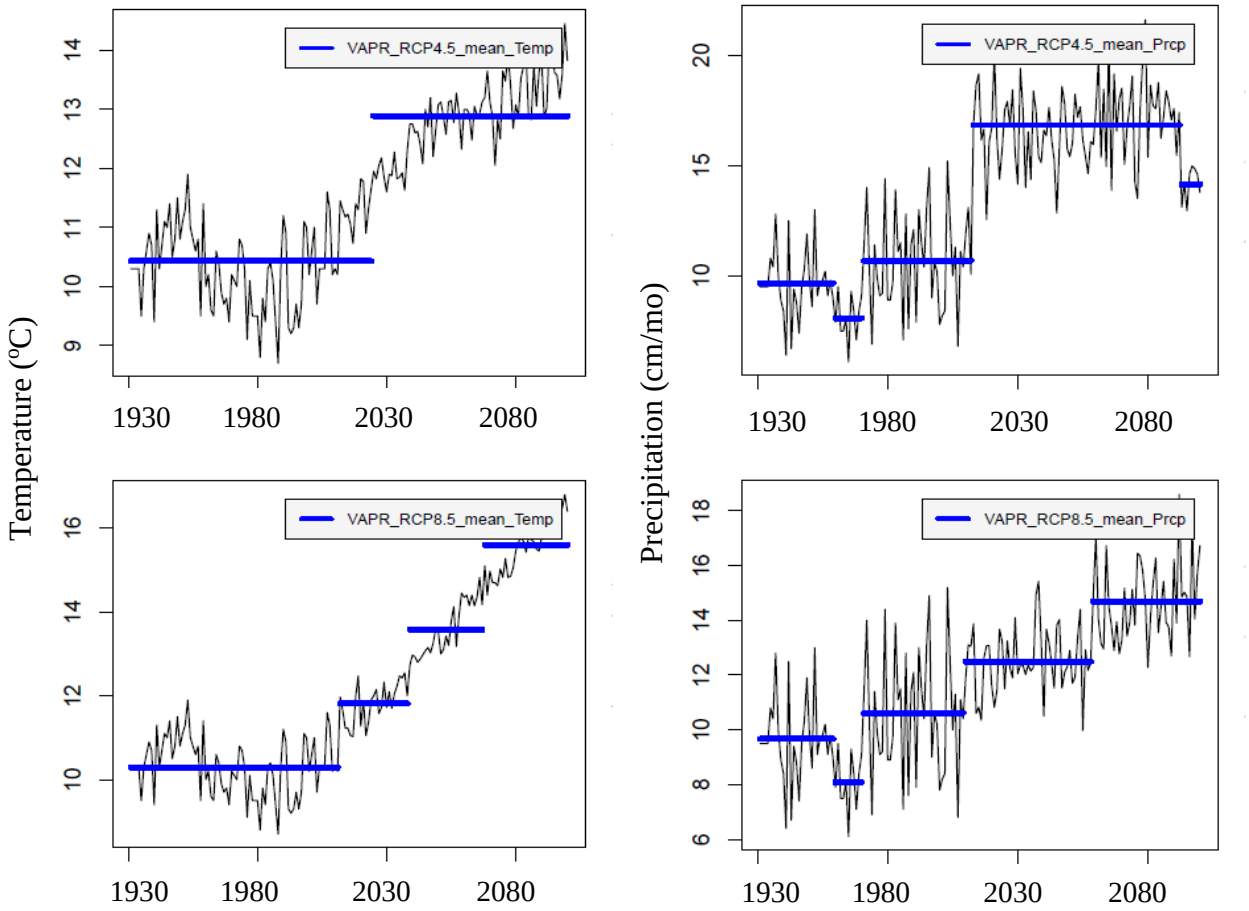

Fig. S3-1a SNP PR climate changing point between 1931 and 2100 (temperature and precipitation)

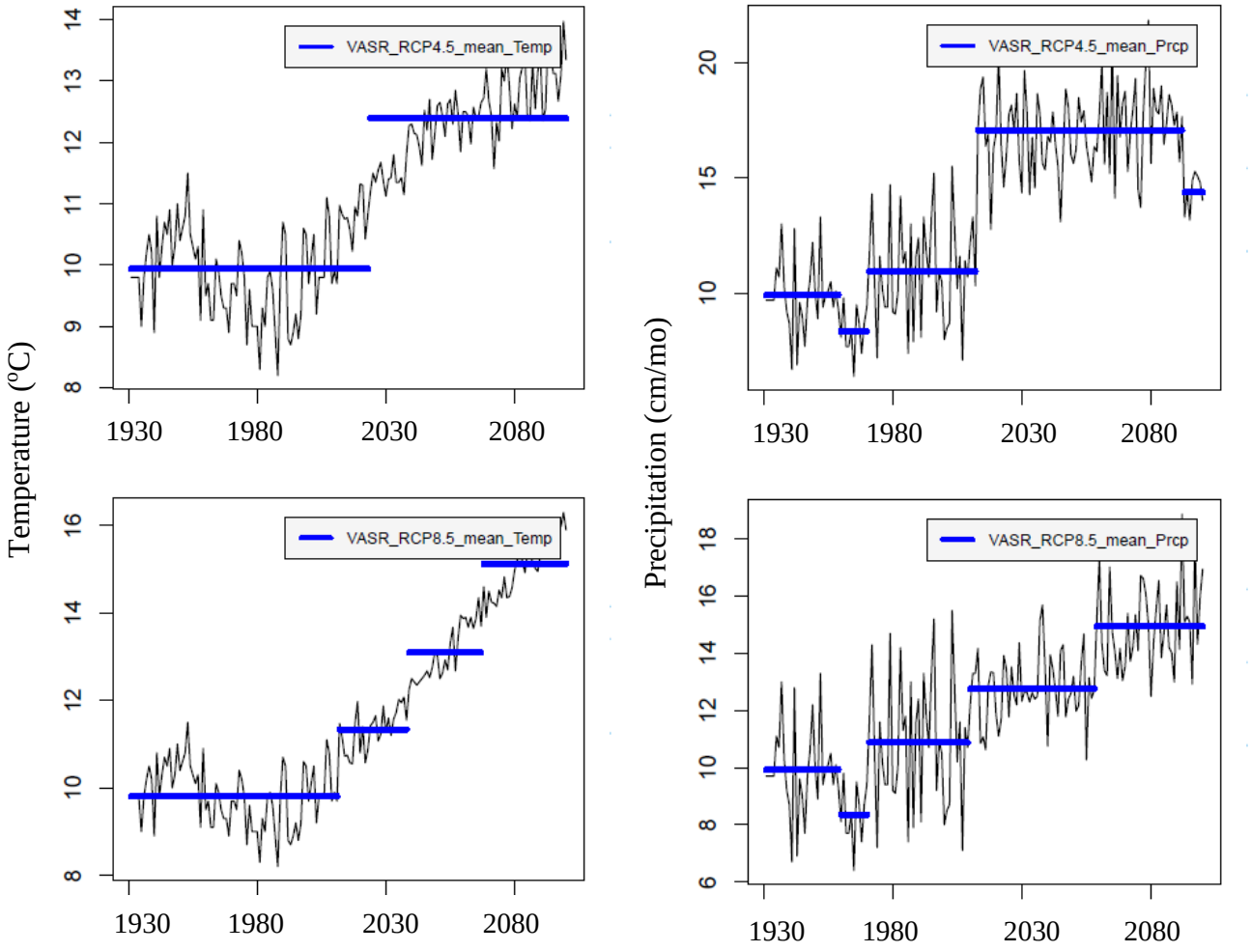

Fig. S3-1b SNP SR climate changing point between 1931 and 2100 (temperature and precipitation)

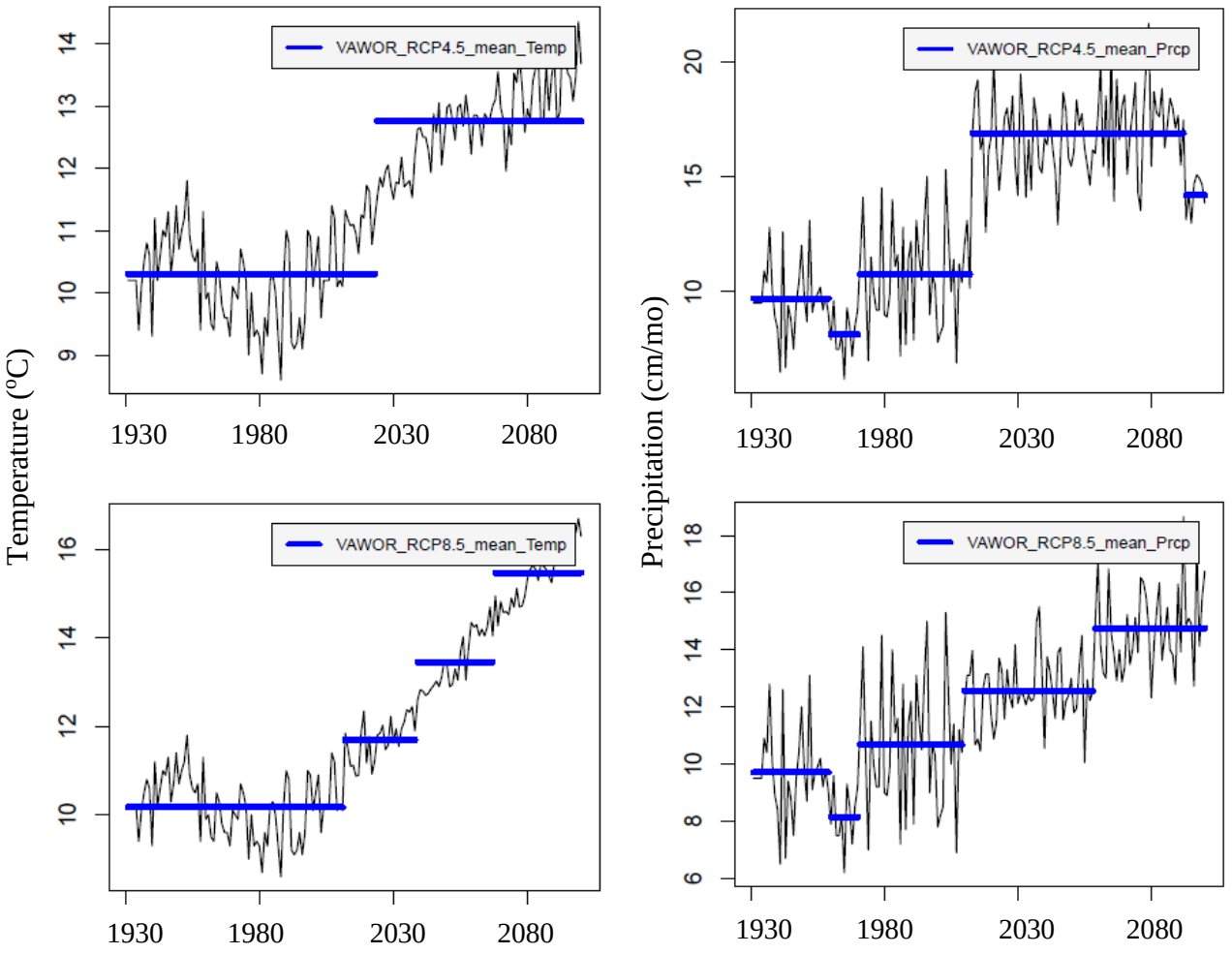

Fig. S3-1c SNP WOR climate changing point between 1931 and 2100 (temperature and precipitation)

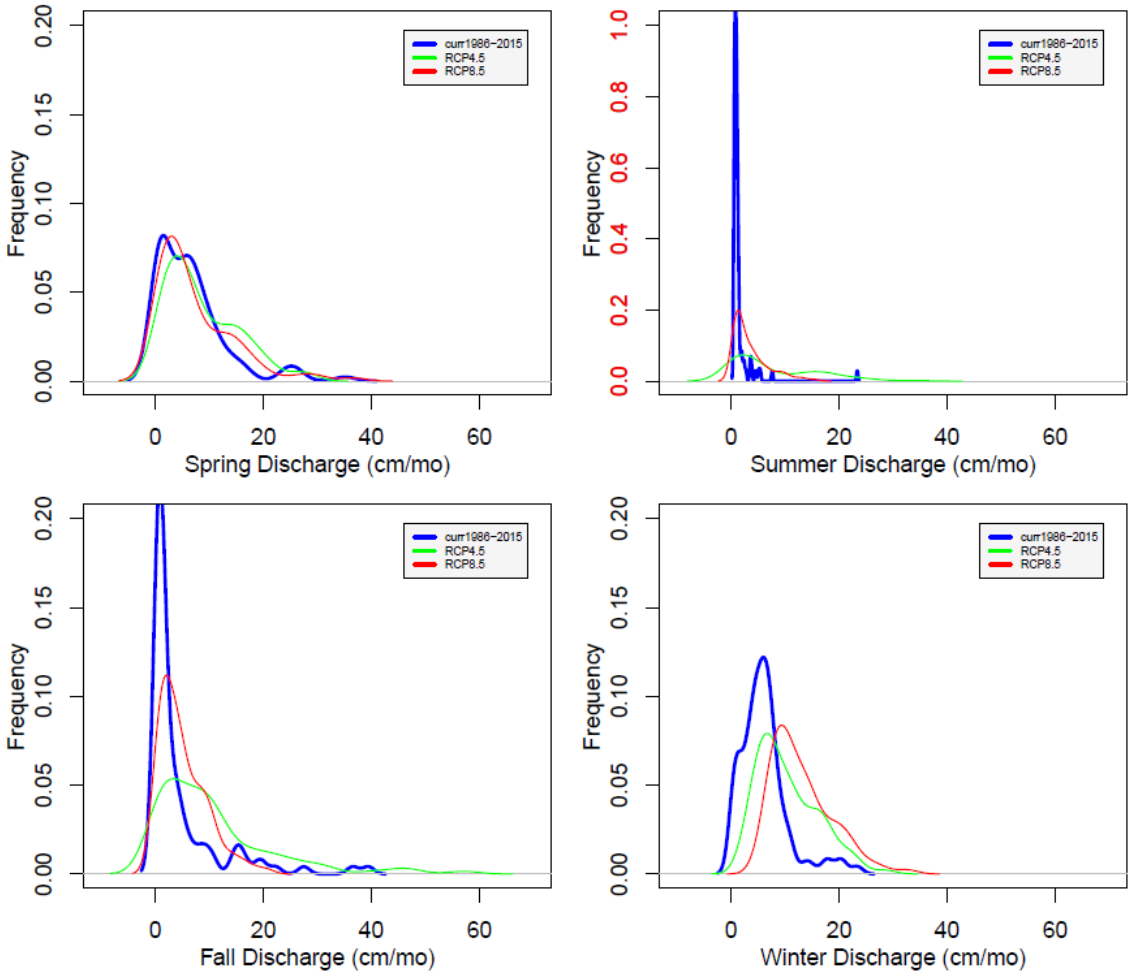

Fig. S3-2a SNP PR comparison of Discharge between current (1986-2015) and future climate scenarios (2071-2100, RCP4.5 and 8.5 – average of four climate models)

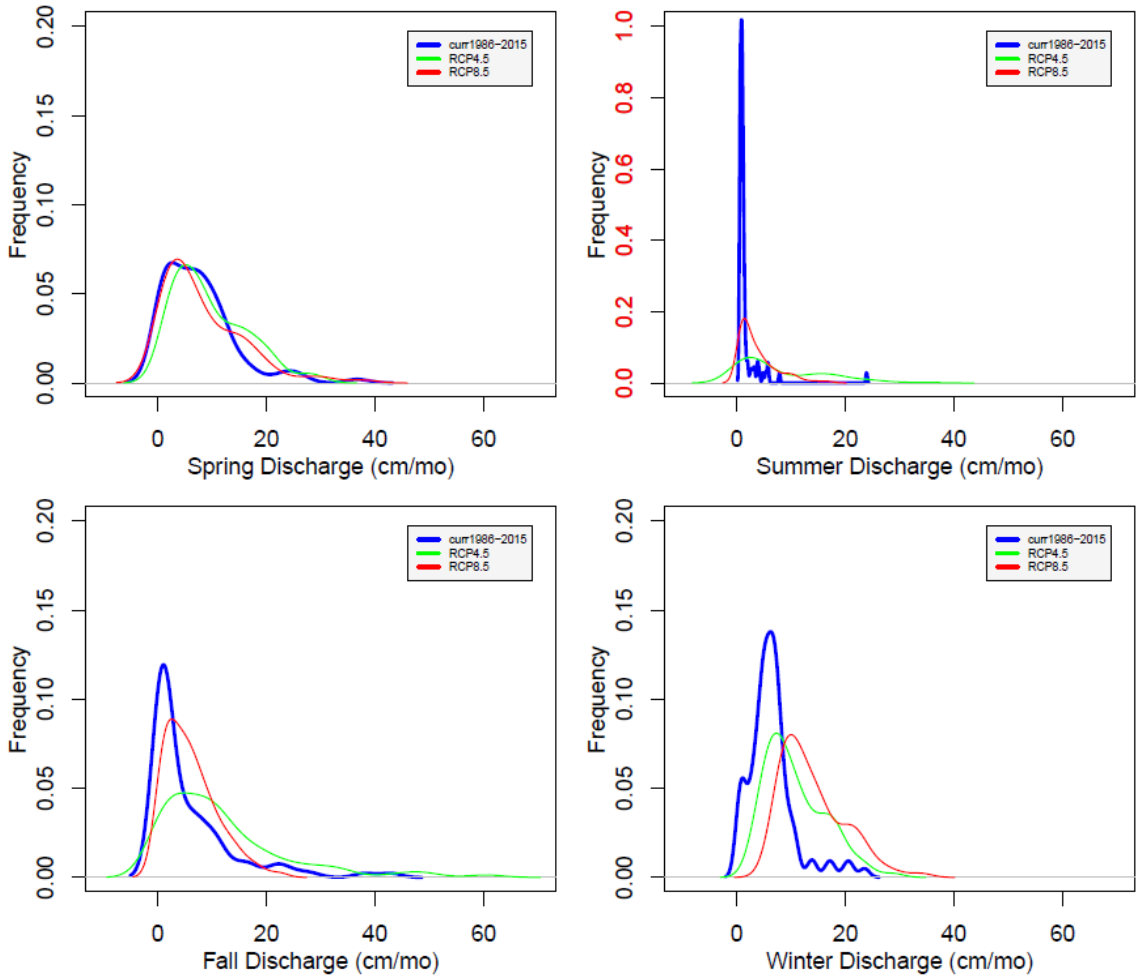

Fig. S3-2b SNP SR comparison of Discharge between current (1986-2015) and future climate scenarios (2071-2100, RCP4.5 and 8.5 – average of four climate models)

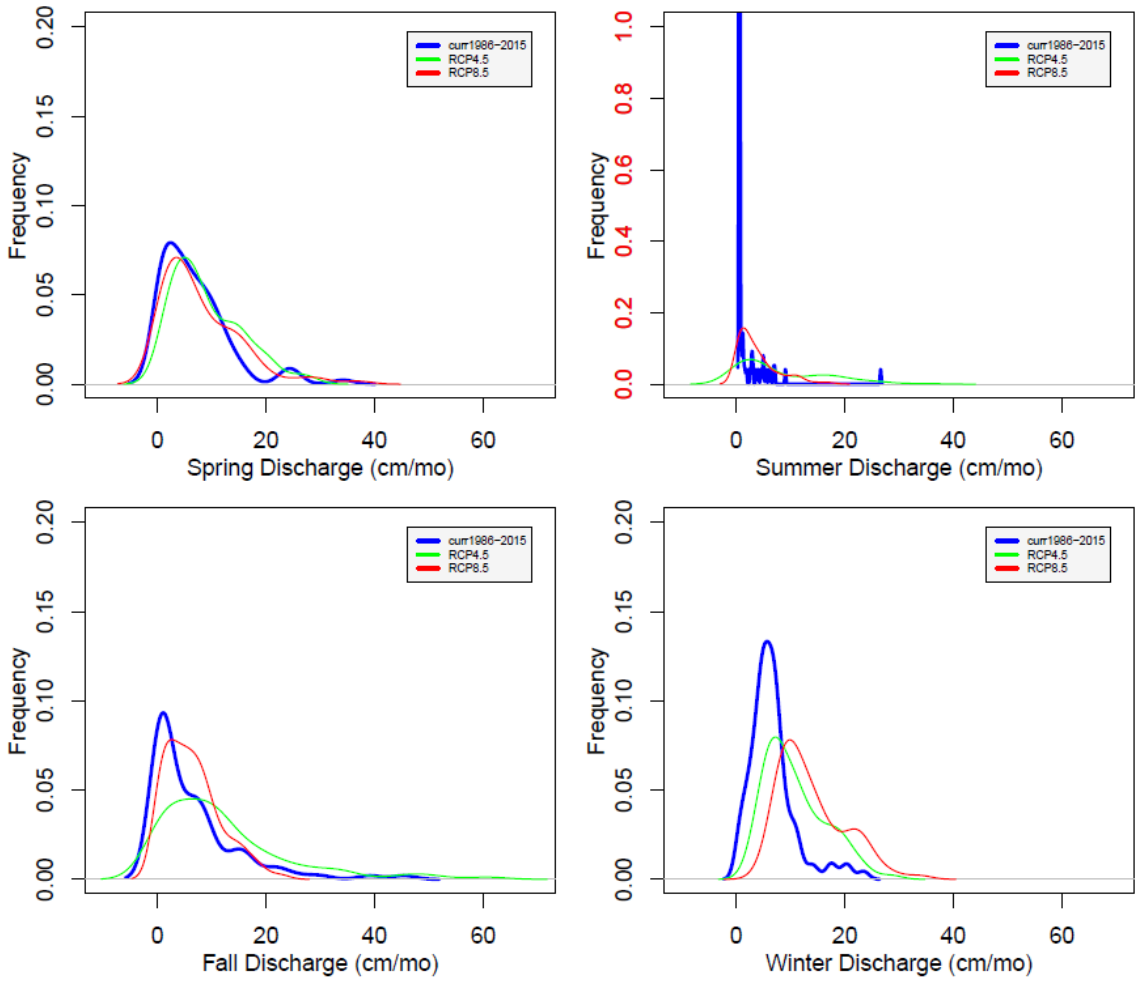

Fig. S3-2c SNP WOR comparison of Discharge between current (1986-2015) and future climate scenarios (2071-2100, RCP4.5 and 8.5 – average of four climate models)

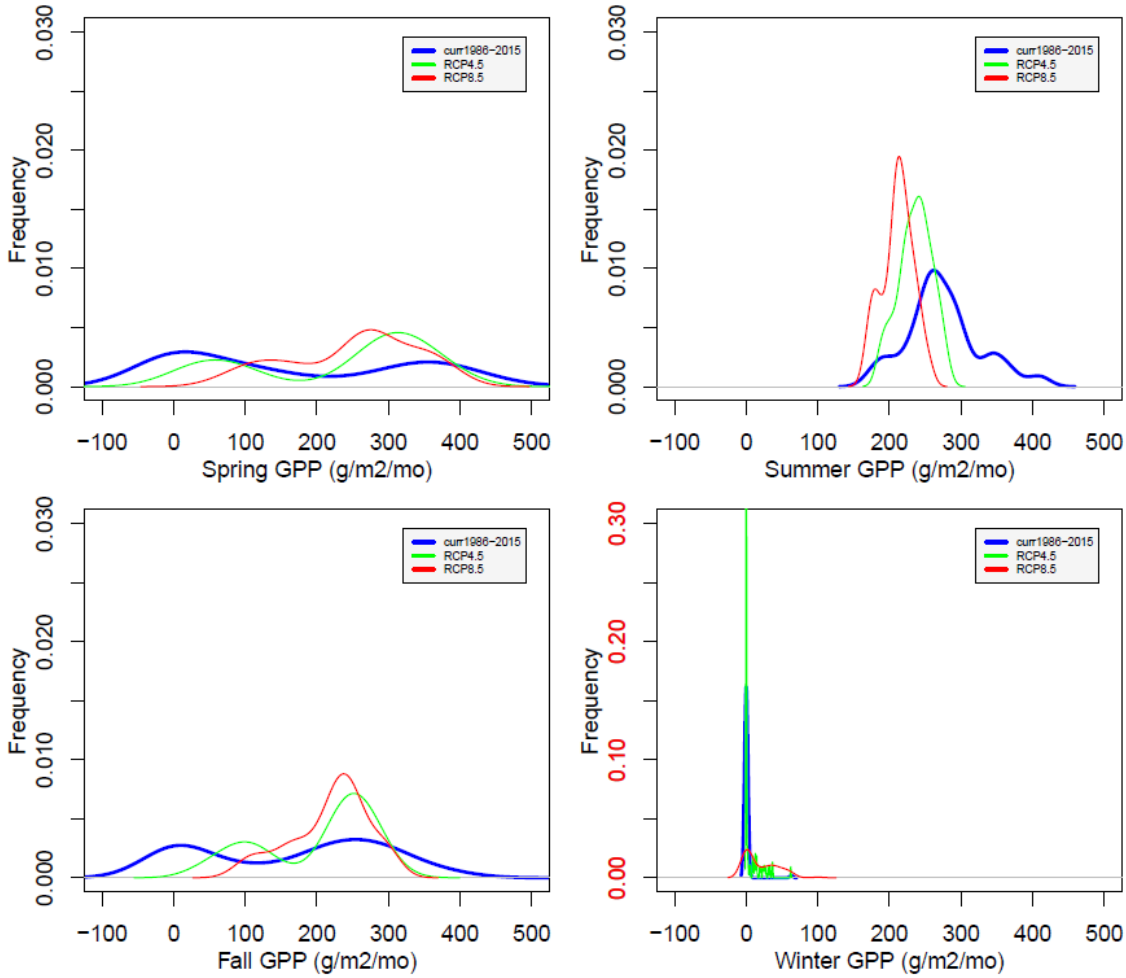

Fig. S3-3a SNP PR comparison of GPP between current (1986-2015) and future climate scenarios (2071-2100, RCP4.5 and 8.5 – average of four climate models)

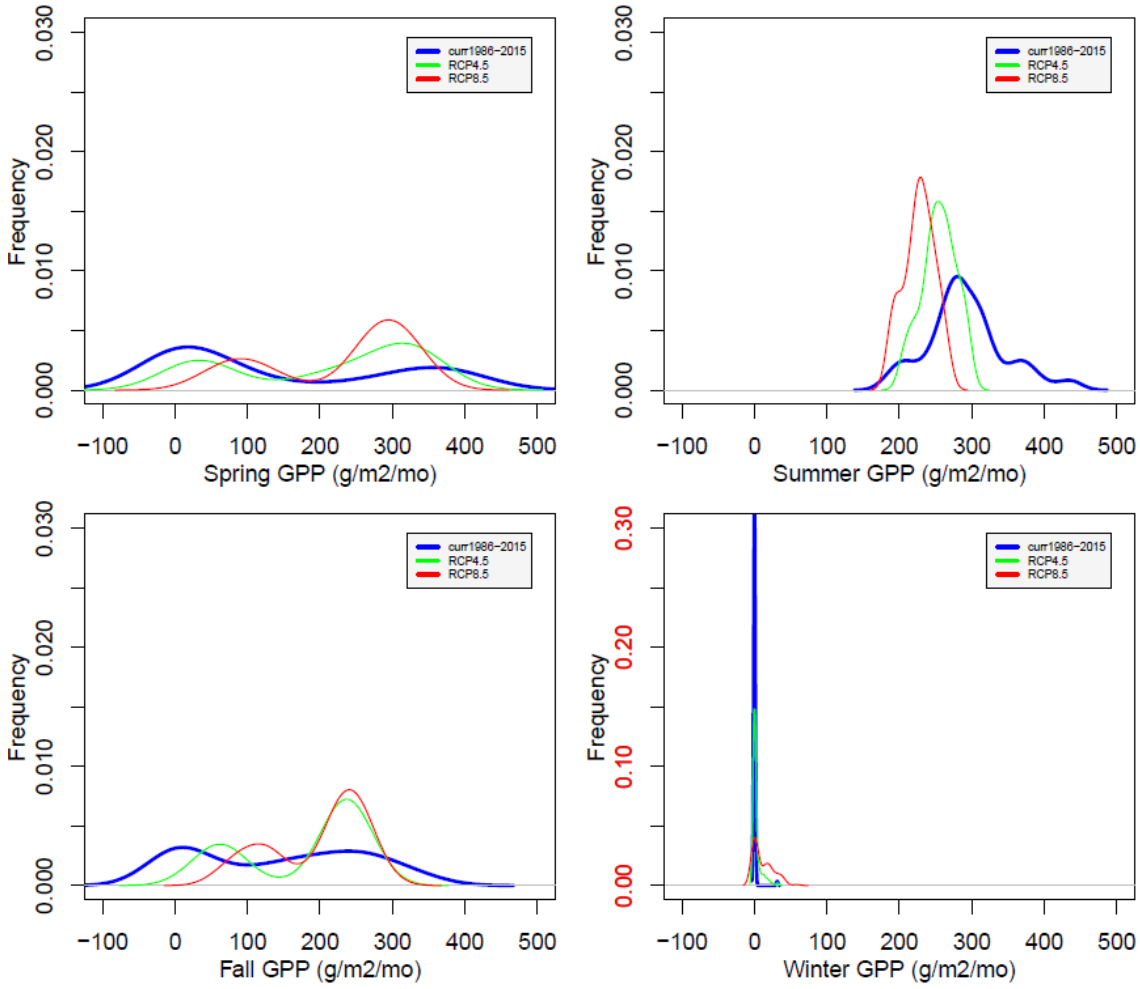

Fig. S3-3b SNP SR comparison of GPP between current (1986-2015) and future climate scenarios (2071-2100, RCP4.5 and 8.5 – average of four climate models)

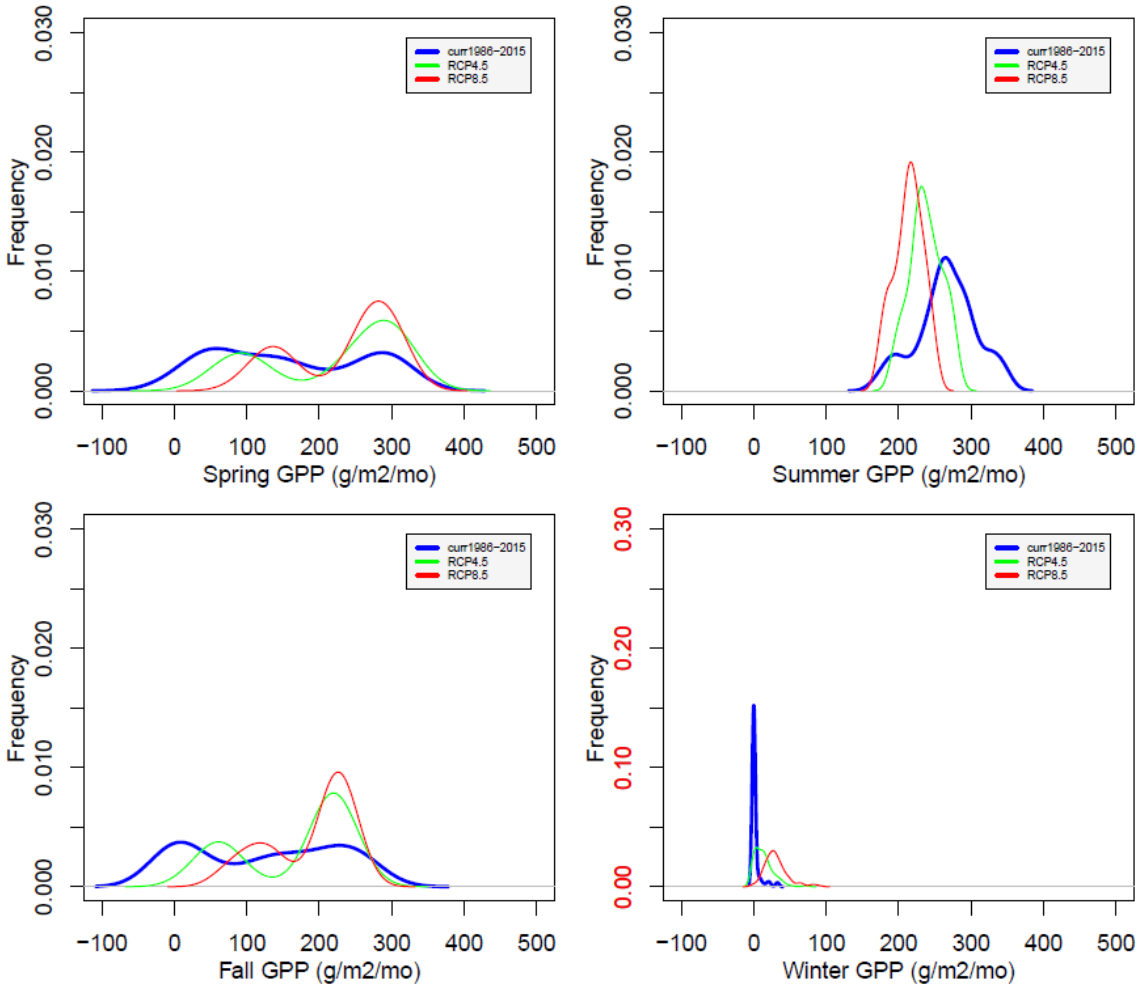

Fig. S3-3c SNP WOR comparison of GPP between current (1986-2015) and future climate scenarios (2071-2100, RCP4.5 and 8.5 – average of four climate models)

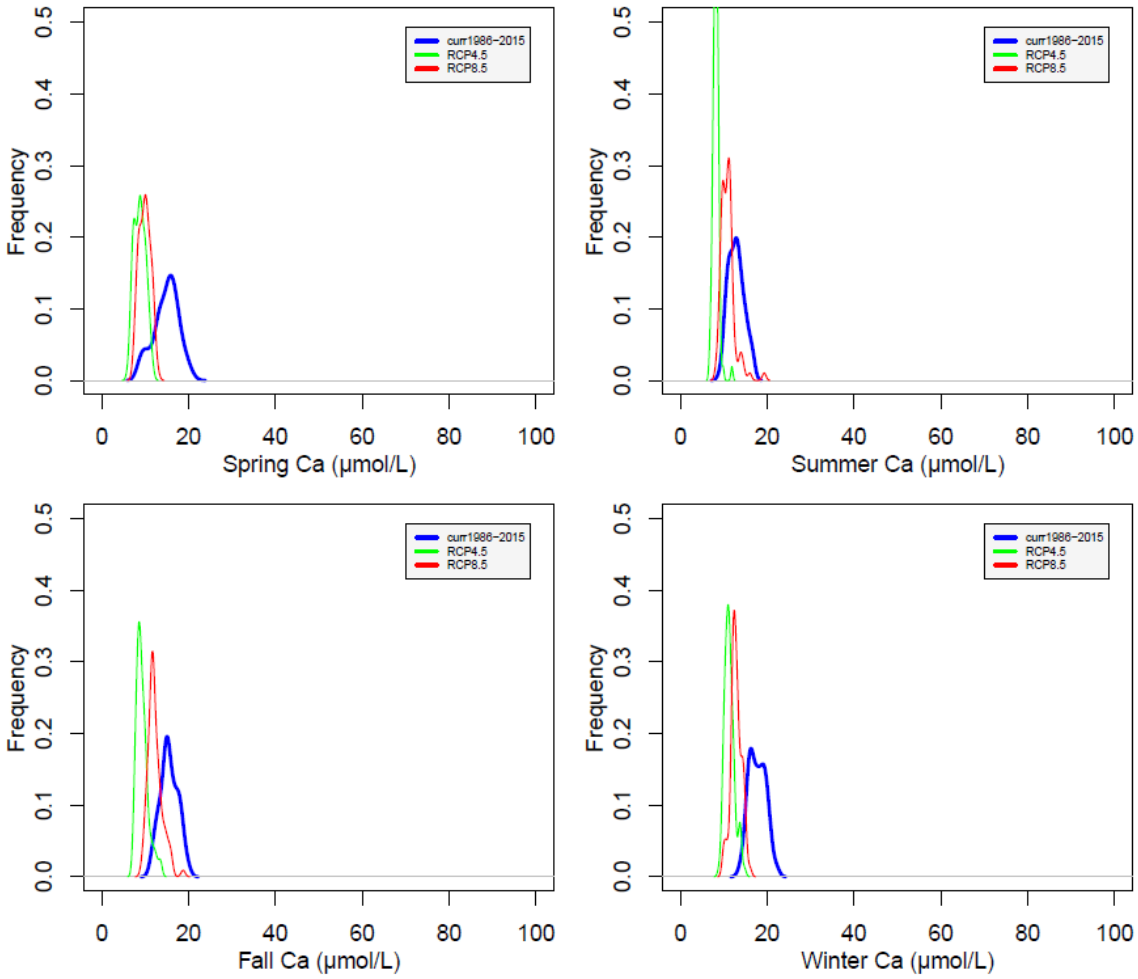

Fig. S3-4a SNP PR comparison of stream Ca^{2+} between current (1986-2015) and future climate scenarios (2071-2100, RCP4.5 and 8.5 – average of four climate models)

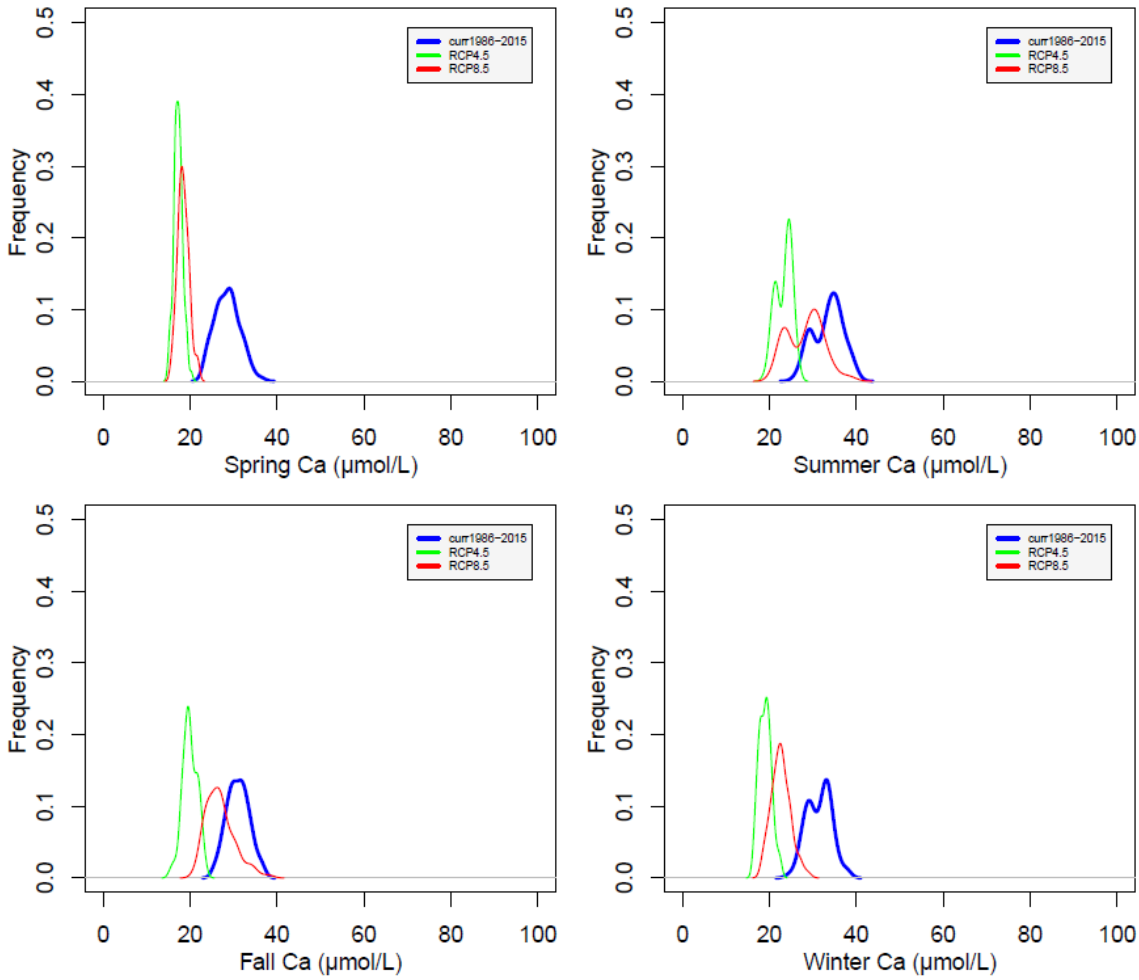

Fig. S3-4b SNP SR comparison of stream Ca^{2+} between current (1986-2015) and future climate scenarios (2071-2100, RCP4.5 and 8.5 – average of four climate models)

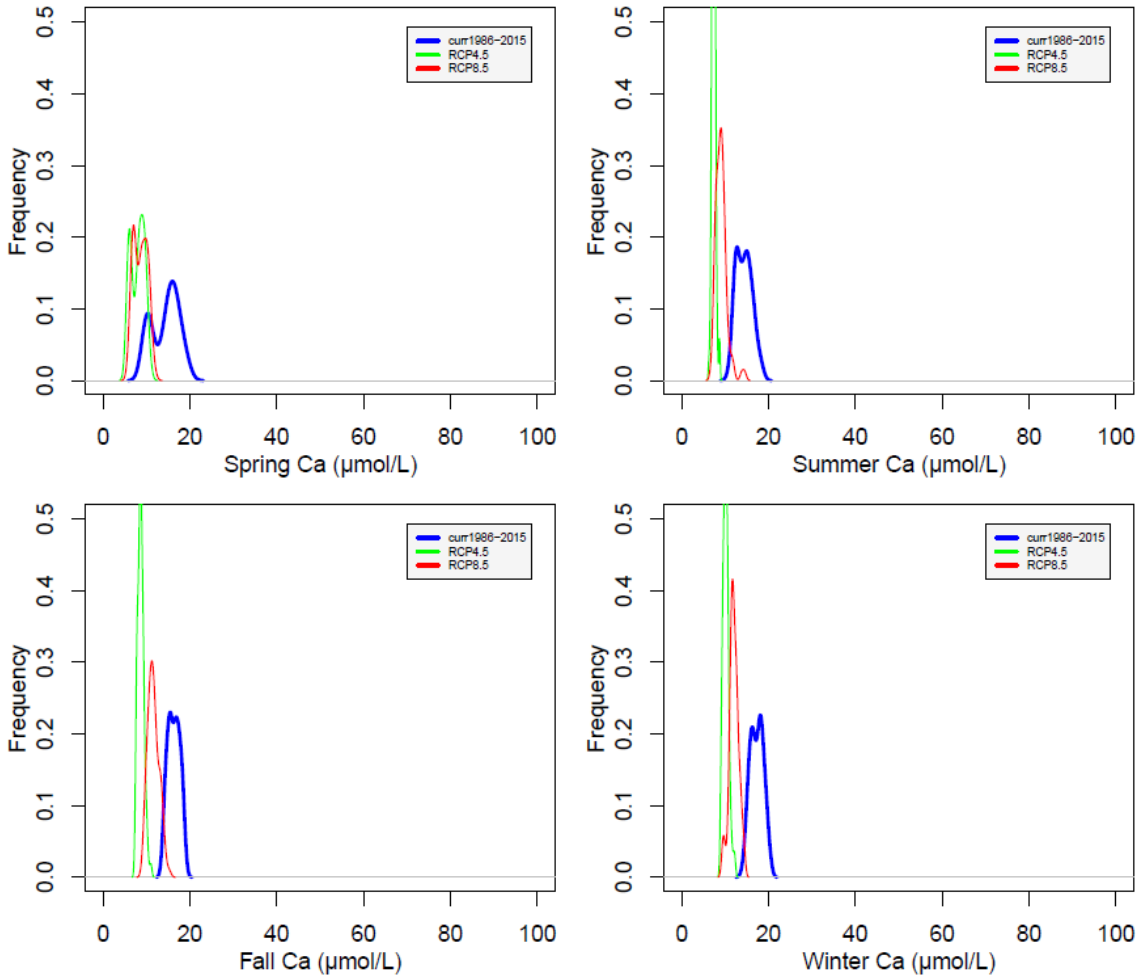

Fig. S3-4c SNP WOR comparison of stream Ca^{2+} between current (1986-2015) and future climate scenarios (2071-2100, RCP4.5 and 8.5 – average of four climate models)

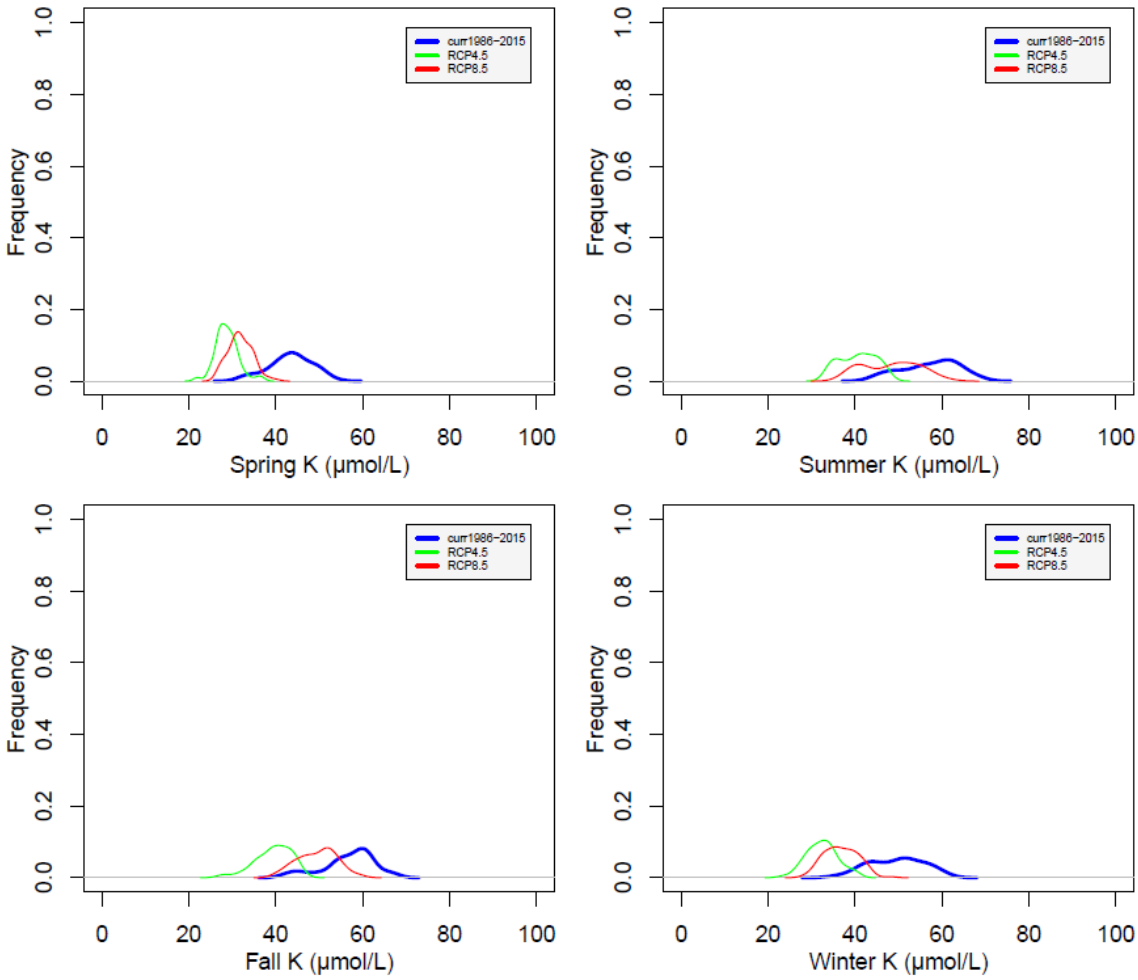

Fig. S3-5a SNP PR comparison of stream K^+ between current (1986-2015) and future climate scenarios (2071-2100, RCP4.5 and 8.5 – average of four climate models)

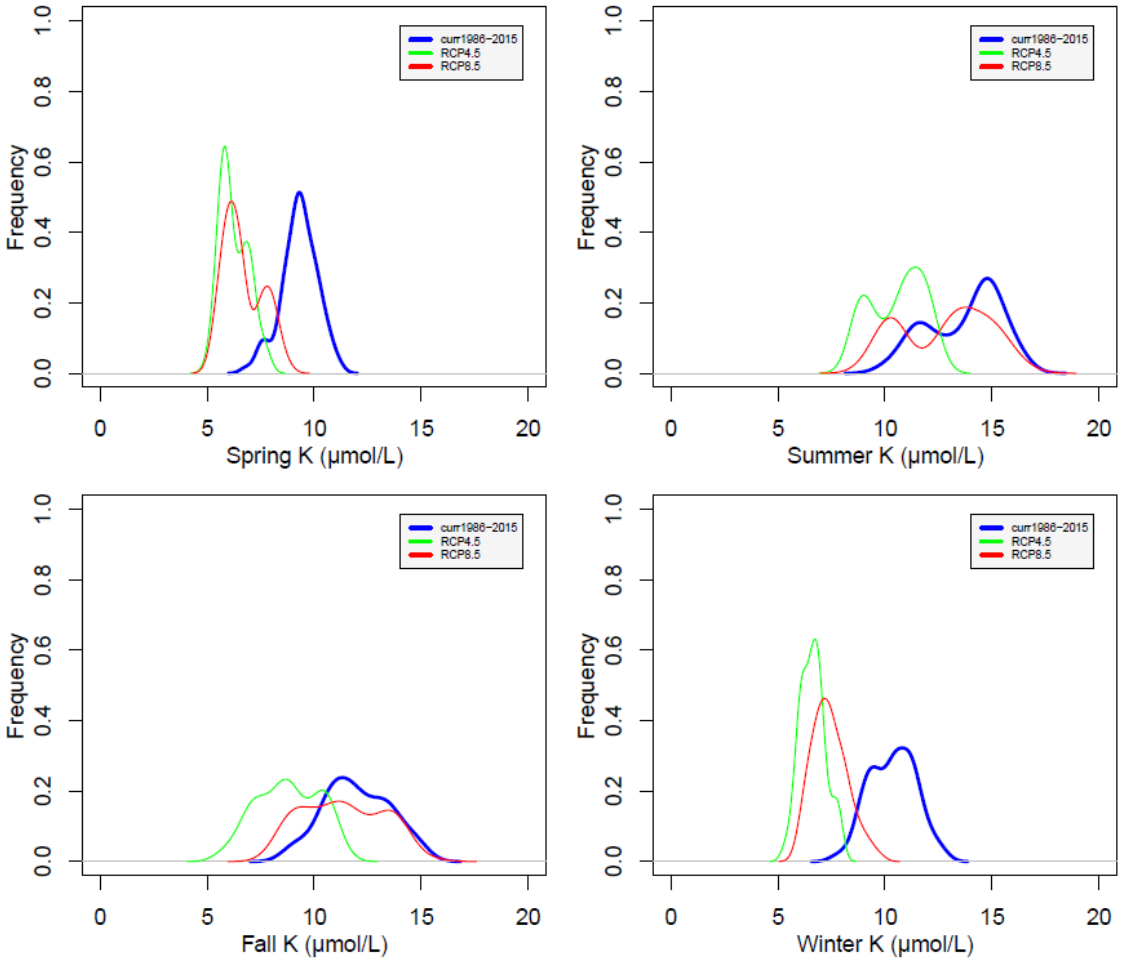

Fig. S3-5b SNP SR comparison of stream K^+ between current (1986-2015) and future climate scenarios (2071-2100, RCP4.5 and 8.5 – average of four climate models)

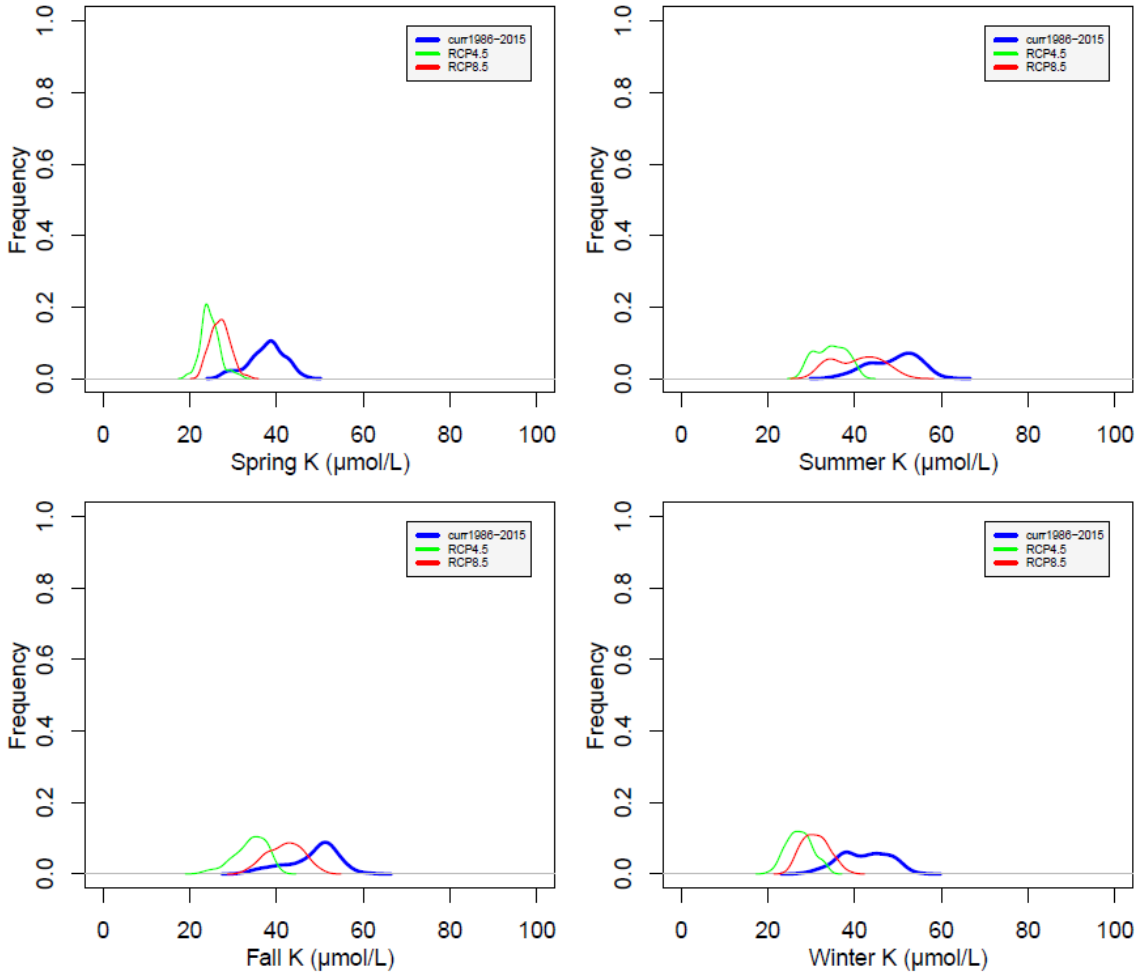

Fig. S3-5c SNP WOR comparison of stream K^+ between current (1986-2015) and future climate scenarios (2071-2100, RCP4.5 and 8.5 – average of four climate models)

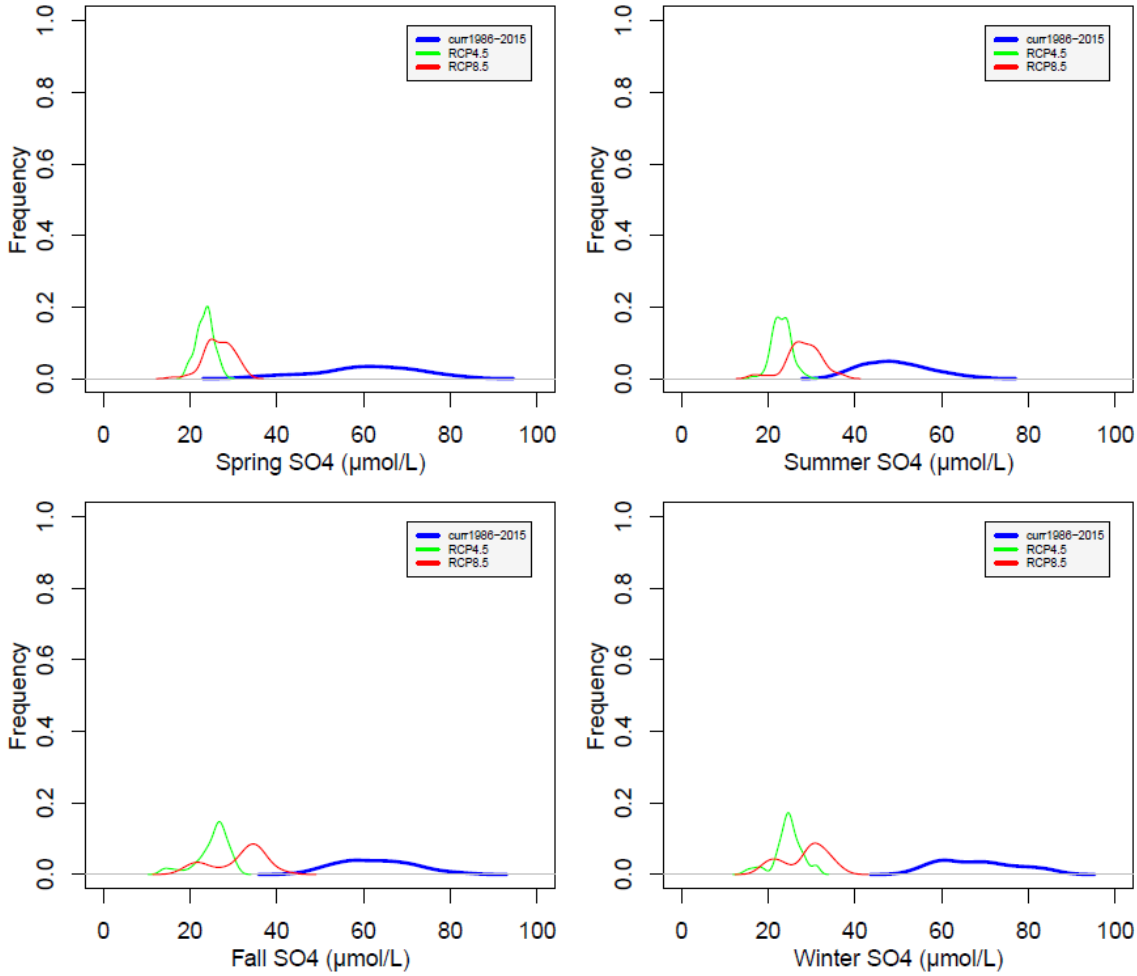

Fig. S3-6a SNP PR comparison of stream SO_4^{2-} between current (1986-2015) and future climate scenarios (2071-2100, RCP4.5 and 8.5 – average of four climate models)

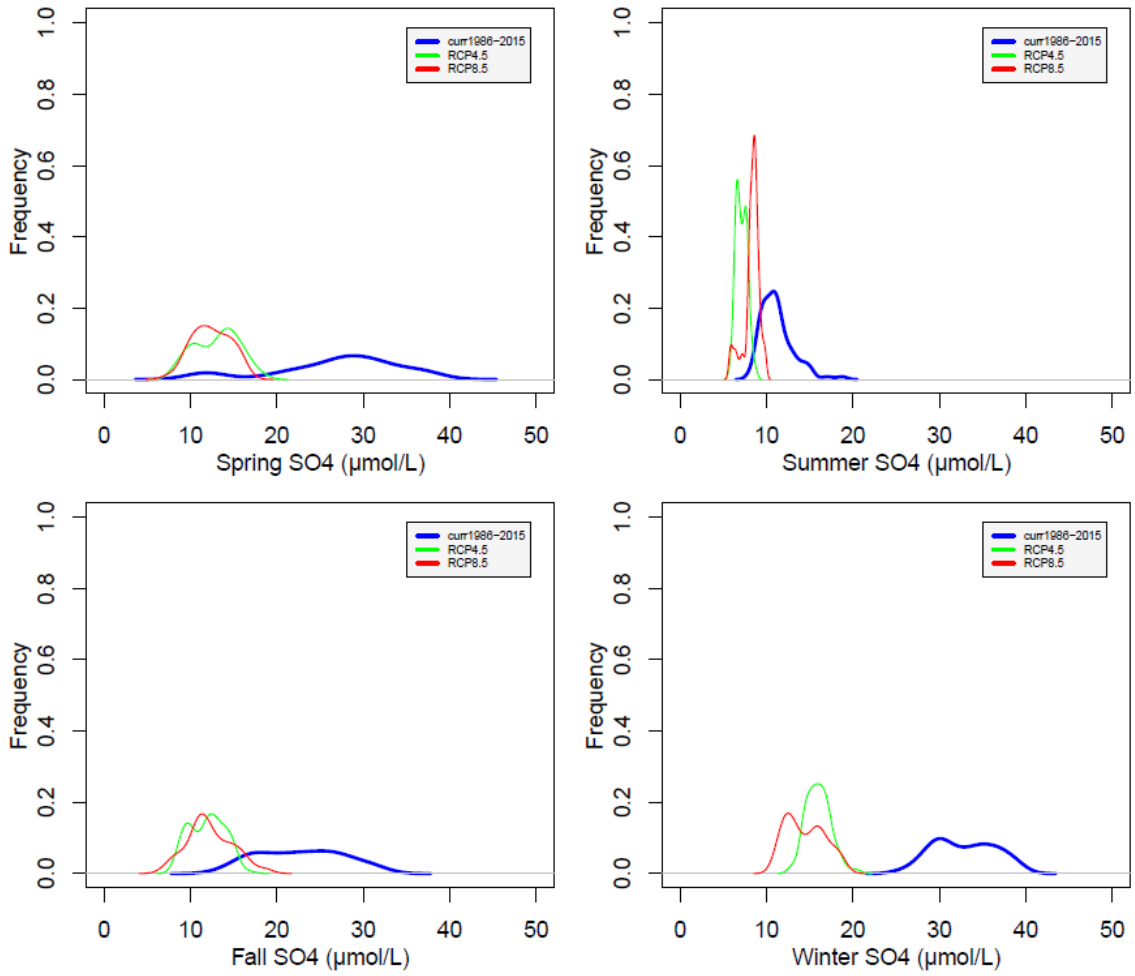

Fig. S3-6b SNP SR comparison of stream SO_4^{2-} between current (1986-2015) and future climate scenarios (2071-2100, RCP4.5 and 8.5 – average of four climate models)

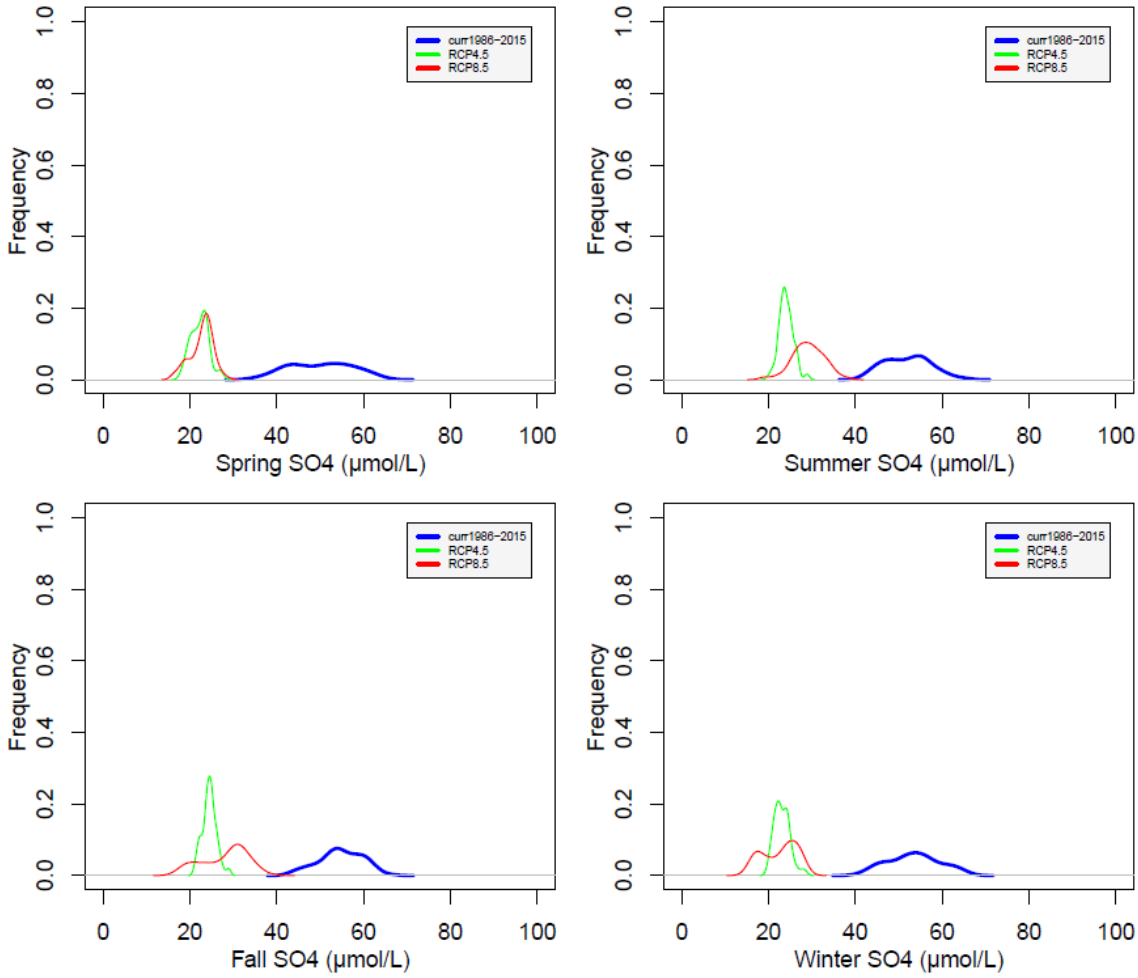

Fig. S3-6c SNP WOR comparison of stream SO_4^{2-} between current (1986-2015) and future climate scenarios (2071-2100, RCP4.5 and 8.5 – average of four climate models)

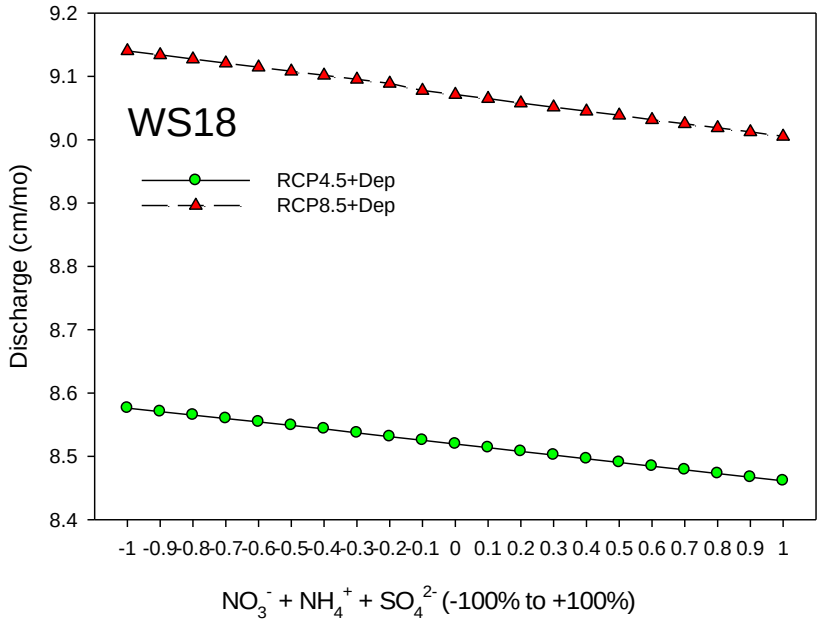

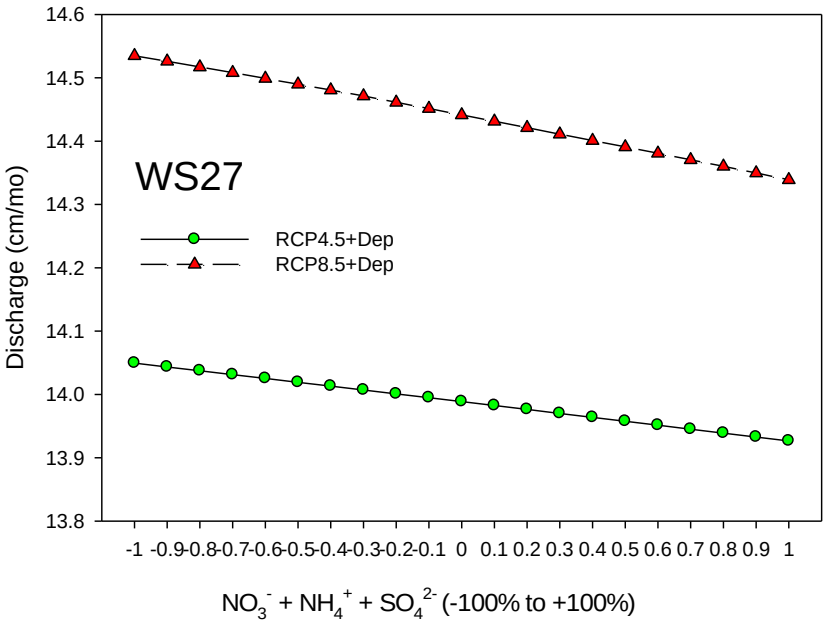

Fig. S3-7 Discharge vs. Deposition changes in NO_3^-, NH_4^+, and SO_4^{2-} (data between 2071 and 2100)

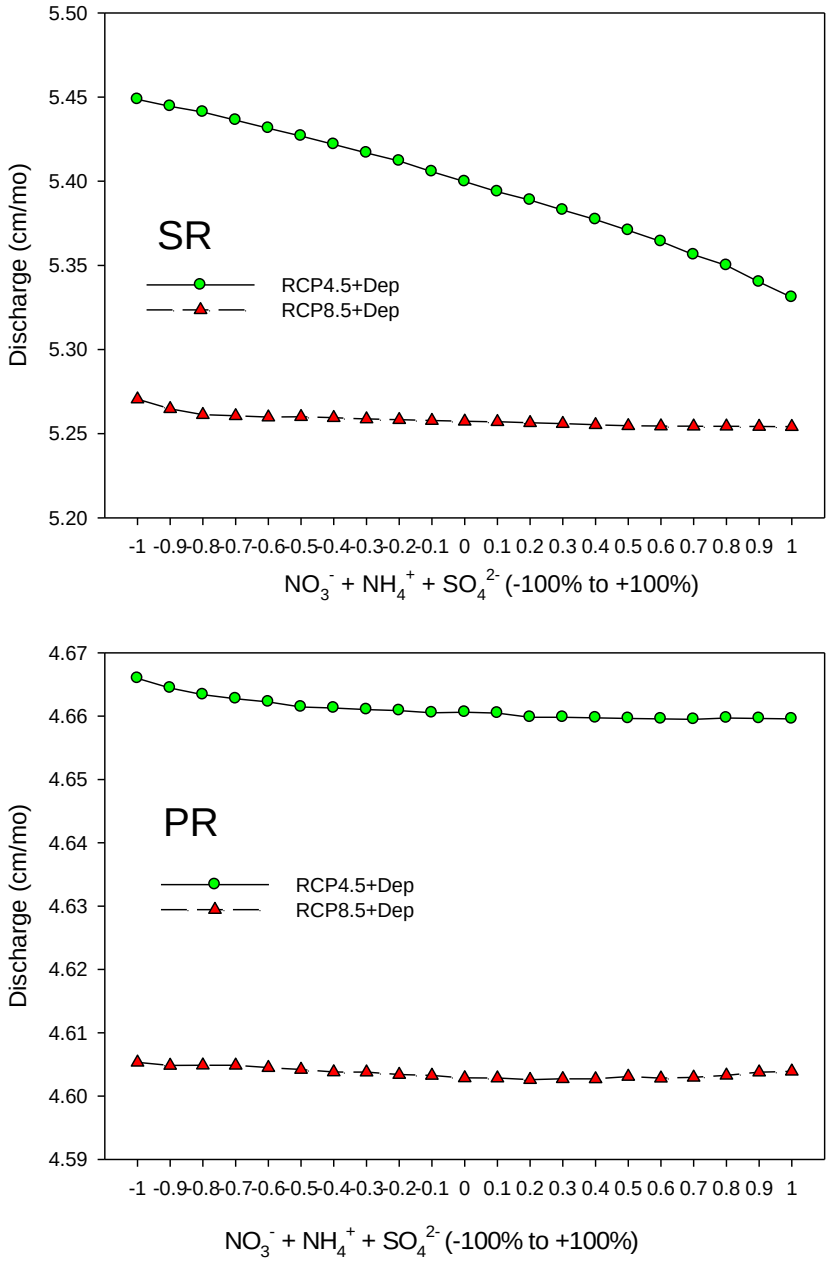

Fig. S3-7 Continued Discharge vs. Deposition changes in NO_3^-, NH_4^+, and SO_4^{2-} (data between 2071 and 2100)

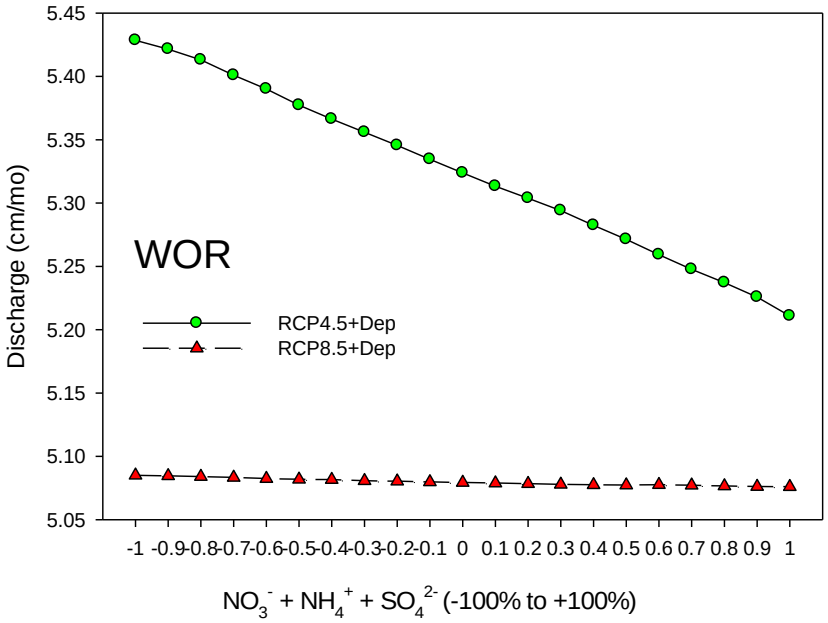

Fig. S3-7 Continued Discharge vs. Deposition changes in NO_3^-, NH_4^+, and SO_4^{2-} (data between 2071 and 2100)

Table S3-1. Coweeta basin, NC and Shenandoah National Park, VA watersheds climate (1935 to 2012)

	Latitude (°)	Elev. (m)	Area (ha)	Prcp. (cm/yr)	Annual Temp. (°C)	Discharge (cm/yr)
WS18	35.0495N	726-993 (887)	13	192	14.0 (8.9-19.6)	96
WS27	35.0340N	1,061-1,454 (1,398)	39	229	10.2 (5.9-14.5)	163
Paine River	38.1986N	434-1,040 (657)	1,390	128	10.4 (4.9-15.9)	40
Staunton River	38.4446N	309-1,181 (768)	1,010	132	9.9 (4.7-15.2)	69
White Oak Run	38.2508N	674-1,594 (685)	1,480	124	10.2 (4.7-15.6)	37

Table S3-2 SNP climate, deposition, discharge, and stream chemistry data

Climate	Tmax	1935.08-2015.12	NCDC
	Tmin	1935.08-2015.12	NCDC
	Rain	1935.08-20115.12	NCDC
	Solar	1935.08-2015.12	NCDC
Deposition	wet	1981.05-2015.12	NADP
	dry	1978.01-2015.12	CASTNET
Vegetation		SHWDS - southern hardwoods	
Soil Chemistry		varied soil chemistry publications @ SWAS-VTSSS https://swas.evsc.virginia.edu/POST/scripts/overview.php and last visited on 08012020	
Soil Properties		STATSGO - State Soil Geographic	
Discharge		1992.10-2011.01	SWAS-VTSSS
water chemistry		1992.01-2012.12	SWAS-VTSSS

Table S3-3 Land based weather station used to develop past and current climate data for SNPPR, SNPSR, and SHWOR (data used 1951-2000)

NCDC station name	Elevation (m)
Big Meadows	1,079
Buena Vista	256
Charlottesville	264
Free Union	180
Glasgow	225
Lexington	334
Luray	427
Mount Weather	506
Pedlar	312
Staunton	51
Somerest	155
Wardensville	293
Warrenton	152
Winchester	207
Woodstock	206

Table S3-4 Derivation of precipitation, Tmax, and Tmin regression based on 16 land-based NCDC climate data (1951-2000)

X- Elevation	Y-Prcp			Y-Tmax			Y-Tmin		
	Slope	Intercept	R^2	Slope	Intercept	R^2	Slope	Intercept	R^2
Jan	0.020	50.214	0.352	-0.005	7.551	0.487	-0.003	-4.223	0.315
Feb	0.016	49.232	0.203	-0.006	9.571	0.454	-0.003	-3.370	0.290
Mar	0.014	73.059	0.298	-0.006	14.052	0.478	-0.004	0.648	0.446
Apr	0.022	65.946	0.515	-0.006	20.729	0.480	-0.003	5.825	0.347
May	0.023	75.913	0.485	-0.006	25.347	0.578	-0.003	10.687	0.317
Jun	0.029	84.302	0.685	-0.006	29.498	0.671	-0.003	15.432	0.342
Jul	0.016	88.564	0.128	-0.007	31.616	0.741	-0.003	17.887	0.392
Aug	0.021	74.877	0.346	-0.007	31.016	0.764	-0.003	16.917	0.307
Sep	0.050	76.045	0.729	-0.006	27.488	0.719	-0.003	13.254	0.226
Oct	0.038	60.878	0.582	-0.006	21.622	0.666	-0.001	6.522	0.067
Nov	0.038	48.737	0.801	-0.006	15.066	0.637	-0.002	1.657	0.167
Dec	0.016	54.780	0.255	-0.005	9.385	0.520	-0.002	-2.331	0.267

REFERENCES

Aber, John D.; Knute J. Nadelhoffer; Paul Steudler; Jerry M. Milillo. 1989. Nitrogen saturation in northern forest ecosystems. BioScience, 39(6): 378–386.

Aber, John D. 1992. Nitrogen cycling and nitrogen saturation in temperate ecosystems. Trends in Ecology and Evolution, 7(7): 220-224.

Aber, John D. and C. Anthony Federer. 1992. A generalized, lumped-parameter model of photosynthesis, evapotranspiration and net primary production in temperate and boreal forest ecosystems. Oecologia, 92(4):463-474.

Aber, John D.; Scott V. Ollinger; Charles T. Driscoll. 1997. Modeling nitrogen saturation in forest ecosystems in response to land use and atmospheric deposition. Ecological Modelling, 101: 61-78.

Aber, John D.; William McDowell; Knute Nadelhoffer; Alison Magill; Glenn Berntson; Mark Kamakea; Steven McNulty; William Currie; Lindsey Rustad; Ivan Fernandez. 1998. Nitrogen saturation in temperate forest ecosystems – Hypothesis revisited. BioScience, 48(11): 921-934.

Albrich, Katharina; Werner Rammer; Rupert Seidl. 2020. Climate change causes critical transitions and irreversible alterations of mountain forests. Global Change Biology, 26(7): 4013-4027.

Anandhi, Aavudai and Chance Bentley. 2018. Predicted 21st century climate variability in southeastern U.S. using downscaled CMIP5 and meta-analysis. CATENA, 170: 409-420.

Andersen, Tom; Jacob Carstensen; Emilio Hernandez-Garcia; Carlos M. Duarte. 2009. Ecological thresholds and regime shifts: approaches to identification. Trends in Ecology and Evolution, 24(1): 49-57.

Augustynczik, Andrey L.; Florian Hartig; Francesco Minunno; Hans-Peter Kahle; Daniela Diaconu; Marc Hanewinkel; Rasoul Yousefpour. 2017. Productivity of Fagus sylvatica under climate change—A Bayesian analysis of risk and uncertainty using the model 3-PG. Forest Ecology and Management, 401:192–206.

Barger, Nichole N; Steven R. Archer; John L. Campbell; Cho-ying Huang; Jeffery A. Morton; Alan K. Knapp. 2011. Woody plant proliferation in North American drylands: a synthesis of impacts on ecosystem carbon balance. Journal of Geophysical Research: Biogeosciences, 116(G4): G00K07.

Bassirirad, Hormoz. 2000. Kinetics of nutrient uptake by roots: responses to global change. New Phytologist, 147(1): 155-169.

Bernal, Susana; Lars O. Hedin; Gene E. Likens; Stefan Gerber; Doc C. Buso. 2012. Complex response of the forest nitrogen cycle to climate change. Proceedings of the National Academy of Sciences of the United States of America (PNAS), 109 (9): 3406–3411.

Boisvenue, Celine and Steven W. Running. 2006. Impacts of climate change on natural forest productivity – evidence since the middle of the 20th century. Global Change Biology, 12(5): 862-882.

Both, A. J., David R. Mears, Eugene Reiss, and William J. Roberts. 2002. Floor heating in greenhouses. Horticultural Engineering, 17(3): 8.

Bowman, William D.; Cory C. Cleveland; Lubos Halada; Juraj Hresko; Jill S. Baron, 2008. Negative impact of nitrogen deposition on soil buffering capacity. Nature Geoscience, 1(11): 767–770.

Buermann Wolfgang; Bikash R. Parida; Martin Jung; Donald H. Burn; Markus Reichstein. 2013. Earlier springs decrease peak summer productivity in North American boreal forests. Environmental Research Letters, 8(2): 024027.

Calder, Catherine; Michael Lavine; Peter Müller; James S. Clark. 2003. Incorporating multiple sources of stochasticity into dynamic population models. Ecology, 84, 1395–1402.

Caldwell, Peter V.; Chelcy F. Miniat; Katherine J. Elliott; Wayne T. Swank; Steven T. Brantley; Stephanie H. Laseter. 2016. Declining water yield from forested mountain watersheds in response to climate change and forest mesophication. Global Change Biology, 22(9): 2997–3012.

Campbell, John L., Charles T. Driscoll, Afshin Pourmokhtarian, Katharine Hayhoe. 2011. Streamflow responses to past and projected future changes in climate at the Hubbard Brook Experimental Forest, New Hampshire, United States. Water Recourses Research, 47(2), W02514, doi: 10.1029/2010WR009438.

Campbell, John L.; Lindsey E. Rustad; Elizabeth W. Boyer; Sheila F. Christopher; Charles T. Driscoll; Ivan J. Fernandez; Peter M. Groffman; Daniel Houle; Jana Kiekbusch; Alison H. Magill; Myron J. Mitchell; Scott V. Ollinger. 2009. Consequence of climate change for biogeochemical cycling in forests of northeastern North America. Canadian Journal of Forest Research, 39: 264-284.

Campo, Julio. 2016. Shift from ecosystem P to N limitation at precipitation gradient in tropical dry forests at Yucatan, Mexico. Environmental Research Letters, 11(9): 095006.

Center for Climate and Energy Solutions (C2ES). 2019. Climate Essentials – Science and Impacts. https://www.c2es.org/document/science-and-impacts/

Charney, Noah D.; Flurin Babst; Benjamin Poulter; Sydne Record; Valerie M. Trouet; David Frank; Brian J. Enquist; Margaret E. K. Evans. . 2016. Observed forest sensitivity to climate implies large changes in 21st century North American forest growth. Ecology Letters, 19: 1119-1128.

Chen, Hao; Geshere A. Gurmesa; Wei Zhang; Xiaomin Zhu; Mianhai Zheng; Qinggong Mao; Tao Zhang; Jiangming Mo. 2016. Nitrogen saturation in humid tropical forests after 6 years of nitrogen and phosphorus addition: hypothesis testing. Functional Ecology, 30: 305-313.

Chen, Limin; Charles Driscoll; Solomon Gbondo-Tugbawa; Myron J. Mitchell; Peter S. Murdoch. 2004a. The application of an integrated biogeochemical model (PnET-BGC) to five forested watersheds in the Adirondack and Catskill regions of New York. Hydrological Processes, 18(14):2631-2650.

Chen, Limin and Charles Driscoll. 2004b. Modeling the response of soil and surface waters in the Adirondack and Catskill regions of New York to changes in atmospheric deposition and historical land disturbance. Atmospheric Environment, 38(25): 4099-4109.

Chen, Limin and Charles Driscoll. 2005a. Regional application of an integrated biological model to northern New England and Maine. Ecological Applications, 15(5): 1783-1797.

Chen, Limin and Charles Driscoll. 2005b. Regional assessment of the response of the acid-base status of lake watersheds in the Adirondack region of New York to changes in atmospheric deposition using PnET-BGC. Environmental Science and Technology, 39(3): 787-794.

Clark, James S. 2005. Why environmental scientists are becoming Bayesians. Ecology Letters, 8: 2-14.

Clark, James S. and Gelfand Alan E. 2006. Hierarchical modelling for the environmental sciences. Oxford University Press, New York.

Clark, James S.; David M. Bell; Matthew C. Kwit; Kai Zhu. 2014. Competition-interaction landscapes for the joint response of forests to climate change. Global Change Biology, 20(6):1979-1991.

Clinton, Barton D. and Corey R. Baker. 2000. Catastrophic windthrow in the southern Appalachians: characteristics of pits and mounds and initial vegetation responses. Forest Ecology and Management, 126(1):51-60.

Clinton, Barton D.; L. R. Boring; Wayne T. Swank. 1993. Characteristics of canopy gaps and drought influences in oak forests of the Coweeta Basin. Ecology, 74(5): 1551-1558.

Clinton, Barton D.; Alan Yeakley; David K. Apsley. 2003. Tree growth and mortality in a Southern Appalachian deciduous forest following extended wet and dry periods. Gastanea, 68(3): 189-200.

Coder, Kim D. 1999. Heat stroke in trees. University of Georgia. pp 9. https://www.extension.iastate.edu/forestry/publications/PDF_files/for99-024.pdf (Last accessed on 08/01/2020).

Coles, Staurt G. 2001. *An Introduction to Statistical Modelling of Extreme Values*. London: Springer.

Cooley, Daniel. 2013. Return periods and return levels under climate change. In: Extremes in a Changing Climate (pp. 97-114). 10.1007/978-94-007-4479-0_4.

Cosby, Bernard J.; James R. Webb; James N. Galloway; Frank A. Deviney. 2006. Acidic deposition impacts on natural resources in Shenandoah National Park. US Department of Interior Technical Report NPS/NER/NRTR-2006/066. pp. 248.

Davidson, Eric A. and Ivan A. Janssens. 2006. Temperature sensitivity of soil carbon decomposition and feedbacks to climate change. Nature, 440: 165-173.

Day, Frank P. Jr; Philips, Dr. L.; Monk, Carl D. 1988. Forest communities and patterns. In: Swank, W.T. and Crossley Jr., D.A. (Eds), Forest Hydrology and Ecology at Coweeta. Ecological Studies, Vol. 66. Springer-Verlag, New York, NY, pp.141-149.

Day, Frank P. Jr. and Carl D. Monk. 1974. Vegetation patterns on a southern Appalachian watershed. Ecology, 55(5): 1064-1074.

Day, Frank P. Jr. and Carl D. Monk. 1977. Net primary production and phenology on a southern Appalachian watershed. American Journal of Botany, 64(9): 1117-1125.

Diffenbaugh, Noah S. and Moetasim Ashfaq. 2010. Intensification of hot extremes in the United States. Geophysical Research Letters, 37(15), L15701. doi:10.1029/2010GL043888.

Dong, Zheng; Charles T. Driscoll; Sherri L. Johnson; John L. Campbell; Afshin Pourmokhtarian; Anne M. K. Stoner; Katharine Hayhoe. 2019. Projections of water, carbon, and nitrogen dynamics under future climate change in an old-growth Douglas-fir forest in the western Cascade Range using a biogeochemical model. Science of The Total Environment, 656: 608-624.

Drechsler, Martin. 2020. Conservation management in the face of climatic uncertainty – the roles of flexibility and robustness. Ecological Complexity, 43: 100849.

Driscoll, Charles T.; Gregory B. Lawrence; Arthur J. Bulger; Thomas J. Butler; Christopher S. Cronan; Christopher Eagar; Kathleen F. Lambert; Gene E. Likens; John L. Stoddard; Kathleen C. Weathers. 2001. Acidic Deposition in the Northeastern United States: Sources and Inputs, Ecosystem Effects, and Management Strategies: The effects of acidic deposition in the northeastern United States include the acidification of soil and water, which stresses terrestrial and aquatic biota, *BioScience*, 51(3):180–198.

Driscoll, Charles T.; Michael D. Lehtinen; Timothy J. Sullivan. 1994. Modeling the acid-base chemistry of organic solutes in Adirondack, New York, lakes. Water Resources Research, 30*:*297–306.

Driscoll, T. Charles; Gregory B. Lawrence; Arthur J. Bulger; Thomas J. Butler; Christopher S. Cronan; Christopher Eagar; Kathleen F. Lambert; Gene E. Likens; John L. Stoddard; Kathleen C. Weathers.. 2001. Acidic deposition in the northeastern United States: Sources and inputs, ecosystem effects and management strategies: The effects of acidic deposition in the northeastern United States include the acidification of soil and water, which stresses terrestrial and aquatic biota. BioScience, 51(3): 180-198.

Duran, Jorge; Jennifer L. Morse; Peter M. Groffman; John L. Campbell; Lynn M. Christenson; Charles T. Driscoll; Timothy J. Fahey; Melany C. Fisk; Gene E. Likens; Jerry M. Melillo; Myron J. Mitchell; Pamela H. Templer; Matthew A. Vadeboncoeur. 2016. Climate change decreases nitrogen pools and mineralization rates in northern Hardwood forests. Ecosphere, 7(3): e01251.

Eck, Montana A.; Baker Perry; Peter T. Soule; Johnathan W. Sugg; Douglask K. Miller. 2019. Winter climate variability in the southern Appalachian Mountains, 1910-2017. International Journal of Climatology, 39(1):206-217.

Elliott, Katherine and Wayne T. Swank. 1994. Impacts of drought on tree mortality and growth in a mixed hardwood forest. Journal of Vegetation Science, 5(2): 229-236.

Elliott, Katherine J. and James M. Vose. 2006. Fire effects on water quality: a synthesis of response regulating factors among contrasting ecosystems. In: Second interagency Conference on Research in the watersheds, May 16-18, 2006. pp. 11.

Elliott, Katherine J. and Wayne T Swank. 2008. Long-term changes in forest composition and diversity following early logging (1919–1923) and the decline of American chestnut (*Castanea dentata*). Plant Ecology, 197: 155–172.

Elliott, Katherine J.; Chelcy F. Miniat; Neil Pederson; Stephanie H. Laseter. 2015. Forest tree growth response to hydroclimate variability in the southern Appalachians. Global Change Biology, 21: 4627-4641.

Elliott, Katherine J.; James M. Vose, Ronald L. Hendrick. 2009. Long-term effects of high intensity prescribed fire on vegetation dynamics in the Wine Springs Creek watershed, Western North Carolina, USA. Fire Ecology, 5(2): 66-85.

Elliott, Katherine J.; Stephanie L. Hitchcock; Lisa Krueger. 2002. Vegetation response to large scale disturbance in a southern Appalachian forest: Hurricane Opal and salvage logging. Journal of the Torrey Botanical Society, 129(1): 48-59.

Ellis, R. A.; D. J. Jacob; M. P. Sulprizio; L. Zhang; C. D. Holmes; B. A. Schichtel; T. Blett; E. Porter; L. H. Pardo; J. A. Lynch. 2013. Present and future nitrogen deposition to national parks in the United States: critical load exceedances. Atmospheric Chemistry and Physics, 19: 9083-9095.

Engeland, K.; H. Hisdal; A. Frigessi. 2004. Practical extreme value modeling of hydrological floods and droughts: a case study. Extremes, 7:5-30.Environmental Protection Agency (US EPA). 2000. National air pollutant emission trends, 1900-1998. EPA-454/R-00-002.

Evans, John R. 1989. Photosynthesis and nitrogen relationship in leaves of C_3 plants. Oecologia, 78(1): 9-19.

Fakhraei, Habibollah; Charles T. Driscoll; James R. Renfro; Matt A. Kulp; Tamara F. Blett; Patricia F. Brewer; John S. Schwartz. 2016. Critical loads and exceedances for nitrogen and sulfur atmospheric deposition in Great Smoky Mountains National Park, United States. Ecosphere, 7(10): E01466.

Furniss, Michael J.; Brian P. Staab; Sherry Hazelhurst; Cathrine F. Clifton; Kenneth B. Roby; Bonnie L. Ilhadrt; Albert H. Todd; Leslie M. Reid; Sarah J. Hines; Karen A. Bennett; Charles H. Luce; Pamela J. Edwards. 2010. Water, climate change, and forests: watershed stewardship for a changing climate. General Technical Report PNW-GTR-812. Portland, OR: U.S. Department of Agriculture, Forest Service, Pacific Northwest Research Station. 75p. https://doi.org/10.2737/PNW-GTR-812

Gbondo-Tugbawa, S. Solomon and Charles T. Driscoll. 2002. Evaluation of the effects of future controls on sulfur dioxide and nitrogen oxide emissions on the acid–base status of a northern forest ecosystem. Atmospheric Environment, 36(10): 1631-1643.

Gbondo-Tugbawa, S. Solomon; Charles T. Driscoll; John D. Aber; Gene E. Likens. 2001. Evaluation of an integrated biogeochemical model (PnET-BGC) at a northern hardwood forest ecosystem. Water Resources Research, 37(4): 1057-1070.

Ghannoum, Oula and Danielle A. Way. 2011. On the role of ecological adaptation and geographic distribution in the response of trees to climate change. Tree Physiology, 31(12): 1273-1276.

Giang, Pham Quy; Toshiki Kosuke; Masahiro Sakata; Schoichi Kunikane; Tran Quoc Vinh. 2014. Modelling climate change impacts on the seasonality of water

resources in the upper Ca River watershed in southeast Asia. The Scientific World Journal, 279135. https://doi.org/10.1155/2014/279135

Gilleland, Eric and Richard W. Katz. 2016. extRemes 2.0: An extreme value analysis package in R. Journal of Statistical Software. 72(8): doi:10.18637/jss.v072.i08

Gilliam, Frank S. 2016. Forest ecosystems of temperate climatic regions: from ancient use to climate change. New Phytologist, 212(4):871-887.

Goss, Michael; Daniel L. Swain; john T. Abatzoglou; Ali Sarhadi; Crystal Kolden; A. Park Williams; Noah S. Diffenbaugh. 2020. Climate change is increasing the risk of extreme autumn wildfire conditions across California. Environmental Research Letters, 15: 094016. doi: 10.1088/1748-9326/ab83a7

Greaver, T. L.; C. M. Clark; J. E. Compton; D. Vallano; A. F. Talhelm; C. P. Weaver; L. E. Band; J. S. Baron; E. A. Davidson; C. L. Tague; E. Felker-Quinn; J. A. Lynch; J. D. Herrick; L. Liu; C. L. Goodale; K. J. Novak; R. A. Haeuber. .2016. Key ecological responses to nitrogen are altered by climate change. Nature Climate Change, 6(9): 836-843.

Grimm, Nancy B.; F. Stuart Chapin III, Britta Bierwagen; Patrick Gonzalez; Peter M. Groffman; Yiqi Luo; Forrest Melton; Knute Nadelhoffer; Amber Pairis; Peter A. Raymond; Josh Schimel; Craig E. Williamson. 2013. The impacts of climate change on ecosystem structure and function. Frontiers in Ecology and the Environment, 11(9): 474-482.

Groffman, Peter M.; Jill S. Baron; Tamara Blett; Arthur J. Gold; Iris Goodman; Lance H. Gunderson; Barbara M. Levinson; Margaret A. Palmer; Hans W. Paerl; Garry D.

Peterson; N. LeRoy Poff; David W. Rejeski; James F. Reynolds; Monica G. Turner; Kathleen C. Weathers; John Wiens. . 2006. Ecological thresholds: The key to successful environmental management or an important concept with no practical application? Ecosystems, 9:1-13. https://doi.org/10.1007/s10021-003-0142-z

Hansen, James; Makiko Sato; Reto Ruedy; Ken Lo; David W. Lea; Martin Medina-Elizade. 2006. Global temperature change. Proceedings of the National Academy of Sciences (PNAS), 103(39): 14288-14293.

Hatfield, Jerry L. and John H. Prueger. 2015. Temperature extremes: effect on plant growth and development. Weather and Climate Extremes, 10(A): 4-10.

Hayhoe, Katharine; Cameron P. Wake; Bruce Anderson; Xin-Zhong Liang; Edwin P. Maurer; Jinhong Zhu; James Bradbury; Arthur T. Degaetano; Anne Marie Koch Stoner; Donald J. Wuebbles. 2008. Regional climate change projections for the northeast USA. Mitigation and Adaptation Strategies for Global Change, 13(5): 425-436.

Hayhoe, Katharine; Cameron P. Wake; Thomas G. Huntington; Lifeng Luo; Mark D. Schwartz; Justin Sheffield; Eric Wood; Bruce Anderson; James Bradbury; Art DeGaetano; Tara J. Troy; David Wolfe. 2007. Past and future changes in climate and hydrological indicators in the US northeast. Climate Dynamics, 28(4): 381-407.

Hayhoe, Katharine; Daniel Cayan; Christopher B. Field; Peter C. Frumhoff; Edwin P. Maurer; Norman L. Miller; Susanne C. Moser; Stephen H. Schneider; Kimberly Nicholas Cahill; Elsa E. Cleland; Larry Dale; Ray Drapek; R. Michael Hanemann;

Laurence S. Kalkstein; James Lenihan; Claire K. Lunch; Ronald P. Neilson; Scott C. Sheridan; Julia H. Verville. 2004. Emissions pathways, climate change, and impacts on California. Proceedings of the National Academy of Sciences (PNAS), 101(34): 12422-12427.

Heartsill-Scalley, Tamara; F. N. Scatena; C. Estrada; W. H. McDowell; A.E. Lugo. 2007. Disturbance and long-term patterns of rainfall and throughfall nutrient fluxes in a subtropical wet forest in Puerto Rico. Journal of Hydrology, 333: 472-485.

Hellmann, Jessica J.; James E. Byers; Britta G. Bierwagen; Jeffrey S. Dukes. 2008. Five potential consequences of climate change for invasive species. Conservation Biology, 22(3): 534-543.

Hodgkins, Glenn A. and Robert W. Dudley. 2006. Changes in the timing of winter–spring streamflows in eastern North America, 1913–2002. Geophysical Research Letters, 33: L06402.

Horswill, Paul; Odhran O'Sullivan; Gareth K. Phoenix; John A. Lee; Jonathan R. Leake. 2008. Base cation depletion, eutrophication and acidification of species-rich grasslands in response to long-term simulated nitrogen deposition. Environmental Pollution, 155(2): 336-349.

Huang, Yongmei; Ronghua Kang; Jan Mulder; Ting Zhang; Lei Duan. 2015. Nitrogen saturation, soil acidification, and ecological effects in a subtropical pine forest on acid soil in southwest China. Journal of Geophysical Research – Biogeosciences, 120(11): 2457-2472.

Hyvonen, Riitta; Goran I. Agren; Sune Linder; Tryggve Persson; M. Francesca Cotrufo; Alf Ekblad; Michael Freeman; Achim Grelle; Ivan A Janssens; Paul G. Jarvis; Seppo Kellomaki; Anders Lindroth; Denis Loustau; Tomas Lundmark; Richard J. Norby; Ram Oren; Kim Pilegaard; Michael G. Ryan; Bjarni D. Sigurdsson; Monika Stromgren; Marcel van Oijen; Goran Wallin. 2007. The likely impact of elevated CO_2, nitrogen deposition increased temperature and management on carbon sequestration in temperate and boreal forest ecosystems: a literature review. New Phytologist, 173(3): 463-480.

Innes, John L.; L. A. Joyce; S. Kellomäki; Bastiaan Louman; Aynslie E. Ogden; John A. Parrotta; Ian Thompson; Matthew P. Ayres; C. Ong; Heru Santoso; Brent Sohngen; Anita Wreford. 2009. Management for adaptation. In: Seppälä R, Buck A, Katila P (eds) Adaptation of forests and people to climate change: a global assessment report, vol World Series Volume 22. IUFRO Helsinki, pp 135–186.

Intergovernmental Panel on Climate Change (IPCC). 2007. Climate Change 2007: The physical science basis. Contribution of working group I to the fourth assessment report of the Intergovernmental Panel on Climate Change. Solomon, S., D. Qin, M. Manning, Z. Chen, M. Marquis, K.B. Averyt, M.Tignor and H.L. Miller (eds.). Cambridge University Press, Cambridge, United Kingdom and New York, NY, USA.

Intergovernmental Panel on Climate Change (IPCC). 2014. Climate Change 2014: Synthesis report. Contribution of working groups I, II and III to the fifth assessment report of the Intergovermmental Panel on Climate Change. Core

writing team, R. K. Pachauri and L.A. Meyer (eds.). IPCC, Geneva, Switzerland, pp151.

Jandi, Robert; Peter Spathelf; Andreas Bolte; Cindy E. Prescott. 2019. Forest adaptation to climate change – is non-management an option? Annals of Forest Science, 76: 4363.

Janssen, P. H. M. and Heuberger, P. S. C. 1995. Calibration of process-oriented models. Ecological Modelling, 83(1-2): 55-66.

Jarvis, Andrew J. and William J. Davies. 1998. The coupled response of stomatal conductance to photosynthesis and transpiration. Journal of Experimental Botany, 49: 399-406.

Jeong, Seco-Hee; Ji-Young Eom; Joo-Yeon Park; Jung-Hwa Chun; Jae-Seok Lee. 2018. Effect of precipitation on soil respiration in a temperate broad-leaved forest. Journal of Ecology and Environment, 42:10.

Jobbágy, E. G. and R. B. Jackson. 2000. The vertical distribution of soil organic carbon and its relation to climate and vegetation. Ecological Applications 10(2): 423–436.

Jolliffe, Ian T.; Jorge Cadima. 2016. Principal component analysis : a review and recent developments. Subject Areas. Philosophical Transactions of Royal Sociegy A, 374(20150202), 1–16.

Kanakidou, M.; Stelios Myriokefalitakis; Nikos Daskalakis; George Fanourgakis; Athanasios Nenes; A. R. Baker; Kostas Tsigaridis; N. Mihalopoulos. 2016. Past, Present and Future Atmospheric Nitrogen Deposition. Journal of Atmospheric Sciences, 73(5): 160303130433005.

Keenan, Rodney J. 2015. Climate change impacts and adaptation in forest management: a review. Annals of Forest Science, 72: 145-167.

Keim, Barry D.; Royce Fontenot; Claudia Tebaldi; David Shankman. 2011. Hydroclimatology of the U.S. Gulf Coast under global climate change scenarios. Physical Geography, 32(6): 561-582.

Kienast, Felix. 1991. Simulated effects of increasing atmospheric CO_2 and changing climate on the successional characteristic of Alpine forest ecosystems. Landscape Ecology, 5(4): 225-238.

Killick, Rebecca and Idris A. Eckley. 2014. Changepoint: An R package for changepoint analysis. Journal of Statistical Software.

Kloeppel, Brian D.; Barton D. Clinton; James M. Vose; Aaron R Cooper. 2003. Drought impacts on tree growth and mortality of southern Appalachian forests. In: Climate variability and ecosystem response at long-term ecological research sites. eds. Greenland, D.; Gooding, D.G.; Smith, R.C. Oxford University Press, New York, p. 43-55.

Klos, Ryan J.; G. Geoff Wang; William L. Bauerle; James R. Rieck. 2009. Drought impact on forest growth and mortality in the southeast USA: an analysis using forest health and monitoring data. Ecological Applications, 19(3): 699-708.

Knoepp, Jennifer D. and James M. Vose. 2007. Regulation of nitrogen mineralization and nitrification in Southern Appalachian ecosystems: separating the relative importance of biotic vs. abiotic controls. Pedobiologia, 51: 89-97.

Knoepp, Jennifer D. and Wayne T. Swank. 1998. Rates of nitrogen mineralization across an elevation and vegetation gradient in the Southern Appalachians. Plant and Soil, 204: 235-241.

Knoepp, Jennifer D. and Wayne T. Swank. 2002. Using soil temperature and moisture to predict forest soil nitrogen mineralization. Biology and Fertility of Soils, 36:177–182.

Knoepp, Jennifer D.; James M. Vose; William A. Jackson; Katherine J. Elliott; Stan Zarnoch. 2016. High elevation watersheds in the southern Appalachians: indicators of sensitivity of acidic deposition and the potential for restoration through liming. Forest Ecology and Management, 377: 101-117.

Krishna, M. P. and Mahesh Mohan 2017. Litter decomposition in forest ecosystems: a review. Energy, Ecology and Environment, 2: 236-249.

Kunkel, Kenneth E.; Michael Palecki; Leslie Ensor; Kenneth G. Hubbard; David Robinson; Kelly Redmond; David Easterling. 2009. Trends in twentieth-century U.S. snowfall using a quality-controlled dataset. Journal of Atmospheric Oceanic Technology, 26:33-44.

Lambert, Paul C.; Alex J. Sutton; Paul R. Burton;Keith R. Abrams; David R. Jones. 2005. How vague is vague? A simulation study of the impact of the use of vague prior distributions in MCMC using WinBUGS. Statistics in Medicine, 24(15): 2401–2428.

Lapenis, Andrei G.; Gregory B. Lawrence; Alexander Heim; Chengyang Zheng; Walter Shortle. 2013. Climate warming shifts carbon allocation from stemwood to roots in calcium-depleted spruce forests. Global Biogeochemical Cycles, 27(1): 101-107.

Laseter, Stephanie H., Chelcy R. Ford, James M. Vose, and Lloyd W. Swift. 2012. Long-term temperature and precipitation trends at the Coweeta Hydrologic Laboratory, Otto, North Carolina, USA. Hydrology Research, 43(6):890-901.

Lavergne, Alienor; Heather Graven; Martin G. De Kauwe; Trevor F. Keenan; Belinda E. Medlyn; Lain Colin Prentice. 2019. Observed and modelled historical trends in the water-use efficiency of plants and ecosystems. Global Change Biology, 25(7): 2242-2257.

Lee, Sukyoung. 2014. A theory for polar amplification from a general circulation perspective. Asia-Pacific Journal of Atmospheric Sciences, 50(1): 31-43.Lewis, William. 2011. Thesis: The effects of acid deposition on high-elevation ecosystems: values and duties to protect in an ecocentric-based environmental ethic. University of Tennessee, Knoxville. pp 28.

Li, Yi; Bret A. Schichtael; John T. Walker; Donna B. Schwede; Xi Chen; Christopher M. B. Lehmann; Melissa A. Puchalski; David A. Gay; Jeffrey L. Collett Jr. 2016. Increasing importance of deposition of reduced nitrogen in the United States. Proceedings of the National Academy of Sciences (PNAS), 113(21): 5874-5879.

Lindquist, Erik J.; Remi D'Annunzio; Adam Gerrand; Kenneth MacDicken; Frederic Achard; Rene Beuchle; Andreas Brink; Hugh D. Eva; Philippe Mayaux; Jesus San-Miguel-Ayanz; Hans-Jurgen Stibig. 2012. Global forest land-use change 1990–

2005. Food and Agriculture Organization of the United Nations and European Commission Joint Research Centre, Rome. FAO Forestry Paper No. 169. http://www.fao.org/3/i3110e/i3110e.pdf

Liu, Ying and Chaoyang Wu. 2020. Understanding the role of phenology and summer physiology in controlling net ecosystem production: a multiscale comparison of satellite, PhenoCam and eddy covariance data. Environmental Research Letters, 15:104086.

Lovett, Gary M. and Adriana E. Ruesink. 1995. Carbon and nitrogen mineralization from decomposing gypsy moth frass. Oecologia, 104(2): 133–138.

Lovett, Gary M. and T. Peter. 1993. Carbon and nitrogen assimilation in red oaks (*Quercus rubra L.*) subject to defoliation and nitrogen stress. Tree Physiology, 3: 259-269.

Lu, Aigang, L., W. Tianming, et al. .2009. On the Relationship between Latitude and Altitude Temperature Effects. Rendiconti Del Seminario Matematico E Fisico Di Milano, 51(1): 43-76.

Lu, Xiankai; Peter M. Vitousek; Qinggong Mao; Frank S. Gilliam; Yiqi Luo; Guoyi Zhou; Xiaoming Zou; Edith Bai; Todd M. Scanlon; Enqing Hou; Jiangming Mo. 2018. Plant acclimation to long-term high nitrogen deposition in an N-rich tropical forest. Proceedings of the National Academy of Sciences (PNAS), 115(20): 5187-5192.

Lydersen, Espen; Rolf Hogberget; Clara E. Moreno; Oyvind A. Garmo; and Per Christian Hagen. 2014. The effects of wildfire on the water chemistry of dilute, acidic lakes in southern Norway. Biogeochemistry, 119:109-124.

Maaroufi, Nadia I.; Jonathan R. De Long. 2020. Global change impacts on forest soils: linkage between soil biota and carbon-nitrogen-phosphorus stoichiometry. Frontiers in Forests and Global Change, doi.org/10.3389/ffgc.2020.00016

Martin, Philip; Adrian C. Newton; Elena Cantarello; Paul M. Evans. 2017. Analysis of ecological thresholds in a temperate forest undergoing dieback. PLOS-ONE, https://doi.org/10.1371/journal.pone.0189578

McColl, J.G.; D. F. Grigal. 1977. Nutrient changes following a forest wildfire in Minnesota: effects in watersheds with different soils. Oikos, 28(1): 105-112.

McKenney, Daniel W.; John H. Pedlar; Kevin Lawrence; Kathy Campbell; Michael F. Hutchinson. 2007. Potential impacts of climate change on the distribution of North American trees. BioScience, 57(11): 939-948.

McKenney-Easterling, Mary; David R. DeWalle; Louis R. Iverson; Anantha M. Prasad; Anthony R. Buda. 2000. The potential impacts of climate change and variability on forests and forestry in the Mid-Atlantic region. Climate Research, 14: 195-206.

Medlyn, Belinda E.; Remko A. Duursma; Melanie J. B. Zeppel. 2011. Forest productivity under climate change: a checklist for evaluating model studies. Wiley Interdisciplinary Reviews: Climate Change, 2(3): 332-355.

Meehl, G. A. and T. F. Stocker, In Climate Change 2007: the Physical Science Basis, Eds. S. Solomon, D. Qin, M. Manning, Z. Chen, M. Marquis, K. B. Averyt, M. Tignor and H. L. Miller, Cambridge University Press, Cambridge, 2007.

Merganicova, Katarina; Jan Merganic; Aleksi Lehtonen; Giorgio Vacchiano; Masa Zorana Ostrogovic Sever; Andrey Lessa Derci Augustynczik; Rudiger Grote; Ina Kyselova; Annikki Makela; Rasoul Yousefpour; Jan Krejza; Alessio Collalti; Christopher Reyer. 2019. Forest carbon allocation modelling under climate change. Tree Physiology, 39(12): 1937-1960.

Mitchell, H. L. and R. F. Chandler. 1939. The nitrogen nutrition and growth of certain deciduous trees of Northeastern United States, with a discussion of the principles and practice of leaf analysis as applied to forest trees. Black Rock Forest Bulletin, 11, 94 pp.

Mitchell, Robert J.; Yongqiang Liu; Joseph J. O'Brien; K. J. Elliott; Gregory Starr; Chelcy Ford Miniat; John Hiers. 2014. Future climate and fire interactions in the southeastern region of the United States. Forest Ecology and Management. 327: 316-326. DOI: 10.1016/j.foreco.2013.12.003

Moore, John C. 2018. Predicting tipping points in complex environmental systems. PNAS, 115(4): 635-636.

Moss, Richard, Jae A Edmonds; Kathy Hibbard; et al. 2010. The next generation of scenarios for climate change research and assessment. Nature, 463(7282): 747-756. doi:10.1038/nature08823

Mote, Philip W.; Alan F. Hamlet; Martyn P. Clark; Dennis P. Lettenmaier. 2005. Decline mountain snowpack in western North America. American Meteorological Society, 39-50.

Munson, Seth M.; Sasha C. Reed; Josep Penuelas; Nathan G. McDowell; and Osvaldo E. Sala. 2018. Ecosystem thresholds, tipping points, and critical transitions. New Phytologist, 218:1315-1317.

Nielsen, Uffe N. and Becky A. Ball. 2014. Impacts of altered precipitation regimes on soil communities and biogeochemistry in arid and semi-arid ecosystems. Global Change Biology, 21(4): 1407-1421.

Niemeyer, Ryan; Kevin D. Bladon; Richard D. Woodsmith. 2020. Long-term hydrologic recovery after wildfire and post-fire forest management in the interior Pacific Northwest. Hydrological Processes, 34(5):1182-1197.

Novick, Kimberly A.; Darren L. Ficklin; Paul C. Stoy; et al. 2016. The increasing importance of atmospheric demand for ecosystem water and carbon fluxes. Nature Climate Change, 6: 1023-1027.

Oishi, A. Christopher; Chelcy F. Miniat; Kimberly A. Novick; Steven T. Brantley; James M. Vose; John T. Walker. 2018. Warmer temperature reduce net carbon update, but do not affect water use, in a mature southern Appalachian forest. Agricltural and Forest Meteorology, 252: 269-282.

Ollinger, Scott V.; John D. Aber; PeterB. Reich; Rita .J. Freuder. 2002. Interactive effects of nitrogen deposition, tropospheric ozone, elevated CO_2 and land use history on

the carbon dynamics of northern hardwood forests. Global Change Biology, 8: 545-562.

Ollinger, Scott V.; C. L. Goodale; Katharine Hayhoe; J. P. Jenkins. 2009. Potential effects of climate change and rising CO2 on ecosystem processes in northeastern U.S. forest, Mitigation and Adaptation Strategies for Global Change, 14: 101-106.

Ontl, T. A. and L. A. Schulte. 2012. Soil carbon storage. Nature Education Knowledge 3(10): 35.

Pachauri, R. and A. Reisinger. 2014. Climate Change 2014: Synthesis Report. Contribution of Working Groups I, II and III to the Fifth Assessment Report of the Intergovernmental Panel on Climate Change. Journal of Romance Studies, 4(2): 85-88.

Pepin, N.; R. S. Bradley; et al. 2015. Elevation-dependent warming in mountain regions of the world. Nature Climate Change, 5: 424-430.

Peters, Emily B.; Kirk R. Wythers; Shuxia Zhang; John B. Bradford; and Peter B. Reich. 2013. Potential climate change impacts on temperate forest ecosystem processes. Can. J. For. Res., 43: 939-950.

Plummer, M., 2017. JAGS: Just Another Gibbs Sampler. https://sourceforge.net/projects/mcmc-jags.

Porter, E., Blett, T., Potter, D. U., Huber, C. 2005. Protecting resources on federal lands: Implications of critical loads for atmospheric deposition of nitrogen and sulfur. BioScience, 55(7), 603–611. https://doi.org/10.1641/0006-3568

Posch, M. and G. J. Reinds. 2009. A very simple dynamic soil acidification model for scenario analyses and target load calculations. Environmental Modelling and Software, 24: 329–340.

Pourmokhtarian, Afshin, Biogeochemical Modeling of the Response of Forest Watersheds in the Northeastern U.S. to Future Climate Change. 2013. Dissertations - ALL. 21. https://surface.syr.edu/etd/21

Pourmokhtarian, Afshin; Charles T. Driscoll; John L. Campbell, Katharine Hayhoe; Anne M. K. Stoner; Mary Beth Adams, Douglas Burns; Ivan Fernandez; Myron J. Mitchell; James B. Shanley. 2016. Modeled ecohydrological responses to climate change at seven small watersheds in the northeastern United States. Global Change Biology, 23(2): 840-856.

Pourmokhtarian, Afshin; Charles T. Driscoll; John L. Campbell; et al. 2016. The effects of climate downscaling techniques and observational data set on modeled ecological responses. Ecological Applications, 26(5): 1321-1337.

Pourmokhtarian, Afshin; Charles T. Driscoll; John L. Campbell; Katharine Hayhoe. 2012. Modeling potential hydrochemical responses to climate change and increasing CO_2 at the Hubbard Brook Experimental Forest using a dynamic biogeochemical model (PnET-BGC). Water Resources Research, 48: W07514.

Prado, A. del; W. J. Corre; P. Gallejones; et al. 2016. NUTGRANJA 2.0: a simple mass balance model to explore the effects of different management strategies on nitrogen and greenhouse gases losses and soil phosphorus changes in dairy farms.

2016. Mitigation and adaptation strategies for global change. https://www.springerprofessional.de/nutgranja-2-0-a-simple-mass-balance-model-to-explore-the-effects/11745358 (Last accessed 08/01/2020)

Pureswaran, Deepa S.; Alain Roques; Andrea Battisti. 2018. Forest insects and climate change. Current Forest Report. 4(2): 35-50.

Rascher, C. M., C. T. Driscoll, et al. 1987. Concentration and Flux of solutes from snow and forest floor during snowmelt in the west-central Adirondack Region of New York. Biogeochemistry, 3(1): 209-224.

Reich, P.B.; M. B. Walters; B.D. Kloeppel; D.S. Ellsworth. 1995. Different photosynthesis-nitrogen relations in deciduous hardwood and evergreen coniferous tree species. Oecologia, 104: 24-30.

Rennenberg, H.; Loreto F.; Polle A.; et al. 2006. Physiological responses of forest trees to heat and drought. Plant Biology, 8(5): 556-571.

Reyer, Christopher P.O.; Niels Brouwers, Anja Rammig et al. 2015. Forest resilience and tipping points at different spatio-temporal scales: approaches and challenges. Journal of Ecology, 103:5-15.

Rice, K. C., T. M. Scanlon, et al. 2014. Decreased atmospheric sulfur deposition across the Southeastern U.S.: when will watersheds release stored sulfate? Environmental Science & Technology, 48(17): 10071-10078.

Rita, Angelo; Jesus Julio Camarero; Angelo Nole; et al. 2019. The impact of drought spells on forests depends on site conditions: The case of 2017 summer heat wave in southern Europe. Global Change Biology, 26(2): 851-863.

Robert, C., Casella, G., 2004. Monte Carlo Statistical Methods, 2nd ed, Springer Texts in Statistics. Springer-Verlag, New York. https://doi.org/10.1007/978-1-4757-4145-2

Robison, A. L. and T. M. Scanlon. 2018. Climate Change to Offset Improvements in Watershed Acid‐Base Status Provided by Clean Air Act and Amendments: A Model Application in Shenandoah National Park, Virginia. Journal of Geophysical Research: Biogeosciences, 123(9): 2863-2877.

Robison, Andrew L.and Todd M. Scanlon. 2018. Climate change to offset improvements in watershed acid base status provided b clean air act and amendments: a model application in Shenandoah National Park, Virginia. JGR Biogeosciences, 123: 2863-2877.

Roots, E. F. 1989. Climate change: High-latitude regions. Climatic Change, 15(1): 223-253.

Ruiz-Pérez, G. and G. Vico. 2020. Effects of Temperature and Water Availability on Northern European Boreal Forests. Frontiers in Forests and Global Change. https://doi.org/10.3389/ffgc.2020.00034

Schlesinger, William H.; Emily S. Bernhardt; E. H. Delucia; David Ellsworth. 2006. The Duke Forest FACE Experiment: CO_2 enrichment of a Loblolly pine forest. In: Managed Ecosystems and CO_2: Case Studies, Processes, and Perspectives. 197-212.

Serreze, M. C., J. E. Walsh, et al. 2000. Observational Evidence of Recent Change in the Northern High-Latitude Environment. Climatic Change, 46(1-2): 159-207.

Shao, S., C. T. Driscoll, T. Sullivan, D. A. Burns, B. Baldigo, G. Lawrence and T. McDonnell. 2020. The response of stream ecosystems in the Adirondack region of New York to historical and future changes in atmospheric deposition of sulfur and nitrogen. Science of Total Environment, 716:137113 doi:10.1016/j.scitotenv.2020.137113.

Shugar, Daniel H.; John J. Clague; James L. Best; et al. 2017. River piracy and drainage basin reorganization led by climate-driven glacier retreat. Nature Geoscience, 10: 370-375.

Shugart, Herman; Roger Sedjo; Brent Sohngen. 2003. Forest & Global climate change potential impacts on U.S. forest resources. https://www.c2es.org/docUploads/forestry.pdfs (Last accessed 08/01/2020)

Smith, N., W. S. Kessler, et al. 2015. Progress in Observing and Predicting ENSO. Boletín - Organización Meteorológica Mundial, 64(1).

Solomon, S., D. Qin, et al. 2007. Climate Change 2007: The Physical Science Basis. Contribution of Working Group I to the Fourth Assessment Report of the Intergovernmental Panel on Climate Change (IPCC). Computational Geometry, 18(2): 95-123.

Stanke, Carla; Marko Kerac; Christel Prudhomme; Jolyon Medlock; and Virginia Murrary. 2013. Health effects of drought: a systematic review of the evidence. PLoS Currents. doi: 10.1371/currents.dis.7a2cee9e980f91ad7697b570bcc4b004

Stark, John M. and Mary K. Firestone.1995. Mechanisms for soil moisture effects on activity of nitrifying bacteria. Applied and Environmental Microbiology, 61: 218-221.

Stewart, Iris T.; Daniel R. Cayan; Michael D. Dettinger. 2005. Changes toward earlier streamflow timing across western North America. Journal of Climate, 18(8): 1136–1155.

Strzepek, K., G. Yohe, et al. 2010. Characterizing changes in drought risk for the United States from climate change. Environmental Research Letters, 5(4): 44012-44019.

Stumm, W. and J. J. Morgan. 1981. Aquatic chemistry. New York: Wiley. ISBN 0-471-04831-3

Swank, Wayne T.; J. B. Waide, D. A. Crossley, Jr., and R. L. Todd. 1981. Insect defoliation enhances nitrate export from forest ecosystems. Oecologia (Berlin). 51: 297-299.

Swank, Wayne T. and James M. Vose. 1997. Long-term nitrogen dynamics of Coweeta forested watersheds in the southeastern United States of America. Global Biogeochemical Cycles, 11(4): 657-671.

Swift Jr. L. W., G. B. Cunningham and L E Douglass. 1988. Climatology and hydrology. In: Swank W. T. and D.A. Crossley Jr. (Eds.) Ecological Studies New York: Springer-Verlag, 35-55.

Thomson, David J. 2009. Shifts in season. Nature, 457: 391-392.

Turnbull, M. H.; D. Whitehead; D.T. Tissue; W.S.F. Schuster; K.J. Brown; K.L. Griffin. 2001. Responses of leaf respiration to temperature and leaf characteristics in three

deciduous tree species vary with site water availability. Tree Physiology, 21: 571-578.

United States Environmental Protection Agency (USEPA). 2000. National air pollutant emission trends, 1900-1998. E. P. Agency. Research Triangle Park, EPA. 454.

United States Environmental protection Agency. 2017. EPA online database: https://www.epa.gov/air-trends/sulfur-dioxide-trends and https://www.epa.gov/air-trends/nitrogen-dioxide-trends (Last accessed on 09/25/2017).

Valipour, Mahnaz; Charles Driscoll et al. 2018. The application of an integrated biogeochemical model to simulate dynamics of vegetation hydrology and nutrients in soil and streamwater following a whole-tree harvest of a northern hardwood forest. Science of the Total Environment. DOI: 10.1016/j.scitotenv.2018.07.066

van Vuuren, Detlef P.; Jae Edmonds; Mikiko Kainuma; et al. 2011. The representative concentration pathways: an overview. Climatic Change, 109:5.

Vaughan, I. P. and Ormerod, S. J. 2005. Increasing the value of principal components analysis for simplifying ecological data: A case study with rivers and river birds. Journal of Applied Ecology, 42(3), 487–497. https://doi.org/10.1111/j.1365-2664.2005.01038.x

Velbel, M, A. 1988. Weathering and soil-forming processes. In Swank, W. T. and Crossley, D. A. Jr. eds, Forest Hydrology and Ecology at Coweeta: New York, Springer-Verlag, 93-102.

Verma, Satyam; Dharmatma Singh; Ajeet Kumar Singh; and Shanmuganathan Jayakumar. 2019. Post-fire soil nutrient dynamics in a tropical dry deciduous forest of Western Ghats, India. Forest Ecosystems, 6: 6. https://doi.org/10.1186

Vose, James M. and Wayne T. Swank. 1994. Effects of long-term drought on the hydrology and growth of a white pine plantation in the southern Appalachians. Forest Ecology and Management, 64: 25-39.

Vose, James M.; James S. Clark, Charles H. Luce, Toral Patel-Weynand. 2016. Effects of drought on forests and rangelands in the United States: A comprehensive science synthesis. USDA. pp302. https://www.fs.fed.us/sites/default/files/DROUGHT_book-web-1-11-16.pdf (Last accessed 08/01/2020)

Wang, Q., X. Fan, et al. 2014. Recent warming amplification over high elevation regions across the globe. Climate Dynamics, 43(1): 87-101.

Wang, Q., X. Fan, et al. 2016. Evidence of high-elevation amplification versus Arctic amplification. Scientific reports, 6(1): 1–8.

Wason, J. W., C. M. Beier, et al. 2019. Acidic Deposition and Climate Warming as Drivers of Tree Growth in High-Elevation Spruce-Fir Forests of the Northeastern US. Frontiers in Forests and Global Change, 2: 63.

Webster J. R. et al. 1992. Catchment disburbance and stream response: Overview of stream research at Coweeta Hydrologic Laboratory. In P.J.Boon; P. Calow, and G. E. Petts (Eds), River Conservation and Management. 1992.

Weih, Martin and P. Staffan Karlsson. 2002. Low winter soil temperature affects summer time nutrient uptake capacity and growth rate of mountain birch seedlings in the subarctic, Swedish Lapland. Arctic, Antarctic, and Alpine Research, 34(4): 434-439.

Westerling, A., T. Brown, et al. 2014. Briefing: Climate and wildfire in western US forests. In: Sample, V. Alaric; Bixler, R. Patrick, eds. Forest conservation and management in the Anthropocene: Conference proceedings. Proceedings. RMRS-P-71. Fort Collins, CO: US Department of Agriculture, Forest Service. Rocky Mountain Research Station. p. 81-102. 71: 81–102.

Wu, Wei and Charles T. Driscoll. 2010. Impact of climate change on three-dimensional dynamic critical load functions. Environmental Science & Technology, 44(2): 720-726.

Wu, Wei; James Clark; James Vose. 2014. Response of streamflow to climate change in the southern Appalachian Mountains using Bayesian inference. *Hydrological Processes* 28(4): 1616-1625, DOI: 10.1002/hyp.9677.

Wu, Wei and Charles T. Driscoll. 2009. Application of the PnET-BGC – An integrated biogeochemical model – to assess the surface water ANC recovery in the Adirondack region of New York under three multi-pollutant proposals. Journal of Hydrology, 378: 299-312.

Wu, Wei, Matthew Bethel, Deepak Mishra, Tyler Hardy, 2018. Model selection in Bayesian framework to identify the best WorldView-2 based vegetation index in

predicting green biomass of salt marshes in the northern Gulf of Mexico. *GISceince & Remote Sensing* https://doi.org/10.1080/15481603.2018.1460934.

Wu, Wei, Patrick Biber, Matthew Bethel, 2017. Thresholds of sea-level rise rate and sea-level rise acceleration rate in a vulnerable coastal wetland. *Ecology and Evolution* 7(24), 10890-10903, doi: 10.1002/ece3.3550.

Wu, Wei; James S. Clark; James M. Vose. 2012a. Application of a full hierarchical Bayesian model in assessing streamflow response to a climate change scenario at the Coweeta Basin, NC, USA. Journal of Resources and Ecology, 3(2): 118-128.

Wu, Wei; Patrick D. Biber; Mark Peterson; and Chongfeng Gong. 2012b. Modeling photosynthesis of *Spartina alterniflora* (smooth cordgrass) impacted by the Deepwater Horizon oil spill using Bayesian inference. Environmental Research Letters, 7: 045302.

Xie, Yingying; Xiaojing Wang; and John A. Silander Jr. 2015. Deciduous forest responses to temperature, precipitation, and drought imply complex climate change impacts. PNAS, 112(44): 13585-13590.

Yao, Shuren. 2003. Effects of fire disturbance on forest hydrology. Journal of Forestry Research, 14(4): 331-334.

Zhai, Jing; Charles T. Driscoll; Timothy J. Sullivan; Bernard J. Cosby. 2008. Regional application of the PnET-BGC model to assess historical acidification of Adirondack lakes. Water Resources Research, 44, W01421.

Zhou, Qingtao. 2014. Developing critical loads and dynamic critical loads for acidification for watersheds in the Adirondack region of New York and Great

Smoky Mountain National Park (GRSM). Ph.D. Dissertation, Syracuse University. pp174.

Zhou, Qingtao; Charles T. Driscoll; Timothy J. Sullivan; Afshin Pourmokhtarian. 2015. Factors influencing critical and target loads for the acidification of lake-watersheds in the Adirondack region of New York. Biogeochemistry, 124(1-3): 353-369.

Zohner, Constantin M.; Lidong Mo; Thomas A. M. Pugh et al. 2020. Interactive climate factors restrict future increases in spring productivity of temperate and boreal trees. Global Change Biology, 26(7): 4042-4055. https://doi.org/10.1111/gcb.15098